Probabilistic Deterioration Modelling and Time-Dependent Reliability Analysis of Coastal Defences

Mehrdad Bahari Mehrabani

Thesis submitted in partial fulfilment of the requirements
of the University of Greenwich for the
Degree of Doctor of Philosophy

March 2018

In loving memory of

My Dear Brother

Dr. Mehdi Bahari Mehrabani

Aged 35 Years

Tragically Taken From Us

in July 2016

DECLARATION

I certify that the work contained in this thesis, or any part of it, has not been accepted in substance for any previous degree awarded to me, and is not concurrently being submitted for any degree other than that of Doctor of Philosophy being studied at the University of Greenwich. I also declare that this work is the result of my own investigations, except where otherwise identified by references and that the contents are not the outcome of any form of research misconduct.

PhD candidate: Mehrdad Bahari Mehrabani

1st Supervisor: Prof. Hua-Peng Chen

2nd Supervisor: Dr. Kong Fah Tee

ACKNOWLEDGMENTS

Pursuing PhD has been a truly life-changing experience for me, and it would not have been possible to do without the support, guidance and encouragement that I received from many people. I wish to express my sincere appreciation to all those who have contributed to the successful outcome of this research. I would like to thank the University of Greenwich for giving me an opportunity and providing the resources to complete this research successfully.

My special thanks go to my supervisor, Professor Hua-Peng Chen who took time out of his busy schedule to provide expert advice and direction in every step during the research. Especially after the tragedy that I have faced in the second year of my research. I would like to express my profound gratitude to him for his constant inspiration and encouragement. My thanks are also extended to Dr Kong Fah Tee for his support.

I am grateful to all my colleagues and friends within the research unit who provided the laughs and social relief during those hectic, frustrated and stressful days. I would like to extend my sincere thanks and appreciation to my best friends for their continuous support.

ABSTRACT

The prediction of coastal flood defence performance deterioration in the future plays an essential role in the reliability analysis and management process of these structures. The climate change effects and sea level rise will increase the hydraulic loads and frequency of the future extreme events, which lead to a more challenging performance deterioration prediction. The main failure mechanisms in coastal flood defences, e.g. wave overtopping and piping will be affected due to the change in hydraulic parameters and deterioration processes, which may decrease the reliability of the structures. Also, the uncertainties arising from the mentioned problems lead to a more expensive and inefficient management strategy to protect the lands, people and properties against floods.

Hence, continuous innovations in flood asset management and structural reliability analyses methods are necessary to improve the accuracy and efficiency of the future performance evaluation in a changeable environment, and then to decrease the maintenance and management costs. In practice, parameters of probabilistic deterioration models can be estimated using available data from routine inspections and observations. For coastal defences, the condition assessment results and observations are collected using different inspection strategies, and deterministic grade-based deterioration curves are available in order to estimate structures residual life with respect to the structural conditions. However, probabilistic approaches to model the stochastic deterioration process with consideration of the changes in hydraulic loading parameters are not studied yet in coastal flood defences.

This thesis proposes probabilistic state-based deterioration models and time-dependent reliability analyses for coastal flood defences, which help to predict the future performance deterioration and condition grades of the assets. The proposed deterioration models have four components: 1) using homogeneous (i.e. stationary) and non-homogenous (i.e. time-dependent and non-stationary) Markovian models to forecast a coastal defence deterioration process, 2) employing stochastic theory and simulation techniques to establish the Markovian transition probability matrices for the assets, 3) utilising performance-based reliability models to predict the reliability of the structures regarding the predicted deteriorations and projected changes in hydraulic variables, and

4) utilising renewal replacement theory, and sequential decision-making model to select optimal multi-objective maintenance actions under partial information.

The deterioration models were established through a process of conversion from deterministic data and conventional framework in coastal flood defences to a probabilistic system. The process of the system conversion is described, and the validation of the conversion is demonstrated by a number of numerical examples. The elements of the time-dependent transition probability matrices are calculated using Weibull distributed waiting times and non-linear optimisation techniques. The limit state equations for the reliability-based model are updated regarding the sea level rise and deterioration models, and the future performance is predicted using time-dependent reliability analyses. The validation and efficiency of the time-dependent reliability analysis are demonstrated by case studies. A Partially Observable Markov Decision Process is utilised to provide the optimal maintenance strategies for each time interval. Cost of imperfect information is adopted to control the optimisation process at each time-step based on the stochastic deterioration model.

The obtained results from the proposed method are examined by experimental and field data available. The applicability of the method is demonstrated by numerical examples, and the results show that the proposed methodology is capable of assessing the structural performance in the future and also can provide multi-objective optimised repair and inspection schedule during the lifetime of coastal defence structures. The knowledge gained in this study contributes to the better understanding of the performance deterioration of flood defences. Furthermore, the methodology presented in this study could be helpful in assessing the actual state of deterioration and to decrease the cost of management for flood defences.

Table of contents

1. Introduction 1

1.1. Background 1

1.2. Research significance and contributions 4

1.3. Aim and objectives 5

1.4. Scope of the thesis 5

1.5. Methodology and outline of the thesis 6

2. Literature review 9

2.1. Introduction 9

2.2. Current risk evaluation methods in UK 9

2.3. Hydraulic conditions for coastal flood defences 13

2.3.1. *Hydraulic loads and parameters* *13*

2.3.2. *Climate change impacts on hydraulic loads* *18*

2.3.3. *Projected sea level rise* *19*

2.3.4. *Projected wave conditions* *19*

2.4. Coastal flood defence condition assessment 21

2.4.1. *Condition grading system* *21*

2.4.2. *Quantitative damage assessment* *24*

2.5. Deterioration processes and modelling 24

2.5.1. *Deterministic vs stochastic deterioration models* *25*

2.5.2. *Stochastic deterioration models* *26*

2.5.3. *Lifetime reliability models* *28*

2.5.4. *Sources of deteriorations in coastal defences* *29*

2.6. Structural reliability analyses 30

2.6.1. *Failure modes of coastal flood defences* *31*

2.6.2. *Limit state equation* *34*

2.6.3. *Fault tree analysis* *35*

2.6.4. *Time-dependent reliability* *38*

2.6.5. *Fragility curves* *39*

2.7. Optimal maintenance strategies 40

2.7.1. *Renewal maintenance model* *41*

2.7.2. *Markov decision process* *42*

2.8. Research questions and gaps 43

2.9. Summary and conclusions 44

3. Monitoring and assessment of coastal defences' condition 46

3.1. Introduction 46

3.2. Grade-based condition assessment 46

3.3. Performance-based asset management 50
3.3.1. *Quality of inspection strategies* *51*
3.3.2. *Correlating quantitative assessment and failure mechanisms* *54*
3.4. Translating quantitative assessment to a probabilistic framework 59
3.5. Hydraulic load monitoring and evaluation 63
3.5.1. *Extreme values analysis* *64*
3.5.2. *Joint probability of sea level and significant wave height* *75*
3.6. Climate change impacts 80
3.7. Case study at Portsmouth 82
3.7.1. *Selecting the deterioration curve* *83*
3.7.2. *Probability distributions of the dyke damage* *83*
3.7.3. *Extreme values analysis* *88*
3.7.4. *Effects of sea level rise on extreme values* *94*
3.7.5. *Joint probability evaluations* *97*
3.8. Summary and conclusions 100
4. Stochastic deterioration modelling for coastal defences 101
4.1. Introduction 101
4.2. Stochastic Gamma process 101
4.2.1. *Parameter estimation* *102*
4.2.2. *Simulation* *103*
4.3. Homogenous Markov chain 104
4.3.1. *Transition probability matrix* *105*
4.3.2. *Calibration of transition probability matrix* *107*
4.3.3. *Model verification* *108*
4.3.4. *Limitation of homogeneous Markov chain* *108*
4.4. Non-homogenous Markov chain 109
4.4.1. *Time-dependent transition probability matrix* *110*
4.4.2. *Weibull-distributed sojourn time* *111*
4.4.3. *Parameter estimation* *113*
4.5. Case study at Sheerness 117
4.5.1. *Effect of deterioration rates on condition grades evolution* *118*
4.5.2. *Effect of repair maintenance on condition grades evolution* *120*
4.6. Case study at Thames estuary 122
4.6.1. *Survival probabilities estimated from two-state approach* *123*
4.6.2. *Survival probabilities estimated from transition approach* *125*
4.6.3. *Comparison of results from two approaches* *128*
4.7. Summary and conclusions 128
5. Reliability-based performance assessment for coastal defences 130
5.1. Introduction 130

5.2. Failure risk assessment 130
5.3. Fragility curves and fragility surfaces 134
5.4. Excessive wave overtopping failure 136
5.5. Piping failure 141
5.6. Case Study at Sheerness 144
5.6.1. *Evaluation of the fragility curves* *144*
5.6.2. *Effects of deterioration rates on the fragility curves* *149*
5.6.3. *Effects of repair maintenance on fragility curves* *150*
5.7. Case study at Thames estuary 152
5.7.1. *Effects of sea level rise on overtopping* *153*
5.7.2. *Evaluation of time-dependent failure probability* *156*
5.8. Summary and conclusions 160
6. Optimal maintenance strategy for coastal defences 161
6.1. Introduction 161
6.2. Single-objective vs multi-objective decision process 161
6.3. Evaluating effectiveness matrices for repair actions 163
6.4. Cost of inspection error in decision making process 164
6.5. Bi-objective optimised inspection strategy regarding risk consequences 167
6.6. Optimal maintenance and replacement policy 168
6.7. Case study at Thames estuary: POMDP optimisation 170
6.7.1. *Single objective optimisation* *170*
6.7.2. *Multi-objective POMDP optimisation* *172*
6.8. Case study at Thames estuary: Renewal maintenance optimisation 174
6.9. Summary and conclusions 176
7. Conclusions and suggestions for future research 178
7.1. Summary and conclusions 178
7.2. Recommendations for future study 180
Reference 182
Appendices 195
Appendix 1: List of publications 195
Appendix 2: Summary of condition grade assessment in UK adopted from Environment Agency 2014. 196

List of tables

Table 2.1 Condition grades and descriptions adopted by Environment Agency (EA 2006).....21

Table 2.2 Example calculation of condition grade from grade and weighting for a flood defence adopted from Environment Agency (2014). 22

Table 2.3 Consequence of mean overtopping discharge on flood defence structures (Van der Meer et al., 2016). 32

Table 3.1 Parameters associated with three inspection strategies. 52

Table 3.2 Parameters associated with three inspection strategy. 53

Table 3.3 Details of failure modes and measurable properties for an earth dyke (adopted from Long et al. 2013).....55

Table 3.4 Surface features related to damage and failure for an embankment (adopted from Long et al. 2013).....57

Table 3.5 Seepage length loss in earth embankments (Long et al 2013) and suggested condition grade. 58

Table 3.6 Slope loss in earth embankments (Long et al 2013) and suggested condition grade. 58

Table 3.7 Crest height loss in earth embankments (Long et al 2013) and suggested condition grade. 59

Table 3.8 Transition of the dykes condition grades from 1 to 5 over time (Harlcrow 2013).....82

Table 3.9 Suggested condition grade for geometrical loss in earth sea embankments and their density distribution referred to Tables 3.5-3.7. 84

Table 3.10 Verification of the estimated lognormal distribution parameters for the example. 87

Table 4.1 Parameter estimation utilising two-state approach. τ: years after the initial date that the sea dyke is in the same condition grade with 50% probability. SSE: the sum of squares due to error (Goodness-of-Fit test). 115

Table 4.2 Parameter estimation using transition approach. τx: years after initial date that the sea dyke is in the same condition grade with x% survival probability. SSE: sum of squares due to error (Goodness-of-Fit test). 116

Table 4.3 Parameter estimation for three different scenarios using two-state approach. 123

Table 4.4 Parameter estimation for three different scenarios using transition approach. 126

Table 5.1 Suggested vertical crest level loss (Long et al. 2013) for a sea dyke related to condition grade system. 140

Table 5.2 Suggested seepage length loss (Long et al. 2013) in water flow direction for a sea dyke related with condition grade system. 143

Table 6.1 Pareto optimum samples for single-objective optimisation. 171

Table 6.2 Pareto optimum samples for multi-objective optimisation. 172

List of figures

Figure 1.1 A train passes through the coast at Saltcoats in Scotland (Picture from BBC, 2014).....2

Figure 2.1 Source-pathway-receptor-consequence model to evaluate the risk for flood defences.....9

Figure 2.2 Flood-map-planning online application demostratres the recommendations for flood risk in Chatham area.....11

Figure 2.3 The defined datum in UK and their approximate relevant position to each other.....14

Figure 2.4 The schematic of wave changes when entering surf zone. 15

Figure 2.5 Cross section of a coastal defence embankment with its geometrical surfaces (adopted from Hall et al. 2007). 16

Figure 2.6 Approximate contributions to coastal flooding, SW England, early January 2014.....17

Figure 2.7. Projected UK mean significant wave height (m) relative changes at various locations from 1990–1999 to 2090–2099 (adopted from Jenkins et al. 2011).....20

Figure 2.8. Sea defences examples with different condition grades, the second asset is in condition grade 2 due to animal burrow and erosions. The arrows show the defects areas.....23

Figure 2.9 Grade (*G*) transition and transition time (*t*) of a typical Markov process.....26

Figure 2.10 Illustration of probabilistic limit state equations; Pf failure probability; β is reliability index; and σ standard deviation of the safety distribution (Adopted from Allsop et al. 2007). 35

Figure 2.11 Failure probabilities and extract of fault tree for a typical dyke (adopted from Naulina et al. 2008). 37

Figure 2.12 Illustration of the time-dependent failure probability and the lifetime *L* (Adopted from Buijs et al 2005). 39

Figure 3.1 Example of deterioration curves provided by Environment Agency for coastal defence structures with toe/slope protection (Halcrow group 2013). 47

Figure 3.2 The stages of evaluating the current condition grade and selecting an appropriate deterioration curve. 49

Figure 3.3 Probability of damage detection for three inspection strategies. 54

Figure 3.4 Conservative random distribution of deterioration for an asset in condition grade 2 (CG2) when inspecting are correct at 92% of the time. 61

Figure 3.5 The probability density and cumulative lognormal distribution for the example. 62

Figure 3.6 GEV probability density function with various parameter values. 66

Figure 3.7 Frequency of hypothesis daily water levels for 5 years. 66

Figure 3.8 The probability density of the block maxima values with a GEV fitted line. 67

Figure 3.9 The smallest R_{10} value achieved within the critical region of the shape parameter. 68

Figure 3.10 GPD probability density for various parameter settings. 69

Figure 3.11 Frequency of the the wave heights. 71

Figure 3.12 Mean residual life plot for the significant wave heights (dots) with 95^{th} percentile (dashed lines). 72

Figure 3.13 Diagnostic plots for the GPD model with a threshold value of 1.30 m. 73

Figure 3.14 Diagnostic plots for the GPD model with a threshold value of 2.50 m. 74

Figure 3.15 Illustration of a joint probability distribution example. 75

Figure 3.16 The effect of various dependency coefficients between two arbitrary parameters. 79

Figure 3.17 Joint exceedance probabilities for wave overtopping failure mechanism (Adopted from HR Wallingford, 2000). 81

Figure 3.18 Estimated times to next condition grade from condition grade 1 for the dyke system. 83

Figure 3.19 Probability density distributions associated with condition grade (CG) of the earth sea dyke regarding the Tier 3 inspection strategy. 85

Figure 3.20 Probability density distributions associated with condition grade (CG) of the earth sea dyke regarding the Tier 1 inspection strategy. 86

Figure 3.21 Verification of the estimated normal distribution parameters. 87

Figure 3.22 Mean residual plots for present water level and significant wave height. ..89

Figure 3.23 Diagnostic plots for the GEV analysis of the present water levels data. 90

Figure 3.24 Diagnostic plots for the GPD analysis of the present water levels data. 91

Figure 3.25 Diagnostic plots for the GEV analysis of the present significant wave height data. 92

Figure 3.26 Diagnostic plots for the GPD analysis of the present significant wave height data. 93

Figure 3.27 Recurrence interval plots for present sea water level (SWL) and significant wave height (SWH). 94

Figure 3.28 Relative increase in sea level for the different emission scenarios with 95th confidence intervals (dashed lines). 95

Figure 3.29 Recurrence interval plots with and without sea level rise after 50 years subject to low (L), medium (M) and high (H) emission scenarios for two extreme value models. 96

Figure 3.30 Scatter plot of original and simulated data for wave periods against significant wave heights. 97

Figure 3.31 Joint probability return periods in contour lines and simulated data marked in dots for water level and significant wave height for the case without sea level rise. 98

Figure 3.32 Joint probability return periods (contour lines) for water level and significant wave height subject to various scenarios. 99

Figure 4.1 Simulated Gamma deterioration process for a sea dyke crest level subject to three different deterioration rates. 104

Figure 4.2 Progress of asset pmf over time regarding time-dependent transition probability. 110

Figure 4.3 Weibull density function with different shape and scale parameters. 113

Figure 4.4 Assumed Weibull survival function and two-state stationary Markov deterioration for the transition from condition grade 1 to 2. 114

Figure 4.5 Assumed Weibull survival function and linear deterioration for the transition from condition grade 1 to 2. 116

Figure 4.6 Deterioration times (year) to specified condition grades CG from new with three different deterioration rates subject to do-nothing maintenance. 117

Figure 4.7 Time-dependent condition grade probabilities from the Markov model for the earth sea dyke subject to varoius deterioration rates. 119

Figure 4.8 Effect of maintenance on time-dependent condition grade probabilities from the Markov model for the earth sea dyke subject to slow deterioration rate. 121

Figure 4.9 Effect of maintenance on time-dependent condition grade probabilities from the Markov model for the earth sea dyke subject to medium deterioration rate. 121

Figure 4.10 Effect of maintenance on time-dependent condition grade probabilities from the Markov model for the earth sea dyke subject to fast deterioration rate. 122

Figure 4.11 Sketch of the earth sea dyke section along Thames estuary. 122

Figure 4.12 Deterioration times to specified condition grades from new with various deterioration rates (Halcrow group 2013). 123

Figure 4.13 Survival functions of cumulative waiting times in different condition grades (CG) subject to fast deterioration rate. 124

Figure 4.14 Survival functions of cumulative waiting times in different condition grades (CG) subject to medium deterioration rate. 125

Figure 4.15 Survival functions of cumulative waiting times in different condition grades (CG) subject to slow deterioration rate. 125

Figure 4.16 Survival functions of cumulative waiting times in different condition grades (CG) subject to fast deterioration rate. 126

Figure 4.17 Survival functions of cumulative waiting times in different condition grades (CG) subject to medium deterioration rate. 127

Figure 4.18 Survival functions of cumulative waiting times in different condition grades (CG) subject to slow deterioration. 127

Figure 5.1 Schematic of a reliability function. 131

Figure 5.2 Typical S-shape fragility curves (solid line) and the uncertainty area (dashed line).....134

Figure 5.3 Fragility surf as a failure mechanism as a function of water level and time after initial date.....135

Figure 5.4 Schematic diagram of wave overtopping discharge over a sea dyke.....137

Figure 5.5 Schematic diagram of piping under a typical sea dyke over time. 142

Figure 5.6 Fragility curves for diffrent wave overtopping discharge limits in specific condition grades and medium deterioration rate. 146

Figure 5.7 Failure probability over time at certain sea water levels for various wave overtopping discharge imits. 147

Figure 5.8 Fragility curves for various wave overtopping discharge limits with sea level rise after present day. 148

Figure 5.9 Fragility curves for 1 l/s/m wave overtopping as a function of water level at 30 years after present condition subject to different deterioration rates. 149

Figure 5.10 Fragility curves for 2 l/s/m wave overtopping as a function of water level at 30 years after present condition subject to different deterioration rates. 149

Figure 5.11 Fragility curves for 1 l/s/m wave overtopping as a function of water level at 30 years subject to slow deterioration rate and two maintenance plans.....150

Figure 5.12 Fragility curves for 1 l/s/m wave overtopping as a function of water level at 30 years subject to medium rate and two maintenance plans. 151

Figure 5.13 Fragility curves for 1 l/s/m wave overtopping as a function of water level at 30 years subject to fast deterioration rate and two maintenance plans. 151

Figure 5.14 Probability density distribution of the sea dyke crest level and seepage length loss associated with condition grade (CG). 153

Figure 5.15 Different rates of crest level deterioration to give the same overtopping rate at 1000-year return period after 50 years from the initial date.....154

Figure 5.16 The relative changes of overtopping discharge in the future subject to different deterioration rates. 155

Figure 5.17 Average mean overtopping discharge for the 1000-year return period event associated with the sea level rise after 50 years from the initial day with 95% percentiles shown by bars. 155

Figure 5.18 Failure probability of the sea dyke due to wave overtopping and piping subject to different deterioration rate. 157

Figure 5.19 Fragility surface for overtopping failure mechanism subject to various deterioration rates. 158

Figure 5.20 Fragility surface for piping failure mechanism subject to various deterioration rates. 159

Figure 6.1 Example of the dominance and Pareto optimally. 162

Figure 6.2 The deterioration curve for a class-44 sea dyke subject to do-nothing and major maintenance action.....164

Figure 6.3 Sequential decision process with partial information. sk: states, ak: actions, ok: observations, bk: belief states, Rk: reward value. 166

Figure 6.4 Pareto sets of solutions for the sea dyke subject to different deterioration rates. 173

Figure 6.5 Expected annual relative costs without discounting as a function of time for different deterioration rates of the crest level. 175

Figure 6.6 Expected relative costs with discounting at an annual rate of 5% as a function of time for various deterioration rates of crest level. 175

Figure 6.7 Expected relative costs with discounting and the medium deterioration rate of crest level as a function of time for various preventive maintenance costs Cp. 176

1. Introduction

1.1. Background

The world in its postmodernism era relies on civil infrastructure for protecting people, assets and economy. Coastal and fluvial floods defence structures are supposed to protect lands and coastlines which is necessary for running economies and societies. Coastal defence assets are aimed to be servicing for extended periods to protect shorelines, particularly infrastructure and habitats against flooding and coastal erosion. Sea defences provide essential protection for coastal lowlands against flooding. Hence they are considered as critical assets.

The risk of land flooding can increase in the future due to the rise of sea level and change of wave conditions caused by climate change. Coastal flood defence structures are facing new challenges such as sea level rise due to climate change. Sea level rise results in storm amplifications, stronger wave attacks and undesirable changes in hydraulic parameters (Donovan et al. 2013). The influences of coastal floods and coastal erosions due to changing environment are significant to society and economy. The sea level rise affects the future hydraulic loading conditions acting on sea defence structures, leading to further deterioration of structural reliability and safety. It is essential to assess the reliability and integrity of the coastal defence structures accurately to make sure that the assets perform reliably during their service life.

In order to effectively manage these risks, reliability analysis is often employed to provide a useful tool for quantitatively evaluating the risks of sea defence structures under future conditions and accurately predicting the probability of failure of the structures over time. As a result of reliability analysis, the dominant failure mechanisms that may lead to failure of the structure can be identified, and the decision for the risk-cost optimised maintenance strategy can be evaluated.

Time-dependent analysis of coastal defence systems is essential in order to assess the reliability performance of the structures over time. A time-dependent analysis involves looking at the deterioration process, sea level rise and the maintenance strategy during the structure’s lifespan. Deterioration processes such as internal or external erosions,

crest level settlement, sliding and instability are types of time-dependent processes that affect the resistance of a structure during the expected lifespan (Udale-Clarke 2009). Climate change effects such as sea level rise lead to increase in the frequency and intensity of extreme events (such as the event in Figure 1.1), which cause a faster deterioration process.

Figure 1.1 A train passes through the coast at Saltcoats in Scotland (Picture from BBC, 2014).

Changing environments due to global warming pose a new challenge for the structural performance of the coastal defences by increasing the hydraulic loads in the future. The projected climate change by United Kingdom Climate Projection 2009 (UKCP09) show a considerable increase in hydraulic parameters in UK waters. For example, in UK, it is expected to have an average rise in sea levels between +12 cm and +76 cm by the end of the 21st century for different emission scenarios. Wave heights are projected to change between -150 cm to +100 cm in UK waters (Jenkins et al. 2011). Wave heights are sensitive to the local (or site) conditions, for example, the South-West of UK will face increases in mean wave heights, while the North will face to a decrease.

Over the last decade, the world has suffered from fatal and deadly coastal floods which raised new concerns about the capacity and effectivity of coastal defence structures. Unprecedented floods happened over the last century. For example, the disasters happened in UK during winter 2013/14, in the US in 2005 (Sandy and Hurricanes Katrina), in Myanmar in 2008, and in the Philippines in 2013 (Hallegatte et al. 2013;

Rosenzweig et al. 2011; Antonioli et al. 2017; Diakakis et al. 2015). The US storms killed about 2000 people and caused damage worth more than 200 billion pounds. In Myanmar, 84000 people were killed, and 50 km of inland coastal width were submerged. In the Philippines, the event killed 8,000 people and destroyed tens of thousands of houses, mostly due to high sea levels.

During winter 2013/14 UK storms, at least 17 people died, and it was estimated that the damage was more than £1bn. In other reports, more than 11 major storms occurred over various coastal cities, and flood defences failed to defend the cities (Burcharth et al. 2014; Wadey et al. 2014; Dahl and Fitzpatrick 2017). These events are a reminder of the ever-present risks facing coastal flood defence scheme over the sea level rise and coastal population grow. The adverse impacts of climate change are likely to worsen with consideration of shoreline erosion and structural degradations. Recently, resilient flood defence criteria are proposed to protect coastlines against future environmental conditions (Agrawala et al. 2011; Wilby and Keenan 2012). The previous standards in coastal defence structures were based on the prevention of wave overtopping and other failure mechanisms, while a resilience flood defence mitigates the failure consequences regarding the priorities. Eliminating failure consequences (e.g. zero failure probability) approach is no longer cost-efficient and not reliable due to the changing environments.

New approaches are not based on the “preventing” but based on the “mitigating” of failure in extreme events. Decision makers consider the new approach to be the new policy shifting to resiliency in coastal structures rather than avoiding the floods entirely. The time-dependent analysis of major hydraulic parameters, the return period and modified remaining life are taken into account as the main factors in this methodology (Sekimoto et al. 2013). The uncertainty in the projection of the sea level rise and the structural deterioration process are the primary problems to achieve a reliable flood defence in the future.

1.2. Research significance and contributions

The reliability-based performance assessment techniques based on stochastic deterioration modelling has remarkable potential to provide cost-effective maintenance management such as inspection, repair, strengthening, and reconstruction in flood defences. For the time-dependent reliability analysis of coastal defences subject to deterioration process and changing environments, a practical evaluation of the damage associated with the resistance parameters during their service life is required. It is always beneficial to have a link between the deterioration levels and the asset condition grades to make the management policy more efficient.

The developed method in this research will provide more accurate assessments of the failure risk in coastal defence structures for the researchers and professionals involved in managing these structures. The proposed method may be socio-economic and a reliable tool for decision makers regarding the future changing environments and deterioration processes to plan necessary maintenance strategies. Also, by consideration of imperfect information and possible errors in the inspection outcomes, the efficiency of the proposed model will be increased. The main contributions of this thesis are listed as follows:

- The effects of sea level rise and changing environments over the hydraulic variables and the structural reliability are investigated. The changes in hydraulic variables such as water level, wave period and depth-limited significant wave heights are considered concerning different sea level rise scenarios.
- A stochastic and grade-based deterioration model is developed to assess the deterioration process of coastal defence structures.
- A time-dependent reliability analysis framework is proposed with consideration of the proposed deterioration model and the adopted functions for sea level rise effects.
- A multi-objective maintenance model is proposed to optimise the maintenance strategies regarding partial observations and imperfect inspections. A Multi-Objective Partially Observable Markov Decision Process (Mo-POMDP) is utilised to consider the effects of deterioration process, maintenance strategies, inspection techniques and structure's condition grade.

1.3. Aim and objectives

The research aim is to investigate how changing environments and non-stationary deterioration process of coastal flood defences can be incorporated into a reliability-based approach, to assess the reliability of the structures against different failure mechanisms in the future, and to optimise maintenance strategy regarding partial information. The following objectives are defined:

- To understand the mechanism of deteriorations and its effect of the structural reliability of the coastal defences.
- To investigate climate change impacts such as sea level rise on hydraulic parameters on the future performance deterioration.
- To define a quantitative link between the current qualitative condition grade system and structural damage.
- To investigate the effects of crest level deterioration and internal erosion on overtopping and piping failure mechanisms.
- To develop an analytical model to assess the time-dependent probability of failure with consideration of structural deterioration and changing environments
- To propose a maintenance model to optimise multiple objectives concerning incomplete information/inspections.

1.4. Scope of the thesis

The primary focus of this thesis was the development of stationary and non-stationary deterioration models of coastal defences. The model uses condition assessment manual (Environment Agency 2006) by application of available deterministic deterioration curves and inspection data. The deterioration models are used to assess time-dependent reliability analysis and generic fragility curves. The proposed models are sensitive to the accuracy of the initial quantitative and qualitative data. Hence, it is limited to use when the proper data are not available. Both deterioration models can be used in existing UK coastal and fluvial flood defences. Some calculations, assumptions and selections were considered to provide a proper and realistic analysis and maintenance optimisation.

The response of a coastal flood defence to hydraulic loads depends on the geometry, material and operational conditions. The analysis of many dyke breaches (Nagy and

Toth, 2005; Horlacher, 2005) shows that structural failures of earth sea dykes due to overtopping and piping failure mechanisms are more than 85% of all various types of failures. Therefore, overtopping and piping failure mechanisms have been considered as major threats to the structural performance of sea dykes, and this thesis focuses on these two failure mechanisms.

1.5. Methodology and outline of the thesis

This research will first carry out a literature review on how failure mechanisms and deterioration processes affect the performance of the coastal defence structures like sea dykes in changing environments. For this, an extensive literature review has been undertaken on the following topics: climate change, sea level rise, deterioration processes, failure mechanisms, and time-dependent reliability analysis methods. The next step is to develop deterioration models to evaluate the resistance of the structures over time. Then, a stochastic and analytical model has established to assess a time-dependent reliability with consideration of the possible hydraulic changes due to sea level rise. Available published field data by Environment Agency are investigated to provide necessary information to estimate the relevant parameters of the proposed models.

A numerical model of failure probability assessment with consideration of joint probability between key variables will also be developed using MATLAB as programming and data processing tools. Evolutionary Algorithms will be applied for the effect of the deterioration process such as settlement in the developed model. Monte Carlo simulations will be utilised for sampling the future and current conditions. During the simulation and analysis processes, various methods of statistics and software such as MATLAB, R-CRAN or EXCEL will be used as analysis tools. The proposed model will be verified with the existing observed and experimental data. Case studies on sea dykes will be utilised for the application of the developed model.

This thesis consists of seven chapters (Chapter 1 to 7), and a brief outline of each chapter is as follows:

Chapter 1: introduction

This chapter describes the background and significance of the research and introduces the aim and objectives and scope of the thesis.

Chapter 2: Literature Review

This chapter presents fundamental theories and state-of-art methods in the relevant research. First, a brief overview of the existing coastal defences and reliability methods in this field are discussed. Then available publications about hydraulic variables and the effects of climate change are studied. Available condition assessment frameworks for coastal defences in UK are presented, and an overview of the deterministic deterioration curves is provided. Stochastic deterioration models are studied, and the applicability of the models for different types of deterioration processes are reviewed. Then reliability theory for coastal defences is investigated to understand the time-dependent reliability and performance evaluation methods. Finally, available maintenance models in this area are studied to find out the developments and the gaps regarding the maintenance policies in UK.

Chapter 3: Condition monitoring and evaluating for coastal flood defences

In this chapter, condition assessment model, hydraulic load monitoring, and climate change impacts on hydraulic boundary conditions are discussed. A quantitative link between structural damage and condition grading system is proposed. The available inspection strategies and deterioration curves are translated into probabilistic forms to use in the reliability model. A practical model is described to apply the impacts of sea level rise on the hydraulic parameters, and the model is utilised for extreme value analysis. A new technique is proposed to improve the dependence estimating between the joint extreme variables via a copula function.

Chapter 4: Stochastic deterioration modelling for coastal defences

In this chapter, new stochastic deterioration models are developed for coastal defence structures to model the deterioration processes such as crest level settlement and seepage length loss. A homogenous Markov model is adopted to model stationary deterioration process for a coastal defence that will be used in a generic fragility curve analysis. An inhomogeneous Markov model is utilised to model non-stationary and grade-based deterioration process for a coastal defence that will be used in a time-dependent reliability analysis. Case studies are provided at the end of the chapter to demonstrate the applicability of the models.

Chapter 5: Reliability-based performance assessment for coastal defences

This chapter proposes reliability assessment models for the coastal defence structures with considering the impact of climate change and deterioration processes. Wave overtopping over the crest and piping underneath the dyke failure mechanisms are studied in a reliability analysis as two major failure mechanisms in coastal defences. Fragility curves are developed utilising the proposed homogeneous Markov deterioration model to analyse the reliability of the coastal defence. Time-dependent reliability analyses is considered utilising the proposed non-stationary deterioration model for coastal defences. Finally, fragility surfs are proposed for time-dependent reliability analyses associated with specific loads. Serviceability limit state (SLS) and Ultimate limit state (ULS) are also described in this section. SLS is defined in two distinct types: 1) the state that the performance of the structure is acceptable, and 2) the state where the structure is no longer serviceable. ULS is defined in two distinct states as: 1) the state that the structure is no longer serviceable, and 2) the state that the structure has collapsed. Overtopping limit state equation is an example of serviceability limit state and piping limit state equation is an example of ultimate limit state.

Chapter 6: Optimal maintenance strategy for coastal flood defences

This chapter investigates the repair strategy for the deteriorating earth sea dyke on the basis of the estimations of failure probability, inspection strategies, available repair actions, costs of imperfect information, and the costs for the repairs. The effects of errors in inspection strategies over the maintenance optimisation process are considered. In order to model the maintenance optimisation regarding the inspection errors, Partially Observable Markov Decision Process (POMDP) is utilised. A renewal maintenance model is also studied to evaluate the optimal repair and inspection intervals.

Chapter 7: Conclusions and suggestions for future research

This chapter presents the summary and main conclusions drawn from the present research work followed by some suggestions for prospective studies.

2. Literature review

2.1. Introduction

In this chapter, firstly an overview of the existing coastal defences and conventional analysis methods in this field are discussed. Then available studies about estimating hydraulic parameters and the effects of climate change on the parameters are studied. Available condition assessment frameworks for coastal defences in UK are presented, and an overview of the deterministic deterioration curves is provided. Stochastic deterioration models are studied, and the applicability of the models for different types of deterioration processes is reviewed. Then reliability analysis theory for coastal defences is investigated to understand the time-dependent deterioration process and performance evaluation methods. Finally, available maintenance models in this area are studied to find out the developments and the gaps regarding the maintenance policies in UK.

2.2. Current risk evaluation methods in UK

In UK, common flood risk assessment methods are based on the source-pathway-receptor-consequence (SPRC) framework as shown in Figure 2.1. The SPRC model has mainly four stages (Kortenhaus et al. 2002; McMillan et al. 2011): 1) sources of hydraulic loads (e.g. water levels or wave heights); 2) structures and their failure mechanisms; 3) receptors (e.g. the people, property and everything that are defenced against floods); and 4) consequence or damage that might occur if the flood defence does not function properly.

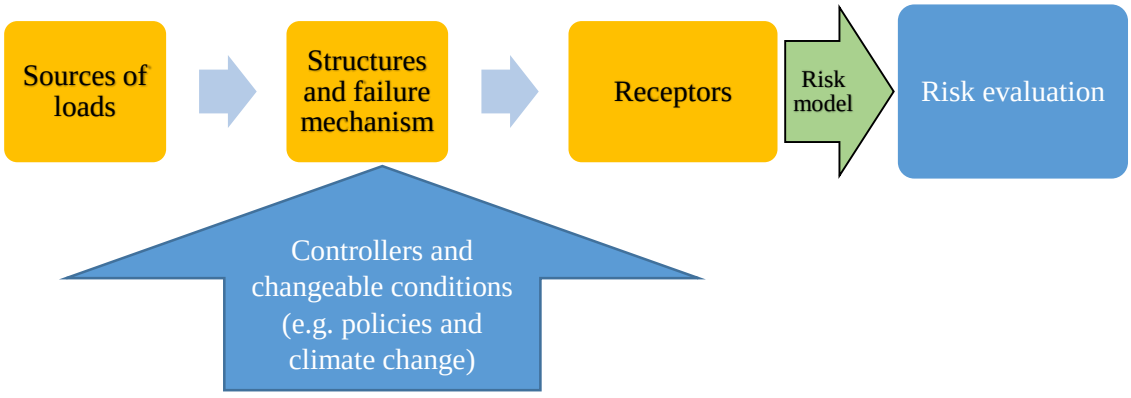

Figure 2.1 Source-pathway-receptor-consequence model to evaluate the risk for flood defences.

The method is well known as a risk-based method, and it is aimed to manage and maintain the flood defence structures in an acceptable performance level and minimum consequences for the receptors. The principles and standards of the conventional risk-based methods are described and guided by Environment Agency in many publications (see Bown et al. 2014; Flikweert et al. 2009). Also, Environment Agency provides "flood map for planning" to support the risk-based management (the map includes interactive tools and data in the local and national scales) (Environment Agency, 2017). Figure 2.2 shows an example of the mentioned map for Medway area. Flood zone definitions are set out in the National Planning Policy Guidance as:

- Flood zone 1 - land assessed as having a less than 1 in 1,000 annual probability of river or sea flooding (<0.1%).
- Flood zone 2 - land assessed as having between a 1 in 100 and 1 in 1,000 annual probability of river flooding (1% – 0.1%), or between a 1 in 200 and 1 in 1,000 annual probability of sea flooding (0.5% – 0.1%) in any year.
- Flood zone 3 - land assessed as having a 1 in 100 or greater annual probability of river flooding (>1%), or a 1 in 200 or greater annual probability of flooding from the sea (>0.5%) in any year.

Furthermore, in 2004, a tiered framework is developed in Performance Based Asset Management System (PAMS) (Long et al. 2013), to improve flood risk management methods, especially in local scale. The conventional reliability analysis methods (risk models) in flood defence scheme are composed of three main stages as (Gelre et al. 2008): 1) objective setting, 2) condition assessment, and 3) performance assessment. The objective setting means to set a goal or threshold for a structure or asset that is going to perform against a specific load, and usually, the objectives are set by decision makers regarding the priorities. The condition assessment stage is currently assessed through deterministic models, visual inspections or quantitative measurements (Long et al. 2013). Finally, the performance assessment stage is commonly based on probabilistic methods and generic fragility curves as high-level risk evaluation approach (Simm et al. 2008).

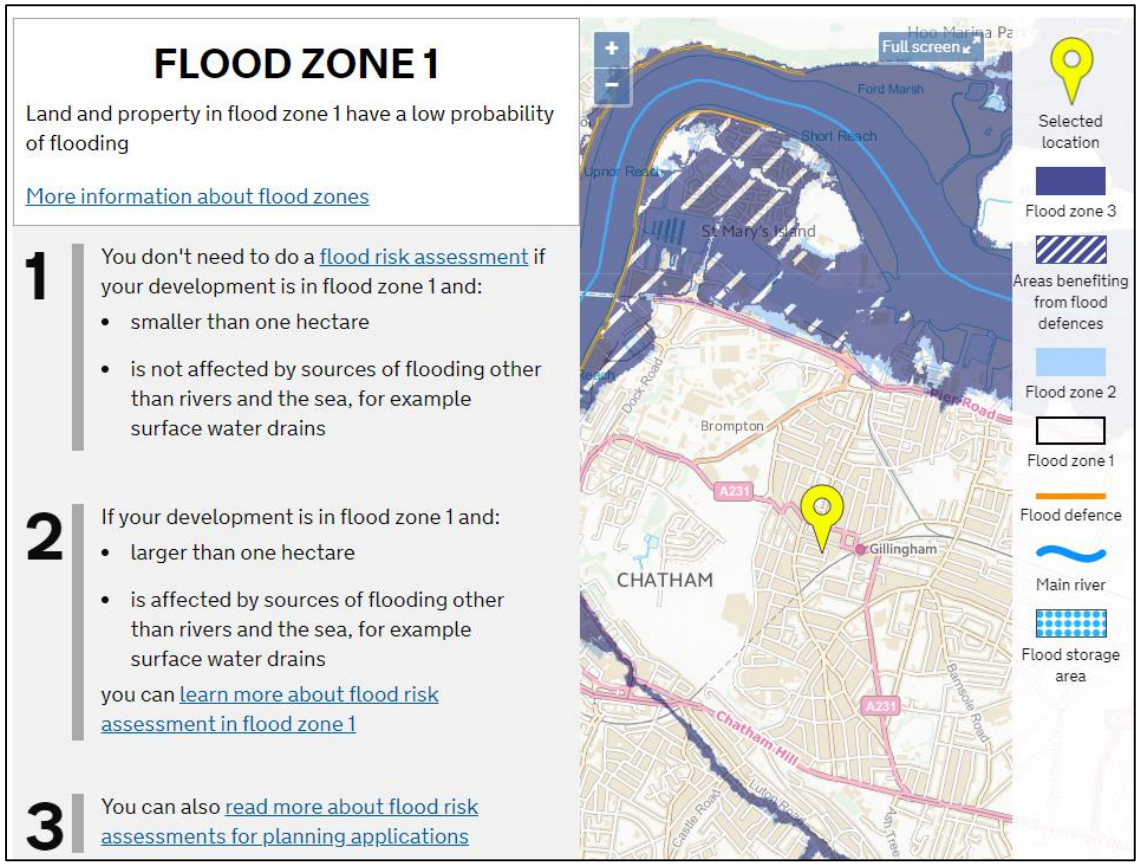

Figure 2.2 Flood-map-planning online application demostratres the recommendations for flood risk in Chatham area.

Joint probability methods for the source of loads in UK

Significant research into joint probability methods has been carried out by the Environment Agency and researchers since the 1990s. Several variables (e.g. wave height, wave period, wave direction, water level, beach elevation and traffic loads) influence some of the primary failure mechanisms in flood defences. Joint probability estimations for various variables and the application of these methods in coastal defences have been studied (e.g. Hawkes 2008; Reeve 2007; Jonathan et al. 2013). Conventional joint probability methods in flood defence structures for combination and interpretation of the source data can be divided into four approaches:

- Event definition approach.
- Desk study approach.
- JOIN-SEA approach.
- Dependence Measure and Monte Carlo simulations approach.

An event definition is a more sophisticated version of the single-variable extreme analysis. In this method, the traditional statistical analysis is carried on one specific variable to find out the extreme variables. Then a subsequence analysis is also carried out to assess another extreme aspect of the first variable. For example, a statistical analysis of peak river flow is conducted, and then a subsequent river modelling will be undertaken to assess flow duration. This method can produce some distributions from two different types of data (which could be unmatched). This method is used in several applications (e.g. Taylor et al. 2014). This method is simple and useful for an initial evaluation of extreme events for small areas, however, not capable to consider the effects of time-dependent and changeable parameters.

Desk study approach to joint probability analysis is a method for creating a table of joint exceedance extremes. The dependency estimation between the critical variables in this method is deterministic, and it is from UK dependency maps provided by Environment Agency (Hawkes and Svensson 2006). Desk study method is widely used in UK, as the technical instructions and necessary tools are available publicly. However, it is not suggested for important structures due to lack of flexibility to adjust site-specific information and time-dependent variables in the model (Gelder et al. 2004).

JOIN-SEA approach to joint probability analysis is a method based on freely available software provided by Environment Agency. The software is designed and developed for joint probability extreme analysis on a FORTRAN programme. The programme fits distributions, estimates dependency between the key variables and extract extreme values from the simulated data. JOIN-SEA algorithms are based on formulas from Owen et al. (1998). Although the software covers joint probability analysis comprehensively, some level of computer knowledge and considerable time-consuming practices are needed for individual operators (HR Wallingford 2000). Also, since the presenting of the project, some equations such as overtopping rate formulae has been adjusted, so the software is out of date and will not be discussed in this thesis.

The last approach (Dependence Measure and Monte Carlo simulations approach) is still considered as a research topic. This approach is still a research topic because the correlations of major variables in a flood risk model and the effect of changing

environments on the variables in the future is not clear yet (e.g. Lorenzoni et al. 2016) . The main steps in this method are similar to the previous approaches such as extreme value analysis of the key variables and preparation of the initial data. Following the mentioned steps, marginal distribution analysis, fitting of the dependence, joint extreme analysis and result presentation should be investigated and will be discussed later. In a joint probability analysis for a coastal defence, often, sea level and wave heights are considered as major variables. However, other combinations of variables are also common, e.g. (rainfall + tidal surge) and (wave height + tidal surge) (Hawkes et al. 2005).

2.3. Hydraulic conditions for coastal flood defences

2.3.1. Hydraulic loads and parameters

Sea level

Sea water level is a crucial parameter to estimate loads on coastal defence structures and estimating crest level of a coastal defence structure. Accurate estimation and prediction of extreme values of sea level are essential for a reliable performance of coastal defence structures during their operation. Sea level term may describe values of (CIRIA 2007):

- Mean sea level.
- Tide level.
- Storm surge level.

Mean sea level is a site-specific parameter and should be obtained from a consistent recorded period/data of local gauges. Climate change and its effects such as sea level rise considerably increase the amount of uncertainty for evaluating mean still water in the future (Nicholls and Cazenave, 2010). Tidal levels are consequences of astronomical effects and then entirely predictable with an acceptable degree of accuracy. Tidal levels change due to the astronomical forces, and they are expressing as relative values to a zero of the chart datum (Purvis et al. 2008). Hence, there is a low-high or neap-spring cycle of tide levels, which should be considered in the prediction of extreme water levels. Storm surge is an abnormal rise of water generated by a storm, over and above the predicted astronomical tide. It's the change in the water level that is due to the presence of the storm (Met office 2017). Figure 2.3 shows the schematic of the described datum and their differences.

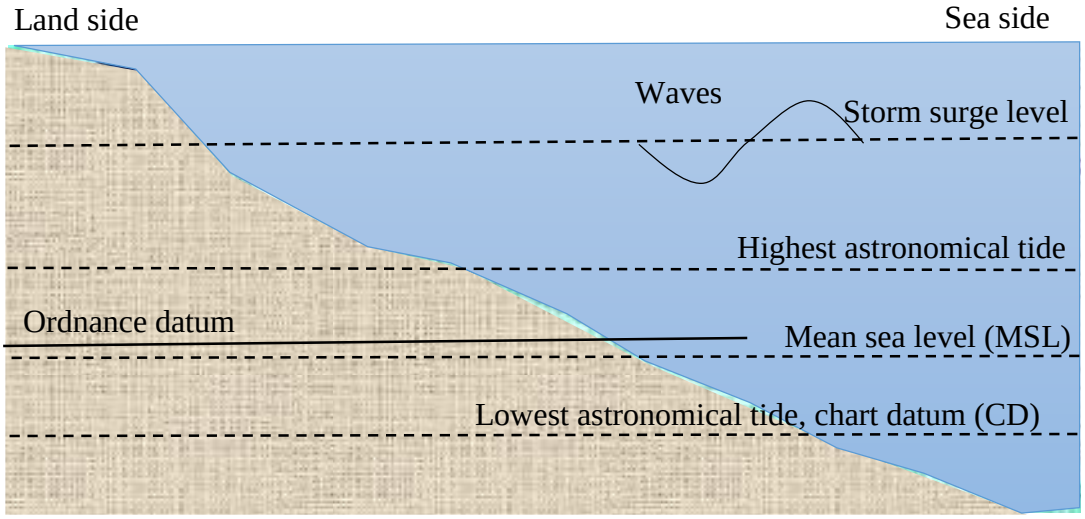

Figure 2.3 The defined datum in UK and their approximate relevant position to each other.

Wave conditions

Wave height is another major parameter for estimation of hydraulic loads in some failure mechanisms. Wave data/observations including height and period are obtained or generated through many techniques such as buoys, laser measurements, satellite images, and numerical wave models. The reliability of buoy measurements is more than other methods, but the spatial coverage is limited. Satellite data are the most available and may be an alternative for estimation of wave heights. However, the level of uncertainty in this technique is high (Khon et al. 2014; Vincest 1982).

The behaviour of wave heights changes when they transit from deep waters to surf zone due to depth-limited effects. In general, parameters such as wave steepness, the slope of bathymetry and offshore wave heights have significant influences on the evaluation of depth-limited wave heights. Goda (2010) and Owen (1980) suggested two empirical models estimating depth-limited wave heights by considering shoaling and wave breaking factors. Goda's method uses an upper limit of significant wave heights while Owen's method provides an initial estimate of depth limited significant wave height in any water depth.

Significant wave height at the toe of a structure is a critical variable in hydraulic loads, and it is defined as the average of the highest third of the waves $H_{1/3}$. Zero moment wave

heights H_{m0} and the highest third of the waves $H_{1/3}$ are often called significant wave heights because they have similar values in deep water zone (Goda 2010). However, the effects of wave breaking and depth-limited in surf-zone could change the behaviour of significant wave heights considerably as shown in Figure 2.4. Hence, significant wave heights in deep and shallow waters are different due to wave breaking process (Pullen et al. 2007; Van-der-Meer et al. 2016). Wave period is another critical parameter in hydraulic load evaluation. Literature before 2012 supposed that wave period remains consistent subject to sea level rise because in the process of wave breaking the wave periods remain unchanged (Pullen et al. 2007). However, new pieces of evidence show that wave periods increases over time due to climate change (Van-der-Meer et al. 2016).

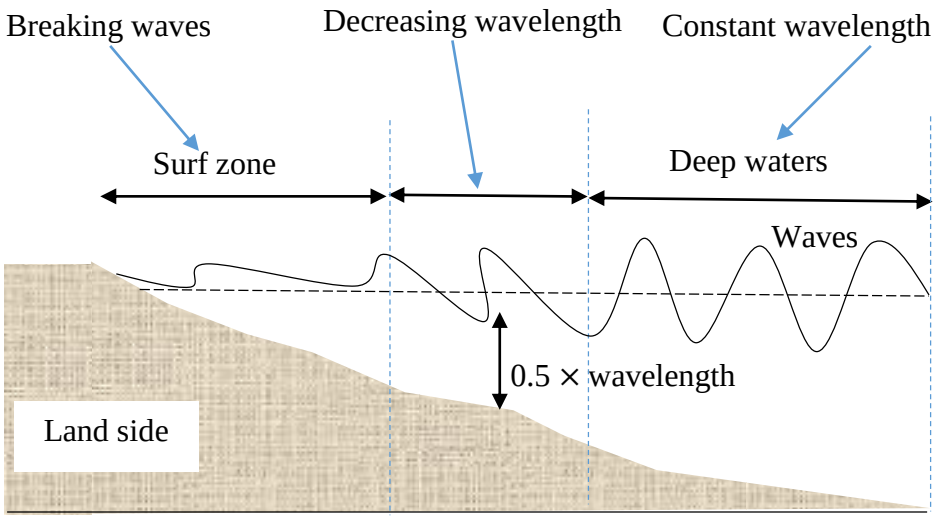

Figure 2.4 The schematic of wave changes when entering surf zone.

Causes of coastal floods

The leading causes of coastal floods for a typical flood defence shown in Figure 2.5 include (Gouldby et al. 2014; Batstone et al. 2013):

- Combination of high tides, storm surges and waves.
- Rising sea levels (Eustatic) and land movement (Isostatic).
- Tsunamis.
- Reclaimed lands.

Sea level rise due to climate change or land movements is considered as one of the sea flood causes. However, the effect of climate change is still vague, as the climate change

may increase the likelihood and severity of storm surges and winds (Dahl et al. 2017). Tsunamis are giant waves resulting from earthquakes, volcanic eruptions, meteor impacts, and any significant displacement of water in the ocean. The tsunami waves surf very quickly and not easy to be detected immediately (Atwater et al. 2016). Fortunately, it is very uncommon for the British Isles to be affected by tsunami waves. During the last century, only two weak tsunamis are recorded within UK, i.e. Meteo-tsunami (1929) and South-east tsunami (2011). The first one killed two people and had 3.5 metres peak wave heights struck the south coast including beaches at Worthing, Brighton, Hastings and Folkestone. The second one was a small tsunami with a peak wave height of 0.40 m occurred along the south coast of England (British Geological Survey 2017).

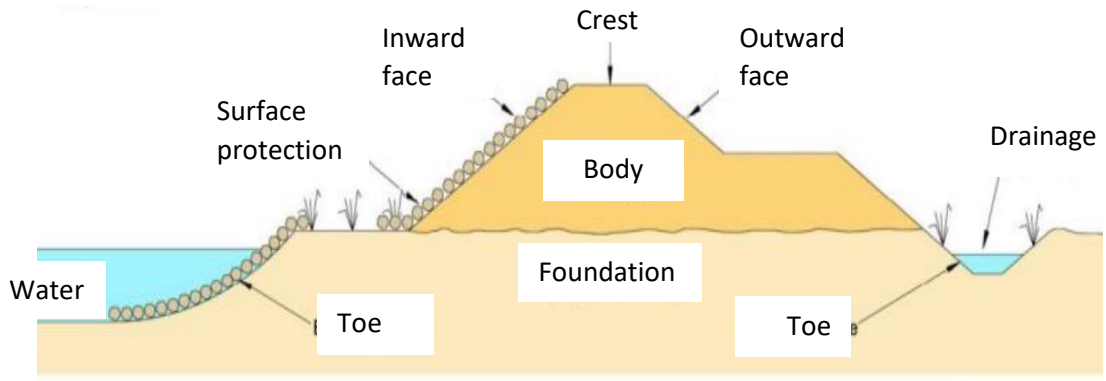

Figure 2.5 Cross section of a coastal defence embankment with its geometrical surfaces (adopted from Hall et al. 2007).

Land reclamation, also known as reclamation, is the process of creating new land from the sea and other water sources. The land reclaimed is known as reclamation ground or landfill, and it is because of coastal management or intends to attach and spread more lands to the beach (Lorenzoni et al. 2016). In UK, land reclamation has been implemented since the 1600s, for example in Dogger Bank in the North Sea, Chatham maritime in Kent, and St Mary Island in Chatham. These areas are low lying, flat and willing to significant settlements, so a small rise in sea level from a mild storm surge is enough to flood it and cause extensive damage.

Regarding the mentioned causes of the coastal floods, it is also important to consider the contribution of each one in floods. Unfortunately, there is not much research undertaken to analyse the role for each cause of the flood. Schaller et al. (2016) and Wadey et al.

(2016) are two interesting studies that investigated the leading causes of several floods in England during winter 2013/14. Also, in the briefing report on the 2014 winter storms, UK Met Office (Met office 2017) provides a comprehensive description of the tide, wave and storm surge contributions to UK floods in the main body of the report.

In the mentioned literature, Newlyn in Cornwall was the datum of the tidal contribution in South-west England. Results show an exceptionally high tide of 5.4 m in the evening and low tide of 0.7 m at Newlyn on 5th January 2014. It is known that 1 mbar pressure change can result in a change on the water level of 1 cm (Met office 2017). The mean barometric pressure along the South coast of England is about 1016 mbar. However, the atmospheric pressure on the mentioned day was about 950 mbar, which means about 66 cm increase in water level only due to pressure change (Met office 2017).

According to the Met Office report, the observed significant wave heights were 16.0 m at the south-west of UK, in January 2013, consistent with other estimates of wave heights exceeding 15.0 m. The Newlyn tide gauge has shown a total sea level rise of 18.0 cm and -11.0 cm land movement in the period 1910 to 2010 (Met office 2017). Hence, coastal flooding of south-west England, in winter 2013/14 caused by a storm surge with exceptionally high tides. The direct contribution from rising sea levels might consider negligible. However, the indirect contribution of climate change such as stronger winds and longer storm surges is still unclear. Figure 2.6 shows the approximate contribution of different causes to the 2014 winter floods.

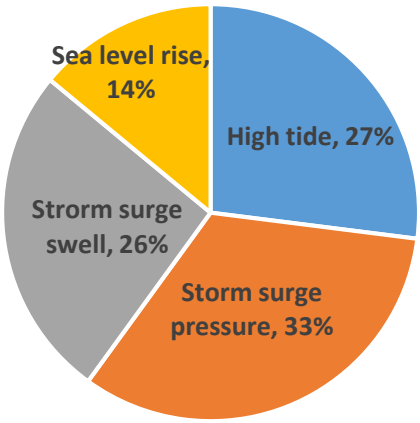

Figure 2.6 Approximate contributions to coastal flooding, SW England, early January 2014.

2.3.2. Climate change impacts on hydraulic loads

Climate change refers to change in the statistical distribution of weather patterns over an extended period of times. It caused by many natural or human activities. Human activities have a significant contribution to climate change which is often referred to global warming according to International Projection of Climate Change IPCC (Hansen 2013). Small increases in global mean temperature and just a few degrees of polar warming relative to the pre-industrial period lead a substantial increase in global mean sea level rise, which affects the performance of coastal defence structures in particular.

Coastal flood defences can be affected by changing environments such as sea level rise and storms, which may lead to failures against unexpected loads. Hydraulic variables such as sea level, wave heights and wave periods are often considered as critical parameters in a coastal defence structure, which are affecting from sea level rise (Mehrabani and Chen 2015; Sterr 2007). Overtopping related failures, as most common failure mechanisms are sensitive to wave parameters and sea level. Hence, both discharge rate and frequency of overtopping events are expected to increase.

Hinkel et al. (2014) assessed coastal flood damage and adaptation costs regarding the projected climate change scenarios with consideration of a wide range of parameters, including vertical land movement, population size, maintenance strategies, socio-economic developments and sea level rise. The results show that without adaptation plans by assuming poor or late time investments, 0.2% to 4.6% of global population is expected to be flooded annually before 2100 due to 25 to 123 cm sea level rise, respectively. The expected economic losses due to sea level rise are predicted to be 0.3% to 9.3% of the global production. The estimated value of damage is too significant for some countries and may lead to fall of societies and governments.

Hallgate et al. (2013) demonstrated that the magnitude of losses and damage due to the future coastal floods on coastal structures would increase more than 50% by 2050 as the strength and frequency of the floods will increase due to sea level rise. Bosello et al. (2013) presented that without adaptation to the projected sea level rise, 12% of lands in European continent will be sunk by the end of the century, while the loss could be reduced more than 85% by adopting the protection in coastal defence structures. The

projected future changes in environments have a unique impact on coastal defence systems as well as 6 % of the European population who live in flood area during the next 100 years (Hallgate et al. 2013).

Changes in sea level and significant wave heights due to global warming have considerable influence on the performance of earth sea dykes. The deterioration process will be boosted dramatically due to sea level rise (Rangel-Buitragoa et al. 2015; Esteban et al. 2014). The structural reliability of the coastal defence structures in the next decades will reduce significantly if the resistance of the structures is not improved (Chen 2015; Buijs et al. 2009; Mehrabani and Chen 2016; Firth et al. 2013). It has been demonstrated that the probability of failure of coastal defence structures due to overtopping and piping failure mechanisms will increase, and without structural adaptations e.g. increase in crest level height, it is expected that the lifespan of the structures decreases significantly (Chen 2015; Mehrabani and Chen 2015).

2.3.3. Projected sea level rise

The projected sea level rise is different in different regions. Also, the vertical movement of lands should be considered to project long-term sea water level rise. The projection of rising above mean sea level in UK waters is provided in the United Kingdom Climate Projection UKCP09 (Jenkins et al. 2011). A summary for estimated changes in sea water level is presented in this section. Mean sea level has projected to increase between +22 to +82 cm with a 95^{th} percentile confidence level for various emission scenarios by 2095 (Jenkins et al. 2011). In order to estimate efficient extreme sea water level in the future to consider the sea level rise effects, UKCP09 suggests to utilise skew surge method to find out storm surge level (Jenkins et al. 2011). The details of the projected sea level rise and mathematical model to consider the influences of the sea level rise will be discussed in next chapter.

2.3.4. Projected wave conditions

Significant wave heights are also estimated to have a change between -1.50 m to +1.00 m, as shown in Figure 2.7. Meanwhile, Anglia Coastal Monitoring programme published site-specific reports for different stations around UK to provide a more accurate

estimation of local wave conditions (Eade 2015). The wave steepness S_{op} is expected to have a linear increase due to sea level rise over time and given as (Pullen et al. 2007)

$$S_{op} = \frac{H_{so}}{L_{op}} \tag{2.1}$$

where H_{so} is wave height; and L_{op} is wave length. There are large uncertainties associated with projected changes in wave heights due to sea level rise, especially with the extreme values. Projections of more extreme, i.e. longer return periods, wave heights reflect the same pattern as the mean changes but with increased uncertainty (Jenkins et al. 2011).

Townend and Burgess (2004) proposed a model to estimate change of wave heights due to change in sea level, which is derived from Weggel's (1972) formula, and based on laboratory experiments. Townend and Burgess (2004) used Weggel (1972) formula for calculation of relative change of wave heights due to sea level rise. The accuracy of the proposed model is tested by Oh et al. (2009) and Lee et al. (2013), and has compared with other verified models such as Goda (2010). The model by Townend and Burgess calculates roughly larger wave heights than the classic models especially on a surf-zone.

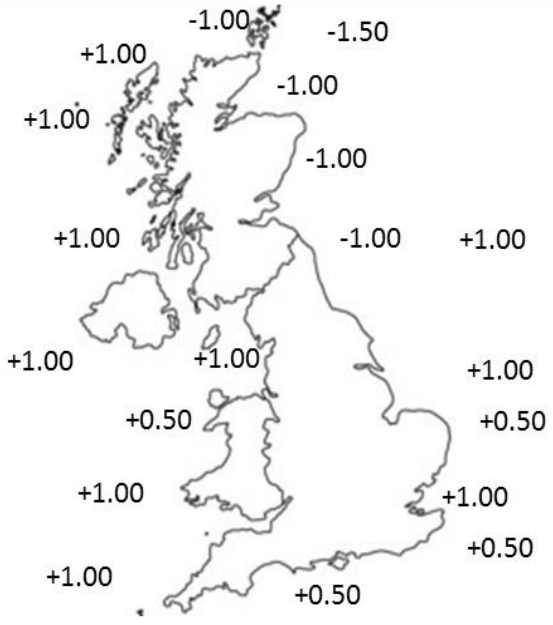

Figure 2.7. Projected UK mean significant wave height (m) relative changes at various locations from 1990–1999 to 2090–2099 (adopted from Jenkins et al. 2011).

2.4. Coastal flood defence condition assessment

2.4.1. Condition grading system

Coastal flood defence structures are designed to serve reliably for decades. By considering changing environments and climate change effects such as sea level rise, it is a significant challenge for authorities to keep existing structures at an acceptable level of structural performance. Therefore, routine condition assessments are essential for observing the assets performance level and for a sufficient management policy (Mehrabani and Chen 2016; Chen and Alani 2013). Condition Assessment Manual (CAM) is a condition grade assessment criterion in the context of grade-based asset management (Environment Agency 2006). Condition grades are defined to offer a standardised approach to assess the deterioration of flood defence structures and to assist decision makers to manage the maintenance strategies. In an inspection process based on CAM, each component is visually inspected by a trained inspector, and it is ranked into one of five condition grades from 1 to 5 (1 for very good and 5 for very poor), as described in Table 2.1.

Table 2.1 Condition grades and descriptions adopted by Environment Agency (EA 2006).

Grade	Rating	Description
1	Very Good	Cosmetic defects that will have no effect on performance.
2	Good	Minor defects that will not reduce the overall performance of the asset.
3	Fair	Defects that could reduce the performance of the asset.
4	Poor	Defects that would significantly reduce the performance of the asset.
5	Very poor	Severe defects are resulting in complete performance failure.

Environment Agency keeps records of individual flood defence asset's inspection results to have a better understanding of their structural performance. The database is also essential for flood risk management regarding the present condition and the deterioration rate. Generic deterioration curves are determined based on CAM system to quantify the residual life of an asset with and without maintenance plans (Simm et al. 2008). Although the provided deterministic deterioration curves are used to determine the residual life of

flood defence structures, the level of uncertainty is still significant due to nature of deterioration process.

In order to assess the condition grade of the structures by inspectors, each organisation or firm has its own approach to assessing asset condition. However, all approaches need to follow Environment Agency practice built on the following documents:

- Condition Assessment Manual (CAM).
- Internal Operational Instructions used by the Environment Agency to standardise the approach to inspections and the frequency of these relating to the risks.
- Asset inspectors' training and accreditation through the T98 programme.

In addition, the principle of weighting for different elements in an asset is described in section 2.3.3 of asset inspection guidance APT 2 report (Environment Agency 2014). An example of the Environment Agency method is shown in Table 2.2. As shown in the figure, the overall grade of the asset is the sum of (weightings × condition grades) divided by the sum of the weightings. However, if any individual element with a weighting of 9 (a critical element) falls below the target condition and the above calculation shows the asset is numerically meeting its target condition, this should be overridden to give an overall condition grade below the target. Full description of the inspection guidance, data quality, reports and inspection approaches for different parts of an asset is provided in the appendix section. Figure 2.8 provides examples of flood defences in different condition grades.

Table 2.2 Example calculation of condition grade from grade and weighting for a flood defence adopted from Environment Agency (2014).

Element	Weighting (W)	Condition grade (CG)	W*CG
Channel side	3	3	9
Berm	5	2	10
Exposed face	8 (9)	4	32 (36)
Crest	8	1	8
Landward face	8	2	16
Sum (W)	32 (33)		
Sum (W*CG)			75 (79)
Overall CG		75/33=2.34= CG2 79/33=2.39= Override to CG3	

Figure 2.8. Sea defences examples with different condition grades, the second asset is in condition grade 2 due to animal burrow and erosions. The arrows show the defects areas.

2.4.2. Quantitative damage assessment

Quantitative Assessment Manual for the monitoring and inspection of flood defences provides a framework to monitor the structures through the collection of quantitative data (Long et al. 2013). In the same year of publishing CAM manual, an improved approach to condition assessment was published to undertake a quantitative condition assessment based on expert judgment, damage level, and performance deterioration. The report suggests ranking assets according to their performance level, surface conditions and risk posed. In fact, the report was one of the first steps to rank an asset by considering the intensity (slight, minor and major) and magnitude of the damage.

According to the manual, slight damage is defined as condition grade 1, minor damage for condition grades 2-3, and major damage for condition grades 4-5. The condition grade of dykes is considered as an indicator of the robustness of the dykes and their likely performance when subjected to extreme loads (Long et al. 2013). This manual improves the efficiency of condition assessment manual by integrating quantitative measurement into visual inspection and provides a more accurate assessment of condition grades. The framework provides instruction for different types of flood defence structures (e.g. vertical walls and sheet piles) and various inspection techniques (not only visual inspection).

2.5. Deterioration processes and modelling

The existing deterioration models are classified into two main categories based on their evaluation process:

- Deterministic models
- Stochastic models

Linear and nonlinear models are two well-known types of deterministic models. In deterministic models, the output of the model is fully determined by the parameter values and the initial conditions. In a deterministic model, the relationship between input and output is described by a mathematical function, and it is suitable for a stable environment. However, this model is not appropriate for a complex system where the correlation between the critical parameters needs to be assessed, and the phenomenon of the structure is changeable (Edirisinghe et al. 2013). Stochastic calculation methods can be

categorised into three levels since each level satisfies the specific amount of accuracy. Level 3 methods approximate the integral of limit state equation (Voortman and Vrijling, 2000). Monte Carlo and directional sampling methods are examples of level 3 probabilistic methods where a large number of simulations are generated for the defined parameters of the limit state function (Wadey et al. 2014). Gamma process and Markov Chain are two examples of stochastic models.

2.5.1. Deterministic vs stochastic deterioration models

In a deterministic model, all variables are individually determined by parameters in the model and by sets of the previous history of the variables. Hence, a deterministic model always has the same outcome for given input variables. In contrary, in a stochastic model variables are defined with respect to uncertainty parameters, and are not described by unique values, but rather by probability distributions. In flood defences, deterministic models cannot describe the nature of problems due to the inherent stochastic behaviour of the input variables. In a deterministic model, hydraulic events, loading and conditions of the asset are defined in the model based on exact and constant values. By defining some or all the input parameters in a stochastic form, the simulation becomes stochastic. Hence, in a stochastic approach, every time the simulation is run, it will have a slightly different outcome, although the input variables are the same.

In deterministic models, the relationship between loading and probability of failure is established by a safety factor, to describe the strength of the asset. Deterministic models in flood defence structures are adopted from European standards, where the standards are absolute values of the strength or resistance divided by a factor. Hence, the probability of failure is zero until the design load event is reached at the point where the failure probability is equal to 1.

In a stochastic analysis, many uncertainties in the estimation of the input variables are considered to evaluate failure probabilities (generally with lower and upper bound). For example, in a stochastic model, one can say the possibility of occurring each sea level rise scenario is equal in a period of 100 years. However, the probability of rising sea level in a period of five years is in a specific range according to today's information, and cannot suddenly rise or drop over or below a specific value.

2.5.2. Stochastic deterioration models

Gamma process

Gamma process is an appropriate model for stochastic deterioration modelling to failure assessment (lifetime), and the average rate of deterioration per unit time is defined as random variables with a gamma distribution. Since deterioration is uncertain and non-decreasing i.e. if the structure is subjected to do-nothing maintenance strategy, it can be regarded as a gamma process (Abdel-Hameed 1975), which gives an appropriate model for random deterioration over time. Initially, Abdel-Hameed (1975) was the first to propose the gamma process as an appropriate model for deterioration process over time and called this model as "gamma wear process".

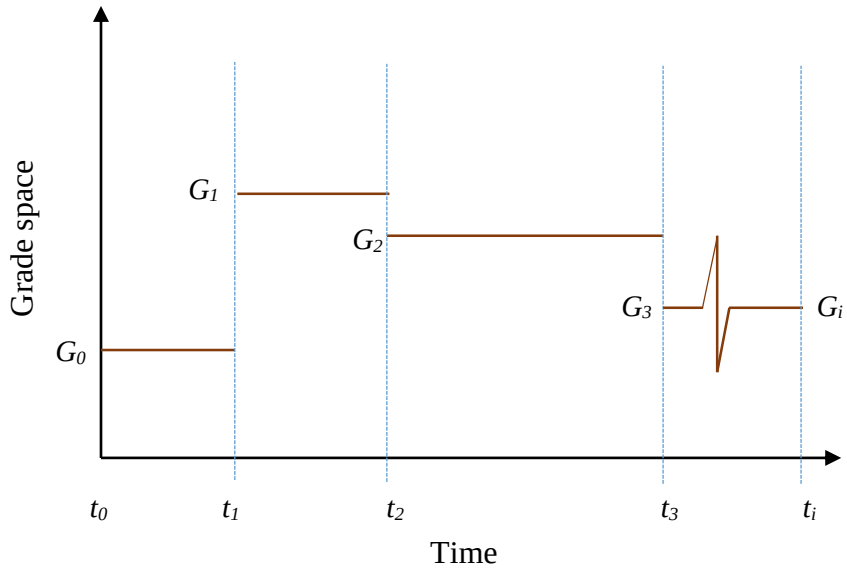

Figure 2.9 Grade (G) transition and transition time (t) of a typical Markov process.

The Gamma process has independent and non-negative increments defined by a gamma distribution with identical scale parameter and a time-dependent shape parameter. Details about the mathematical aspects of gamma processes and its application in deterioration modelling can be found in literature (Pinsky and Karlin 2011; Noortwijk, 2009; Chen 2006), and will be discussed in detail in Chapter 4. Noortwijk (2012) investigated the applicability of gamma process to predict infrastructure degradation in the future and demonstrated that it is a suitable model to estimate evolving deteriorations such as settlement on crest level. A stochastic gamma process can be incorporated the temporal uncertainty associated with the evolution of deterioration (Chen and Alani, 2012; Noortwijk, 2009). The gamma process is, therefore, suitable to model gradual damage

that are monotonically accumulating over time in coastal flood defences. An advantage of modelling deterioration processes through gamma processes is that the required mathematical calculations are relatively straightforward.

Markov chain

Markov chain is a stochastic process to estimate the future event as random outcomes based on the present condition of the system (Bocchini et al. 2012; Duchesne et al. 2013). It is a homogeneous process if the transition probabilities are independent of time. For example, for the same length of 2 years as a time step, the deterioration follows the same pattern no matter when it starts. A non-homogeneous Markov chain model has a transition probability matrix that is not a constant but a function of time. For example, hydraulic loads subject to a scenario of climate change may change the deterioration rate of coastal defence due to more frequency of extreme events. Markov chain is a common tool to predict the deterioration of structures and helps to deal with deterioration uncertainties (Norris 1997). A Markov chain is considered as a series of transitions between certain condition grades. Figure 2.9 shows a schematic diagram of a Markov process with its transition points.

The transition probability matrices are estimated using available data (e.g. inspection results for a period) and can be calibrated by minimising the difference between the observed and the predicted condition grades of the asset, typically:

1. By minimising the sum of the squared differences between each of the data points and the average condition calculated from the distributions of the condition.
2. A regression analysis is performed first using the collected data. Then, the squared differences between the regression line and the observed data are minimised.
3. The initial data are presented in the form of distributions and the squared differences between the observed distributions and the predicted distributions should be minimised.

Also, for homogeneous of Markov chain models, a zoning concept needs to be applied if the lifespan of the structure is long. The zone times help to overcome the limitation of the model about changing deterioration rate over time. For example, in most realistic

infrastructures the deterioration rate is higher when the structure is closer to the end of its lifespan than the time where the structure is newly constructed. A zone is a specified period that assumed to produce constant transition probabilities, and the period for a zone is based on expert judgment and inspection intervals.

Markov chain vs Gamma process

Although both Markov chain and Gamma process are widely used in deterioration modelling, they have their specific features. Gamma process can only to be used for non-decreasing processes, while Markov chain can be transited to a new condition grade, e.g. improved or deteriorated. Markov chain models are often used in a discrete-time and single step degradation model, while Gamma process is suitable for continuous deterioration process. Both Gamma and Markov processes can be utilised in grade-based case studies. For example, Bocchini et al. (2012) applied Markov chain to a condition-based deterioration model for future assessment of a component condition, while Edirisinghe et al. (2013) applied Gamma process in a condition-based deterioration model for bridge elements. It should be noted that Gamma process is not independent of the history of the structure's condition, while Markov chain model is only based on the present condition of the system.

2.5.3. Lifetime reliability models

Continues and non-decreasing statistical distributions can describe time to failures (TTF) of a system, in order to simulate the behaviour of a structure in a lifetime reliability model with consideration of parameter uncertainties. Then, the lifetime reliability model can be utilised to plan (or optimise) inspection, repair and maintenance strategies.

Lifetime reliability using gamma process

In the gamma process model, the cumulative deterioration at time t follows a gamma distribution with the shape function $\lambda(t) > 0$, and a constant scale parameter β. To represent the increase of deterioration rate over time, the shape function may be an increasing function of time. The damage increment from any time step is an independent random variable, and it is a consequence of Gamma process parameters, hence, the cumulative deterioration is also gamma distribution. The cumulative distribution function of the lifetime can be derived as (Le Son et al. 2013)

$$F_T(t) = \Pr[X(t) \geq \rho] = 1 - GA(\rho_m|\lambda(t), \beta) \quad (2.2)$$

where $X(t)$ is the random variable at time t; and ρ_m is the design margin or a deterioration threshold.

Lifetime reliability using Markov process

In Markov process, the system provides information for the future state (including deterioration level), where the future state is independent of the past state given that the present state is known. The statistical parameters such as mean and variance of the deterioration level depend on whether the process is stationary or non-stationary. In the case of a stationary process, the parameters will not change, while in a non-stationary process, the parameters are time-dependent. Since the initial condition state S_{t_0} is known, the expected condition of the next state $E(X)$ regarding the loading parameters ℓ and time-step t is given as (Bocchini et al. 2012)

$$E(X) = S_{t_0} \cdot P^n(\ell) \quad (2.3)$$

where P is the transition probability matrix regarding the load ℓ.

2.5.4. Sources of deteriorations in coastal defences

Deterioration is defined as the act or process of becoming worse. In a structural concept, it involves a decline in the state of structural resistance and material. Processes of deteriorations in coastal defence structures are categorised into three groups as:

- External erosion; External erosion is the wearing of a surface (bank, embankment or another surface) by floods, waves, wind or any other natural process (Rangel-Buitragoa et al. 2015).
- Internal erosion; Internal erosion occurs when soil particles within a levee or its foundation are carried downstream by seepage flow (Bonelli et al. 2013).
- Instability; Instability occurs when the strengths of soil particle movement exceed the resistant strengths. Excessive loading on a levee, or weak physical properties of the levee materials or the foundation soils generates sliding along a shear surface within the levee embankment and/or foundation soils that damage the levee (Sayers et al. 2015).

External erosions occur when the shear stress in the outer surfaces of a structure (levee), which is induced by hydrodynamic forces. Currents, waves and tides, when transforming to an overtopping or overflowing, may act as the principal inducer of the surface erosion (Rangel-Buitragoa et al. 2015). Internal erosions occur when soil particles inside the structure induced by hydrodynamic forces (most often in porous layers). The primary cause for the development of internal erosions is seepage. Bonelli et al. (2013) categorised the mechanism of internal erosion into two groups as; 1) piping or backward erosion when the seepage gradient exceeds the flotation gradient of the soil with concentrated erosion; 2) contact erosion where the fine soil is washed into the coarse soil by the horizontal flow.

An important type of instability is due to the geotechnical configuration of the structure such as consolidation and settlement (Baars and Kempen 2009). Coastal defence foundations are built on layers of soft clay and expected to undergo relatively time-dependent settlement and consolidation under the imposed load, especially for embankment higher than two meters. The time-dependent nature of consolidation and settlement processes may increase the level of uncertainty in reliability assessment and maintenance plans. Another problem caused by the settlement is distortion-induced cracking of the potentially brittle fill material. The cracks will make the embankment more permeable as well as be more prone to damage and possibly breach because of overtopping/overflowing (Sayers et al. 2002).

A case study in Germany provided by Baars and Kempen (2009) showed the contribution specific deterioration processes to different failure mechanisms in coastal defence structures. Studies of 100 levee breaches demonstrated that almost 70% of the failures are related to external erosions due to wave overtopping. 17% of the breaches are related to stability failures due to instability erosions such as settlement and slope breach, 12% related to internal erosions due to piping, and 1% for other deterioration processes (Baars and Kempen 2009).

2.6. Structural reliability analyses

The risk posed by the combined effect of two or more extreme variables and the effect of sea level rise on the hydraulic variables have significant impacts on the performance

of coastal defences. Many failure modes in coastal defence structures such as overtopping may occur in extreme events, which shows the necessity of joint extreme analysis in failure probability estimation for the structures (CIRIA 2007). The failure mechanisms in coastal defences are mainly relevant to two major types of limit states (CIRIA 2007):

- Ultimate Limit State (ULS) - corresponding to the maximum load carrying resistance such as piping and uplifting.
- Serviceability Limit State (SLS) - corresponding to the criteria applicable to normal use or durability such as overtopping.

Therefore, time-dependent analysis of serviceability failure mechanisms such as wave overtopping and ultimate failure mechanisms such as piping appears to be necessary to improve reliability and integrity of coastal defence structures (Chen 2015). Sea level rise and deterioration processes are considered as significant threats to coastal flood defences due to their uncertainties. Hence, probabilistic methods for risk evaluation will be more appropriate to evaluate the risk of changing environments.

2.6.1. Failure modes of coastal flood defences

A failure is a state to express the inability to achieve a defined performance threshold or performance indicator for a given function (Hall et al. 2008), which is categorised into hydraulic and structural failures in coastal defence context (Gouldby et al. 2014):

- Hydraulic failures; they happen if water ingress into the leveed area by overflow or overtopping of the structure without prior damage to the coastal defence structure.
- Structural failures; they happen by a breach in the coastal defence system due to damage.

Hydraulic failures are classified into three main groups (Reeve 2009):

- Wave-hydraulic failures: failure and breach is a result of overtopping and wave forces.
- Geo-hydraulic failures: failure and breach are because of seepage flow through dyke core or foundation, which lead to piping or macro-instability.

- Global static failures: failure and breach are because of water, wind or ice pressure.

A structural failure scenario may lead to a breach, and it includes a failure mode involving both physical and functional phenomena. Deterioration and damage are part of the physical domain that might lead to failure in the functionality of a coastal defence (Allsop et al. 2007). A failure mechanism is a time-dependent process resulting in deterioration, damage and finally failure. A failure mechanism is expressed by a limit state function, a function in which describes the process of failure mathematically.

The response of a coastal flood defence to hydraulic loads depends on the geometry, material and operational conditions. The analysis of 117 historical dyke breaches in Hungary (Nagy and Toth, 2005) and 84 dyke breaches in Saxony (Horlacher, 2005) are two examples to show the weight of various failure mechanisms in coastal flood defence. Structural failures of earth sea dykes due to overtopping, piping and other failure mechanisms in the first study are reported as 69%, 20%, and 11%, respectively. In the second study, failure rates of coastal defences due to overtopping, piping and other failure mechanisms were 71%, 10%, and 19%, respectively. Therefore, overtopping and piping failure mechanisms have been considered as major threats to the structural performance of sea dykes, and this thesis focuses on these two failure mechanisms.

Table 2.3 Consequence of mean overtopping discharge on flood defence structures (Van der Meer et al., 2016).

Mean overtopping discharge $(l/s/m)$	Consequence of overtopping discharge
$q < 0.1$	Insignificant
$q = 1.0$	Crest and inner slopes may start to erode
$q = 10.0$	Significant for dykes and embankments
$q = 100.0$	Crest and inner slopes have to be highly protected

Excessive wave overtopping failure mode

Wave overtopping is often described as mean discharge q per meter of width in $m^3/s/m$ or $l/s/m$ (Van der Meer et al. 2016). Wave overtopping rate is described as mean or average term because in reality there is no constant discharge over the crest of a structure. Wave overtopping discharge increases significantly by increase in the height of waves. For example, lower waves will not produce overtopping while a high wave can result in

a large amount of overtopping discharge in a shorter time less than a wave period (Van Der Meer 1998). A predefined mean overtopping discharge is often considered as threshold criteria to meet the quality performance of a structure. The allowable values of mean overtopping discharge are different more or less in various references (for example EurOtop manual (Van der Meer 2016)). Table 2.3 shows classification of different range for mean overtopping discharge rates by EurOtop manual (Pullen et al. 2007; Van der Meer et al. 2016).

Piping failure mode

Piping failure belongs to geo-hydraulic failure type with hidden indicators that warn the high possibility of piping failures such as seepage through the sand layer beneath the dyke, rupture of clay layer in a landslide, and progressive erosion at the toe dyke (Weijers and Sellmeijer 1993). Piping in the dyke foundation and slope occurs because of seepage flow through a dyke core (micro-instability) (Vorogushyn et al. 2009). In the dyke foundation, the deterioration processes result in a formation of pipes, which decrease the stability of structure due to piping failure mechanism (Voortman and Vrijling 2001). Finally, inner erosion of the dyke core may occur as a result of material transport via flow paths such as animal holes towards the seaside dyke slope leading to the slope and core failure.

A critical resistant element to protect sea dykes is the sheet piling under the structure that prevents seepage & piping, and increases stability. Some significant failures during Hurricane Katrina occurred because of an insufficient length of these sheet pilings (Liu et al. 2005). A dyke fails due to piping when two subsequent failure mechanisms occur. First uplifting failure mechanism causes openings in the impervious clay layer covering the sand layer. Secondly, a flow of water through these openings initialises a deterioration process. The deterioration process takes the form of pipes undermining the foundation of the dyke and eventually causes failure (Baars et al. 2009).

Piping is the sub-mechanism that describes the growth of water-bearing ‘pipes’ due to increasing pressure of the water on the outside of the dyke. The dyke fails as a consequence of piping if the difference between the local water level and the inside water level reduced with a part of the vertical seepage length exceeds the critical water level. Weijers and Sellmeijer (1988) defined the critical parameters of a piping failure

mechanism as: (1) water level as a function of a factor reflecting the effect of the finite thickness of the water-bearing layer, (2) the characteristics of the sand properties in the resistance layer, and (3) the seepage length. Vorogushyn et al. (2009) defined the piping failure probability related to rupture and seepage by

$$P_f = P_{piping} \cdot P_{cr|piping} \tag{2.4}$$

$$P_{piping} = P_{rs} \cdot P_{h_{cr}|rs} \tag{2.5}$$

$$P_{rs} = P_{seepage} \cdot P_{r|seepage} \tag{2.6}$$

where P_f is the probability of dyke failure due to piping; $P_{cr|piping}$ is conditional probability of piping associated with the critical seepage length after erosion or deterioration; P_{piping} is the probability of progressive piping; $P_{h_{cr}|rs}$ is the conditional probability rupture after water level reaches to critical head difference; P_{rs} is the probability of rupture and seepage; $P_{r|seepage}$ is the conditional probability of rupture associated with the seepage level.

2.6.2. Limit state equation

In structural reliability analysis, the first step is to define the desired/required performance of the structure. The decision maker or authorities are asked to describe the required/desired target service life, and the period that coastal defences are needed to service regarding the budget, the expected extreme events and the importance of the receptors. Performance of the structure represents the combined short term and long term fulfilment of the functional requirements including safety, serviceability and functionality of the structure during the service life. In a performance-based context, these functional requirements are defined as the limit states (Van et al. 2007).

The limit state is the function of the boundary conditions including its loads and the state of the structure including its resistance. In order to evaluate the risk of each specific failure, a limit state equation Z should be described. A limit state equation in its general form is expressed by (Allsop et al. 2007)

$$Z = R - S \tag{2.7}$$

where failure is defined when $Z \leq 0$; R is the strength of the structure; and S is the loading on the structure. Both strength and load may interpret to time-dependent stochastic random or deterministic variables. For a probabilistic approach, the schematic diagram of a limit state equation and the visual interpretation of failure probability is illustrated in Figure 2-14. In the case of environmental change over time, hydraulic variables may change due to rise in sea level, and the resistance of the structure is decreased due to deterioration processes.

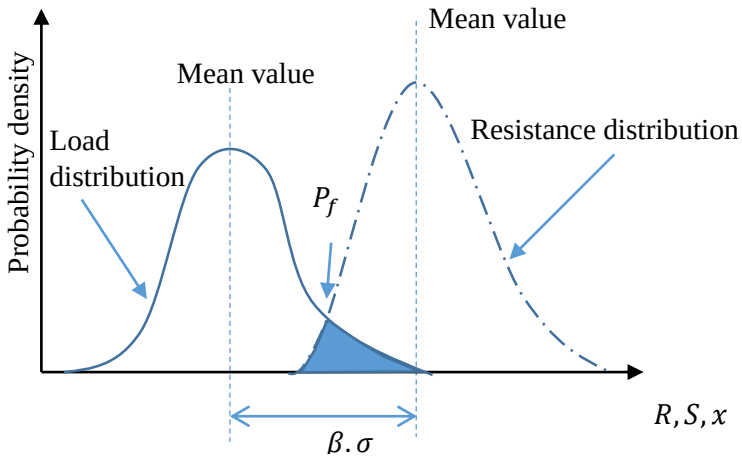

Figure 2.10 Illustration of probabilistic limit state equations; P_f failure probability; β is reliability index; and σ standard deviation of the safety distribution (Adopted from Allsop et al. 2007).

2.6.3. Fault tree analysis

A fault tree is a logical tree shape diagram to describe the interaction and influence of extreme events or component failures in a system into the total system failure (Gelder 2013). A fault tree is useful as it illustrates a general overview of the system and contains the different chains of events/failure modes, leading to a top event representing the total failure. In other words, the reliability of an element or a system is expressed visually and logically. The primary purpose of constructing a fault tree is to describe the logical connection between component failures, and to estimate the probability of system reliability, eventually to calculate the probability of the major event occurring.

The eventual failure probability of whole system failure is estimated according to logical gates in the fault tree. In a parallel coastal defence ring (system), the final probability of

failure is the maximum failure probability between each asset. In contrary, in a series ring system, the reliability of the ring system is calculated from the reliability of its defence structures in which failure probability is passed from one hierarchical level to the next (Kortenhaus et al. 2002). However, in a single dyke or systems, different failure mechanisms may be in parallel or series relationships. In the case of n parallel failure mechanisms such as wave overtopping and overflow, the total probability of failure is expressed as

$$\Pr[\ total\ failure\ probability|parallel] = \prod_{1}^{n} P_{f,i} \tag{2.8}$$

while the total probability of failure of n series failure mechanisms such as piping and uplifting is given as

$$\Pr[total\ failure\ probability|series] = 1 - \prod_{1}^{n}(1 - P_i) \tag{2.9}$$

Most systems, including coastal flood defences, cannot be described in a simple parallel or series system, as they are often a combination of both models (OUMeRAcI 2005). Hence, fault tree analysis is best fits to systems with two-state components (e.g. binary systems) and not appropriate to a complex phenomenon such as coastal defence systems. However, most UK authorities in flood defence scheme including Environment Agency use fault trees to describe qualitative risk assessment (Reeve 2009).

Figure 2.11 shows a generic fault tree which illustrated the hierarchic of the failure modes in coastal defence structures (Naulin et al. 2011), and it describes a detailed view of a fault tree. The figure shows each of the failure mechanisms is organised in a fault tree, and the structure of a fault tree represents the different chains of events leading to an overall failure of a sea dyke (top event), which is defined as breaching the structure and flooding in the protected lands. Conventional fault trees in coastal defence structure describe according to structural failures (ultimate failures) and non-structural failures (serviceability failures). Naulin et al. (2011) investigated the fault trees in coastal defences and concluded the following shortcomings as:

- Insufficient data to assign failure probabilities to individual components.
- Fault trees are essentially binary (e.g. components either work or fail). However, in coastal defence structures, different levels of performance are available.

- The events and failure mechanism in coastal defences have significant overlap in functions, and they are too correlated together to be considered as independent parts.

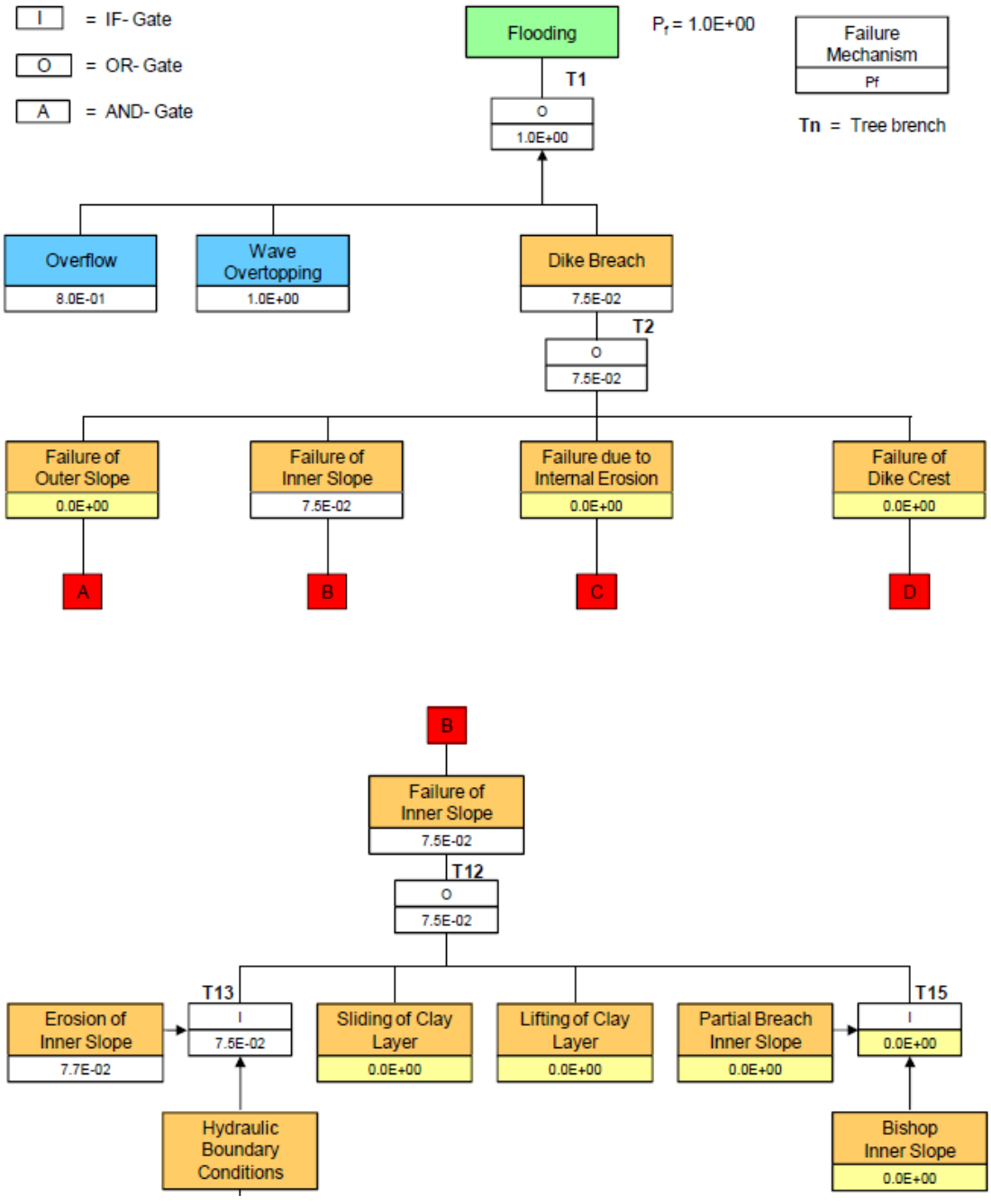

Figure 2.11 Failure probabilities and extract of fault tree for a typical dyke (adopted from Naulina et al. 2008).

The gaps in the conventional fault trees have prompted cause-consequence fault tree diagrams (Naulin et al. 2011). The cause-consequence fault trees can describe possible changes in the system and link these to consequences, then provide a complete

description of the system. Cause-consequence fault tree for a flood defence summarises the combination of the different limit state equations and some technical failure mechanisms concerning the correlation between them. The steps of establishing the diagram are as follows:

1. Consider some or all modes of failure, other modes of failure are excluded.
2. Recognise the events that are affecting the structure.
3. Assign probabilities of failure to each failure mechanism.
4. Define a time scale as an event has a duration (e.g. the probabilities of failure are interpreted as annual probabilities).

The lower parts of the cause-consequence trees have less influence on the main extreme event, and the highest raw of the tree, which is considered as significant failures or events, is also dependent on another sub-failures. It means that in a coastal defence structure the process of failure is not a sudden event and needs several sub-failures, (except poor estimation of load). The cause-consequence fault trees are giving the decision makers enough time to improve the reliability performance of the structure after observing of low-level sub-failures/events (Naulin et al. 2011).

2.6.4. Time-dependent reliability

Coastal flood defence structures need to be analysed over time as described in Buijes et al (2009):

1. Hydraulic loads are time-dependent especially with consideration of sea level rise and changing environments.
2. The strength of the coastal defences is time-dependent because of the deterioration process.

As discussed in the previous section, failure mechanism can be defined by a limit state equation. Thus a general time-dependant limit state equation can be written as

$$Z(t) = R(t) - S(t) \tag{2.10}$$

Let the lifetime probability distribution function be (Buijs et al. 2005; Li et al. 2015)

$$\Pr[lifetime] = f_{L\leq t} = f_L[t|Z(t) \leq 0] = \frac{dF_L(t)}{dt} \tag{2.11}$$

where L is the lifetime; t is the time of interest; and $f_L(t)$ is the probability of structural failure in the interest time period. The lifetime probability density function can be written as $f_L(t)$ (Allsop et al. 2007)

$$f_L(t)dt = \Pr[failure\ for\ (t, t+dt) \cap (no\ failure\ for\ (0,t)] \quad (2.12)$$

The above equation means the probability of failure for a specified period of time. The failure surface and the domain of integration change with time. Thus the failure probability itself is time-dependent. The time-dependent process can be described as failure events that out-crossed of the load distribution over the strength distribution during the operation time, as shown in Figure 2.12. The exact solution/estimation of the out-crossed area provides the reliability of the system. However, it is not possible to find the exact solution due to uncertainty and inherent stochastic features.

In coastal defence engineering, the time-dependent parameters for limit state equation are often both strength and loads. The strength, which could be decreased or increased due to deterioration or repair, and the hydraulic loads on the asset, which are often increased due to environmental changes, often need to be evaluated in terms of extreme values for a specific period of time, e.g. 250 years return period.

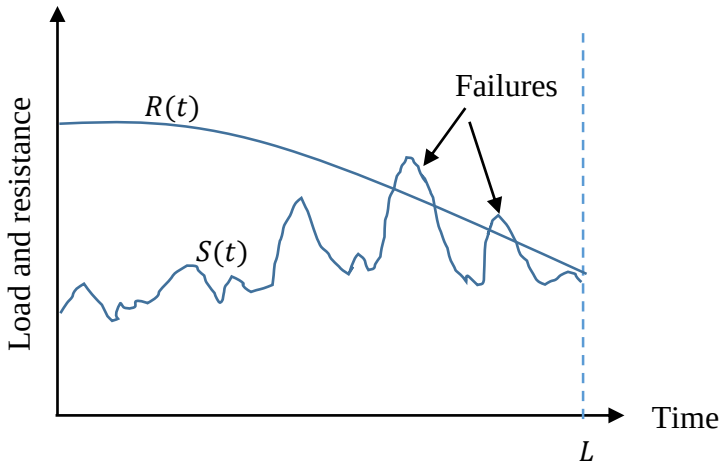

Figure 2.12 Illustration of the time-dependent failure probability and the lifetime L (Adopted from Buijs et al 2005).

2.6.5. Fragility curves

The probability of failure for a structure concerning loading variables creates a curve which calls “fragility curve” (Simm et al. 2008). Fragility curves are utilised to

demonstrate the probability of failure on a given load, and to describe the function of failure, not the point of failure. Fragility curves are interpreted in absolute terms to provide a more comprehensive understanding of the reliability of a structure. The curves provide more information regarding system response associated with the load variables. Effectiveness and benefits of fragility curves for coastal flood defences have been investigated and demonstrated in many kinds of literature (e.g. Buijs et al. 2005; Suppasri et al. 2012).

Carter et al. (2013) utilised fragility curves for joint probabilities of waves and water level in coastal defences to determine the reliability of a structure over time with consideration of deterioration processes. VanderMeer et al. (2013) applied and compared various methods to improve reliability assessment with a combination of different data sources, and demonstrated that fragility curves provide better understanding in comparison with other failure probability presentation models.

The fragility curves give the ability to illustrate the performance of a coastal defence structure or system in a curve, and it is practical for a reliability analysis. For each fragility curve, materials, failure mechanisms and load variables are considered to understand the structural response to environmental conditions in a defence system. There are five stages of drawing a fragility curve given as (Simm et al. 2008):

1. Recognize the relevant failure modes.
2. Provide limit state functions.
3. Define the critical parameters and their uncertainties.
4. Provide fault tree analysis (hierarchy of failure modes).
5. Carry out reliability analysis.

2.7. Optimal maintenance strategies

Reliability of civil engineering infrastructure including coastal defence systems is not only affected by quality and reliability of its components against different failure mechanisms but also depends on maintenance and inspection strategies. This means that maintenance and inspection activities should be optimally planned in order to ensure the performance of the structure stays higher than the predefined threshold, while minimising the maintenance and operational costs.

2.7.1. Renewal maintenance model

Preventive maintenance and inspection models are defined with repair or replacement actions (preventive or corrective maintenances) of a structure or part of it. In corrective maintenance, a repair action is implemented after failure event (or below the required serviceability levels) to restore the structure to the predefined performance level (often as good as new). In preventive maintenance, the action is carried out at predetermined intervals or corresponding to prescribed criteria, and is intended to reduce the probability of failure or the degradation rate of the structure. Preventive and replacement maintenance models are developed mainly targeting based on (Grall et al. 2002; Hong et al. 2014):

- Cost minimisation: to achieve the minimum cost of maintenance per unit time for constant interval replacement policy or replacement at a predetermined age.
- Downtime minimisation: to minimise the unavailability of the structure per unit of time for constant interval replacement policy or replacement at a predetermined age.

Damnjanovic and Zhang (2008) presented a flexible framework for quantifying the reliability-based maintenance regarding cost optimisation for preventive maintenance and replacement strategies. The developed framework consists of three components, the reliability-based performance model, the preventive and corrective maintenance, and the cost model. The results show that the model can be used to estimate a reasonable cost for a reliable maintenance strategy.

Saydam and Frangopol (2014) proposed a risk-based maintenance optimisation model for bridges to find the optimum maintenance options and their time intervals. The model is formulated as a multi-criteria optimisation in which the maximum lifetime value of expected losses associated with failure and the lifetime total expected maintenance cost. It also accounts for different deterioration levels of bridge components and consequences of both component failure and system failure, which provides comprehensive information and solution for decision makers. Chen and Alani (2012) applied optimal repair planning during the service life of sea defence structures, based on reliability analysis by optimising the balance between the risk of failure and the costs of

maintenance. The results show that the optimal repair time largely depends on the deterioration rate of structural resistance and the relative cost of preventive maintenance.

2.7.2. Markov decision process

Markov decision process (MDP) provides a mathematical framework for modelling decision making in situations where outcomes are both dependent on the transition matrices and the decision maker actions (Frangpool et al. 2004). A Markov decision process is a discrete-time transition process, and the system or structure moves through a sequence of defined states. The transition between the states is not only dependant on the deterioration rate and transition matrix, but also depends on the maintenance actions during its lifetime. Hence, the outcomes of the actions of the system or the structure are not deterministic. Objective functions (single or multiple) may control the maintenance strategy by choosing optimal policies at each time-step in a period of the finite or infinite horizon (Cheng et al. 2015).

Policies $\Pi = \{\pi_1, \dots, \pi_n\}$ represent available strategies in Markov decision processes which map from states to actions. In order to evaluate a policy, total rewards for deterministic actions or expected total rewards for stochastic actions are estimated. Note that the state of the structure over time with or without performing maintenance actions can be modelled, the optimisation of inspection and maintenance policies using this process can be performed. For example, when the system is in state i, the expected discounted costs over an unbounded horizon are given by the recurrent relationships given here as (Frangpool et al. 2004)

$$V_\alpha(i) = C(i,a) + \alpha \sum_{1}^{N} P_{ij}(a) V_\alpha(j) \tag{2.13}$$

where α is the discount factor for one year; V_α is the value function using α; $P_{ij}(a)$ is the transition function; and $C(i,a)$ is the cost function regarding the action a over state i. A cost-optimal decision can now be found by minimising the above equation with respect to the action a. MDP based models are used in pavement management systems (e.g. Cheng et al 2015) and Bridges (e.g. Papakonstantinou and Shinozuka 2014). Bennett and Hauser (2013) illustrates how to maximise the condition of the road system under a budget constraint or how to minimise the maintenance cost under a minimum safety

constraint. This can be achieved by using the original linear programming formulation or with its dual formulation.

Markov decision processes are able to model sequential decision problems in which there is a decision required at each time-step. Other advantages of using MDPs is the computational time required for solving MDP models, which is much smaller than that for solving other maintenance models. This is useful particularly when the problem is very complex, and has large state and action spaces. Markov decision processes also have some limitations. First, extensive data are required because data are needed to estimate a transition probability function and a reward function for each possible action. In infinite horizon MDPs it is assumed that the rewards and the transition probabilities are stationary. In cases where rewards and transition probabilities are not stationary, finite horizon MDP is suggested to solve because of the difficulties in computational calculations. Furthermore, there is no available user friendly software for solving MDPs, and some level of programming are needed to simulate the concerned problem.

2.8. Research questions and gaps

In this chapter, an overview of the climate change effects, deterioration processes, and deterioration models in coastal defences is presented. Also, the conventional methods to evaluate failure probability as well as maintenance optimisation models are discussed. From the review of existing studies following gaps and research questions are identified:

- Performance deterioration of coastal defence structures mainly depends on the future hydraulic variables and resistance degradation of the geometrical surface of the assets. However, only a few investigations have been carried out to study the effect of changing environment over the resistance degradation such as crest freeboard loss.
- Although few attempts have been made using analytical approach but there is still a need to investigate the impacts of climate change on the reliability of coastal defences in the future with consideration of different failure modes.
- The life cycle performance of coastal defence structures associated with serviceability (i.e. excessive wave overtopping) and ultimate (i.e. piping

underneath a dyke) limit state equations considering the realistic behaviour of deterioration process is not investigated comprehensively.

- In lifecycle performance assessment, implication of a stochastic and state-based deterioration model (i.e. using Markov model) on time-dependent reliability analysis is less studied. Although few stochastic models are studied to simulate the deterioration process in coastal defences, state-based deterioration model is not yet studied.
- Condition-based maintenance model to investigate the optimal repair strategy of coastal defence structures with consideration of inspection errors is not yet studied. The effects of imperfect information on maintenance optimisation in flood defences are not investigated. Additionally, sequential decision making models (i.e. Markov Decision Process) are not studied in coastal defence structures, while these models are useful as the environment of the assets are changeable, i.e. due to climate change, and a sequential decision making model can be adopted accordingly in each time-step.
- There are many disagreements in literatures dependency evaluation between the key hydraulic parameters for coastal defences are limited, and few studies are carried out to investigate the effect of climate change on dependency coefficient. Hence, more investigations are necessary to discover the effects of climate changes on the dependency parameters.
- In quantitative and qualitative methods for condition grade assessment of flood defence structures, probalistic models to investigate the condition of the assets in the future in not yet studied.
- The correlation between damage indicators (i.e. the visual indicators in a sea dyke such as crest level settlement) and condition grading system is not available. Hence, it is not possible to translate the qualitative inspection results into quantitative values for risk assessment.

2.9. Summary and conclusions

This chapter provides a literature review and background information about hydraulic parameters, climate change, reliability analysis, deterioration processes and maintenance models in coastal defence structures. The existing and common risk evaluation approaches for the existing structures are investigated and summarised. The concept of

the joint probability, the extreme values of the hydraulic variables and impacts of climate change on the key variables are studied. Causes of floods, the contribution of each cause and the projection of flood defence scheme over the next century are discussed to give a transparent background of main issues in this field. In particular, sea level and wave height features are reviewed to assess their change over time and the impacts on performance of the coastal defences.

Stochastic deterioration models such as Gamma process and Markov chain are studied and aimed to be embedded into coastal defence deterioration modelling. The sources of deteriorations, the weaknesses of current coastal defences and common failure modes are discussed. The fragility curve concept in reliability based method is studied. The definitions in structural reliability are given, and probabilistic approaches are explained. Performance deteriorations in coastal defence scheme are discussed in detail for various types of damage and failure. A general overview of failure probability calculation is provided. Finally, available maintenance models for different types of reliability analysis are discussed.

In order to develop the methodologies and to cover some of the mentioned gaps, this research aims to:

1. Develop and translate current deterministic deterioration curves to stochastic state-based models with consideration of the quantitative condition assessment and damage inspection results.
2. Develop appropriate limit state equations to consider changing environments for different failure mechanisms in coastal defences with consideration of the degradation in the resistance of the strictures over time in order to apply in reliability analyses.
3. Investigate homogeneous and inhomogeneous (stationary and non-stationary) effects of deterioration rates in the proposed deterioration models in a time-dependent reliability analysis for coastal defences.
4. Develop maintenance model in order to optimise the cost of inspection and repair in coastal defences while maintaining the assets at a reliable performance level concerning the cost of imperfect information such as inspection error.

3. Monitoring and assessment of coastal defences' condition

3.1. Introduction

For an effective reliability and maintenance management, it is necessary to understand the consequence of failure, the expectation of performance, and the actual loading on the coastal defence. Without the understanding of these topics, it is difficult to target resources for necessary inspections, maintenance and developments. In this chapter, condition assessment model, hydraulic load monitoring, and climate change impacts over these topics are discussed. The main contributions of this chapter are as follow:

- A link between structural damage and condition grading system is proposed. This relationships will help to standardise the deterioration model used in the reliability analyses.
- The available inspection strategies and deterioration curves are translated into probabilistic forms used in the reliability analyses.
- A practical model is proposed to apply the impacts of sea level rise on the hydraulic parameters, and the model is utilised for extreme value analysis.
- A new technique is proposed to improve the dependence estimating between the joint extreme variables via a copula function.

3.2. Grade-based condition assessment

The condition observations have been collected since 1990s, and condition assessment manual (CAM) is proposed to guide and train the inspectors, as mentioned in the literature review (Environment Agency 2006). The deterministic deterioration curves are developed based on the collected data and expert judgement for various types of flood defence structures (Halcrow Group 2013). However, existing deterioration curves are deterministic and may not provide a reliable grade-based deterioration model for a long period due to uncertainties. To tackle the limitation, the deterministic deterioration curves and the outcome of the inspection strategies should translate to probabilistic frameworks in order to use them in a stochastic model.

Deterministic deterioration curves

In 2013, Environment Agency proposed a series of asset deterioration curves for different types of coastal and fluvial defences to estimate the residual life of an asset or structure

concerning the condition grading system (Halcrow group 2013), as shown in Figure 3.1. Deterioration curves predict the condition grade of assets associated with time based on historical data and expert judgments. The curves are categorised according to the asset class, materials, asset type, and environment of the asset. Two more factors affect the deterioration curves: the rate of deterioration and maintenance strategy.

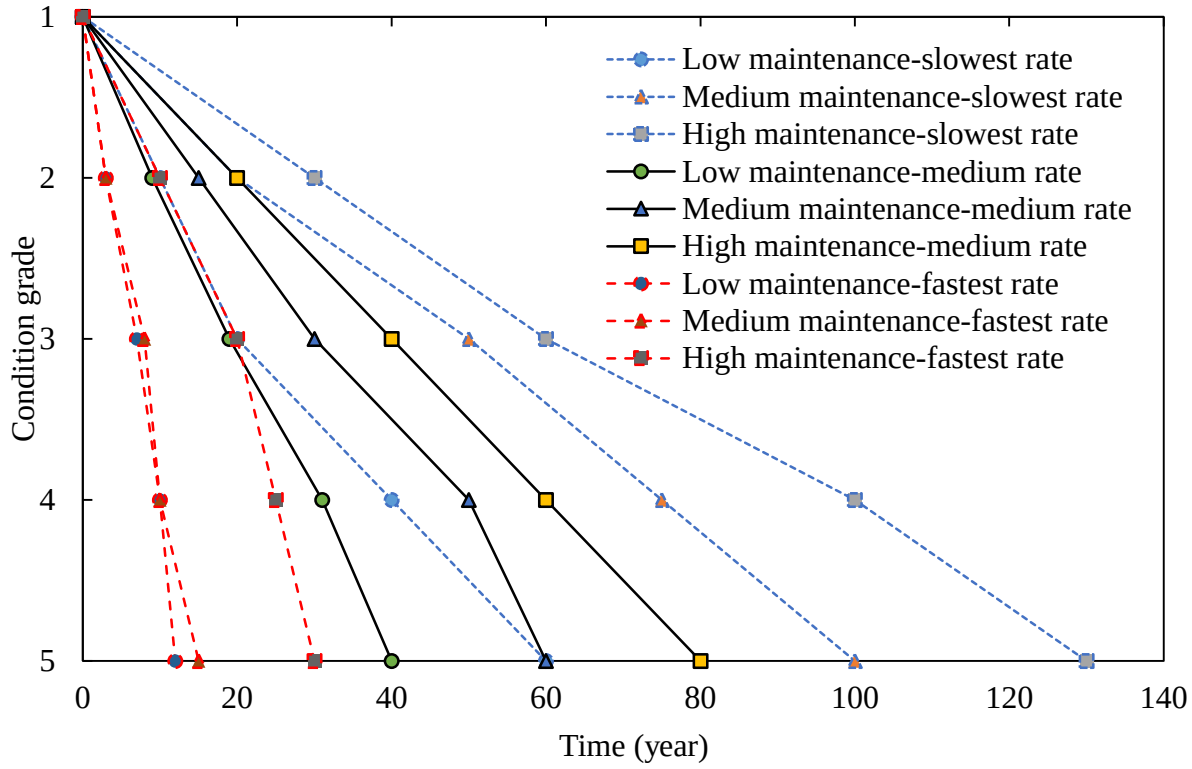

Figure 3.1 Example of deterioration curves provided by Environment Agency for coastal defence structures with toe/slope protection (Halcrow group 2013).

Parameters of selecting a deterioration curve for an existing flood defence

The parameters that are considered in a deterioration curve selection are (Halcrow Group 2013)

- Asset class, e.g. earth dyke, vertical walls
- Asset type, e.g. defence, embankment
- Materials, e.g. concrete, clay
- Environment, e.g. fluvial, coastal
- Rate of deterioration, e.g. medium or fast
- Maintenance strategy, e.g. low, high

The first four parameters are constant, time-independent and deterministic, and can be identified or recognised in a site inspection. In contrary, the rate of deterioration and maintenance strategy need to be investigated and determined, which is also changeable over time, e.g. due to change in the maintenance strategy because of requirements. Deterioration rates are classified into slow, medium and fast rates with respect to the pace of structural deterioration. In order to choose the appropriate rate, site-specific information about the loads and environmental conditions should be considered.

The medium deterioration rate assumes standard or average conditions, and a faster or slower rate of deterioration should be chosen based on the severity of the environmental conditions (Flikweert and Simm. 2008; Taylor et al. 2014). However, each case study needs to be expertly judged to determine the appropriate deterioration rate with consideration of site-specific observations. In coastal defence context, three major types of maintenance are defined by Environment Agency as (Flikweert et al. 2009):

- Regime 1: Low or basic maintenance with the minimum repair.
- Regime 2: Medium maintenance for maintaining at target condition grade 3.
- Regime 3: High maintenance for maintaining at target condition grade 2.

Regime 1 or low maintenance is non-structural maintenances, e.g. handrail maintenance or painting if necessary. Hence it does not improve the structural strength or performance. Thus, it is a do-nothing maintenance in a reliability analysis and does not affect deterioration rate. Regime 2 and 3, are also considered as minor and major maintenances, respectively, and both of them are implemented in specific time intervals (Flikweert et al. 2009; Thorne 2014).

Apart from the mentioned parameters in deterioration curves, some other site-specific parameters need to be considered regarding the type of the structure. For example, for a sea dyke, site-specific parameters that should be considered are a risk of vandalism, level of traffic, increase/lose vegetation condition, the degree of cracking and reduction in foreshore level. Figure 3.2 shows the process of evaluating the current condition grade and selecting deterioration curve.

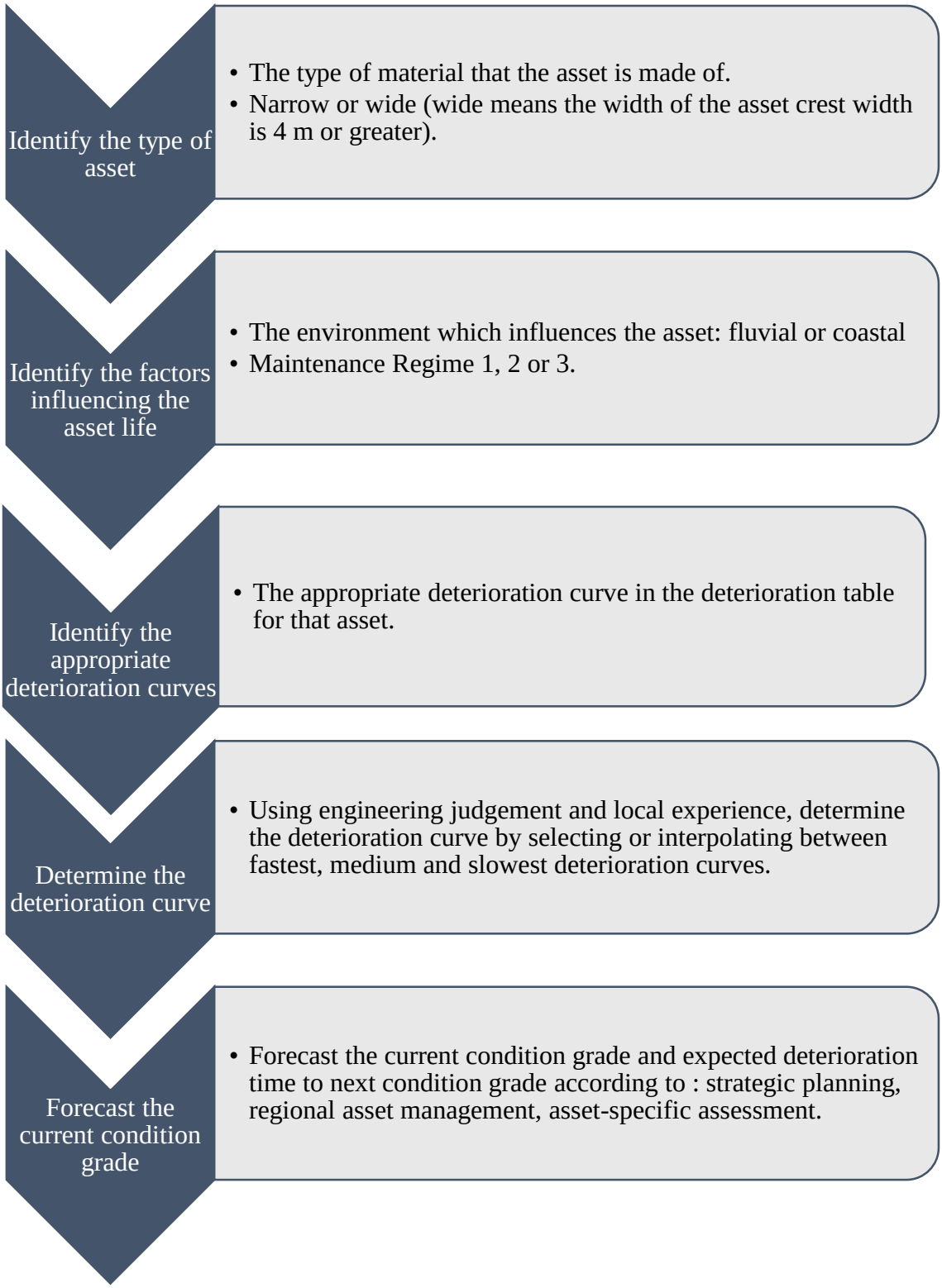

Figure 3.2 The stages of evaluating the current condition grade and selecting an appropriate deterioration curve.

Limitations of the deterministic deterioration curves

The deterioration curves are designed to predict the deterministic transition through the five condition grades for the asset. Although the deterioration rates account for a wide range of parameters including environmental aspects, the outcome of the curves is too generic. Hence, it cannot be utilised for prediction of asset performance without stochastic analysis and expert judgment. Moreover, the inspection outcomes are qualitative, while quantitative data are needed for a structural failure analysis. For example, assume an inspector assigns the condition grade of different parts of a sea dyke as 1, 3 and 4, respectively. The overall condition grade of the dyke will be 4. However, it is not clear that which part is more vulnerable to a specific failure mechanism. Consequently, the deterministic method to evaluate overall structural performance is not scientific and it is ambiguous.

3.3. Performance-based asset management

Quantitative damage measurements are essential for evaluating the performance level of an asset, e.g. measuring crest height loss to evaluate the strength of a sea dyke against wave overtopping. Also, accurate assessment of an asset geometry is useful for reliability performance assessment, while the qualitative judgment of an asset, such as discussion in the previous section, is not sufficient for statistical models. For example, crest height has a critical role in the asset performance against wave overtopping, and it represents the standard of protection, which cannot be assessed through visual inspection accurately (Long et al. 2013). In addition, some geotechnical parameters related to subsurface or the core of the flood defences can only be assessed via specific inspection techniques, not visual inspections. The primary objectives of quantitative asset monitoring are (Long et al. 2013):

1. To have a more accurate condition grade assessment.
2. To understand the performance of the asset rather than its residual life.
3. To identify optimal maintenance strategy.

Inspection strategies

Effective management of valuable and vital assets in coastal and fluvial areas is one of the leading objectives for Environment Agency in UK. Routine inspections of these assets help authorities to have essential information about the performance of the assets

level by observing and recording the structural condition. Eventually, with studying and analysing the recorded data, it is possible to achieve the optimal maintenance plan. The asset inspection strategy needs to be regularly reviewed and updated in response to changing conditions such as changes in asset condition grade or loading conditions. There are three main types of inspection strategy, as (Flikweert et al. 2009):

- Tier 1: the default level, routine inspection.
- Tier 2: more detailed, non-intrusive inspections.
- Tier 3: highly detailed, intrusive inspections.

A tier 1 inspection is routine asset inspection which discussed in the Environment Agency Condition Assessment Manual, and it is the lowest level of monitoring. It includes the techniques that operate at a fixed location or single asset, e.g. traditional methods of visual inspection. Tier 2 and 3 inspections are activities that seek more detailed information than is routinely collected in tier 1 strategy. Both Tier 2 and 3 need to be carried out by appropriate experts, and each can be triggered after proper consideration about the general condition of the structure (Flikweert et al. 2009).

3.3.1. Quality of inspection strategies

One of the main objectives of condition grade assessment and inspections is to evaluate the performance level of the structure. Hence, the accuracy of the inspection technique and utilising the results for a risk assessment model is critical. The accuracy of an inspection method is defined as the closeness of a measured quantity to the actual true value (Papakonstantinou and Shinozuka 2014). It is almost impossible (or too expensive) to have a 100% accuracy in the observation results. However, inaccuracy in the condition assessment may lead to inefficient and more expensive maintenance costs.

The gathered information during damage and condition assessment is used as the basic information of reliability analysis, which means the errors may cause the entire analysis in danger. Especially, this happens when the quantitative observation outcomes are relative values (Ossa et al. 2016), because the difference between two measurements may show the difference between the upper bound and lower bound observations, not the mean values. In other words, the measured damage may not reflect the change of real damage in a time interval but instead may reflect the imprecision of the inspection results.

This problem could be mitigated by repeating the inspections at each time-step to increase the precision of the results. However, it does not improve the accuracy of the inspection technique. Hence, it is essential to translate the effectiveness of the inspection techniques and condition grade observation results into a probabilistic from.

The probabilistic form can describe the accuracy and precision of an inspection strategy by considering the error and standard deviation of the observations. The inspections in coastal defences are not a continuous function, but a series of discrete observations and sometimes for specific damage detection. Table 3.1 shows the three main inspection strategies, lower bound and upper bound errors, and their standard deviations of possible error for each strategy. The values and assumed distribution in Table 3.1 are from the referenced case studies. According to the case studies, the assumption of normal distribution is arbitrary, however, the observations and empirical results show that the assumed distribution is suitable. The quality of inspection techniques are also stated in the case studies, and they are evaluated according to the Asset Inspection Guidance (Environment Agency 2014) with respect to the inspector skills and the applied instruments. The standard deviations σ_{ins} are evaluated based on the upper bound UB and lower bound LB errors, and the values represent the average of LB-UB based on various case studies observations. The case studies are from UK, and the results are observed by different companies/contractors with different inspection techniques.

Table 3.1 Parameters associated with three inspection strategies.

Inspection strategy	Inspection technique	Case study/ report	LB (m)	UB (m)	σ_{ins} (m)	Distribution
Tier 3	Local GPS	Thames Estuary 2100	-0.01	+0.01	0.0078	Normal
Tier 2	LIDAR	HR Wallingford (2006)	-0.27	+0.27	0.2100	Normal
Tier 2	N/A	Statutory Defence Levels	-0.30	+0.30	0.2610	Normal
Tier 2	N/A	Haskoning Defence Database	-0.37	+0.37	0.3130	Normal
Tier 1	N/A	IA3	-0.47	+0.47	0.3390	Normal
Tier 1	Visual	Thames Tidal Database	-0.50	+0.50	0.3640	Normal
Tier 1	Visual	Thames Estuary 2100	-0.60	+0.60	0.3900	Normal

This ability/quality is defined based on the intensity of the structure damage. The damage intensity factor η is described here as (Blong 2003),

$$\eta = \frac{L_{ini} - L_t}{L_{ini}} \tag{3.1}$$

where L_t is the deteriorated length at time t (in X, Y or Z direction); L_{ini} is the initial length (in X, Y or Z direction).The damage intensity is from 0, indicating no damage, to a value of 1, indicating entire length loss. Table 3.2 shows the parameters that describe the quality of inspection strategies, where $\eta_{0.5}$ is damage intensity where the probability of observing the damage is 50%, and the suggested values in the table are according to Lin and Breslow (1996); η_{min} is minimum damage observation and below this level is impossible to be detected; η_{cer} is the certainty level that above this level the damage is certainly observed by the inspector; and the inspection cost in arbitrary unit represent the schematic cost difference between the strategies. η_{cer} and η_{min}values are calculated from three standard deviation above and below the mean, namely

$$\eta_{cer} = \eta_{0.5} + 3\,\sigma_{inp} \tag{3.2}$$

$$\eta_{min} = \eta_{0.5} - 3\,\sigma_{inp} \tag{3.3}$$

where σ_{inp} is the standard deviation of the inspection strategy.

Table 3.2 Parameters associated with three inspection strategy.

Inspection strategy	$\eta_{0.5}$	η_{min}	η_{cer}	σ_{ins}	Inspection cost (unit)
Tier 3	0.10	0.01	0.19	0.03	80
Tier 2	0.30	0.12	0.48	0.06	30
Tier 1	0.60	0.30	0.90	0.10	10

The probability of observing the damage at an inspection session is given here as (Ang and Tang 2007)

$$p_{det} = \Phi\frac{\eta - \eta_{0.5}}{\sigma_{inp}} \tag{3.4}$$

where Φ is the standard normal value and can be found in normal distribution table from Ang and Tang (2007). Figure 3.3 shows the cumulative distribution of the results estimated by Equation (3.4) for the three inspection strategies for flood defence context.

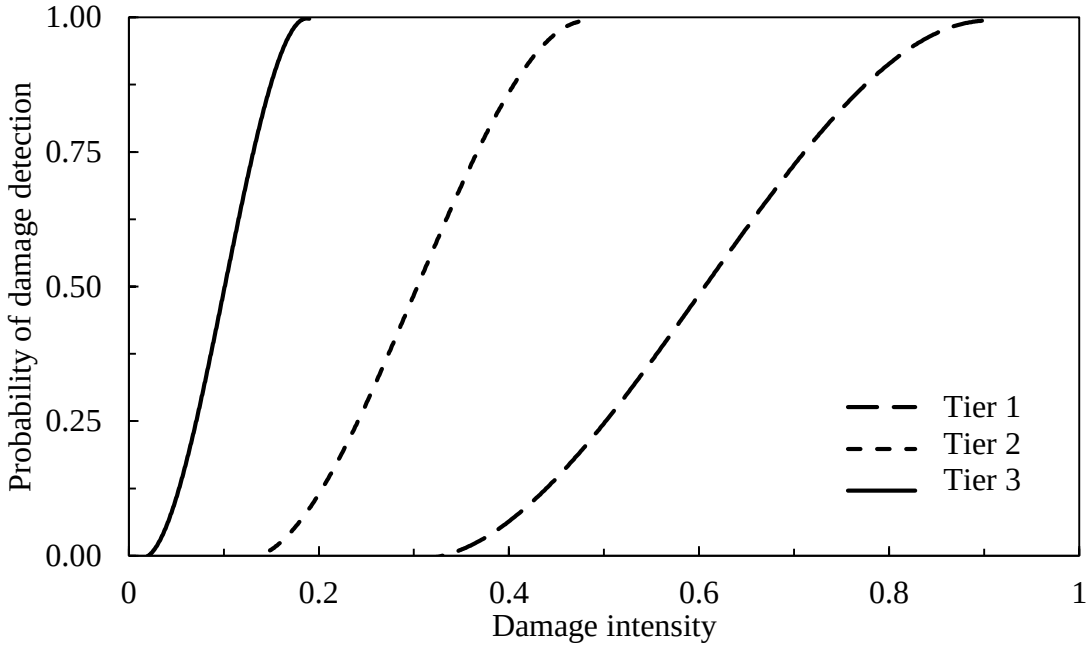

Figure 3.3 Probability of damage detection for three inspection strategies.

3.3.2. Correlating quantitative assessment and failure mechanisms

Deterioration curves focus explicitly on condition grades and do not necessarily provide information about structural deteriorations such as settlement. In order to cover the limitation, it is necessary to estimate structural deterioration by utilising transition probabilities between condition grades through stochastic process. The first step to describe the deterioration transition process is to establish a link between visual damage indicators, which are observable through inspection processes, and structural failure mechanisms. Table 3.3 shows overtopping and piping failure mechanisms with their measurable properties and physical evidence that are used for inspectors to grade the conditioning surface of a dyke or embankment.

Failure mechanisms and visual indicators

An improved approach for condition assessment was suggested to develop the inspection quality based on expert judgment and quantitative measurements (Long et al. 2013). The approach was conducted with objectives of finding accurate linkage between indicative structural damage and their relative failure mechanisms. The damage in the surface of an earth dyke divided into slight, minor, and major deteriorated conditions to characterise the intensity of damage level, and the relevant failure mechanism is specified (Long et al. 2013).

Table 3.3 Details of failure modes and measurable properties for an earth dyke (adopted from Long et al. 2013).

Failure mode	Description	Measurable properties	Physical evidence of potential problems
Overtopping	Water running down outer slope leads to degradation of surface protection and eventual erosion of outer slope over time. Eventually, leads to a breach of defence.	Crest height. Grass quality. Slope angle.	Rutting of the crest. Crest height below the standard of protection. Vegetation on outer slope.
Piping	A pathway for water to pass through or under the embankment forms (due to poor soil condition and/or vermin infestation etc.). Water seeps into the asset washing out fill material. Eventual creation of a piping channel from inner to the outer side of the embankment.	Embankment width. Soil coefficients. Seepage length. Water level Difference. Creep ratio.	Signs of seepage. Presence of washed out Fines. Animal burrowing. Altered vegetation on Bank.

The report suggests to rank assets damage according to their likely performance, general conditions and risk posed. Regarding the magnitude and intensity of eroded surface, slight damage are considered for condition grade 1, minor damage for condition grades 2-3, and major damage for condition grades 4-5. The condition grade of a dyke is considered as an indicator of the robustness of the dykes and their likely performance when subjected to extreme loads.

In Chapter two, the main failure modes for an earth sea dyke were discussed (e.g. Allsop et al. 2007, Hall et al. 2007). In this thesis, two main failure mechanisms are focused, wave overtopping and piping. Visual indicators in a condition assessment framework may be evident that the failure modes are occurring. Visual indicators for overtopping progress gradually, which means that they appear earlier than the critical point to the inspectors. In contrary, visual indicators for piping underneath the dyke progress with little visual warnings and after passing the safety threshold rapidly close to the critical

point. Geometrical features and dimensions of the asset are required to correlate between the visual indicators and failure modes.

Table 3.3 (previous table) shows the measurable properties that could be indicators of a deterioration process for two primary failure mechanisms in a sea dyke. According to Long et al. (2013), some performance parameters related to failure mechanisms are identified to conduct surface condition appraisal and monitoring. The performance parameters are measurable properties that are used to assess the dyke's performance. In order to have a quantitative assessment of physical evidence or visual indicator, their location in an earth dyke needs to be identified. However, it should be noted that the severity of defects strongly depends on the local situation. Table 3.4 illustrates the location of each visual indicator with their likely position and direction on an earth dyke or embankment. The value of damage is also divided into three different intensities as slight, minor and major evaluated from expert judgment (Long et al. 2013).

Table 3.4 will be used throughout the following sections as the table illustrates the size of features that any inspection method should be able to identify. However, in this table, the linkage between condition grades and surface damage is not available. It is suggested to link the dimension values given in Table 3.4 in a condition grade ranking system defined by Environment Agency. Table 3.5-3.7 show the combination of a qualitative condition grading system with quantitative damage evaluations for three main structural parts, i.e. seepage length, slope angle and crest level, respectively.

Seepage length has a crucial role in the reliability of a sea dyke against piping failure mechanism, as discussed in the literature review, while slope angle and crest level will be considered for overtopping failure mechanism. The tables help to set a relationship between the visual indicators of a specific failure mechanism and the condition grade system to develop a grade-based deterioration model. To translate the condition grades into probabilistic parameters, it is assumed that condition grade transition over time is linear and the deterioration intensity has a normal distribution.

Table 3.4 Surface features related to damage and failure for an embankment (adopted from Long et al. 2013).

Visual Indicator	Location	Description	Dimension (m)		
			Slight	Minor	Major
Rutting	Crest Slope	Wearing of crest or slope due to traffic (human or livestock)	X: 0.1–0.3 Y: 0.2–0.5 Z:0.05–0.1	X: 0.3–0.6 Y: 0.5–1.0 Z: 0.1–0.3	X: 0.6+ Y: 1.0+ Z: 0.3+
Vermin holes	Slope	Holes in slope caused by vermin: slight = hole/rat size minor = rabbit size major = badger/fox size	X: 0.05–0.1 Y: 0.05–0.1 Z: 0.05–0.2	X: 0.1–0.3 Y: 0.1–0.5 Z: 0.1–0.3	X: 0.3–0.6 Y: 0.3–0.6 Z: 0.3–0.6
Slumping	Toe Crest	Depression at toe or crest. If at toe, there may also be movement of slope above slump leading to a change in slope angle (SA)	X: 0.1–0.2 Y: 0.1–0.3 Z: 0.02–0.05	X: 0.2–1.0 Y: 0.2–1.0 Z: 0.05–0.4	X: 1.0+ Y: 1.0+ Z: 0.4+
			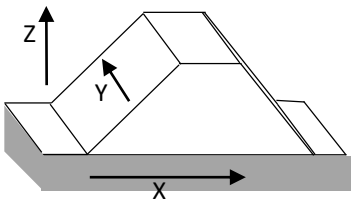		

The distributions are normal except the first and last condition grades, which assumed to be lognormal, as the dyke will not improve due to deterioration for condition grade 1. Dyke failures occur with very tiny visual indicators at the surface, but large-scale change may be occurring within the dyke. For example, Table 3.5 shows likely seepage length loss for various condition grades that is useful to evaluate piping in the embankment or dyke. Table 3.5-3.7 show the expected crest height and slope angle loss for condition grades from 1 to 5 with other visual indicators, such as surface protection that may be considered in overtopping discharge calculations. The value of loss in the tables are referred to critical values of surface feature related to damage according to Table 3.4.

The slight damage is categorised into condition grade 1, minor damage into condition grades 2-3, and major damage into condition grades 4 and 5. For example, rutting and slumping may degrade the crest level as stated in column 2 of Table 3.4. Hence, the slight degradation in the crest height direction (Z direction) is between 0.05 m and 0.1 m due to rutting, and 0.02 m to 0.05 m due to slumping. Therefore, the critical values for slight degradation is between 0.02 to 0.05 m, and it is assumed that the structure's crest level is in condition grade 1 since the deterioration level is less than 0.05 m. It should be noted that the severity of defects strongly depends on the local situation and values given in the tables are illustrative, not absolute. Apart from the mentioned parameters, some other visual indicators such as soil conditions and holes in slope should be considered to evaluate the deterioration level.

Table 3.5 Seepage length loss in earth embankments (Long et al 2013) and suggested condition grade.

Condition grade	Intensity of surface damage	Description	Loss of seepage length (m)
1	Slight	Cosmetic defects, very good soil condition, no vermin holes, slight width loss (<5 cm).	0.00-0.05
2	Minor	Good soil condition, slight (rat size) holes in slope, slight width loss (>5 cm but <15 cm).	0.05-0.15
3	Minor	Fair soil condition, minor (rabbit size) holes in slope, minor width loss (>15 cm but <30 cm).	0.15-0.30
4	Major	Poor soil condition, major (fox size) holes in slope, major width loss (>30 cm but <60 cm).	0.30-0.60
5	Major	Very poor soil condition, major (fox size) holes in slope, major width loss (>60 cm).	0.60+

Table 3.6 Slope loss in earth embankments (Long et al 2013) and suggested condition grade.

Condition grade	Intensity of surface damage	Description	Loss of slope (degree°)
1	Slight	Cosmetic defects (<2.5 °).	0-2.5
2	Minor	Slight depression at toe or crest (>2.5 ° but < 4 °).	2.5-4.0
3	Minor	Depression at toe or crest, lowering of slope section (> 4 ° but < 6 °).	4.0-6.0
4	Major	Depression and lowering in crest and toe, movement of slope above slump leading to change in slope angle (>6 ° but <10 °).	6.0-10.0
5	Major	Presence of sever slope change (>10 °).	10.0+

Table 3.7 Crest height loss in earth embankments (Long et al 2013) and suggested condition grade.

Condition grade	Intensity of surface damage	Description	Loss of height (m)
1	Slight	Cosmetic defects, very good surface protection, the slight wearing of crest elevation (< 5 cm).	0.00-0.05
2	Minor	Slight rutting, good embankment surface protection, slight wearing of crest elevation (> 5 cm but <10 cm).	0.05-0.10
3	Minor	Minor rutting, fair embankment surface protection, the minor wearing of crest elevation (> 10 cm but <20 cm).	0.10-0.20
4	Major	Major rutting, poor embankment surface protection, the major wearing of crest elevation (> 20 cm but <40 cm).	0.20-0.40
5	Major	Major rutting, very poor embankment surface protection, the major wearing of crest elevation (>40 cm).	0.40+

3.4. Translating quantitative assessment to a probabilistic framework

A probabilistic approach for the dyke may provide a more comprehensive understanding of the structural condition in the present and the future. If the condition assessment is probabilistic and is defined by the condition grading system, then a stochastic and grade-based risk assessment would be possible. In this section, the deterministic and qualitative inspection results are transformed into a probabilistic framework by the properties of the statistical distribution. In the probabilistic approach used in condition grading system, the following assumptions are considered:

- It is assumed that the distribution for each condition grade is normal and independent. However, for the first and the last condition grades, e.g. grades 1 and 5, a different type of distributions may be used to have a better presentation.
- The second assumption is that the accuracy of the inspection results is consistent with an accuracy of inspection strategies. The accuracy of three different inspection strategies is discussed earlier this chapter.

Statistical distributions and parameter estimations

For middle condition grades, e.g. grades 2, 3 and 4, it is assumed that deterioration intensity is normally distributed. To have a conservative evaluation, it is also assumed that the structural element, e.g. crest level or seepage length, is initially at the halfway point of a specific condition grade and progressively shifts to the right over time. The standard deviation of the distribution is determined by the quality of the inspection strategy, to include the error in the inspection strategy. Normal (or Gaussian) distribution is a standard continuous probability distribution. Normal distributions are important in statistics and are often used to represent real-valued random variables whose distributions are not known. The probability density and cumulative distribution function are given here representing as (Coles et al. 2001),

$$f(x;\mu,\sigma) = \frac{1}{\sqrt{2\pi\sigma^2}} e^{-\frac{(x-\mu)^2}{2\sigma^2}} \tag{3.5}$$

$$F(x;\mu,\sigma) = \frac{1}{\sqrt{2\pi\sigma^2}} \int_{-\infty}^{x} e^{-\frac{(y-\mu)^2}{2\sigma^2}} dy \tag{3.6}$$

where x is random variable; and μ, σ are mean and variance, respectively. The density of the normal distribution is symmetric with respect to the line $x = \mu$, and its width depends upon the standard deviation σ.

Assume a sea dyke is in condition Grade 2 for the deterioration of sea dyke crest between 5-10 cm (see Table 3.7). The accuracy of the inspection strategy need to be estimated for different case using the described method in section 3.3.1, however, here an arbitrary assumption of 92% is considered to demonstrate the numerical example. The mean start value is 7.5 cm crest level loss with consideration of the 8% wrong inspection results, which is 4% from each side, e.g. to be higher than 10 cm or lower than 5 cm. The probability of obtaining a value of $5 < \Delta H_d < 10$ cm when the structure is actually in condition grade 2 is 92%, or relative crest settlement $\Delta H_d < 10$ is 96%. The standard deviation can be computed as (Ang and Tang 2007)

$$\Pr(\Delta H_d < 10) = 0.96 = \Phi\left(\frac{10-\mu}{\sigma}\right) = \Phi\left(\frac{10-7.5}{\sigma}\right) \tag{3.7}$$

$$\sigma = \frac{10 - 7.5}{\Phi^{-1}(0.96)} = \frac{2.5}{1.76} = 1.42\ cm \tag{3.8}$$

where Φ is the standard normal value and can be in page 6.0found in normal distribution table (Ang and Tang 2007). As time goes, the structure deteriorates and the mean value shifts to the right side (see Figure 3.4). It means the crest elevation loss will increase over time (move to the right) when the structure is in condition grade 2 until the mean value reaches to condition grade 3. As mentioned earlier, the first and last condition grades, e.g. grades 1 and 5, follow a different pattern, because it is not possible to inspect a negative value of deterioration for condition grade 1. For the last condition grade, all deterioration values more than the specified threshold are considered as the last condition grade. In this case, the normal distribution may not accurate to show the distribution tails, and lognormal distribution is suggested.

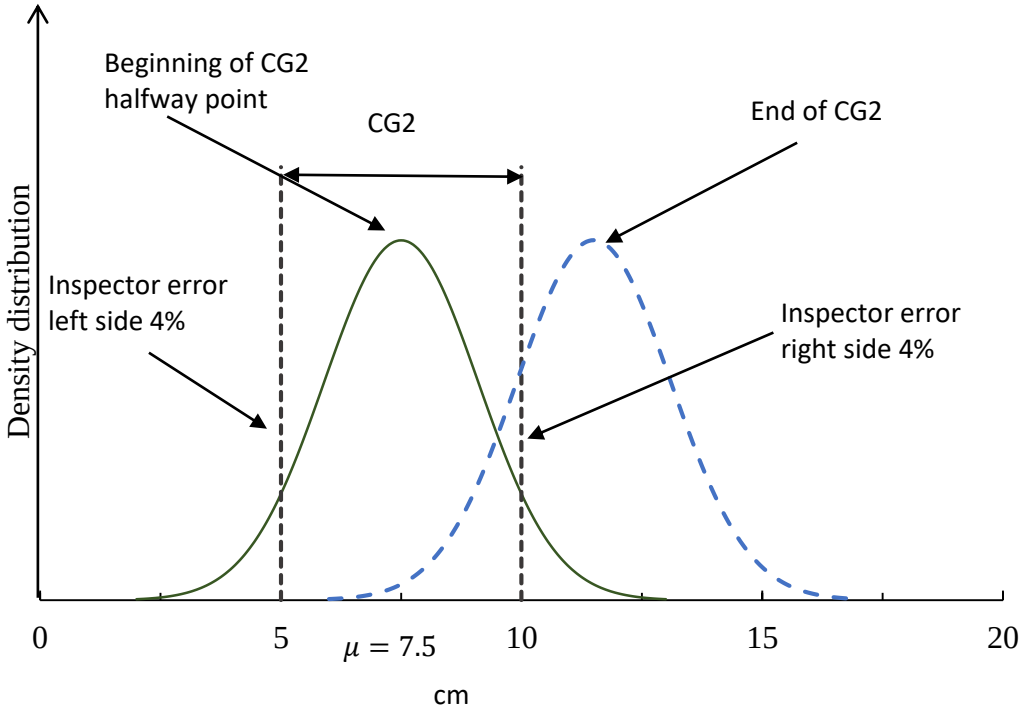

Figure 3.4 Conservative random distribution of deterioration for an asset in condition grade 2 (CG2) when inspecting are correct at 92% of the time.

The lognormal distribution is useful for modelling natural variables and often provides a good representation of a positively skewed physical quantity that extends from zero to infinity (+∞). The probability density and cumulative distribution function for a lognormal distribution are representing here as (Coles et al. 2001)

$$f(x;\mu,\sigma) = \frac{1}{x\sqrt{2\pi\sigma^2}} \cdot e^{-\frac{(\ln \mu x)^2}{2\sigma^2}} \quad ; \ \mu,\sigma > 0 \tag{3.9}$$

$$F(x;\mu,\sigma) = \frac{1}{\sqrt{2\pi\sigma^2}} \int_{-\infty}^{x} \frac{1}{y} \cdot e^{-\frac{(\ln \mu y)^2}{2\sigma^2}} \cdot dy \quad ; \ \mu,\sigma > 0 \tag{3.10}$$

where x is random variable; and μ, σ are mean and variance, respectively. It should be noted that the error of the condition grading results are considered from one side. For example, assume that the quality the inspection assessment for condition grade 1 is 90%, and the right side error tail is 10% (and zero error for left side). Figure 3.5 shows the plot for the lognormal distribution of crest level settlement for a sea dyke assuming in condition grade 1 and 10% error in inspection results.

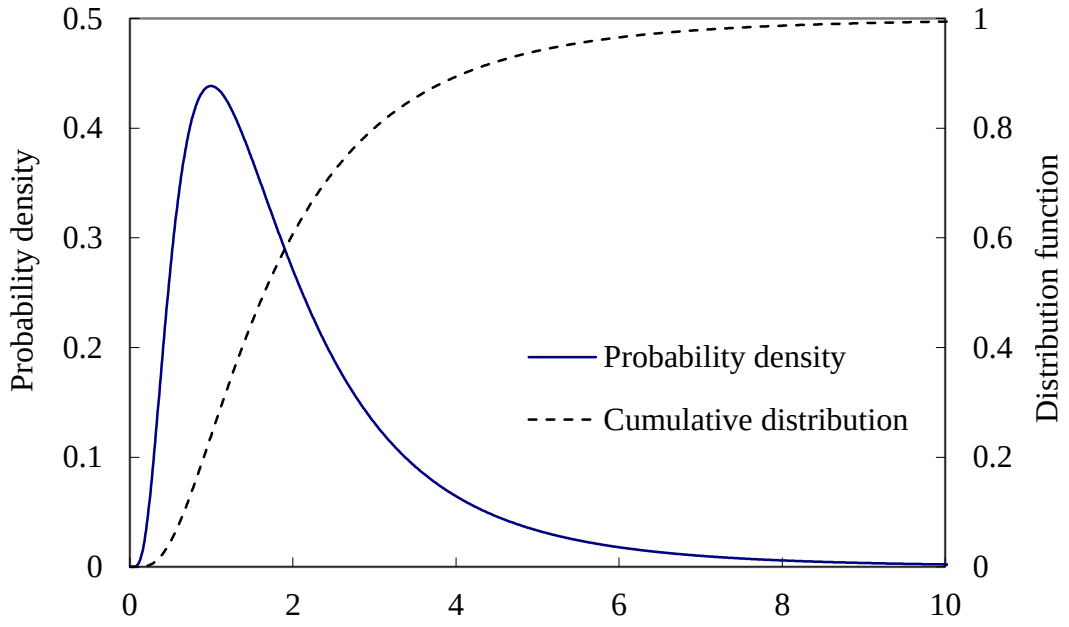

Figure 3.5 The probability density and cumulative lognormal distribution for the example.

Verification of the estimated parameters

There are several methods to verify the values of the estimated parameters (e.g. Garthwaite et al. 2005; Wilks 2011). A simple and straightforward method is utilised here by checking the value of cumulative distribution function. Let $x_{min,i}$ and $x_{max,i}$ be the minimum and maximum values of the loss for condition grade i. For normal

distribution in condition grade i, the cumulative probability of the variables between the minimum $x_{min,i}$ and maximum $x_{max,i}$ values is expressed as

$$F\left(X,\ x_{max,i} \geq x \geq x_{min,i} | \mu_{n,i}, \sigma_{n,i}\right) = 1 - \Pr(inspection\ error) \tag{3.11}$$

For lognormal distributions, the cumulative probability of the first condition grade and the last condition grades is different, as

For the first condition grade:

$$F\left(X, x \geq x_{max,1} | \mu_{log,1}, \sigma_{log,1}\right) = \Pr(inspection\ error) \tag{3.12}$$

For the last condition grade:

$$F\left(X, x \leq x_{min,i} | \mu_{log,i}, \sigma_{log,i}\right) = \Pr(inspection\ error) \tag{3.13}$$

where $F\left(X, x \geq x_{max,1} | \mu_{log,1}, \sigma_{log,1}\right)$ represents the cumulative distribution value where x is more than the expected value for the first condition grade $x_{max,1}$; and $F\left(X, x \leq x_{min,i} | \mu_{log,i}, \sigma_{log,i}\right)$ represents the cumulative distribution value where x is less than the i^{th} condition grade values (for the highest condition grade).

3.5. Hydraulic load monitoring and evaluation

Effective management of flooding requires accurate models that are capable of quantifying failure risk. Quantification of flood risk involves both the quantification of probabilities of extreme events and the associated consequences. Coastal defence risk evaluation models account for the probabilities of extreme hydraulic loading events and also include a probabilistic representation of the performance of defence infrastructure and its associated reliability. The evaluation of the dependency coefficient between the hydraulic variables makes the extreme value evaluations complex. In this thesis, the conventional methods to evaluate dependency between extreme values in England and Wales are developed.

The primary aim of the application of the multivariate approach is to increase the applicability and accuracy of the model with an explicit consideration of the dependence in the extremes of the hydraulic loads. It should be noted that the dependence in the extremes is likely to vary significantly between the sites. The statistical model needs to be sufficiently flexible to capture the range of dependence between the variables

accurately. Of the range of multivariate extreme value models available, the approach of Carter et al. (2013) offers the most flexibility in capturing the range of dependence of hydraulic variables. Other approaches, for example Coles (2001) and Grimaldi and Serinaldi (2006), have restrictive assumptions relating to the dependence among multiple variables. The Carter et al. (2013) approach is therefore the model of choice for this study to be improved regarding dependency estimations.

3.5.1. Extreme values analysis

It is very common in coastal defence context to design a structure to resist a condition so extreme that no similar condition may be found in available measurements or records. This is because even one failure against a rare event may cause to a massive disaster either economically or socially. Hence, probability distributions are utilised to fit the available data and extrapolate the data to find the extreme conditions or events that are likely to occur, taking account of the uncertainties. It should be noted that all hydraulic variables in coastal engineering, e.g. sea levels and wave heights, are continuous functions while measurements are taken at fixed intervals, resulting in a discrete set of values over time or time series. The traditional methods to estimate extreme values, either a high level or low level, relies on the ranking of the quality and period of observations. To have a reliable estimation the minimum period of observed data should not be less than 15 years (Tawn 1992; Weisse et al. 2014).

Block maxima vs peak-over-threshold

The definition of the extreme events in peak-over-threshold is the values that are greater than a threshold value. Instead, in block maxima, the data are "blocked" into sections of a fixed period, and the maximum value from each block is considered for extreme value evaluation. In block maxima method, instead of using all recorded wave heights, the only maximum value of annuals, seasons or defined blocks are considered to estimate extreme wave heights, and this method is compatible with Generalised Extreme Value (GEV) model. On the other hand, in peak-over-threshold (POT), the recorded data over a specific threshold are selected rather than using only maximum annual values, hence, a wider range of data is utilised for estimation, which is appropriate for joint extreme analysis. POT method is a useful technique in Generalised Pareto Distribution (GPD). However, this method is too dependent on the selected threshold value, which needs an

expert judgment to choose an appropriate threshold (Olbert et al. 2017; Karamouz et al. 2017).

Generalised extreme values (GEV)

In probability theory, the generalised extreme value (GEV) distribution is a continuous probability distribution. In coastal defences, the generalised extreme value distribution is the limit distribution of properly normalised maxima of a sequence of independent and identically distributed random variables. Hence, the distribution is often used as an approximation to model the block maxima for sequences of random variables. The cumulative density function is given here as (Bali 2003)

$$F(x;\zeta,\theta,\kappa) = \exp\left[-\left\{1-\kappa\left(\frac{x-\zeta}{\theta}\right)\right\}^{1/\kappa}\right] \tag{3.14}$$

where κ is shape parameter, for $\kappa > 0$ the distribution is Freshet (Type II), for $\kappa < 0$ the distribution is Weibull (Type III), and for $\kappa = 0$ the distribution is Gumbel (Type I); ζ is location parameter; and θ is a scale parameter. The probability density function is given as (Garthwaite et al. 2005)

$$f(x;\zeta,\theta,\kappa) = \frac{1}{\sigma}\{1-\kappa\left(\frac{x-\zeta}{\theta}\right)\}^{\frac{1}{\kappa}-1} \cdot \exp\left[-\{1-\kappa\left(\frac{x-\zeta}{\theta}\right)\}^{1/\kappa}\right] \tag{3.15}$$

Subject to

$$1-\kappa\left(\frac{x-\zeta}{\theta}\right) > 0; \quad \theta > 0 \tag{3.16}$$

The distribution is shown in Figure 3.6 with different shape parameters. There are several mathematical methods in order to estimate parameters of the distributions, which are presents the data for reliability analysis (Martins and Stedinger 2000). This study utilises maximum likelihood method because this method can be applied to a wide range of variables in coastal flood context.

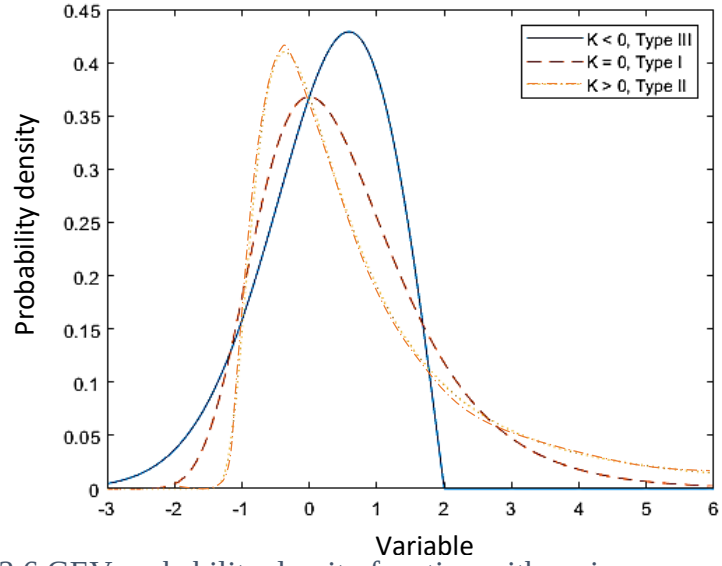

Figure 3.6 GEV probability density function with various parameter values.

Verification of parameters, and simulations

Block maxima and generalised extreme values are often used together because they are naturally compatible. The initial data with its original distribution need to be transformed to a black maxima form with independent time intervals, and the original distribution determines the shape parameter (Garthwaite et al. 2005) of the GEV. For example, assume the frequency of daily water level for five years data is shown in Figure 3.7, where a monthly block within 60 maximum values are considered for 60 months.

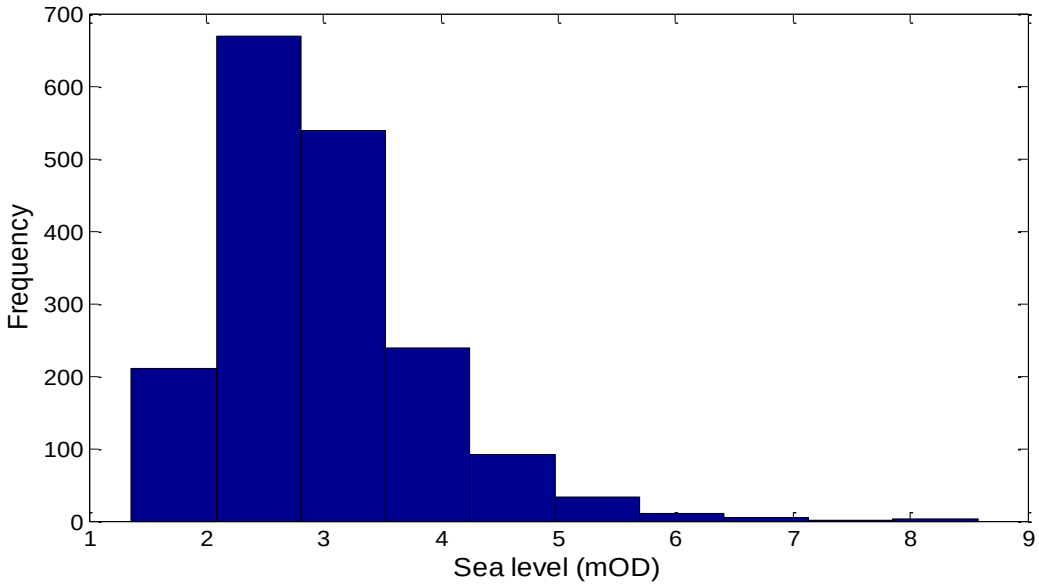

Figure 3.7 Frequency of hypothesis daily water levels for 5 years.

By utilising the MLE method, the values of shape parameter and scale parameter are estimated as 0.0378 and 0.6412, respectively. The 95% confidence interval for the parameters are also calculated, i.e. 0.0050 and 0.0706 are for shape parameter, and 0.6173 and 0.6660 for scale parameter, respectively. The GEV distribution is the type II extreme value distribution as shown in in Figure 3.8, where the tail is heavier than a normal distribution tail. The second step is to check visually whether the estimated parameters are acceptable or not. The fitted probability density function (PDF) is plotted over the block maxima values as shown in Figure 3.8 where the GEV distribution is fitted to the block maxima values, not the original data. It shows that the histogram of the monthly maxima data overlaid with the PDF for the fitted GEV model, with relatively good fit.

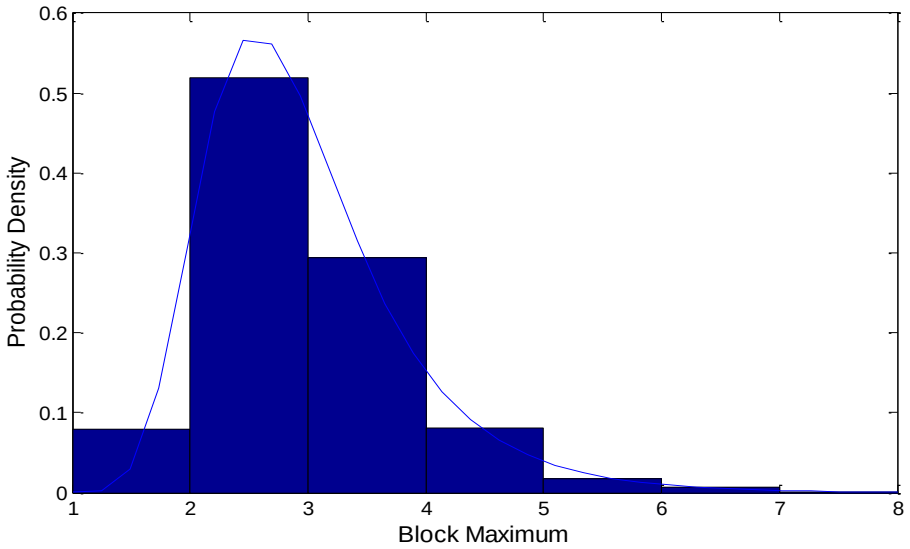

Figure 3.8 The probability density of the block maxima values with a GEV fitted line.

In block maxima, the return level is defined as the block maxima value expected to be exceeded only once in m blocks, which is $(1 - 1/m)$'th quantile. Hence, by adopting the estimated parameters into the inverse cumulative distribution function (CDF), return level R for m is estimated. The critical value that determines the compatible region with the data is based on a chi-square approximation, and lowest confidence level. Therefore, for example for the smallest R_{10} value within the critical region of the estimated shape parameter, the negative log-likelihood is larger than the critical value, which means the estimated shape parameter is acceptable, as shown in Figure 3.9.

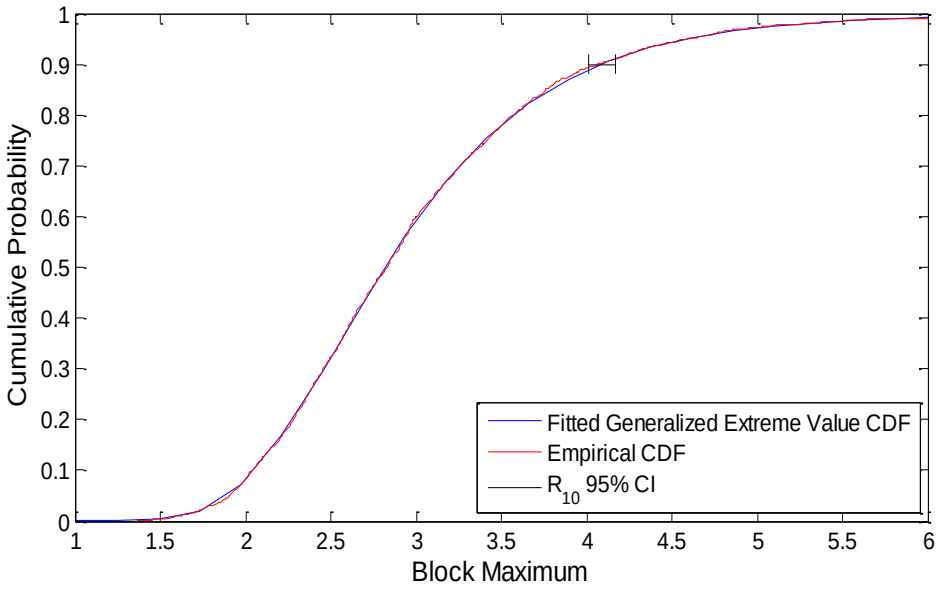

Figure 3.9 The smallest R_{10} value achieved within the critical region of the shape parameter.

Generalised Pareto distribution (GPD)

Generalised Pareto distribution is naturally compatible with peak-over threshold method. The combination of POT and GPD is widely utilised for extreme value analysis, especially for joint extreme values. The threshold value must be chosen properly because the final results are very sensitive to the threshold value u. Let the conditional distribution of the variable X, given $X > u$, be (Coles 2001)

$$\Pr(X \leq x|X > u) = F\,(X \leq x|X > u), \qquad x > u \tag{3.17}$$

where F is the distribution function of X. Then, the generalised pareto distribution function is

$$F(X \leq x|X > u) = 1 - \left\{1 - \frac{\kappa(x-u)}{\theta}\right\}^{1/\kappa} \tag{3.18}$$

where X is greater than the threshold value u; θ ($\theta > 0$) is a scale parameter; and κ is a shape parameter, and for $\kappa = 0$ the function is exponential. Generalised Pareto distribution is often used to model the tails of another distribution. It is useful for extreme value analysis in coastal defence. The generalised Pareto distribution has the following properties (Armagan et al. 2013):

- Generalised Pareto shape parameter of zero when the other distribution's tail decreases exponentially, e.g. normal distributions.
- Generalised Pareto shape parameter of positive value when other distribution's tail decreases as a polynomial.
- Generalised Pareto shape parameter of negative value when other distribution's tail is finite.

Figure 3.10 shows the example of the GPD with different scale parameters that produce tails for various types of distributions.

The probability density function f of a GPD distribution with location ζ, scale θ and shape κ parameters, as expressed here (Coles et al. 2001)

$$f(x) = \frac{1}{\theta}(1+\kappa)^{-(1/\kappa+1)} \tag{3.19}$$

where x stands for the desired variable, e.g. sea level or wave height; and $z = (x-\zeta) / \theta$. The scale and shape parameters can be estimated by the maximum likelihood method discussed in following section. This method estimates unbiased parameters with smallest mean square errors especially for large samples.

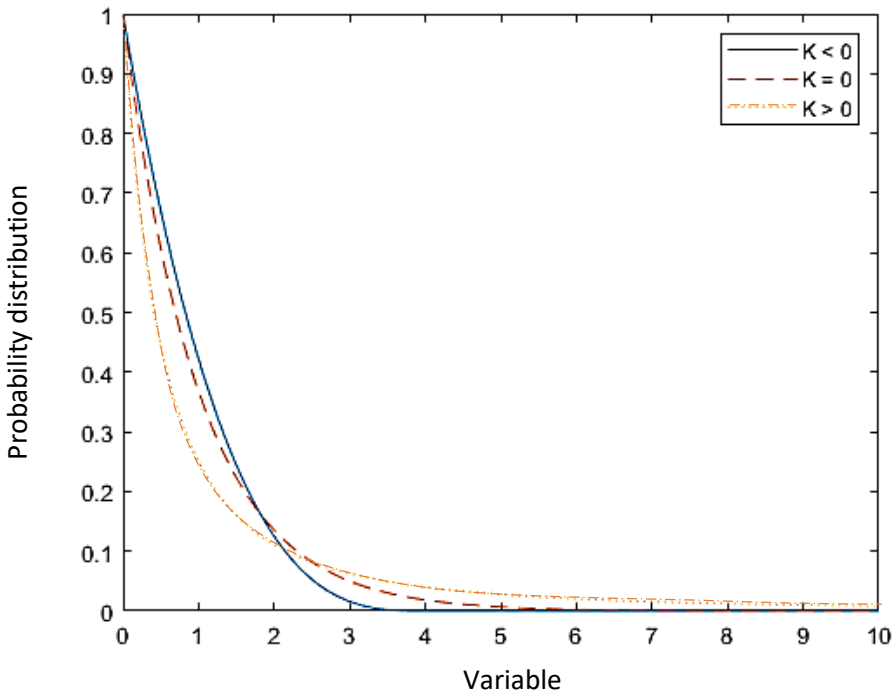

Figure 3.10 GPD probability density for various parameter settings.

Parameter estimation (GPD)

Maximum likelihood method is a common method for parameter estimation process as mentioned before. The first step is to define a likelihood functionι which is the function of observed data and the density function f. The function needs to be maximized with consideration of the selected distribution. The likelihood function is given as (Rakonczai and Zempleni 2012)

$$\iota(x|\theta,\kappa) = \prod_{i=1}^{n} f_X(x_i|\Theta_d) \tag{3.20}$$

where Θ_d is the set of parameters for the density function. As the density function described in the previous section is in exponential form, hence the log-likelihood function is more appropriate for formulation. Let x_i be a sample with size n, the log-likelihood function for generalised pareto distribution is expressed here as (Castillo and Daoudi 2009)

$$\iota(\vartheta,\kappa) = -\log(s\,\kappa\theta) - \frac{1+\kappa}{\kappa\, n}\sum_{i=1}^{n}\log(1+s\left(\frac{x_i}{\theta}\right)) \tag{3.21}$$

where $s = sign\,(\kappa)$ is the sign of the empirical coefficient of variation of the sample. If $\kappa < 0$ it is assumed $\theta > M = \max x_i$, otherwise the likelihood is zero. The restriction $-0.5 < \kappa < 0.5$ is usually assumed for both practical and theoretical reasons, since GPD with $\kappa < -0.5$ has finite end points and the probability density function is strictly positive at each endpoint, and GPD with $\kappa > -0.5$ has infinite variance (Davison and Smith, 1990; Castillo and Hadi, 1997). Then, by equating the derivate of above equation to zero, the parameters can be estimated as (Castillo and Daoudi 2009)

$$\hat{\kappa} = \frac{1}{n}\sum_{i=1}^{n}\log(1+s\left(\frac{x_i}{\theta}\right)) \tag{3.22}$$

Threshold selection for GPD

As discussed earlier, threshold selection is a critical step to have an appropriate GPD fit, because choosing a too high threshold leads to insufficient data to estimate a proper exceedance probability, while choosing a too low threshold leads to overestimated and disqualified data simulations (Davison and Smith 1990). A common and reliable approach to select a suitable threshold u is to use mean residual lie plot suggested by Davison and Smith (1990). Let X be $X - u|X > u$ has a GPD distribution with (θ,κ)

parametres, then for all thresholds $\hat{u} > u$, $X - \hat{u}|X > \hat{u}$ is GPD distribution with $(\theta + \kappa(\hat{u} - u), \kappa)$ parametres. It is expressed here as (Rinker 2013)

$$E(X - \hat{u}|X > \hat{u}) = \frac{\theta + (\hat{u} - u)\kappa}{1 - \kappa} \tag{3.23}$$

where E shows that the mean excess of X over $\hat{u}$ is a linear function of $\hat{u}$. Hence, by plotting the residual life plot, the threshold is the value that the plot shows approximately a linear behaviour.

Verification of the parameters and simulations

Generalised Pareto distribution is often defined in terms of exceedance probability. The original distribution of the variable, e.g. wave height, is divided by the selected threshold, and the values below the threshold are omitted. Hence, the distribution of the retained values is almost a GPD. However, the original distribution controls the shape parameter of the resulting distribution. For example, 1500 recorded data of wave heights are assumed as shown in Figure 3.11. Figure 3.12 shows the mean residual life plot, where a graphical procedure for identifying a suitably high threshold for modelling extremes via the GPD model is used. In this plot, for a range of threshold values, the corresponding mean threshold excess is identified, and the threshold value from linear part in the plot is selected. From the plot, linearity in Figure 3.12 might be suggested above 1.30 m, where information on the far right–hand–side of these plots is unreliable.

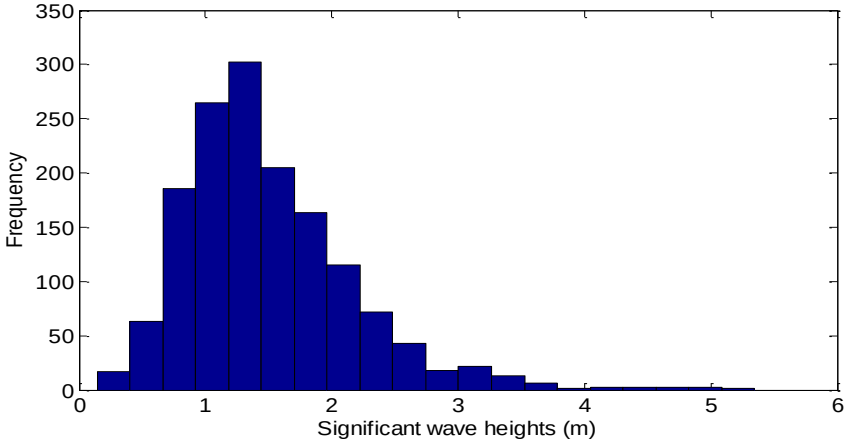

Figure 3.11 Frequency of the the wave heights.

The maximum likelihood method is utilised to estimate the parameters of the distribution for two different threshold values i.e. 1.30 m and 2.50 m for comparison. The MLE gives

0.0331 for shape parameter, and 0.6362 for scale parameter by assuming the threshold is 1.30 m, and gives -0.0243 for shape parameter and 0.5920 for scale parameter, by assuming the threshold is 2.50 m. The diagnostic plots are provided for two selected thresholds in Figure 3.13 and Figure 3.14. A comparison between the plots verifies the superiority of 1.30 threshold value. The density plot shows that how the first GPD fitted models covers more data, and the probability plot proves that the simulated model for the first GPD model is much closer to the original data.

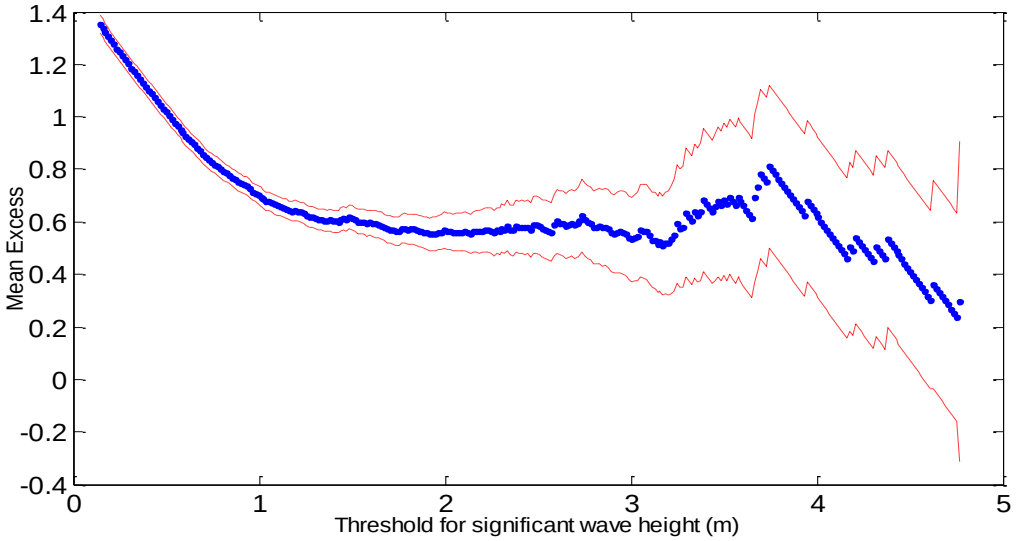

Figure 3.12 Mean residual life plot for the significant wave heights (dots) with 95th percentile (dashed lines).

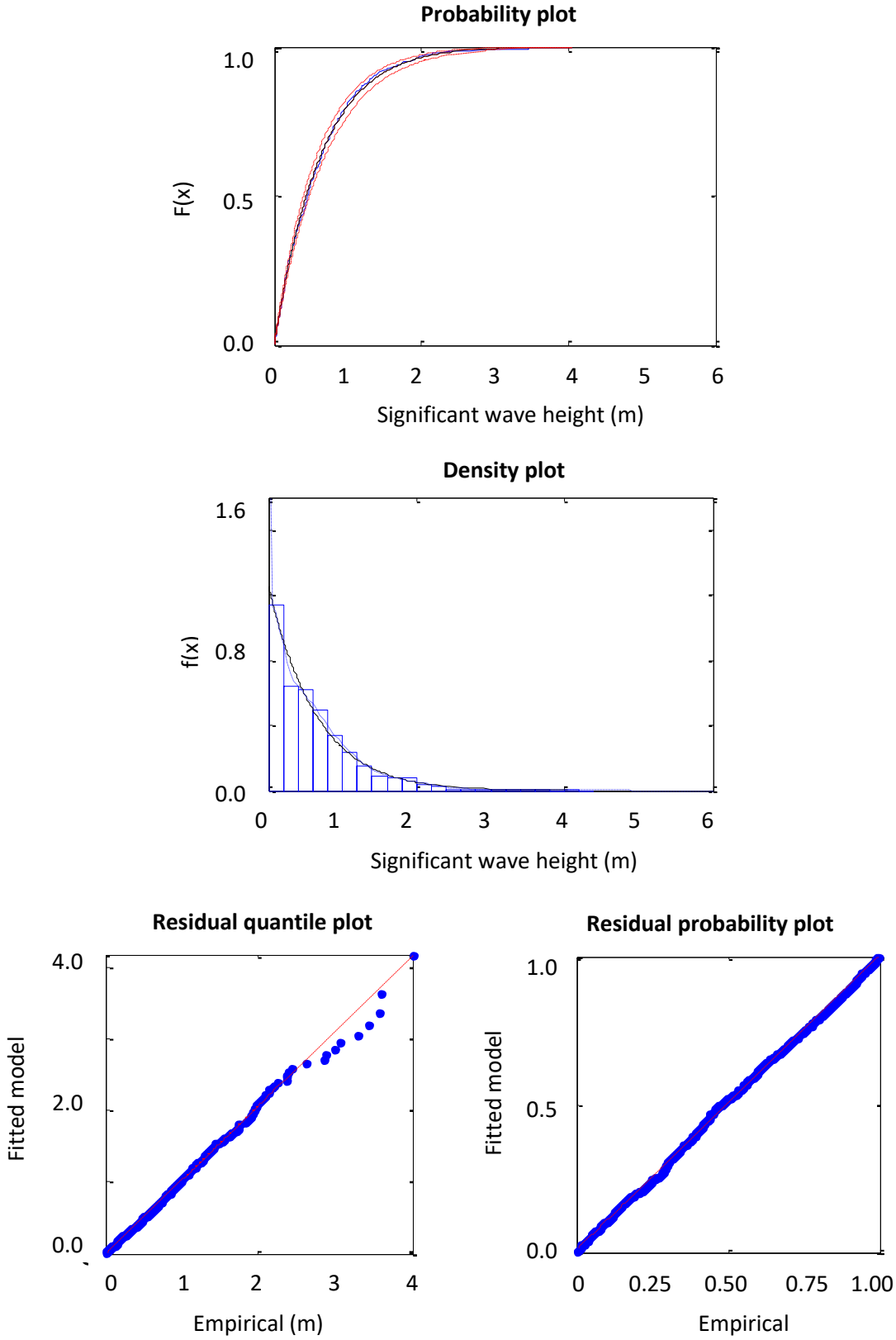

Figure 3.13 Diagnostic plots for the GPD model with a threshold value of 1.30 m.

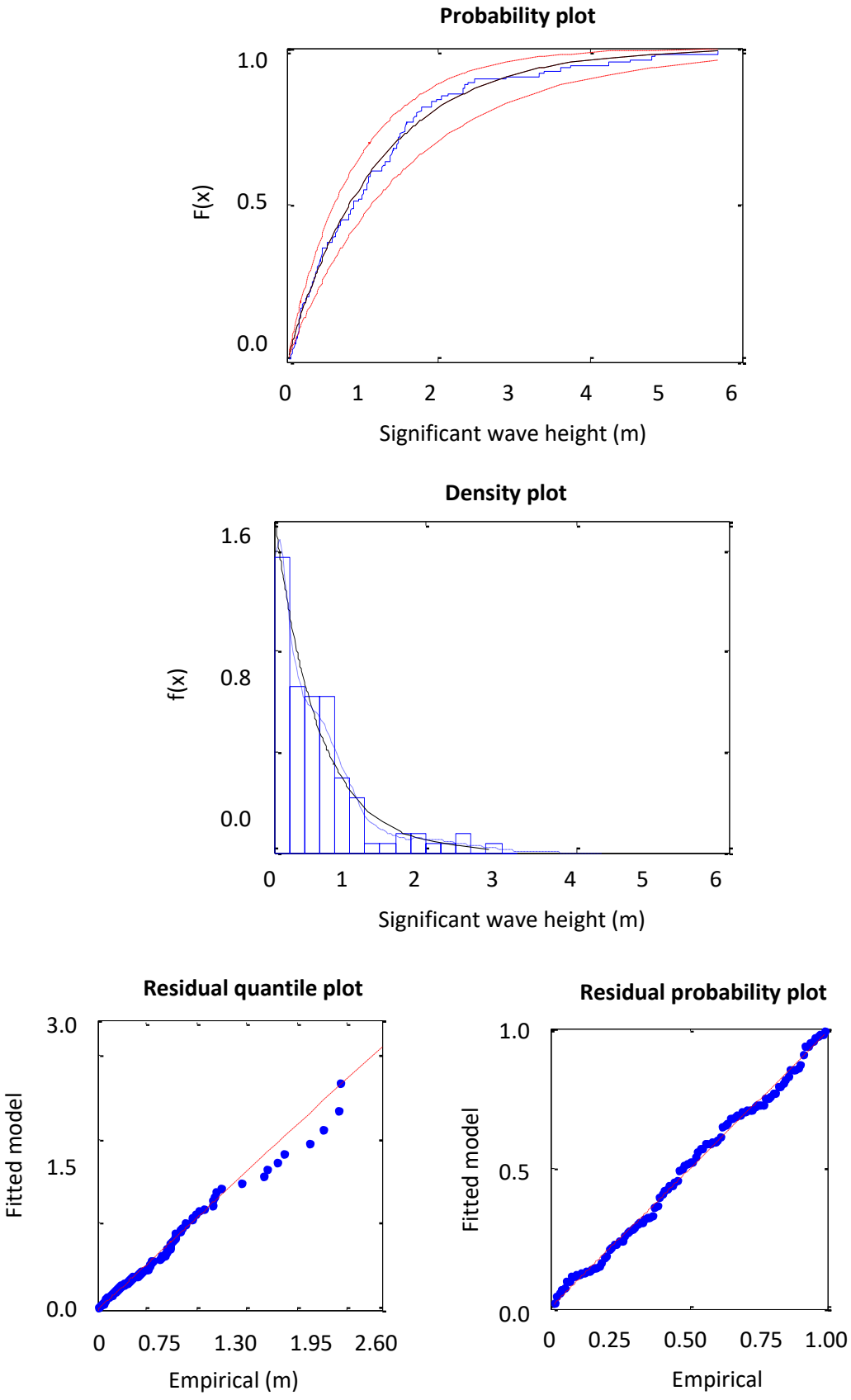

Figure 3.14 Diagnostic plots for the GPD model with a threshold value of 2.50 m.

3.5.2. Joint probability of sea level and significant wave height

Joint probability is useful in the situations that two or more conditions have a chance to occur at the same time. In these circumstances, the dependency between two or more conditions is neither zero (independent) nor one (entirely dependent). In the case of coastal defence structures, there is usually a degree of dependence between critical parameters, which vary from place to place due to hydraulic and meteorological effects (Hawkes 2008; Kuczera et al. 2006).

Therefore, joint probability method is a useful tool to estimate the probability of simultaneous occurrence of crucial hydraulic variables. Figure 3.15 shows an example of joint probability illustration with marginal distributions for arbitrary variables. It shows the density distribution of variables 1 and 2 are at highest probability, when they are around values -0.5 and 2.0, respectively, at the same time. It is essential to evaluate extreme values for the combination of key variables such as significant wave heights and sea level. It is also necessary to evaluate the failures caused by individual variables in risk analysis of coastal flood defences.

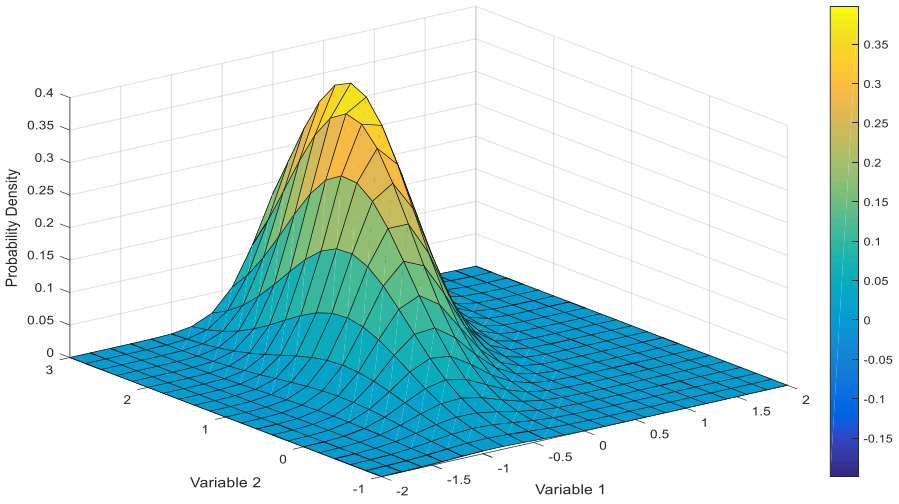

Figure 3.15 Illustration of a joint probability distribution example.

Failures in coastal defence structures may occur due to only high water level such as overflow or excessive overtopping, or may occur due to both high wave heights and high sea level. Studies show main variables in coastal defence hydraulic loads are not independent, and assuming independency between them leads to an underestimated

extreme value evaluation (Ewans and Jonathan 2014; Pugh and Vassie 1980). Technical reports published by Environment Agency consider dependency to use the joint probability mathematical functions. Joint probabilistic methods provide the ability of considering both correlation and uncertainties in the key parameters with consideration changing environments.

Joint probability method in coastal defences

Hawkes (2008) and Hawkes et al. (2008) introduced joint probability methods in coastal defences by several case studies. The joint probability method used in this study focuses on three factors: water level, significant wave height and wave period. Five stages of the method are defined as (Hawkes 2008):

- Preparation of initial data.
- Distribution fitting of single variables.
- Extreme value analysis of single variables.
- Dependency analysis between variables.
- Combination and interpretation of results to understand the behaviour of joint variables together.

Preparation of data and distribution fitting of single variables are based on statistical and observational methods. The initial data should cover an acceptable range of period to provide proper information on hydraulic conditions including extreme events. Then, the data should be fitted to a suitable distribution, e.g. Generalised Extreme distribution. Extreme values of each variable are estimated using the mentioned GEV or GPD models. The next step is an estimation of dependency between variables that are necessary for data simulations. Finally, the results should be combined and present in a proper way to demonstrate the extreme conditions of the case study.

Joint probability methods in coastal and fluvial defence structure risk assessment are still at the level of researching, e.g. Garrity et al. (2006) and Gelder et al. (2004). Cai et al. (2007) developed the correlation assessment methods for simulations of large samples of data. Chini and Stansby (2012) introduced a method for extreme values of wave overtopping to estimate the projected failure due to the joint probability of sea level rise and wave height change. Rakonczai and Zemplénia (2011) developed a joint probability method to evaluate bivariate or multivariate extreme values. The method is suitable for

sea level rise issue. Joint probability methods are still under development to improve the accuracy of estimations (Ewans and Jonathan 2013; Mazas et al. 2014). Generally, the joint distribution of two random variables X and Y are defined as

$$F(x_v, y_v) = \Pr[(X \leq x_v) \cap (Y \leq y_v)] = \iint_{-\infty}^{x_v, y_v} f(x_v, y_v) dx dv \tag{3.24}$$

where x_v and y_v are arbitrary variables; and $f(x_v, y_v) \geq 0$ is the joint probability density function, and the total area under the joint density function is unity. For each variable, e.g. X, F_X and f_X are the marginal cumulative and density functions, respectively. The marginal density functions are given here as (Ewans and Jonathan 2013)

$$\begin{aligned} f_x(x_v) &= \int_{-\infty}^{\infty} f(x_v, y_v) dy \\ f_y(x_v) &= \int_{-\infty}^{\infty} f(x_v, y_v) dx \end{aligned} \tag{3.25}$$

The joint distribution of sea water level H_w and depth limited significant wave height H_{m0} can be expressed as

$$F(H_w, H_{m0}) = \Pr[H_w > x_v,\ H_{m0} > y_v] \tag{3.26}$$

where x_v and y_v are extreme values of the variables. The probability is estimated as above, forms a contour line which is obtained by (Reeve 2009)

$$\begin{aligned} \Pr[x_0 < H_w < x_1,\ y_0 < H_{m0} < y_1] = F(x_0, y_0) + F(x_1, y_1) - \\ F(x_0, y_1) - F(x_1, y_0) \end{aligned} \tag{3.27}$$

In this study, copula dependence function C and Monte Carlo simulations are applied to joint probability analysis for bivariate random variables with identical marginal distributions. The dependence measure provides an estimate of the probability of one variable being extreme, given that the other one is extreme. The dependence model is defined by transforming the variables to a bivariate form. The correlation between the hydraulic variables has a considerable effect on the joint probability results (Hawkes et al. 2008).

Marginal distribution for joint probability

Before considering the joint probability between the variables, the marginal distribution of these variables needs to be determined. For the marginal distributions, the GPD model is selected due to the discussion in this chapter. However, GEV model is also used to

estimate the extreme values. Selection of a suitable threshold for marginal distributions depends on expected lifespan of the structure, hydraulic condition of the site and intended use of the structure. An optimum threshold of acceptable return period will consider both economic and safety matters of a coastal defence system.

Correlation between the variables

The estimate of correlation coefficient ρ between two variables proposed by CIRIA (2007) could be rewritten for sea level H_w and significant wave height H_{m0}, expressed here as (HR Wallingford 2000)

$$\rho = \frac{Cov(H_w, H_{m0})}{\sqrt{Var(H_w)Var(H_{m0})}} \tag{3.28}$$

where Cov is the covariance between the variables, and Var is the variance. The range of correlation interval is between [0, +1], where $\rho = 0$ means the variables are independent and $\rho = 1$ means the variables are fully dependent.

Marginal distributions are determined by fitting either a generalised Pareto distribution (GPD) or generalised extreme value (GEV) to the key variables, as disused in previous sections. In order to combine the marginal distribution and evaluate dependence structure, a copula function is integrated. The copula function C is a multivariate distribution with uniform marginal distributions, and expressed here as (Grimaldi and Serinaldi 2006)

$$C(u, v) = \Pr[u \geq U, v \geq V] \tag{3.29}$$

Let $H(x_v, y_v)$ be the joint distribution of the variable x_v and y_v, e.g. water levels and wave heights, hence

$$H_{x,y}(x_v, y) = C\left(F_x(x_v), F_y(y_v)\right) \tag{3.30}$$

In this study, the Metaellipical copulas model is used, which is described by Genest et al. (2007). The joint exceedance and the joint return period value $T(x_v, y_v)$ is given as (Zhang and Singh 2007)

$$\Pr[X > x_v, Y > y_v] = 1 - F_x(x_v) - F_y(y_v) + H_{x.y}(x_v, y_v) \tag{3.31}$$

$$T(x_v, y_v) = \frac{1}{\lambda_j\left(1 - F_x(x_v) - F_y(y_v) + H_{x.y}(x_v, y_v)\right)} \tag{3.32}$$

where λ_j is the mean number of events per year.

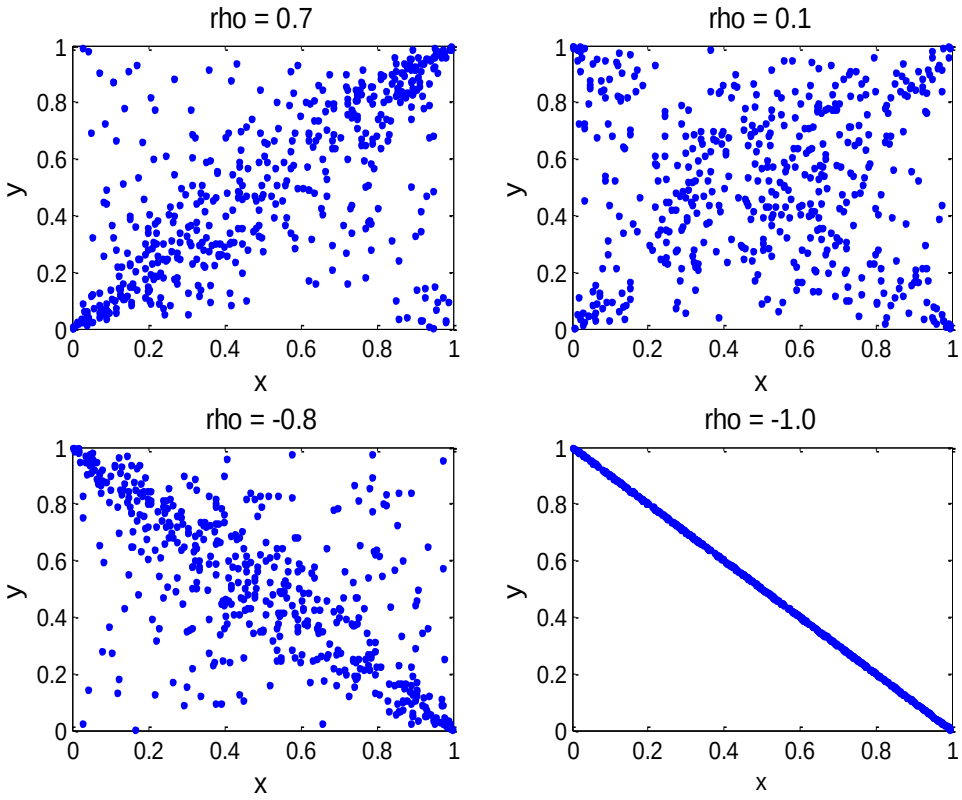

Figure 3.16 The effect of various dependency coefficients between two arbitrary parameters.

Simulation process for major variables

For Monte Carlo simulations, selecting a distribution and its parameters for each individual variable is often straightforward, but deciding what dependencies should exist between the inputs is complicated (Binder et al. 1993; Cai et al. 2007). Original observations data to a simulation should reflect the dependence among the variables being modelled. The process of data analysis and simulation in this thesis is as follows:

1. Fit extreme value to key variables e.g. water level and wave height.
2. Transform each variable, changing the marginal distributions into lognormal. The transformed variables still have a statistical dependence.
3. Transform the data to the copula scale (unit square) using a kernel estimator to find out the dependence value.

Interpretation of the joint probability results

Joint probability results can be presented in three common ways:

- Joint probability density.

- A structure function.
- Joint exceedance.

Joint probability density is a form of joint density function, which is only suitable for full analytical approaches, i.e. JOIN-SEA and dependence measure χ. In this method Monte Carlo simulations of data are visualized as a scatter diagram with the information on probability density, extreme values, and dependency of variables. Structural function illustrates a response based on the selected variables. This method for coastal defence structures can be used for mean overtopping rate and wave run-up, as they can be described as a function of a constant structural function such as crest level or seaside slope. This is an effective method for estimation of high and extreme values of a particular structural variable, which could reduce a joint probability problem to a single-variable problem. However, calculations should be repeated for other structural functions or for other structures in that coastal defence system (Hawkes 2008).

Joint exceedance illustrates the probability of specific values of one variable that will be exceeded at the same time for a given value of the second variable. It could be expressed as return period for extreme values. However, the results should be tested for various combinations of the same return period to find out the most critical combination of design. In this method, the higher joint return values are used, the higher reliability occurs in the future (Hames and Reeve 2006). Figure 3.17 shows joint exceedance and joint structural probabilities on a bivariate diagram.

3.6. Climate change impacts

Studies have been carried out recently to undertake the reliability and failure analysis of coastal defence affected by future climate changes as discussed in literature reviews. However, the knowledge about the effects of climate change over the hydraulic variables is still very limited (Masselink and Russell 2013). For example, most literature published by 2014 claimed that the wave heights remain unchanged during the projected sea level rise (e.g. Hallegatte et al. 2011), but latest studies show that the wave periods will increase due to the sea level rise (e.g. Dahl et al. 2017).

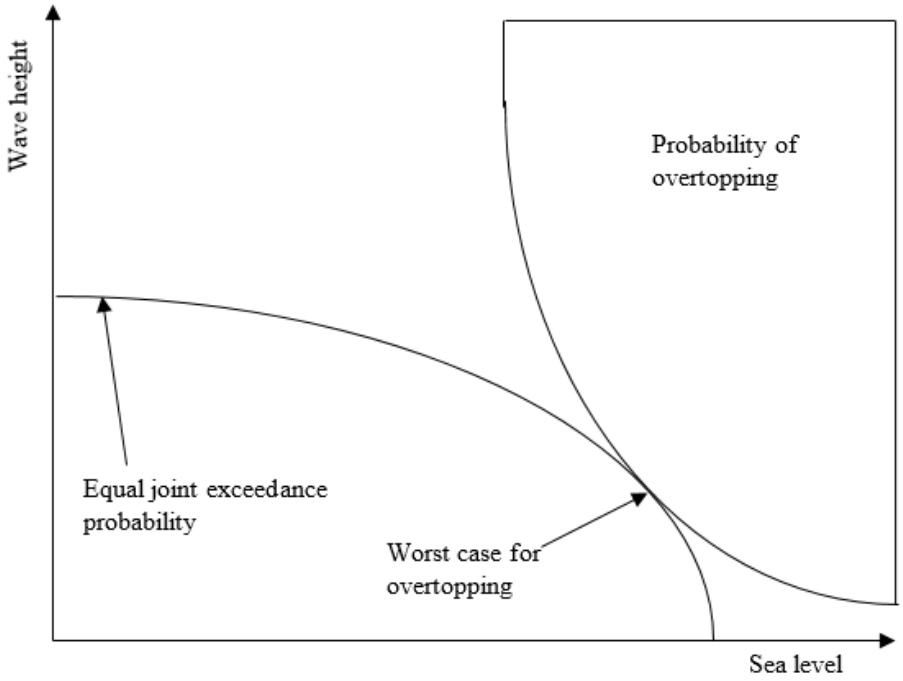

Figure 3.17 Joint exceedance probabilities for wave overtopping failure mechanism (Adopted from HR Wallingford, 2000).

Another problem of the controversial models for estimating the effects of sea level rise on the hydraulic variables are their complexity. The studied models that predict the future behaviour of wave conditions are time-consuming and complicated. This thesis is presenting a straightforward model to estimate the future primary hydraulic variables subject to sea level rise. However, it should be noted that the proposed model is only useful for the studied failure mechanisms described in this thesis (e.g. wave overtopping and piping), and more studies are necessary for other failure mechanisms.

Sea level rise will increase the wave attack on sea flood defences if the wave heights are depth-limited. The depth-limited significant wave height H_{m0} depends on many factors including still water level at the toe of the sea defence. The depth-limited significant wave height H_{m0} is estimated from the interpolation between local relative water depth h_l and deep-water wave steepness S_{op} considering the foreshore slope [25]. The local water level $h_w(t)$ at the toe increases with time due to sea level rise $\Delta h_w(t)$, expressed here as

$$h_w(t) = h_w(0) + \Delta h_w(t) \tag{3.33}$$

where $h_w(0)$ is the initial water level at present day and it is associated with the design water level within a chosen return period. From the energy decay numerical model for

uniform foreshore slope by Van der Meer (1990, 2016), the depth-limited significant wave height H_{m0} can be estimated from hydraulic conditions including local relative depth $h_l(t)$, deep-water wave steepness S_{op} and foreshore slope. The local relative water depth $h_l(t)$ is expressed as

$$h_l(t) = \frac{h_w(t)}{L_{op}} \tag{3.34}$$

where peak wave length L_{op} is related to peak wave period T_p, and it is estimated as

$$L_{op}(t) = \frac{g \cdot T_p^2}{2\pi} \tag{3.35}$$

where g is the acceleration due to the gravity. The rise in wave periods due to climate change is negligible (Van der Meer et al. 2016) and it is ignored in this study. The deep-water wave steepness S_{op} is defined as deep-water significant wave height H_{so} over peak wave length L_{op}, given here as

$$S_{op} = \frac{H_{so}}{L_{op}} \tag{3.36}$$

where H_{so} is significant wave height at deep-water. The depth-limited significant wave height associated with sea level rise over time can be estimated if the wave parameters together with the deep-water significant wave height are available.

3.7. Case study at Portsmouth

A numerical example for a system of three different types of earth dykes situated at Portsmouth, England described by Taylor et al. (2009) is utilised for showing the condition assessment and load evaluation with consideration of the sea level rise. The average crest level is 4.80 mOD, crest width 6.00 m, seaside slope $Cot(\alpha) = 5.5$, seabed slope 1:30 with turf and different core materials. A public access area/walkway is located on the landward side of the dykes. It is assumed that the sea dykes are in very good condition (condition grade 1).

Table 3.8 Transition of the dykes condition grades from 1 to 5 over time (Harlcrow 2013).

	Slowest estimate (yr)					Medium estimate (yr)					Fastest estimate (yr)				
	1	2	3	4	5	1	2	3	4	5	1	2	3	4	5
Dyke 1	0	**18**	35	62	74	0	**14**	32	52	**55**	0	12	**18**	**35**	55
Dyke 2	0	20	**34**	60	70	0	16	**28**	50	60	0	10	20	38	**48**
Dyke 3	0	22	36	**56**	**68**	0	15	30	**48**	58	0	**9**	22	40	50

3.7.1. Selecting the deterioration curve

The first step is to select an appropriate deterministic deterioration curve for the sea dyke. There are three types of earth dykes with turf and impermeable materials, which is situated in coastal and estuary environment. The structures are wide (crest width more than 4.00 m), and according to Halcrow (2013) the lifecycle for the condition grades of these three structures are given in Table 3.8. In order to estimate the critical transition year for the dyke system, the minimum year transition to a new condition grade among the three dykes should be considered for the system, as highlighted in bold in the table. Table 3.8 provides the information for slow, medium and fast deterioration rates, where the medium deterioration rate is often considered for standard conditions. For each deterioration rate between the three types of dykes, the minimum values are identified (bold value). The final deterioration curve is shown in Figure 3.18, and will be used in deterioration process analysis which will be discussed in the next chapter.

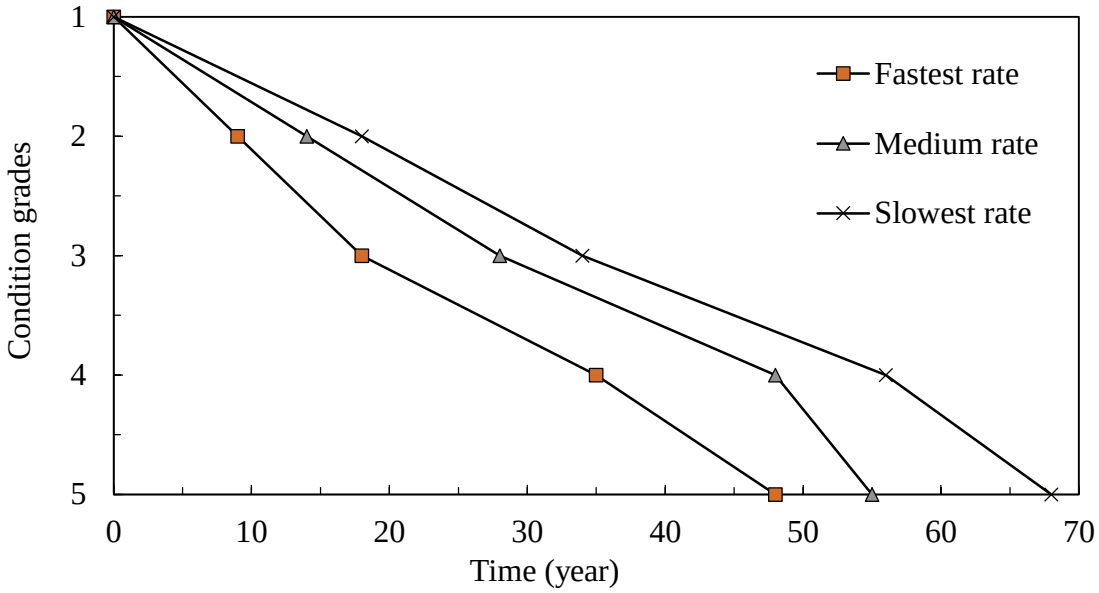

Figure 3.18 Estimated times to next condition grade from condition grade 1 for the dyke system.

3.7.2. Probability distributions of the dyke damage

From the beginning of this chapter, the probabilistic accuracy of available inspection strategies is estimated. Then the measurable visual indicators are correlated to the relevant failure mechanisms, and the damage intensity is defined in a condition grade system. Finally, the methodology to describe the damage using probabilistic distributions

is given. The proposed method is utilised to present grade-based distributions for damage relevant to overtopping and piping failure mechanisms in this case study.

Table 3.9 Suggested condition grade for geometrical loss in earth sea embankments and their density distribution referred to Tables 3.5-3.7.

Condition grade	Seepage length loss (m)	Crest level loss (m)	Slope lowering (degree)	Density distribution
1	0.00-0.05	0.00-0.05	0.00-2.50	Lognormal
2	0.05-0.15	0.05-0.10	2.50-4.00	Normal
3	0.15-0.30	0.10-0.20	4.00-6.00	Normal
4	0.30-0.60	0.20-0.40	6.00-10.00	Normal
5	0.60+	0.40+	10.00+	Lognormal

Table 3.9 shows the suggested condition grade for the loss in seepage length, crest level and slope in the dykes with respect to their condition grade. The values in the table are general values that discussed previously in this chapter and gathered from Environment Agency publications (e.g. Long et al. 2013). It should be noted that the values could be slightly different if a site-specific investigation implemented. The first and the last condition grades are represented by lognormal distributions while the other condition grades are assumed to be normally distributed. The distributions of the loss for three different visual indicators are presented in Figure 3.19 and Figure 3.20, by assuming the inspection strategies are Tier 3 and Tier 1, respectively. The mean and standard deviation of the distributions are calculated using Equations (3.5-3.12) and verified by the proposed method in the current chapter. For example for a sea dyke in condition grade 4, the crest level loss due to deteriorations is between 20 and 40 cm with a mean value of 30 cm. According to the case study report, the accuracy of the inspection strategies are 80% and 94% for Tier 1 and Tier 3 strategies, respectively. The standard deviations of the distributions are 5.3 and 7.9 for Tier 3 (94% correct) and Tier 1 (80% correct) inspection strategies, respectively. Hence, the cumulative probability between the values of minimum and maximum (20 and 40) needs to be about 94% and 80% for Tier 3 and Tier 1 inspection strategies, respectively. Figure 3.21 shows the cumulative probabilities for the condition grade 4 for Tier 3 strategy and verifies the estimated parameters for the distribution are acceptable. The plot is obtained using Equation 3.5 for probability density of normal distribution, and the verification is obtained using Equation 3.11.

The estimated mean and standard deviations for seepage length and crest level loss in condition grade 1 (Lognormal distribution) are 0.60 and 0.58 for Tier 3, 0.60 and 1.19 for Tier 1 inspection strategies, respectively. This means the cumulative probabilities for maximum value in condition grades 1 or 5 should be equal to 0.94 and 0.80 for Tier 3 and Tier 1, respectively. Table 3.10 verifies the estimated parameters for the lognormal distribution and shows the cumulative probabilities for the condition grade 1 for Tier 3 and Tier 1 strategies, which are about 94% and 80%, respectively.

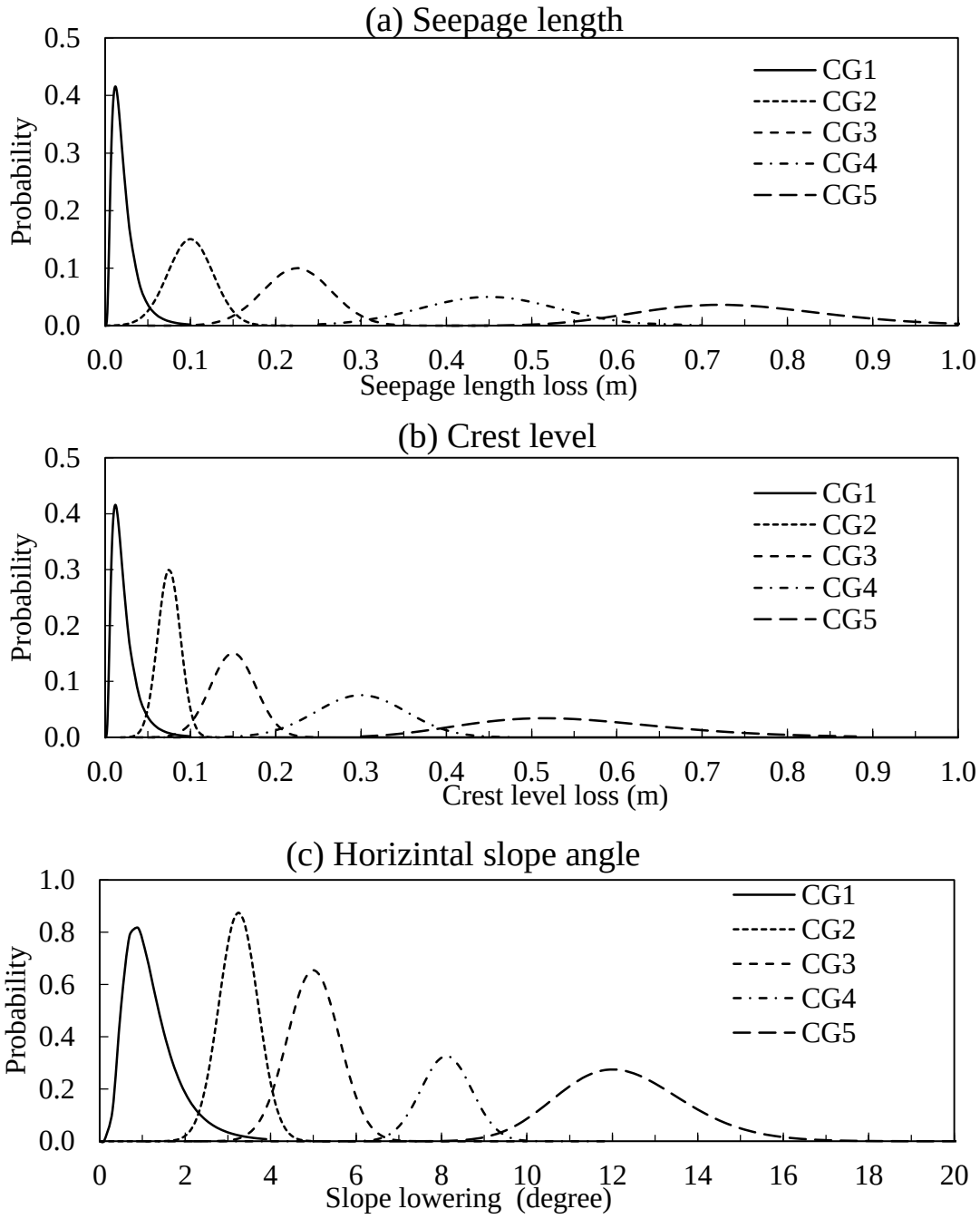

Figure 3.19 Probability density distributions associated with condition grade (CG) of the earth sea dyke regarding the Tier 3 inspection strategy.

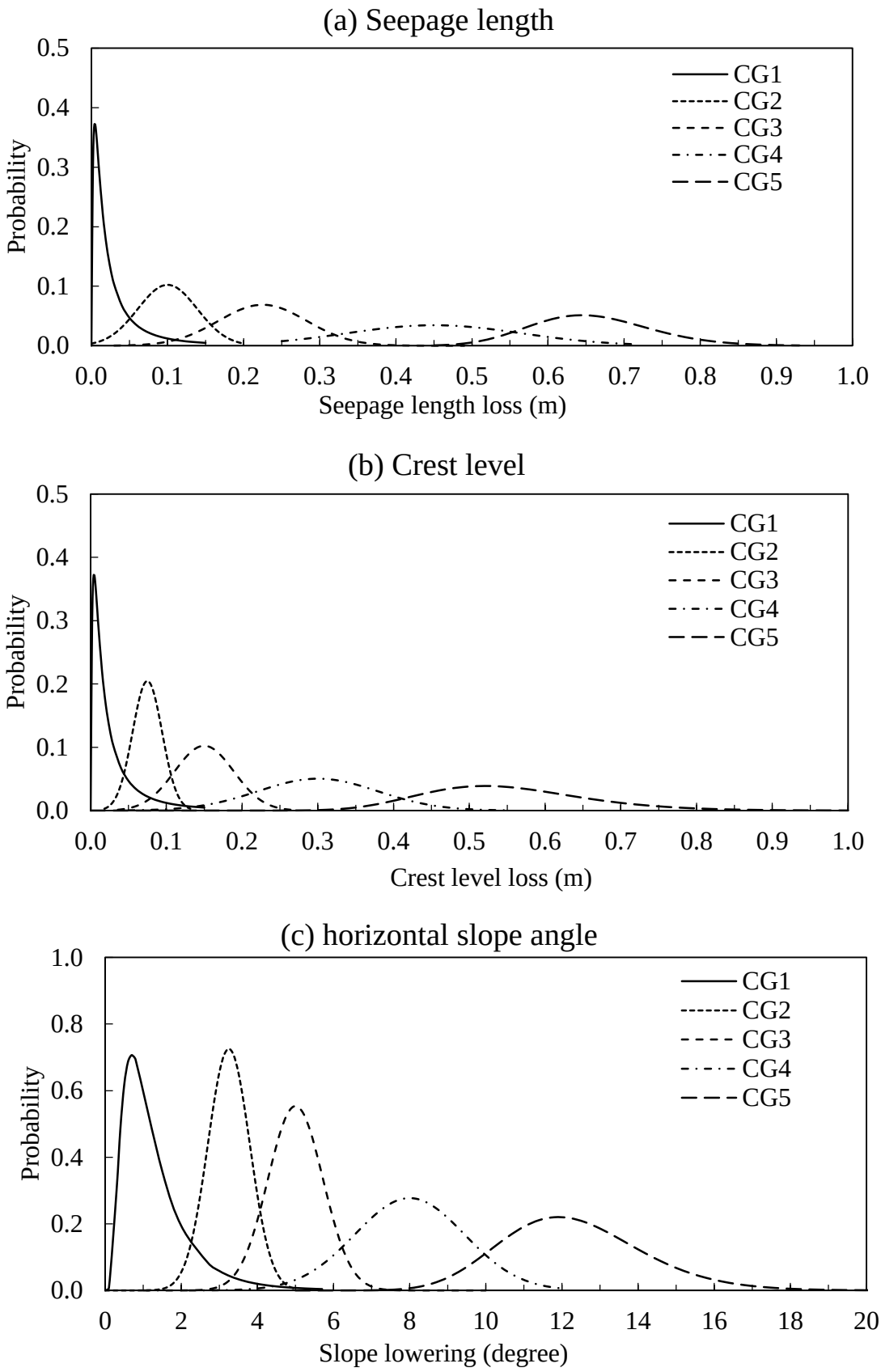

Figure 3.20 Probability density distributions associated with condition grade (CG) of the earth sea dyke regarding the Tier 1 inspection strategy.

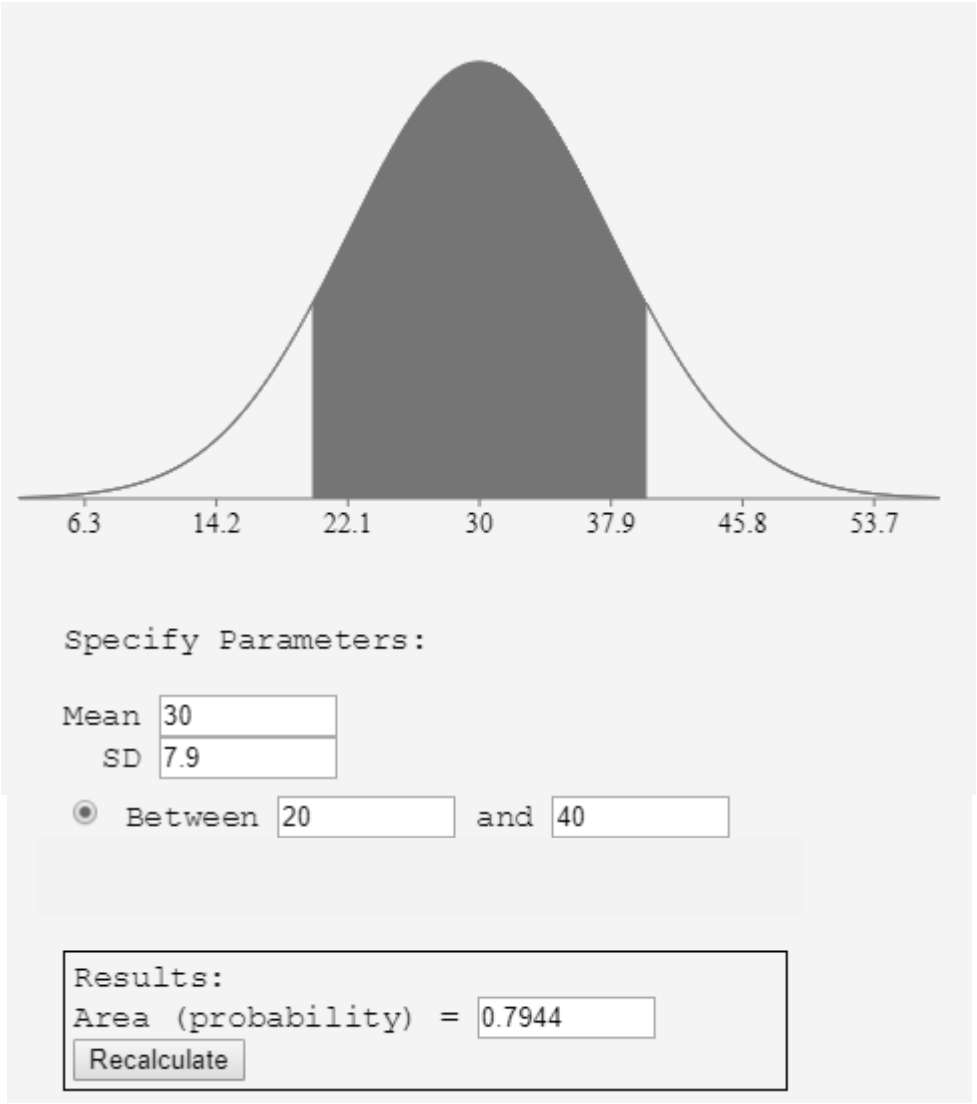

Figure 3.21 Verification of the estimated normal distribution parameters.

Table 3.10 Verification of the estimated lognormal distribution parameters for the example.

$\mu =$	0.60			$\mu =$	0.60		
$\sigma =$	1.19			$\sigma =$	0.65		
Quantiles		Cumulative distribution		Quantiles		Cumulative distribution	
r	q_r	x	$F(x)$	r	q_r	x	$F(x)$
0.1	0.40	1	0.30706	0.1	0.79	1	0.17798
0.25	0.82	2	0.53120	0.25	1.18	2	0.55697
0.5	1.82	3	0.66239	0.5	1.82	3	0.77849
0.75	4.07	4	0.74561	0.75	2.82	4	0.88680
0.9	8.37	5	0.80186	0.9	4.19	5	0.93979

3.7.3. Extreme values analysis

In this section, the extreme values of the hydraulic variables are evaluated for the case study. Original data for sea levels and wave conditions are gathered from south station dataset available from Met-Office within 14 years recorded data. Data from four tide gauge stations nearby the location concerned are used to provide original mean sea level and tidal data. The recorded data for fourteen years during 2000-2014 from the stations are analysed in this study to evaluate the extreme values of the sea water level and significant wave height. Both GEV and GPD models are considered in this section to illustrate the difference between the estimated extreme values.

The mean residual life plots are presented for present significant wave heights and sea levels in Figure 3.22 to estimate high thresholds for modelling extreme values via the GPD fit. In the plots, linearity might be suggested above 1.20 and 0.5 m for water levels and wave heights, respectively, where information on the far right–hand–side of these plots is unreliable. The diagnostic plots are provided for both GEV and GPD models to analyse the suitability of the suggested models from Figure 3.23 to 3.26. The P-P and Q-Q plots for water levels show that the GEV fit may be a more appropriate model for extreme value analysis, because the deviation (errors) between the model and the data are less significant. In another word, the original water level data have a closer pattern to a generalised extreme distribution than a generalised Pareto distribution. However, the level of error for GPD model is not significant, and the original data can be modelled as GPD distribution regarding an appropriate threshold as well.

The comparison between the probability density plots in water levels also suggests that GEV model is a better fit for water level as it covers more data. However, it should be noted that the GEV model tends to estimate higher extreme values than GPD model as shown in Figures 3.23 and 3.24. The P-P and Q-Q plots for significant wave heights show that both models are suitable and the error in both GEV and GPD models is insignificant. However, the probability density plots suggest that the GPD model may cover more realistic extreme values for wave height than a GEV model, as shown in Figure 3.26. The fitted models are used to estimate the return periods for the variables and the results are illustrated in Figure 3.27. The frequency analysis is often used to evaluate the hydraulic

parameter values for various return periods. The return period here refers to the average period between occurrences of an unusually high value of the variable. Recurrence interval plots for sea water level and wave height are provided for the GEV and GPD fitted models, respectively. According to the results, the estimated extreme values for significant wave height at 1000-year return period are 2.53 m and 2.59 m for GPD and GEV fitted models, respectively. The extreme values for water level at the same return period are 4.68 and 4.82 mOD for GPD and GEV fitted models, respectively. The GEV fitted model estimates higher values in comparison with the GPD model, and the difference is more significant for higher return periods.

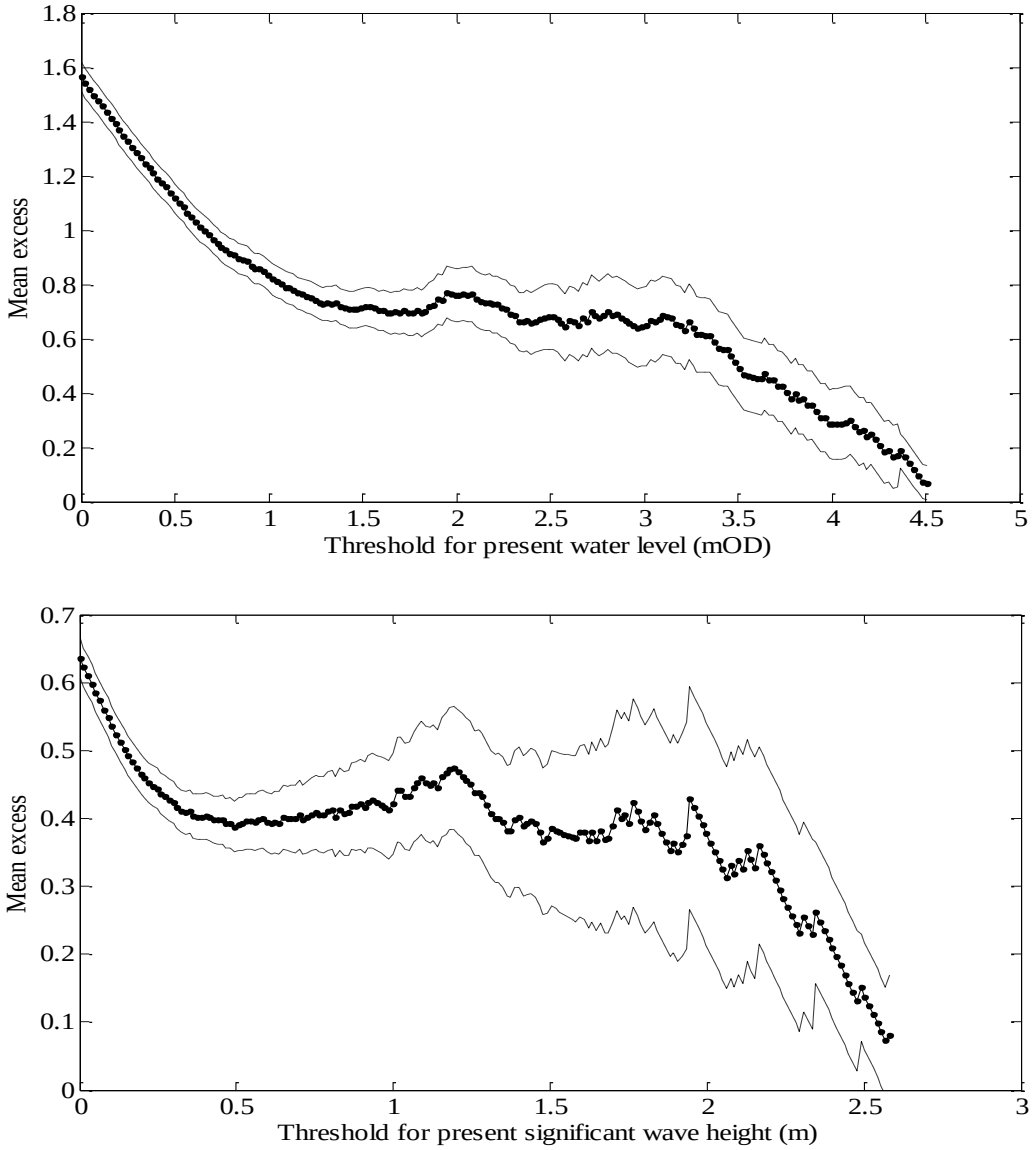

Figure 3.22 Mean residual plots for present water level and significant wave height.

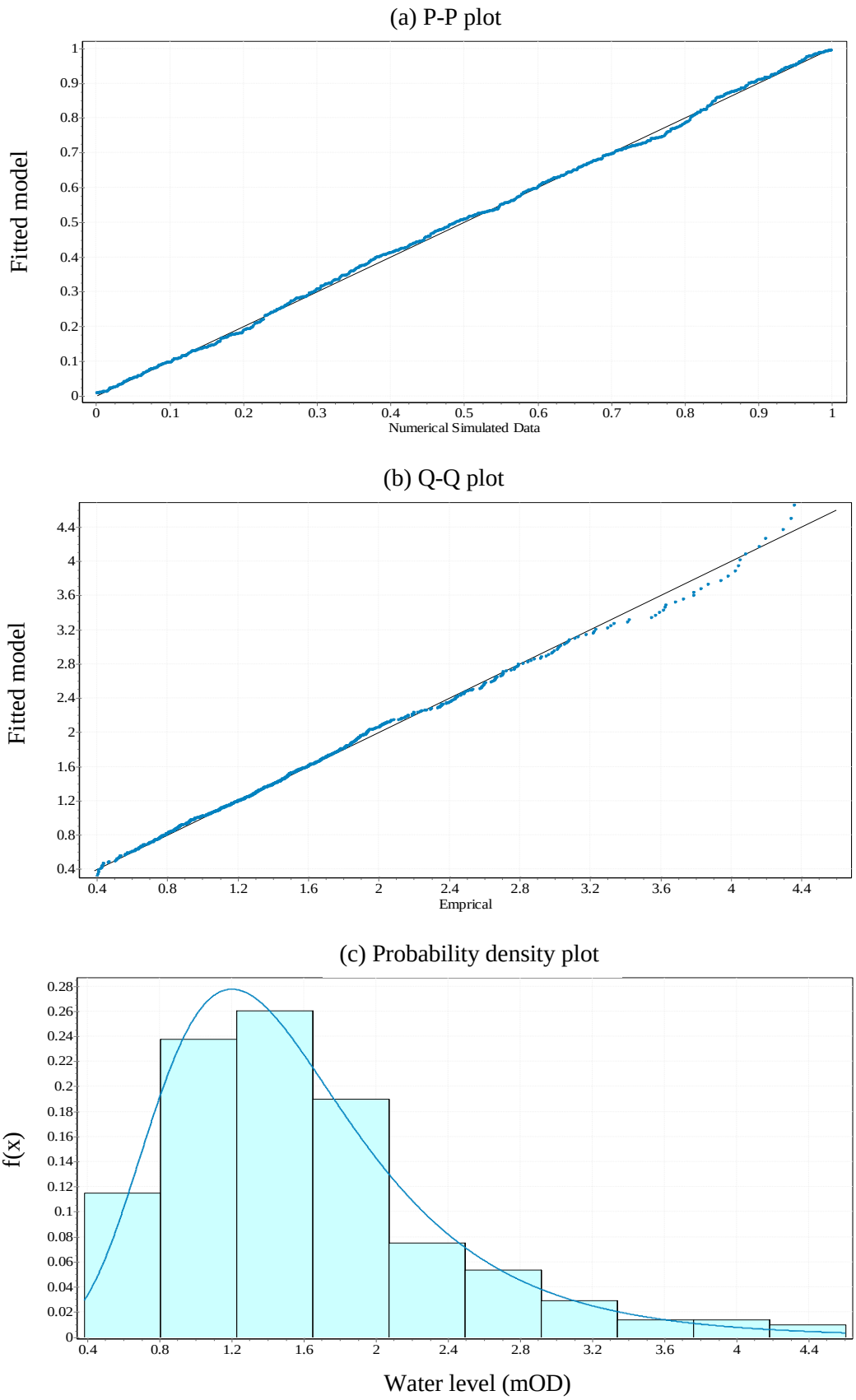

Figure 3.23 Diagnostic plots for the GEV analysis of the present water levels data.

(a) P-P plot

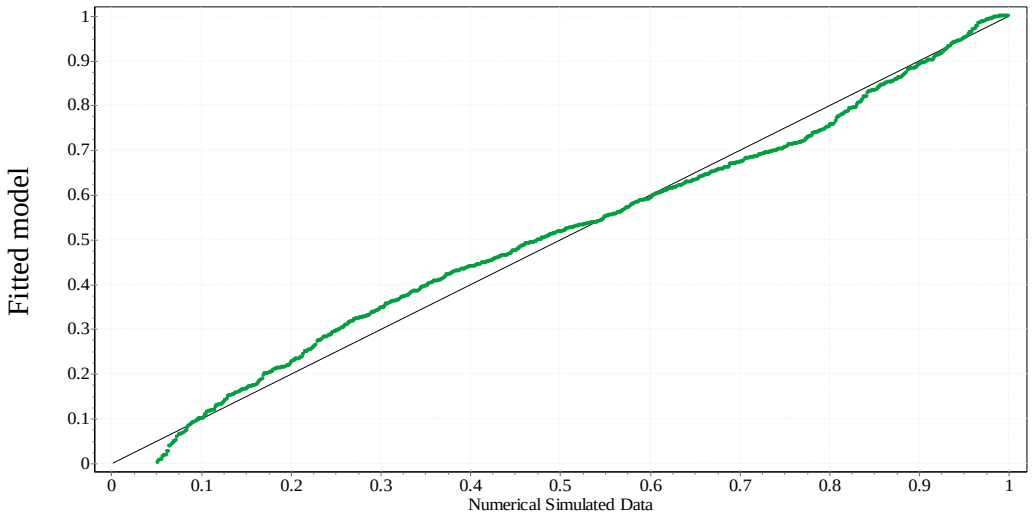

(b) Q-Q plot

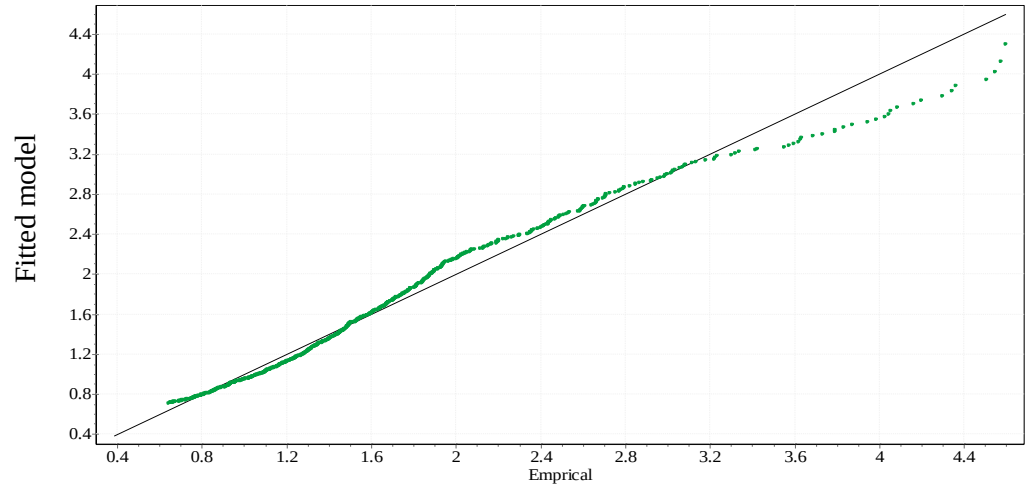

(c) Probability density plot

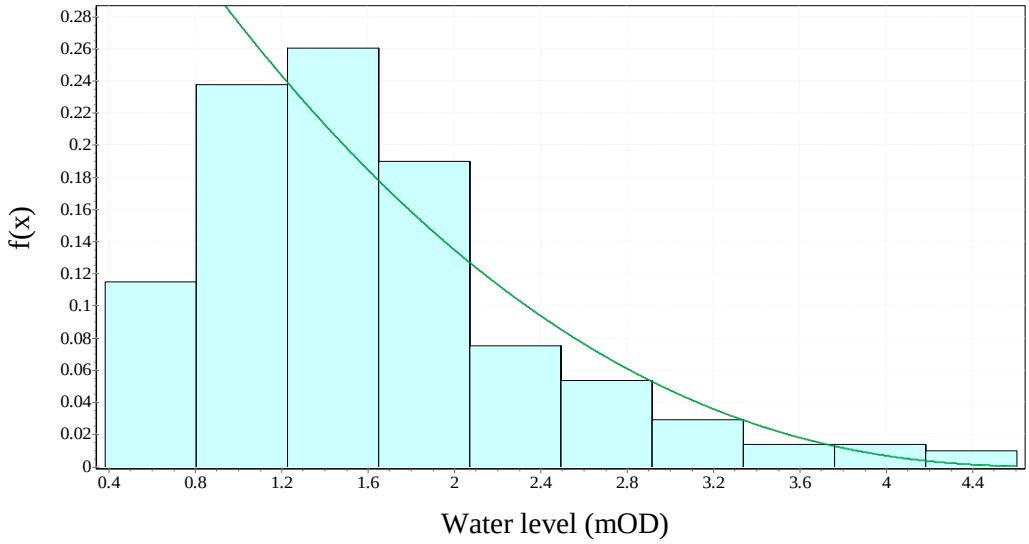

Figure 3.24 Diagnostic plots for the GPD analysis of the present water levels data.

(a) P-P plot

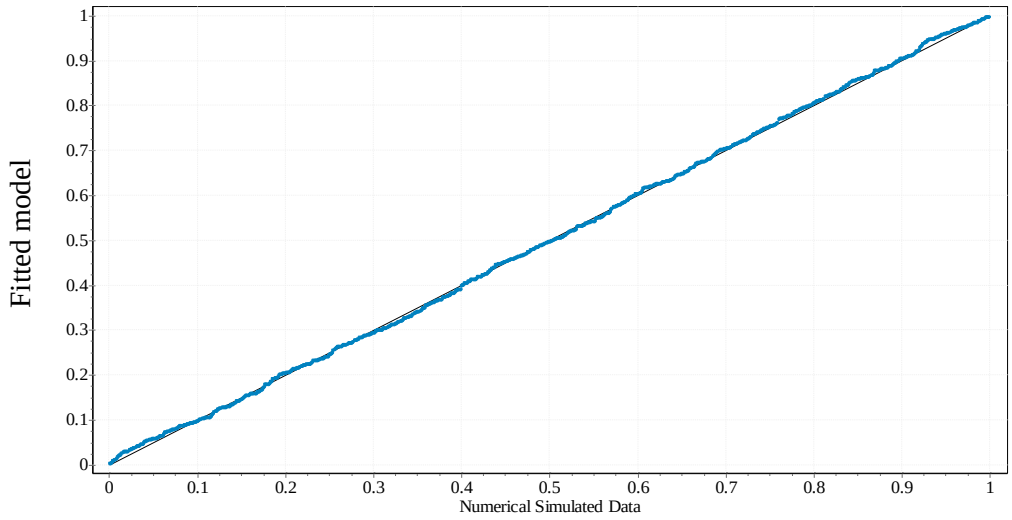

(b) Q-Q plot

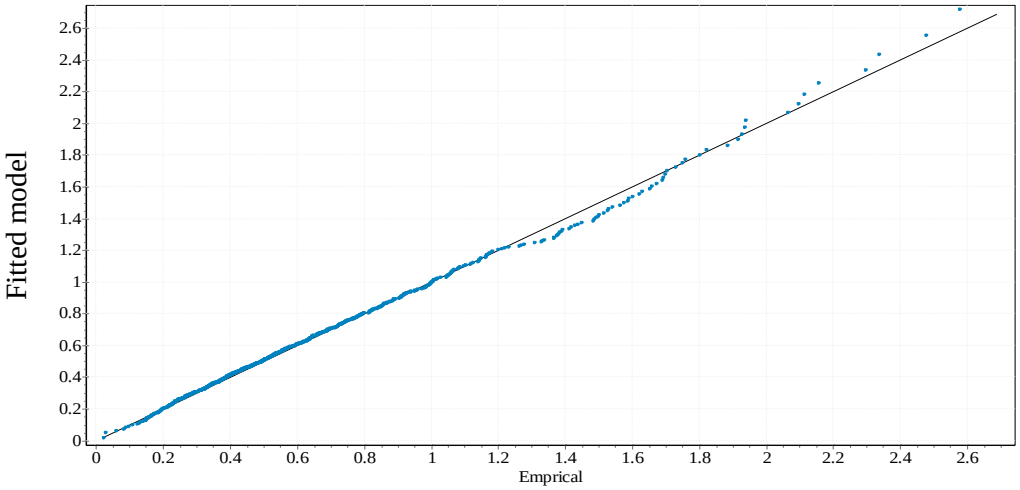

(c) Probability density plot

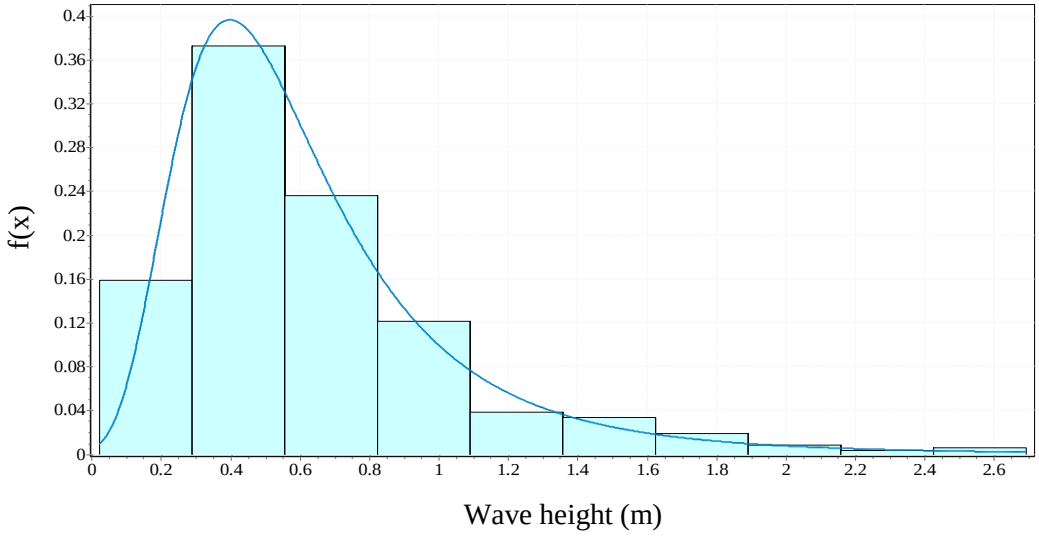

Figure 3.25 Diagnostic plots for the GEV analysis of the present significant wave height data.

(a) P-P plot

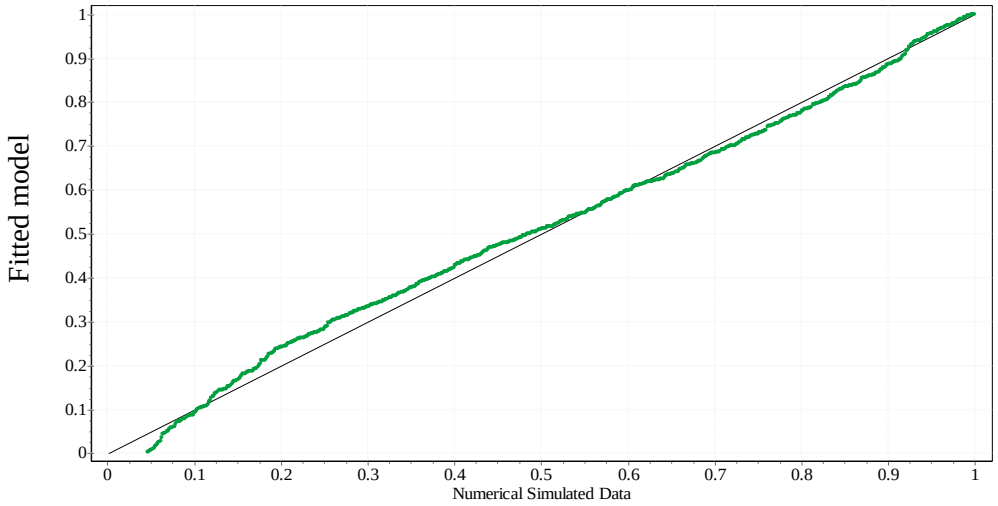

(b) Q-Q plot

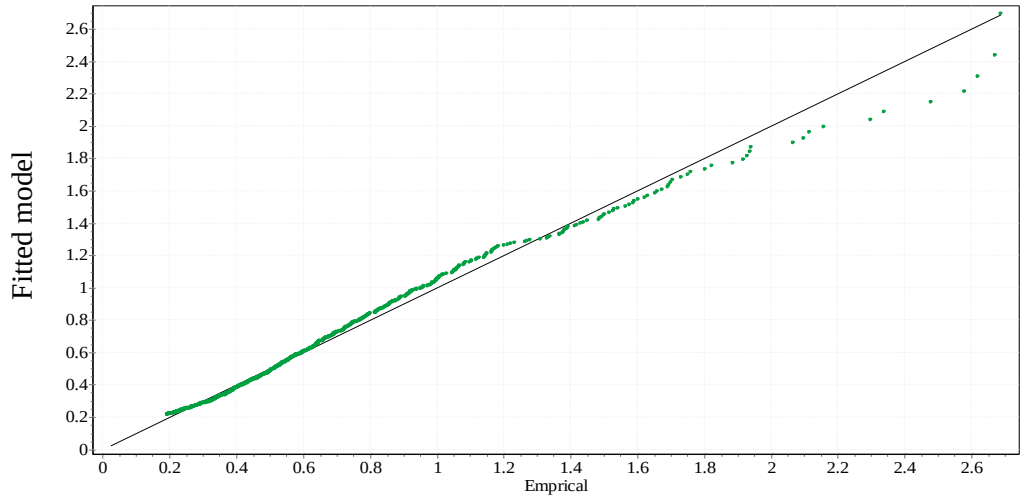

(c) Probability density plot

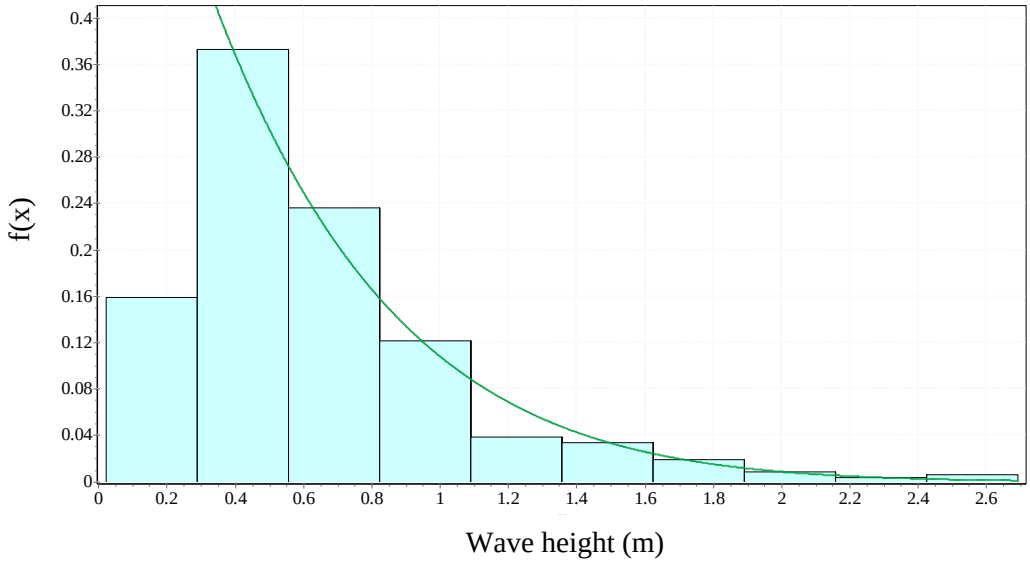

Figure 3.26 Diagnostic plots for the GPD analysis of the present significant wave height data.

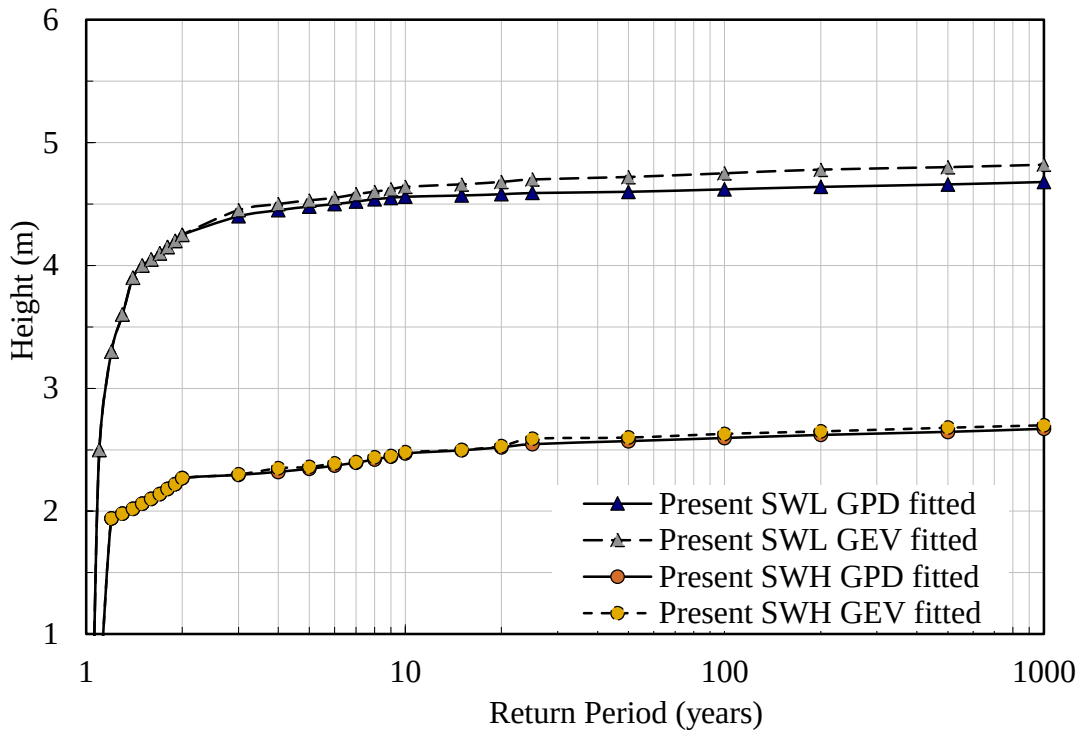

Figure 3.27 Recurrence interval plots for present sea water level (SWL) and significant wave height (SWH).

3.7.4. Effects of sea level rise on extreme values

The projected sea level rise due to low, medium and high emission scenarios is adopted from UKCP09 (Jenkins et al. 2011) to analyse the future hydraulic conditions. According to UKCP09 low emission scenario, the projected sea level rise including vertical land movements over a period of 1990-2095 is between 15-48 cm, or 3.2 mm/year in average (Jenkins et al. 2011). The projected increase in peak wave periods subject to low emission scenario after 50 years from the initial day is about 1% (Dahl et al. 2017). For medium emission scenario, the projected sea level rise including vertical land movements over the same period is between 21-68 cm, or 4.4 mm/year in average (Dahl et al. 2017). The projected increase in peak wave periods subject to medium emission scenario after 50 years from the initial day is about 2% (Dahl et al. 2017). The estimated sea level rise for high emission scenario including vertical land movements over the same period is between 28-84 cm, or 5.6 mm/year (Dahl et al. 2017). The increase in peak wave period subject to high emission scenario is about 4% after 50 years from the present day.

Figure 3.28 shows the relative increase in sea level rise with the lower and higher confidence intervals for the three mentioned scenarios. The projected sea level rises are

applied to the original data to estimate the extreme values in the future, as shown in Figure 3.29. The extreme values of water level at a 1000-year return period subject to the different emission scenarios are between 4.92 and 5.52 mOD, which shows a significant increase in the hydraulic loads. For the significant wave heights, the estimated extreme values subject to the different emission scenarios are between 2.90 and 3.27 m.

The results also show that for the lower return periods, i.e. less than 10-year, the difference between the estimated values through GEV or GPD fitted models are insignificant. Both GEV and GPD fitted models have similar return period values for return periods lower than 10 years. However, for the higher return periods, the GEV fitted model estimates higher extreme values, with the more significant difference due to the uncertainty from the predicted sea level rise.

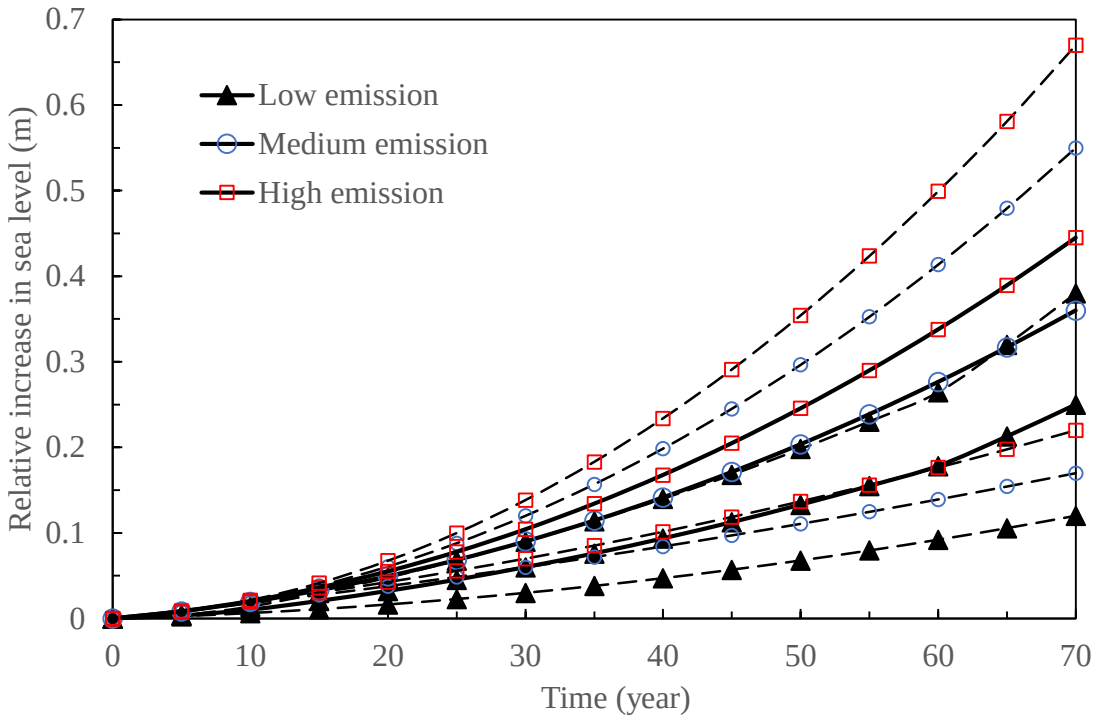

Figure 3.28 Relative increase in sea level for the different emission scenarios with 95th confidence intervals (dashed lines).

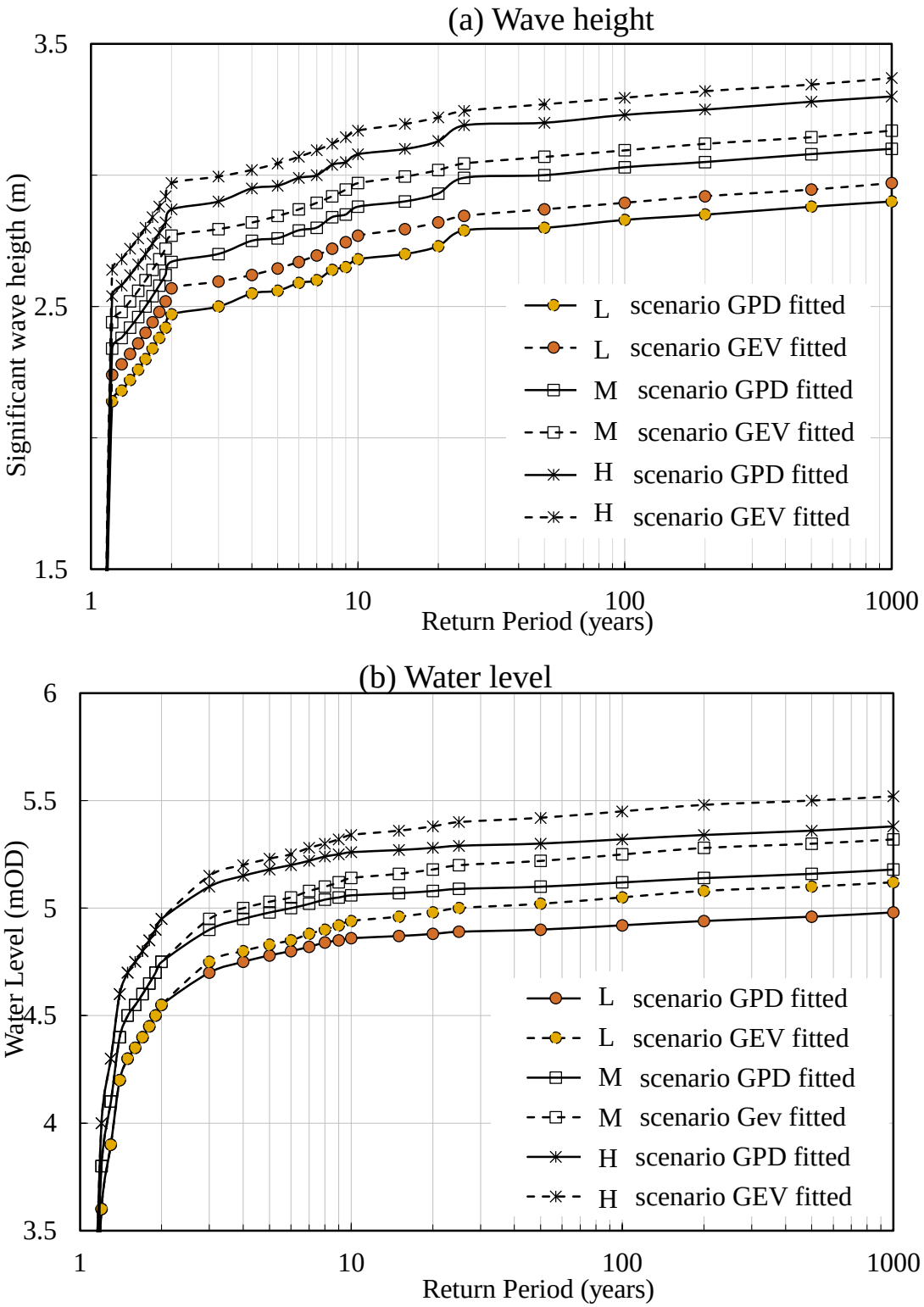

Figure 3.29 Recurrence interval plots with and without sea level rise after 50 years subject to low (L), medium (M) and high (H) emission scenarios for two extreme value models.

3.7.5. Joint probability evaluations

The dependence coefficient matrix between the original data of sea water level and significant wave heights ρ_1, and between significant wave heights and wave periods ρ_2 are estimated for all scenarios. The estimated dependence values for the original data are given here as

$$\rho_1 = \begin{bmatrix} 1.00 & 0.11 \\ 0.11 & 1.00 \end{bmatrix}, \rho_2 = \begin{bmatrix} 1.00 & 0.71 \\ 0.71 & 1.00 \end{bmatrix} \quad (3.37)$$

The estimated parameters are used to generate 10e5 simulated data for all variables subject to the three emission scenarios. Monte Carlo simulations are utilised to generate the samples of water level, significant wave height, and wave period. Figure 3.30 shows scatter plot of the original and simulated data for wave periods against wave heights in the case study. The distribution of the dots show strong correlation between wave height and wave period, and by increasing the wave height the wave period is increased. However, the extreme values of wave periods do not exceed from 6 second.

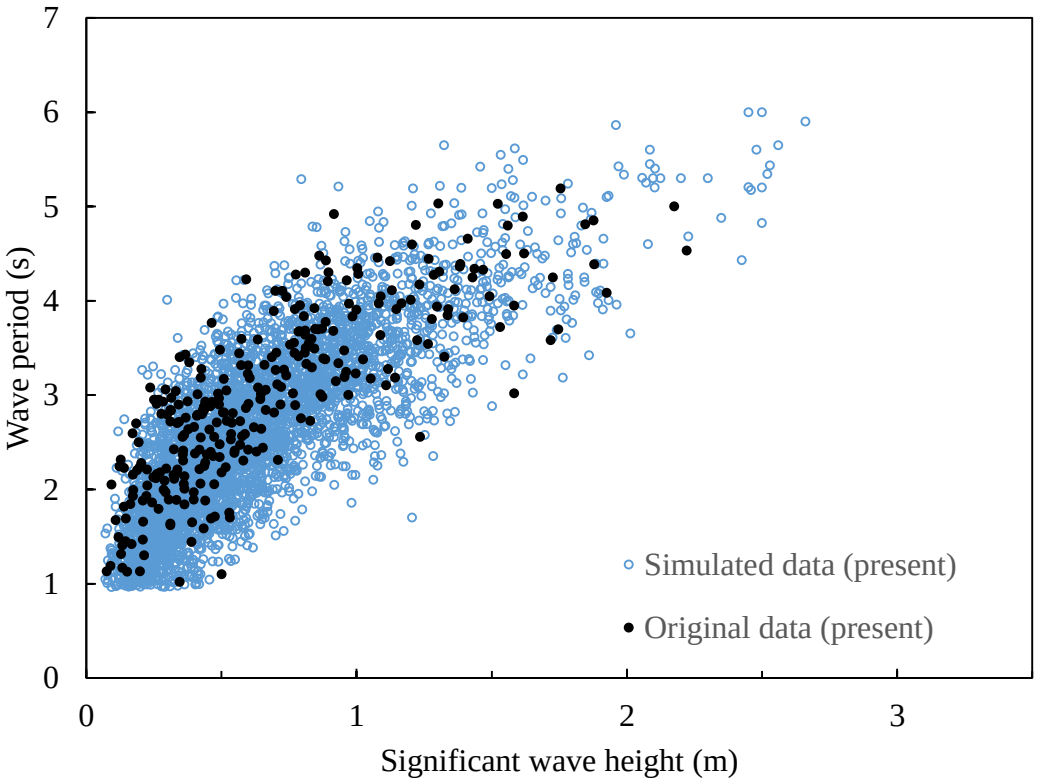

Figure 3.30 Scatter plot of original and simulated data for wave periods against significant wave heights.

The joint exceedance results for the present wave heights and water levels are given in Figure 3.31 as the contour lines. The contour lines, e.g. in 50, 100 and 1000-year return periods for both GEV and GPD fitted models, are presented over the simulated data. The GEV fitted values show a more conservative evaluation of the extreme events in the future. However, the simulated results emphasise that the GPD fitted evaluation may be closer to the reality. The worst case of wave overtopping for present data by assuming a 1000-year event may be at (2.20 m, 4.55 mOD) for significant wave height and water level (GEV model), respectively. On the other hand, the worst point is estimated to be (2.10 m, 4.35 mOD) for GPD fitted model. However, more extreme values, such as (2.30 m, 4.0 mOD) and (1.50 m, 4.60 mOD), should be considered in a failure probability analysis. Figure 3.32 shows the joint exceedance plots for water levels and significant wave heights subject to the three emission scenarios. The estimated worst case (GEV model) for low, medium and high emission scenarios are (2.25 m, 4.80 mOD), (2.30 m, 5.10 mOD) and (2.42 m, 5.25 mOD), respectively. The worst case for the same scenarios but GPD fitted model are (2.20 m, 4.70 mOD), (2.25 m, 4.95 mOD) and (2.30 m, 5.05 mOD), respectively. The results show that for a more cost-efficient result, GPD model is suggested. However, a reliability analysis needs to be undertaken to make sure about the performance level of the structure in the future.

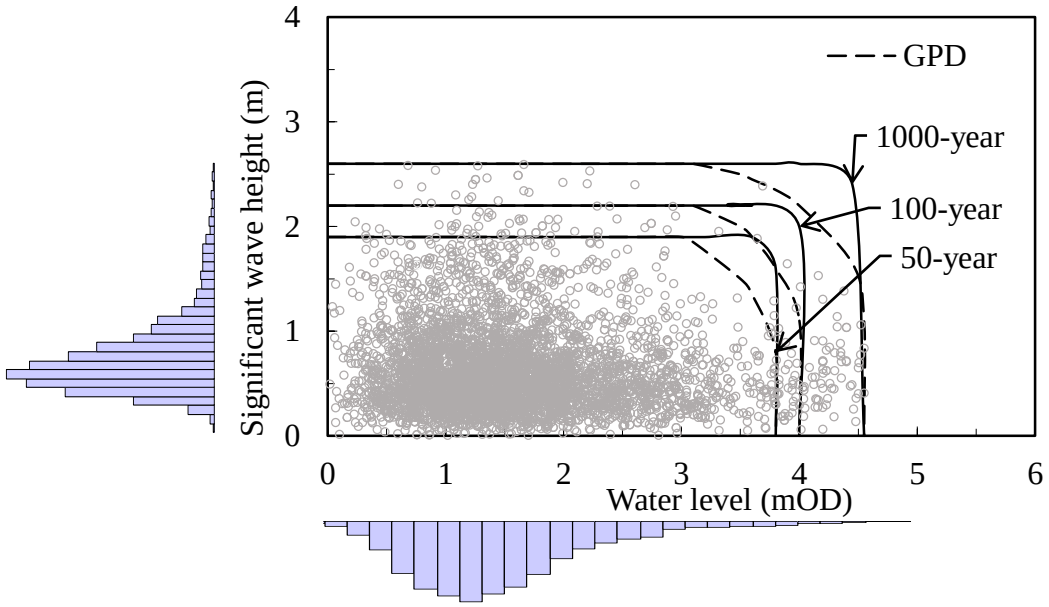

Figure 3.31 Joint probability return periods in contour lines and simulated data marked in dots for water level and significant wave height for the case without sea level rise.

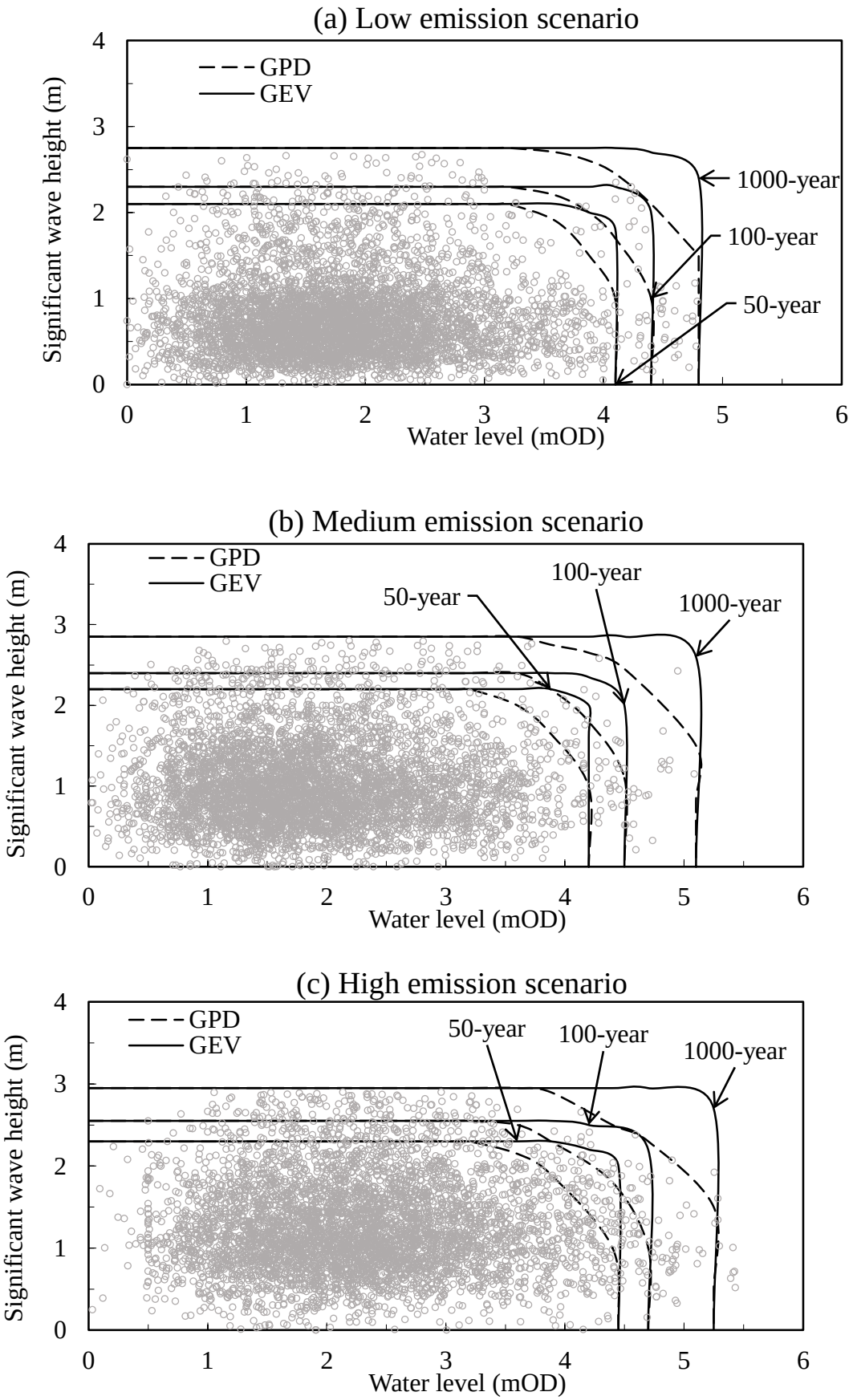

Figure 3.32 Joint probability return periods (contour lines) for water level and significant wave height subject to various scenarios.

3.8. Summary and conclusions

In this chapter, a new probabilistic method for analysing the evolution of flood defence condition grades is proposed regarding Environment Agency condition assessment manual. The available inspection strategies are translated into a probabilistic framework to be capable of using them in reliability analyses. A correlation between the visual indicators of the major failure mechanisms are defined and studied using the proposed method. The effects of climate change on the hydraulic variables are discussed, and a simplified model is developed to estimate the future wave conditions. A dependence copula function model is provided to use in the joint probability model. Finally, a numerical example provided to show the applicability of the proposed models.

From the results obtained by proposed model, following conclusions are drawn: a) the deterministic deterioration curves for coastal defences can be transformed into a probabilistic model to develop a stochastic deterioration model; b) the comparison between the GEV and GPD models show that the GPD model may give a more realistic and cost-efficient results; c) the proposed functions for adopting the effects of sea level rise over major hydraulic variables lead to a more straightforward model for predicting the future conditions, which are less complicated and more accurate; and d) the dependence evaluation through the copula function improves the quality of the simulated results in comparison with the original data.

4. Stochastic deterioration modelling for coastal defences

4.1. Introduction

In reliability analysis, it is often essential to deal with quantities that vary as a function of time, e.g. deterioration processes. To imply the variation of the deterioration process during the desired time in the reliability analysis, the concept of stochastic process is required. Mathematically, a stochastic process is a rule for assigning to every outcome of a simulation through a stochastic function. In this chapter, novel stochastic deterioration models are developed for coastal defence structures to model the deterioration processes such as crest level and seepage length loss. The main contributions of this study in this chapter are as follow:

- A homogenous Markov model is developed to model stationary deterioration process for a coastal defence that will be used in a generic fragility curve analysis.
- An inhomogeneous Markov model is developed to model non-stationary and grade-based deterioration process for a coastal defence that will be used in a time-dependent reliability analysis.

4.2. Stochastic Gamma process

Deterioration process is generally stochastic and non-decreasing process, which is suitable to be modelled by a gamma process (Van Noortwijk 2009). This process is used to model the uncertainty over time to failure and deterioration rate in many engineering fields such as the settlement of crest level in flood defence structures. In a non-stationary gamma deterioration model, let X be the random variable, then the probability density function of X is given as (Van Noortwijk 2009)

$$Ga[x|\kappa,\theta] = \frac{\theta^{\kappa}}{\Gamma[\kappa]} x^{\kappa-1} e^{-\theta x} I_{(0,\infty)}(x) \tag{4.1}$$

where $\kappa(t) > 0$ and $\theta > 0$ are shape function and scale parameter of gamma distribution, respectively; $I(x) = 1$ for $x \in A$, $I(x) = 0$ for $x \notin A$; $\Gamma[v]$ is the gamma function defined as (Van Noortwijk 2009)

$$\Gamma[v] = \int_0^{\infty} z^{v-1} e^{-z} dz \tag{4.2}$$

Let $\kappa(t)$ be a time-dependent and non-decreasing shape function for $t > 0$, then $X(t + \Delta t) - X(t) \approx Ga(\kappa(t + \Delta t) - \kappa(t), \theta)$. The resistance of flood defence structures deteriorates with time due to many factors such as degradation of crest level and seepage length. Here, the gamma process is utilised for modelling a stochastic deterioration process to evaluate the resistance of ageing sea defence structures. The probability density function of the deterioration increments Δy occurring at time t ($t \geq 0$) is given here as

$$f_{\Delta y}(\Delta y) = Ga(\Delta y|\kappa(t), \theta) = \begin{cases} \dfrac{b^{\kappa(t)}}{\Gamma[\kappa(t)]} \Delta y^{\kappa(t)-1} e^{-\theta \Delta y} & , for\ \Delta y > 0 \\ 0\ , & elsewhere \end{cases} \tag{4.3}$$

where the shape function and scale parameter are given as

$$\theta = \frac{\mu}{\sigma^2} \quad , \qquad \kappa(t) = \frac{\mu^2 t}{\sigma^2} \tag{4.4}$$

where μ and σ are the mean and the standard deviation for average deterioration rate, respectively. The process is a pure-jump increasing Levy process (Van Noortwijk 2009).

4.2.1. Parameter estimation

The maximum likelihood method is utilised to estimate the parameters of the gamma process. It is assumed that the expected deterioration at time t is proportional to a power function, given as (Edirisinghe et al. 2013),

$$E\big(X(t)\big) = \frac{\kappa(t)}{\theta} = \frac{c t^{\varrho}}{\theta} \tag{4.5}$$

where c and ϱ are related to the structure and environment conditions and always positive. The likelihood function of the deterioration increments $\delta_i = x_i - x_{i-1}$ is a product of independent gamma densities as

$$\iota(\delta_1, \dots, \delta_n | c, \theta) = \prod_1^n f_{X(\Delta t)}(\delta_i) = \prod_1^n \frac{\theta^{c(\Delta t^{\theta})}}{\Gamma(c\big(\Delta t^{b}\big))} {\delta_i}^{c\left(\Delta t^{\theta}\right)-1} \exp(-\theta \delta_i) \tag{4.6}$$

By solving the first partial derivatives of the two following equations, the values of $\acute{c}$ and $\acute{b}$ can be estimated as

$$\acute{\theta} = \frac{\acute{c}t_n^{\varrho}}{x_n}$$
$$t_n^k \log\frac{\acute{c}t_n^{\varrho}}{x_n} = \sum_1^n \left(\Delta t_{\Delta i}^{\varrho}\right)\left(\psi(\acute{c}\left(\Delta t_{\Delta i}^{\varrho}\right) - \log\delta_i\right) \quad (4.7)$$

where ψ is the derivative of the logarithm of the gamma function.

4.2.2. Simulation

There are many simulation methods for gamma process such as compound Poisson simulation and gamma-bridge sampling. This research uses gamma-increment sampling for the simulation of the discrete time deterioration in flood defence assets such as settlement. Gamma-increment sampling is defined as drawing independent samples of deterioration steps $\delta_i = x_i - x_{i-1}$, where the initial deterioration is zero, expressed here as (Strauss et al. 2015; Strauss et al. 2013)

$$Ga(\delta|\kappa(t_i) - \kappa(t_{i-1}), \theta) = \frac{\theta^{c(\Delta t^{\theta})}}{\Gamma(c(\Delta t^{\theta}))}\delta_i^{\,c(\Delta t^{\theta})-1}\exp(-\theta\delta_i) \quad (4.8)$$

for every $i = 1,2,\ldots,n$.

Figure 4.1 shows the simulated deterioration process for crest level loss of a hypothesis sea dyke subject to three different deterioration rates. The parameter estimation for the gamma process requires in-situ data from the case study. In this example, the parameters for different deterioration rates are assumed not estimated in order to show the simulation process. Hence, the parameters are not evaluated and only utilised to show the applicability of the equation in a coastal defence case study. For each deterioration rate, five distinct simulations are run to increase the accuracy of the results by taking the mean values. The results show that the expected mean crest deterioration over 60 years is about 15, 26, and 44 cm subject to slow, medium and fast deterioration rates, respectively.

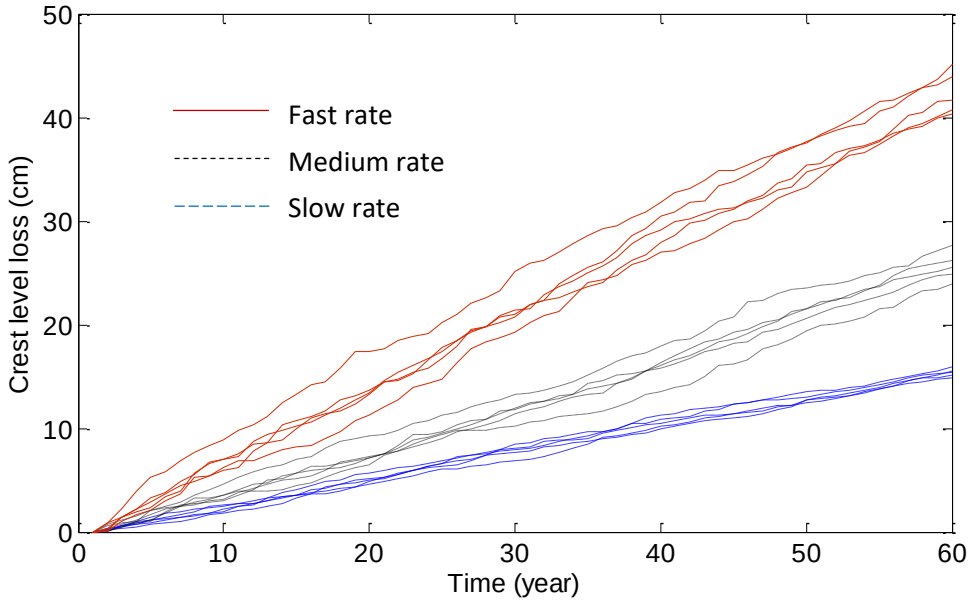

Figure 4.1 Simulated Gamma deterioration process for a sea dyke crest level subject to three different deterioration rates.

4.3. Homogenous Markov chain

As discussed in Chapter 2, a Markov model is a memoryless stochastic process that evolves during time, and the future of the process is only conditional on the current condition of the system or asset (Wellalage et al. 2015). The degradation process for coastal flood defence structures is only conditional on the present deterioration rate of the system and not to its previous deterioration rate. This is because the deterioration rate of the asset depends on its current resistance level and operational parameters. Consequently, the degradation process is memoryless and the deterioration process at random conditions in the future follows different random rates.

A Markov chain is considered as a series of transitions between certain condition grades. The stochastic process $X = \{X_n; n = 0,1,2, \dots\}$ with discrete and finite state space is a Markov chain if the following holds for each $i, j \in E$ (Bocchini et al. 2012)

$$\Pr(X_{n+1} = j | X_n = i_n, X_{n-1} = i_{n-1}, \dots, X_0 = i_0) = \Pr(X_{n+1} = j | X_n = i_n) \tag{4.9}$$

where for any set of states $i_0, \ldots . i_n$ in the state space the conditional probability does not change over time $t \geq 0$. When the Markov chain is used to model deterioration of a system in state i, a fixed probability, i.e. stationary transition probability, exists when a system changes from state i to state j during the period.

$$\Pr(X_1 = j | X_0 = i) = \Pr(X_{n+1} = j | X_n = i) \tag{4.10}$$

The stationary transition probabilities mean that the Markov chain is homogenous. Since the probabilities are stationary, the only information needed to describe the process is the initial condition state and the one-step transition probabilities.

4.3.1. Transition probability matrix

Estimation of the transition probabilities for a defence structure requires adequate available inspection data history. Generating an accurate and reliable transition probability matrix is a critical step in the Markov model (Ortiz-García et al. 2016). The deterioration rate of typical earth sea dykes with the progress of age is represented by five different condition grades as discussed in Chapter 3. The deterioration of flood defences is considered to be discrete in time, and is assumed that:

- Condition grade change over time follows stochastic process.
- The future condition of an asset only depends on present condition.
- The transition matrix is stationary.
- The transition in condition grades is an only one-state transition, i.e. only transit to next state due to deterioration.
- Each transition matrix is only valid for one failure mechanism.

The general form of transition probability matrix P with condition grades $\{1,2, \ldots, m\}$ is expressed as

$$\mathbf{P} = \begin{bmatrix} p_{11} & p_{12} & \cdots & p_{1m} \\ p_{21} & p_{22} & & p_{2m} \\ \vdots & & \ddots & \vdots \\ p_{m1} & p_{m2} & \cdots & p_{mm} \end{bmatrix} \tag{4.11}$$

$$Subject\ to \qquad \sum_{j=1}^{m} p_{ij} = 1 \qquad for\ \ i = 1,2,\dots,m$$

Each element in the transition probability matrix **P** represents the probability that the condition of the system or component concerned will transfer from state i to state j during a certain period of time t. Estimating the transition probability matrix **P** for a flood defence structure is based on available inspection data. Deterioration of flood defence structures is represented through the elapsed time to increase in condition grade ranging from 1 to 5, and it is assumed to have the initial information based on expert judgment and long term observations. Therefore, the transition probability matrix of Markov chains from grade i to j in Equation (4.11) is represented by a 5×5 matrix.

In addition, under the assumption of do-nothing, which means no maintenance is applied to the components or structure during the service life, the asset will gradually deteriorate. Hence the corresponding condition grade either transits to a higher number or remains unchanged during the inspection period. This means the condition to deteriorate by no more than one grade in one specific period of time, in order to simplify the model. However, it is important to choose appropriate time intervals. One more condition applies to the process when it is used to simulate coastal flood defence deterioration, namely $p_{55} = 1$, indicating condition grade where the structure has reached its worst condition (condition grade 5) and cannot deteriorate further. The transition probability matrix **P** in Equation (4.11) by assuming a homogenous condition can be expressed as

$$\mathbf{P} = \begin{bmatrix} p_{11} & 1-p_{11} & 0 & 0 & 0 \\ 0 & p_{22} & 1-p_{22} & 0 & 0 \\ 0 & 0 & p_{33} & 1-p_{33} & 0 \\ 0 & 0 & 0 & p_{44} & 1-p_{44} \\ 0 & 0 & 0 & 0 & 1 \end{bmatrix} \qquad (4.12)$$

A Markov process on a sea dyke is defined once its transition probability matrix and initial condition grade X_0 are specified, where X_0 is described as a distribution vector. In a Markov process, the probability of condition grade i of the stochastic process $\{X_{n+1}, (n > 0)\}$, where the transition time interval could be taken as 1 year for the convenience in calculations, is independent of the previous asset's condition $X_0, X_1, \dots, X_{n-1}$ but depends on X_n. Hence, the probability of the transition from condition grade i to condition grade j within n-steps, can be estimated. The expected condition grade for n transitions $\mathbb{E}X_n$ can be estimated from

$$\mathbb{E}X_n = X_0 \cdot P^n \cdot G^T \tag{4.13}$$

where G^T is the transpose of condition grade vector $G = [1\ 2\ \ldots\ M]$. In most situations, the initial distribution vector X_0 is available, but transition matrices are probabilistic because of the uncertainty in predicting deterioration from inspection data and the inherent stochasticity of the deterioration process.

4.3.2. Calibration of transition probability matrix

A regression-based non-linear optimisation method is utilised to minimise the difference between the observed condition grades and expectation of the model. This study utilises this method because it is useful when the observed data are not sufficiently available (e.g. lack of observations for some periods), which is common for coastal flood defence. The objective of this method is to minimise the squared difference between the regression curve and the expected transition probability fitted curve (Jiang and Sinha 1989).

Non-linear function, $Y(n)$, as a function of step, is obtained using regression curve fitting analysis on deterioration curve, where Y is a condition grade value. Then, transition probability matrix is estimated by solving the constrained nonlinear optimisation problem (Jiang and Sinha 1989; Morcous and Hatami 2011) that minimises the sum of absolute difference between the regression model and the expected condition grade from the objective function. The objective function can be expressed as a function of the transition probability matrix in Markov chain model. It is assumed that for each desired time-step n in a finite set of ages, there are one or more observations of condition grades, and the optimisation function is expressed as follows (Baik et al. 2006)

$$\min_{p_{ij}} \sum\sum (Y(n) - \mathbb{E}X_n)^2$$
$$\text{subject to: } 0 \le p_{ij} \le 1 \; and \; \textstyle\sum_{j=1}^{M} p_{ij} = 1\,, \; for \; i,j = 1,2,\ldots,M \tag{4.14}$$

where $Y(n)$ is an observation of a condition grade at time-step n from the non-linear regression function; and $\mathbb{E}X_n$ is the expected value for condition grade after n transition from Markov model.

4.3.3. Model verification

The chi-square goodness-of-fit test is used in a statistical model to make sure whether the transition matrix reflects the observed data, or whether the observed values are close to the expected distribution matching to the non-linear fitted model. The chi-square test is often used to test the values in two-way tables where the Markov model is evaluated against the observed data. The generalised chi-square test is expressed here as (Norris 1997)

$$\chi^2 = \sum \frac{(\text{Observed} - \text{expected})^2}{\text{Expected}} \tag{4.15}$$

The test will verify or refute whether the Markov model developed for the deterioration prediction of flood defence structure is reliable with the observations. The observed data are available from the Environment Agency (Halcrow 2013). The hypothesis testing method allows finding whether the proposed probability model is consistent with a set of observations used to validate the models (Garthwaite et al. 2002). The chi-square (χ^2) test can be used to compare the observed frequency with the expected condition grades at a particular observed time. The test for the deterioration models developed in this study can be calculated as

$$\chi^2 = \sum_{1}^{5} \frac{(Y(n) - \mathbb{E}X_n)^2}{\mathbb{E}X_n} \tag{4.16}$$

where $Y(n)$ is the observed values; and $\mathbb{E}X_n$ is the model's values. If the chi-square is larger than the critical ${\chi^2}_{0.05,4}$, corresponding to 95% confidence level and four degrees of freedom, the hypothesis is rejected. To ensure that the χ^2 statistic accurately approximates the χ^2 distribution, the traditional rule of thumb is executed, where all values should be at least 1.0, and more than 80% values should be more than 5.0 (Tables are available in appendix section).

4.3.4. Limitation of homogeneous Markov chain

Even though homogeneous Markov chain has been widely used to model the deterioration of various assets, the process has been criticised about the stationary assumptions for the time-dependent deterioration rate. In general, homogeneous Markov chain models have two significant limitations that make it challenging to predict flood

defence deterioration process accurately. The first one is the majority of assumptions for the Markov model are not consistent with the reality. For example, the parameters that might influence of the deterioration process are assumed to be constant, while in reality, the deterioration rates are different in various condition grades. A sea dyke at condition grade 4 is expected to degrade faster than a sea dyke in condition grade 2 due to the resistance and material factors.

This problem makes the simulation results to be different from the reality especially in long-term situations. The problem could be mitigated by using the short-term simulations. Also, Markov chain for the deterioration modelling is assumed to be a single step function. This means the elements do not transmit more than one condition state within a given time-step. The second major limitation of Markov chain models is the process of transition probability evaluation, which is often biased and needs observational data. The transitions matrices are very sensitive to the calibration methods, e.g. by using different calibration methods, the value of probabilities change significantly (Mishalani and Madanat 2002).

In a homogeneous Markov chain model, it is impossible to model the time-dependent deterioration process of flood defences. Hence, some methods overcome the limitation by dividing the lifetime into short and equal segments and then estimates the transition probability matrices for each time segment. The influence of the environmental factors such as hydraulic loads and traffic volume on the flood defence are neglected.

4.4. Non-homogenous Markov chain

A non-homogenous Markov model is more appropriate in flood defence deterioration modelling, as the transition probabilities are inherently time-dependent, for example older assets deteriorates faster. The basic features of the Markov chain are also valid in a time-dependent model such as being memoryless and stochastic. Let $X = \{x_1, x_2, \dots, x_M\}$ be a set of finite states of a flood defence asset. A time-dependent Markov process of a flood defence is defined once its transition probability matrices and initial condition state $X_0(t)$ at time $t \geq 0$ are specified, where $X_0(t) = \{\alpha_1^t, \alpha_2^t, \dots, \alpha_M^t\}, \sum \alpha_i^t = 1$ and $\alpha_i^t \geq 0$. A discrete-time Markov property for the mentioned process X^t at time t $(t > 0)$ is expressed as (Kleiner 2001)

$$p_{ij}^{t,t+1} = \Pr(X^{t+1}|X^1, X^2, \dots, X^t) = \Pr(X^{t+1} = x_j|X^t = x_i) \tag{4.17}$$

where conditional probability $p_{ij}^{t,t+1}$, with constraints $p_{ij}^{t,t+1} \geq 0$ and $\sum_{j=1}^{M} p_{ij}^{t,t+1} = 1$, denotes the transition of the asset from condition grade i to j during a given period of time. Figure 4.2 shows the progress of an asset probability mass function over time regarding time-dependent deterioration rate.

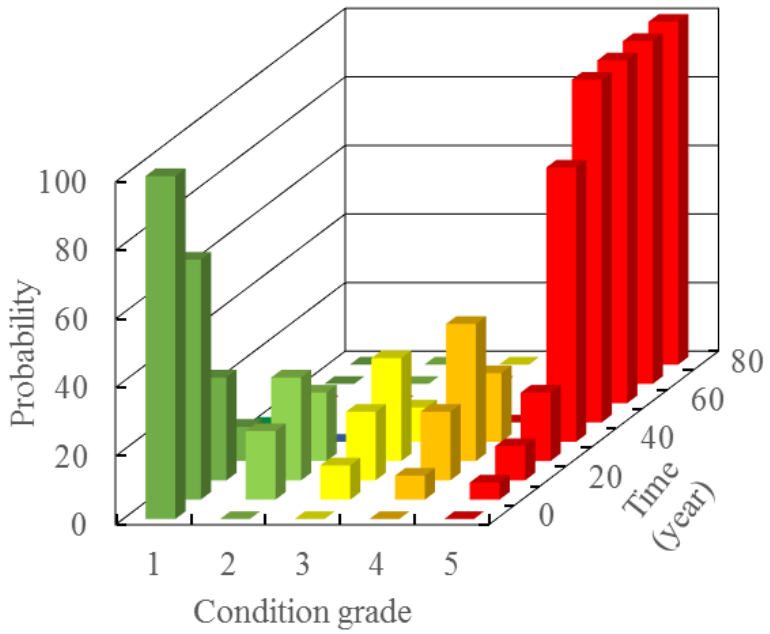

Figure 4.2 Progress of asset pmf over time regarding time-dependent transition probability.

4.4.1. Time-dependent transition probability matrix

The transition probabilities are normally expressed as an $M \times M$ matrix, where M is the number of possible states, referred to as transition probability matrix **P** as

$$\mathbf{P}^{t,t+1} = \begin{bmatrix} p_{11}^{t,t+1} & p_{12}^{t,t+1} & \cdots & \cdots & p_{1M}^{t,t+1} \\ p_{21}^{t,t+1} & p_{22}^{t,t+1} & p_{23}^{t,t+1} & \cdots & p_{2M}^{t,t+1} \\ \vdots & \vdots & \vdots & \vdots & \vdots \\ \vdots & \vdots & \vdots & \vdots & \vdots \\ p_{M1}^{t,t+1} & \cdots & \cdots & \cdots & p_{MM}^{t,t+1} \end{bmatrix} \tag{4.18}$$

In flood defence the deterioration modeling it is assumed that the assets can only transit to the next worse condition grades and cannot improve in condition, e.g. under do-nothing maintenance plan. As discussed earlier, coastal defence structures are categorised into 5 condition grades, where condition grade 1 denotes good as new and

condition grade 5 denotes failure. If a structure is in condition grade 5 under the no-maintenance plan, then cannot transit to a higher (worst) state, and always remains in condition grade 5. The one-step transition probability matrix under do-nothing maintenance plan is expressed here as

$$\mathbf{P}^{t,t+1} = \begin{bmatrix} 1-p_{12}^{t,t+1} & p_{12}^{t,t+1} & 0 & 0 & 0 \\ 0 & 1-p_{23}^{t,t+1} & p_{23}^{t,t+1} & 0 & 0 \\ 0 & 0 & 1-p_{34}^{t,t+1} & p_{34}^{t,t+1} & 0 \\ 0 & 0 & 0 & 1-p_{45}^{t,t+1} & p_{45}^{t,t+1} \\ 0 & 0 & 0 & 0 & 1 \end{bmatrix} \tag{4.19}$$

Once the transition probability matrix is defined, the expected condition of the system in the future can easily be obtained. Thus, suppose the system has an initial distribution vector $X_0(t)$, then the probability that the system being in state j after n time steps is expressed as:

$$X(t+n) = X_0(t) \cdot P^{t,t+1} \cdot P^{t+1,t+2} \cdot \ldots \cdot P^{t+n-1,t+n} \tag{4.20}$$

And accordingly, the expected condition grade is

$$E(t+n) = X(t+n) \cdot G^T \tag{4.21}$$

where G is the condition rating vector; and T is the transpose function

4.4.2. Weibull-distributed sojourn time

In a Markov process, a state space remains in a particular state for a given length of time, then transits to another state. Let $\{T_1, T_2, \ldots, T_M\}$ be random variables denote the sojourn time in states $\{x_1, x_2, \ldots, x_M\}$, respectively. Their corresponding probability density function (PDF), cumulative distribution function (CDF), and survival function are denoted $f_i(t), F_i(t)$ and $S_i(t)$, respectively. Thus, $T_{i,i+1}$ is the time from state i to state $(i+1)$. The random variable denoting the sum of the sojourn times in states $\{i, i+1, \ldots, k-1\}$, $T_{i\to k}$, is calculated as

$$T_{i\to k} = \sum_{i}^{k-1} T_{i,i+1} \quad ; \quad i = \{1,2,\ldots,M-1\}, k = \{2,3,\ldots,M\} \tag{4.22}$$

$T_{i\to k}$ represents the time that will take for the process to go from state i to k. In order to represent the flood defence deterioration process, let the sojourn times in states $i = \{1, 2, \dots, M-1\}$ be $\{T_1, T_2, \dots, T_{M-1}\}$, respectively. The time-dependent transition probabilities from state i at time t to next state at time $t+1$ can be expressed here as (Kleiner 2001)

$$p_{i,i+1}(t) = \Pr\{X_{t+1} = i+1 | X_t = i\} = \frac{f_{1\to i}(T_{1\to i})}{S_{1\to i}(T_{1\to i}) - S_{1\to(i-1)}(T_{1\to i-1})} \quad , \quad i = \{1,2, \dots, M-1\} \tag{4.23}$$

where $T_{1\to i}$ indicates the time that will take for process to go from state 1 to i; and the transition probability $p_{i,i+1}(t)$ is time-dependent and non-homogenous. For example the transition probability from state 4 to state 5 at time t is expressed as

$$p_{4,5}(t) = \frac{f_{1\to 4}(t)}{S_{1\to 4}(t) - S_{1\to 3}(t)} \tag{4.24}$$

Weibull distribution is one of the most widely used lifetimes and continues distributions in reliability analysis. It is a distribution that can take on the features of other types of distributions, based on the value of the shape parameter. The Weibull distribution is almost a normal distribution when shape parameter $\kappa = 3.25$. Figure 4.3 shows Weibull distribution gives a distribution for which the failure rate is proportional to a power of time as:

- Shape parameter $\kappa < 1$ indicates that the failure rate decreases over time.
- A value of $\kappa = 1$ indicates that the failure rate is constant over time hence the Weibull distribution reduces to an exponential distribution.
- A value of $\kappa > 1$ indicates that the failure rate increases with time. This happens if there is an aging or deteriorating process.

Assume that the waiting time T_i follows Weibull distribution. The CDF (F), PDF (f), and survival S function of Weibull distribution are expressed, respectively, as (Birolini 2007)

$$F_i(t, \theta_i, \kappa_i) = 1 - \exp[-(\theta_i t)^{\kappa}] \quad , \quad t > 0; \quad (F(t) = 0 \; for \; t \le 0) \tag{4.25}$$

$$f_i(t, \theta_i, \kappa_i) = \theta_i \kappa_i (\theta_i t)^{\kappa_i - 1} \exp[-(\theta_i t)^{\kappa_i}] \tag{4.26}$$

$$S_i(t, \theta_i, \kappa_i) = 1 - F_i(t, \theta_i, \kappa_i) = \exp[-(\theta_i t)^{\kappa_i}] \quad (4.27)$$

where θ_i and κ_i are scale and shape parameters, respectively. Under the specification of Weibull parameters, the probability of the transition from state i to state $(i + 1)$ can be estimated.

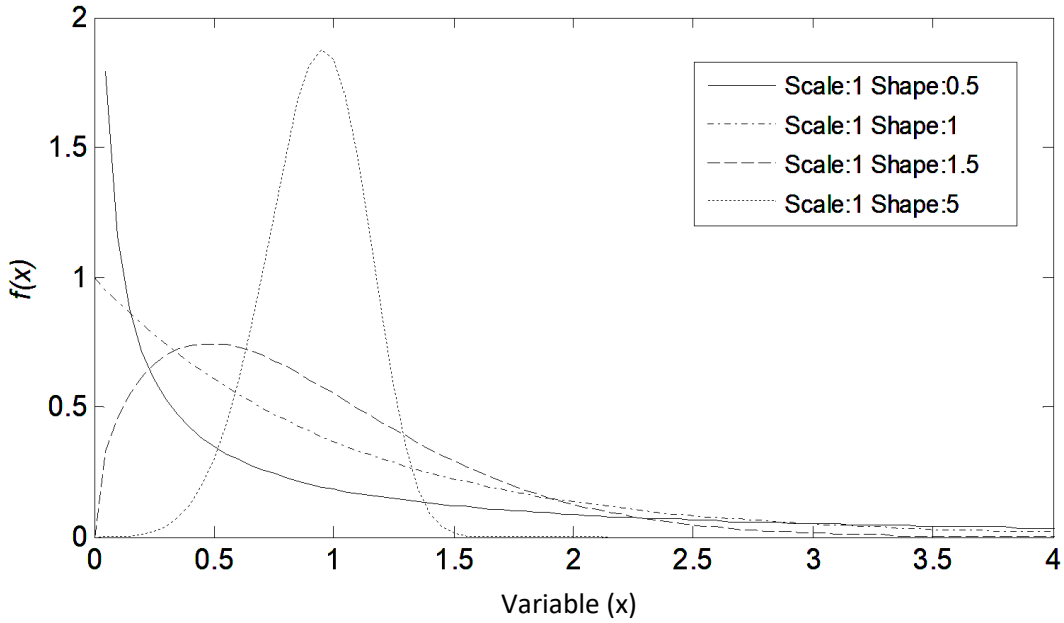

Figure 4.3 Weibull density function with different shape and scale parameters.

4.4.3. Parameter estimation

Two-state approach

The scale θ_i and shape κ_i parameters are estimated based on historical observations and condition assessments, which are available via Environment Agency publications as discussed in Chapter 3 (e.g. Halcrow Group 2013). Deterioration curves are developed by experts to predict the condition grade of assets associated with time according to their environment, material, deterioration rate and maintenance regime. For example, a deterioration curve for a specific asset describes that the structure remains in condition grade i for T years. After selecting an appropriate deterioration curve for the case study, a two-state Markov chain is utilised to estimate the transition probability for condition grade i. The one-step transition matrix is expressed here as

$$\widehat{\mathbf{P}} = \begin{bmatrix} p_{ii} & 1 - p_{ii} \\ 0 & 1 \end{bmatrix} \quad (4.28)$$

where $\widehat{\mathbf{P}}$ is a discrete-time and homogenous Markov transition matrix; and p_{ii} is the probability of being in condition grade i at time step (year). Transition probability that

the coastal defence goes from condition grade i to next condition grade in n steps is called n-step transition probability and is calculated from the n^{th} power of the transition matrix $\widehat{\mathbf{P}}$. Let τ be the time-step (year) that the structure remains in the same condition grade with probability of $p_a = 50\%$. From Equation (4.27) is it written as

$$\exp[-(\theta_i \tau)^{\kappa_i}] = p_a = {p_{ii}}^{\tau} \tag{4.29}$$

Also, it was assumed that the survival function at condition grade i follows a Weibull survival function S_i. A non-linear least squares method is suggested to find the scale θ_i and shape κ_i parameters by minimising the difference between two functions. The scale θ_i and shape κ_i parameters can be estimated by solving the minimization function given here as

$$minimise \ \sum_i (S_i(t) - {p_{ii}}^t)^2 \ ; \quad i = \{1,2,3,4\} \tag{4.30}$$

where $S_i(t) = \exp(-(\theta_i t)^{\kappa_i})$ is the Weibull survival probability at time (year) t. For example, assume a slope sea dyke, which transits from condition grade 1 to condition grades 2, 3, 4, and 5 at years 9, 19, 33, and 56, respectively. The following transition matrix for transition from condition grade 1 to 2

$$\widehat{\mathbf{P}}_{12} = \begin{bmatrix} 0.93 & 0.07 \\ 0 & 1 \end{bmatrix} \tag{4.31}$$

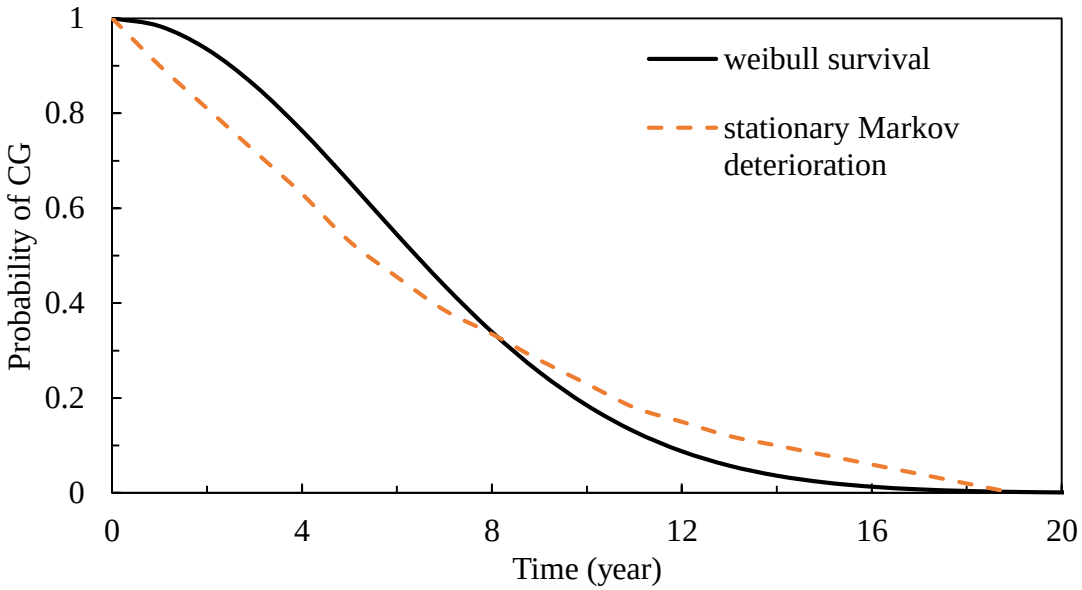

Figure 4.4 Assumed Weibull survival function and two-state stationary Markov deterioration for the transition from condition grade 1 to 2.

Hence, the time-step (year) that the survival probability of the condition grade is about 50% is $\tau = 9$. The next step is to minimise the distance between the Weibull function and transition pattern via objective function as shown in Figure 4.4. The parameters are estimated by solving the objective functions and are provided in Table 4.1. The parameters in the table will be used for Monte Carlo simulations to generate the cumulative survival functions of the condition grades.

Table 4.1 Parameter estimation utilising two-state approach. τ: years after the initial date that the sea dyke is in the same condition grade with 50% probability. SSE: the sum of squares due to error (Goodness-of-Fit test).

	Two state approach example			
	year	Shape	Scale	
Grade	τ	κ_i	θ_i	SSE
1(→ 2)	9	3.510	0.100	4.51e-06
2(→ 3)	10	3.610	0.091	4.51e-06
3(→ 4)	14	2.530	0.063	6.33e-06
4(→ 5)	19	2.924	0.045	4.42e-04

Transition approach

Let τ_x be the time-step (year) that the structure remains in the same condition grade with probability of x%. The deterministic deterioration curves associated with condition grades for different types are provided by Environment Agency as discussed previously Halcrow Group (2013). Let $t_{i\to(i+1)}$ be the time (year) that the asset moves from grade i to grade $(i+1)$. Hence, the probability that the asset is in grade i and $(i+1)$ at year $t_{i\to(i+1)}$ is $\{p_{i,i}^{t,t+1} = p_{i,i+1}^{t,t+1} = 50\%\}$. The probability of being in state i $(i = \{1,2,\dots,M-2\})$ is gradually decreasing until it is equal to zero at time (year) of the next transition $t_{(i+1)\to(i+2)}$. For $i = (M-1)$ the probability of being in the state is gradually decreasing until the mid-time period of the final transition, as the asset is in its worst condition grade and cannot deteriorate further. Hence, from the provided deterioration curves by Environment Agency, $\tau_{50} = t_{i\to(i+1)}$ and $\tau_0 = t_{(i+1)\to(i+2)}$ are available. From Equation (4.27) gives

$$\exp(-(\theta_i\tau)^{\kappa_i}) = p_{i,i+1}^{\tau} \tag{4.32}$$

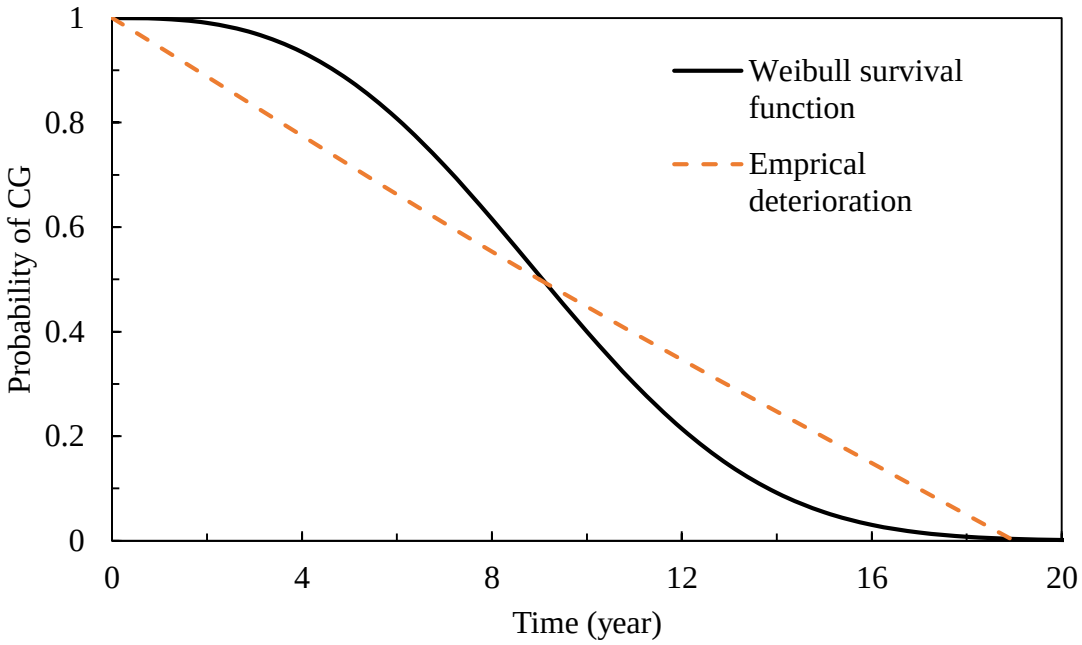

Figure 4.5 Assumed Weibull survival function and linear deterioration for the transition from condition grade 1 to 2.

The scale θ_i and shape κ_i parameters can be estimated by solving the minimisation function, together with Equation (4.32), as

$$minimise\ \sum_i (S_i(t) - p_{i,i+1}^{\tau})^2\ ;\quad i = \{1,2,3,4\} \tag{4.33}$$

where $S_i(t) = \exp(-(\theta_i t)^{\kappa_i})$ is the Weibull survival probability at time (year) t.

Table 4.2 Parameter estimation using transition approach. τ_x: years after initial date that the sea dyke is in the same condition grade with x% survival probability. SSE: sum of squares due to error (Goodness-of-Fit test).

Second approach example					
	year		Shape	Scale	
Grade	τ_{50}	τ_0	κ_i	θ_i	SSE
1(→ 2)	9	19	3.294	0.099	4.51e-6
2(→ 3)	10	24	2.831	0.087	4.51e-6
3(→ 4)	14	37	2.523	0.061	6.33e-6
4(→ 5)	14	23	3.441	0.081	4.42e-4

For example, for the same sea dyke example discussed in the two-state approach, once the sea dyke is in year 9 the probability of being in condition grade 1 and 2 are the same and it is 50%. Then the probability of being in condition grade 1 continues to decrease linearly until year 19. Figure 4.5 shows the linear deterioration and Weibull survival

functions for the second approach. Table 4.2 shows the parameters estimated for all condition grades and the estimated parameters will be used in the Monte Carlo simulations to generate the survival functions of cumulative waiting times in different condition grades.

4.5. Case study at Sheerness

A case study for a sea dyke section is utilised for investigating the deterioration process by utilising the homogeneous Markov model. The structure has a crest height of 4.6 m from the toe, a seaside slope of $Cot\ (\alpha) = 4$, and a land side slope of $Cot\ (\theta) = 3$. The seaside slope is protected by coarse gravel revetment within 0.8 m thickness to prevent wave attacks. The earth dyke rests on a layer of impermeable clay soils within 7.0 m thickness. Below the clay is 5.0 m of water conductive sand layer overlying impervious bedrock. The parameters relevant to the deterioration of crest level are considered. The initial condition vector for the sea dyke crest is assumed to be very good (1 0 0 0 0). The deterministic deterioration curves for the dyke subject to three deteriorating rates are selected from Halcrow group (2013) and presented in Figure 4.6.

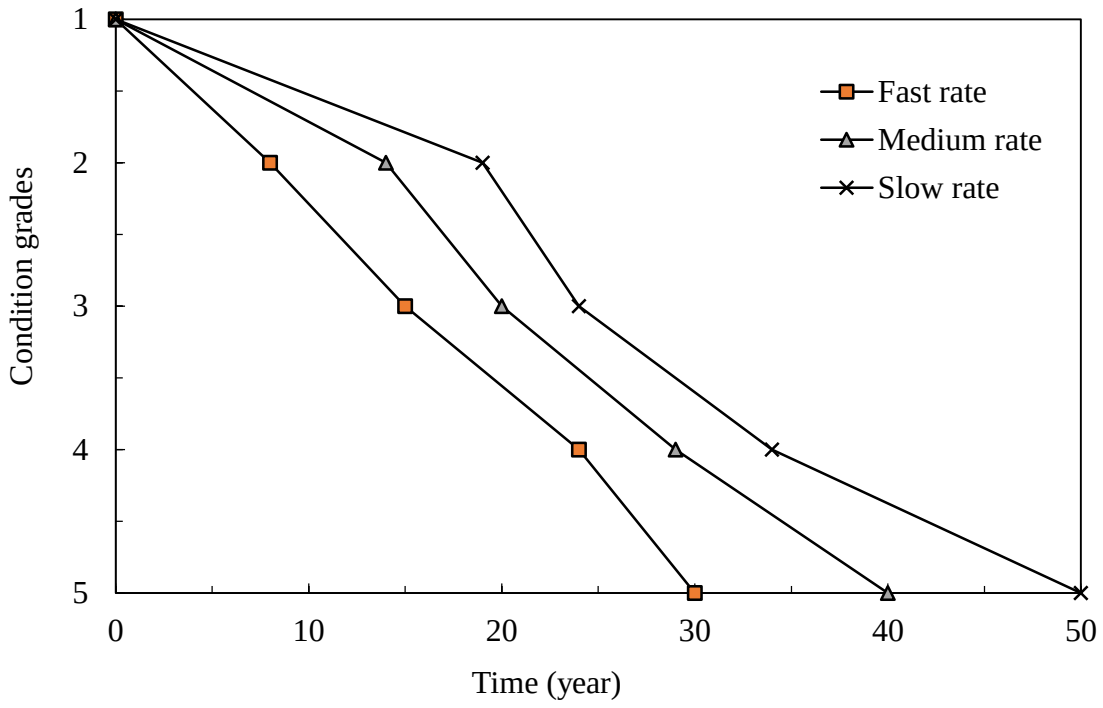

Figure 4.6 Deterioration times (year) to specified condition grades CG from new with three different deterioration rates subject to do-nothing maintenance.

4.5.1. Effect of deterioration rates on condition grades evolution

The sea dyke deterioration curves show the lifecycle of condition grades with a scale of 1 to 5 as shown in Figure 4.6. Nonlinear optimisation based on Equation (4.14) was performed to evaluate the transition probability. A MATLAB code was developed for the proposed state-based stochastic deterioration modelling. The codes solve the nonlinear optimisation based on an evolutionary algorithm for the problem described in Equation (4.14). The algorithm was run for some generations until it converges to the actual condition state. The estimated transition probability matrices for the first stage of transition for different deterioration rates are given as:

$$\mathbf{P}_{Slow} = \begin{bmatrix} 0.61 & 0.39 & 0 & 0 & 0 \\ 0 & 0.72 & 0.28 & 0 & 0 \\ 0 & 0 & 0.75 & 0.25 & 0 \\ 0 & 0 & 0 & 0.64 & 0.36 \\ 0 & 0 & 0 & 0 & 1 \end{bmatrix}$$

$$\mathbf{P}_{Medium} = \begin{bmatrix} 0.56 & 0.44 & 0 & 0 & 0 \\ 0 & 0.58 & 0.42 & 0 & 0 \\ 0 & 0 & 0.73 & 0.27 & 0 \\ 0 & 0 & 0 & 0.72 & 0.28 \\ 0 & 0 & 0 & 0 & 1 \end{bmatrix} \qquad (4.34)$$

$$\mathbf{P}_{Fast} = \begin{bmatrix} 0.51 & 0.49 & 0 & 0 & 0 \\ 0 & 0.55 & 0.45 & 0 & 0 \\ 0 & 0 & 0.79 & 0.21 & 0 \\ 0 & 0 & 0 & 0.71 & 0.29 \\ 0 & 0 & 0 & 0 & 1 \end{bmatrix}$$

Based on the evaluated transition probability matrices, condition grade distribution during the lifecycle can be evaluated using Markov chain model, as plotted in Figure 4.7. The results show how the embankment initially at condition state 1 (i.e. CG1) deteriorates from one state to another (CG1 to CG5) through the progress of time. From the results, it is clear that the probability of CG1 vanishes at approximately 20, 15, and 12 years after the initial day subject to slow, medium and fast deterioration rates, respectively. CG3 has the highest probability, compared with other condition states between the ages of 10 and 20 years when the deterioration rate is slow, while the highest probability for CG3 is between years 12-15 and 9-14 when the deterioration rate is medium and fast, respectively. As expected, CG5 increases steadily with time, reaching approximately a probability of 70%, 82% and 94% at the age of 30 years for slow, medium and fast deterioration rates. The goodness-of-fit test using a Chi-squared test based on null

hypothesis is evaluated using Equation (4.16). The evaluated values of χ^2 for the earth dyke is much less than the critical Chi-square value $\chi^2_{0.05,5}$ of 9.49 in this study, which validates the evaluation of condition grades by using the proposed grade-based stochastic deterioration model.

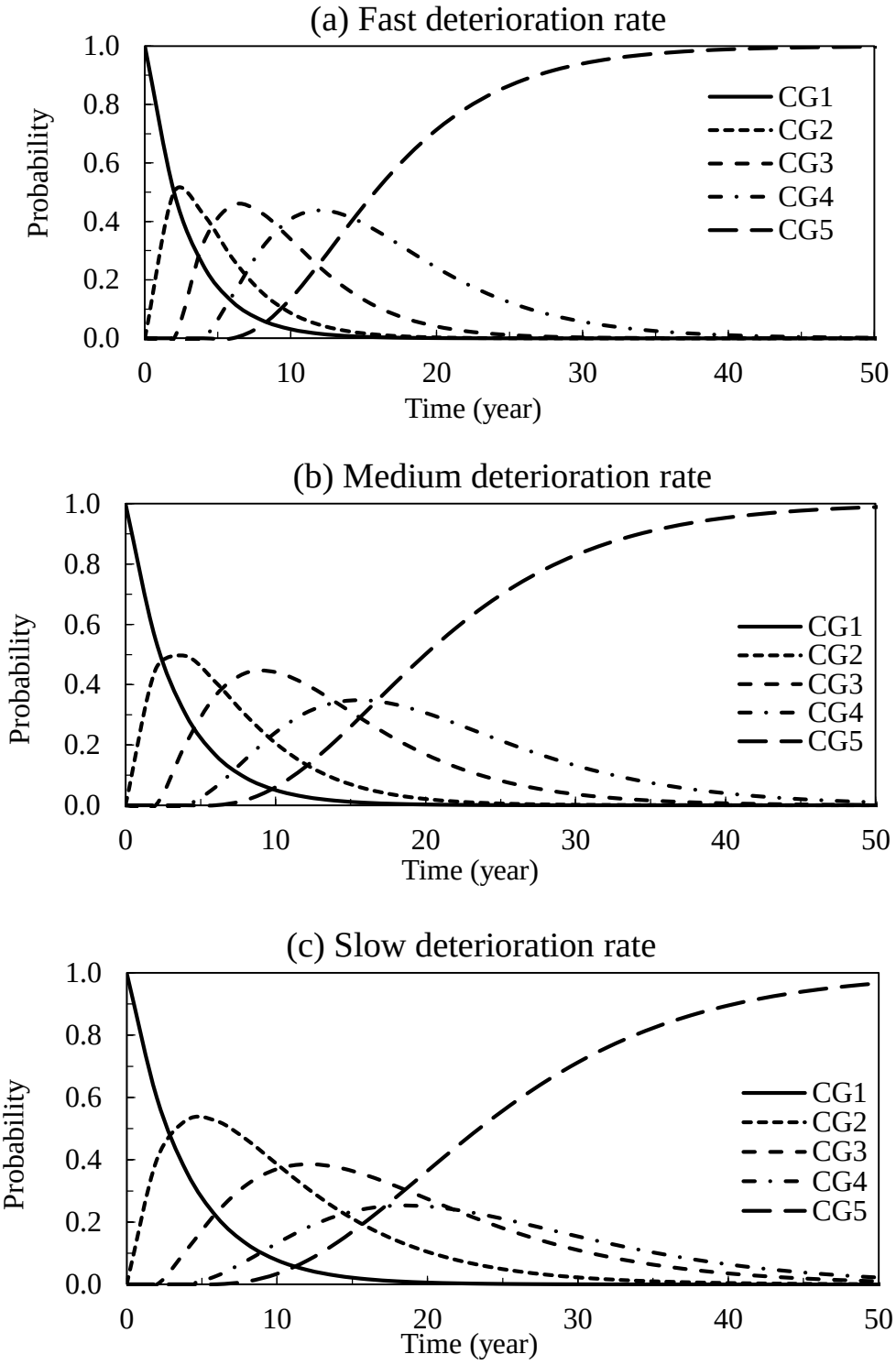

Figure 4.7 Time-dependent condition grade probabilities from the Markov model for the earth sea dyke subject to varoius deterioration rates.

4.5.2. Effect of repair maintenance on condition grades evolution

In this section, the effects of a maintenance plan over the three different deterioration rates are investigated. The repair maintenance strategy in the case study suggests to refurbish sea dyke back to a lower condition grade (one grade better) by applying structural repairs every 4 years. The effectiveness of the repair is estimated using the inspection results before and after the applied maintenance in the case study, and it is suggested that there is 10% probability for the dyke to move to a lower condition grade (HR Wallingford 2006). In this section, it is assumed that the improvement has equal effects on the probabilities of transiting to a higher condition grade or remaining in the same condition grade. The estimated transition probability matrices for the first stage of transition for different deterioration rates subject to minor maintenance are amended as

$$\mathbf{P}_{Slow} = \begin{bmatrix} 0.61 & 0.39 & 0 & 0 & 0 \\ 0.10 & 0.67 & 0.23 & 0 & 0 \\ 0 & 0.10 & 0.70 & 0.20 & 0 \\ 0 & 0 & 0.10 & 0.59 & 0.31 \\ 0 & 0 & 0 & 0.05 & 0.95 \end{bmatrix}$$

$$\mathbf{P}_{Medium} = \begin{bmatrix} 0.56 & 0.44 & 0 & 0 & 0 \\ 0.10 & 0.53 & 0.37 & 0 & 0 \\ 0 & 0.10 & 0.68 & 0.22 & 0 \\ 0 & 0 & 0.10 & 0.59 & 0.31 \\ 0 & 0 & 0 & 0.05 & 0.95 \end{bmatrix} \quad (4.35)$$

$$\mathbf{P}_{Fast} = \begin{bmatrix} 0.51 & 0.49 & 0 & 0 & 0 \\ 0.10 & 0.50 & 0.40 & 0 & 0 \\ 0 & 0.10 & 0.74 & 0.16 & 0 \\ 0 & 0 & 0.10 & 0.66 & 0.24 \\ 0 & 0 & 0 & 0.05 & 0.95 \end{bmatrix}$$

The estimated transition probabilities are used to simulate the Markov process for the evolution of the condition grades over time as shown in Figure 4.8, Figure 4.9 and Figure 4.10. The results show that a significant improvement in the lifecycle of good condition grades. For example, CG1 can survive about 22, 15 and 10 years longer for slow, medium and fast deterioration rates, respectively, due to the implemented maintenance plan. The probabilities of the condition grade 5 show a significant drop, which is about 36%, 30% and 26% decrease at year 50 due to the repairs.

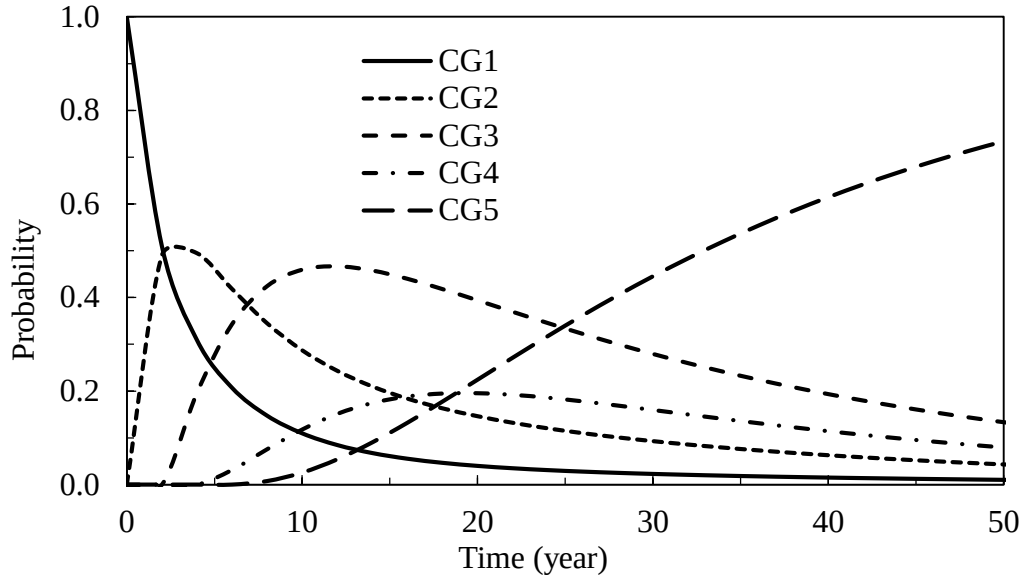

Figure 4.8 Effect of maintenance on time-dependent condition grade probabilities from the Markov model for the earth sea dyke subject to slow deterioration rate.

The maintenance model in this section shows the limitation of the deterministic evaluation of the effectiveness matrix for maintenance action. The effectiveness of the repair actions should be evaluated for all condition grades, not only the neighbour condition grades. Also, assuming similar improvement for all condition grades, e.g. 10% for all, is unrealistic. Because the effects of maintenance for higher condition grades are less than the effects of the repairs in lower condition grades, and the dyke needs more repairs to improve to a better grade. In the next chapters, the mentioned limitations will be addressed to estimate a proper effectiveness matrix due to maintenance actions.

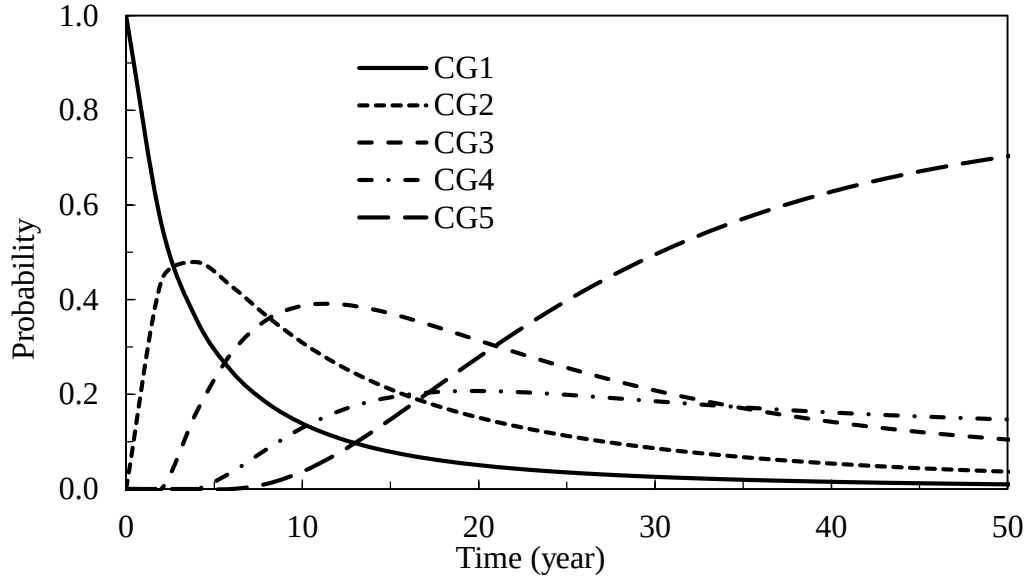

Figure 4.9 Effect of maintenance on time-dependent condition grade probabilities from the Markov model for the earth sea dyke subject to medium deterioration rate.

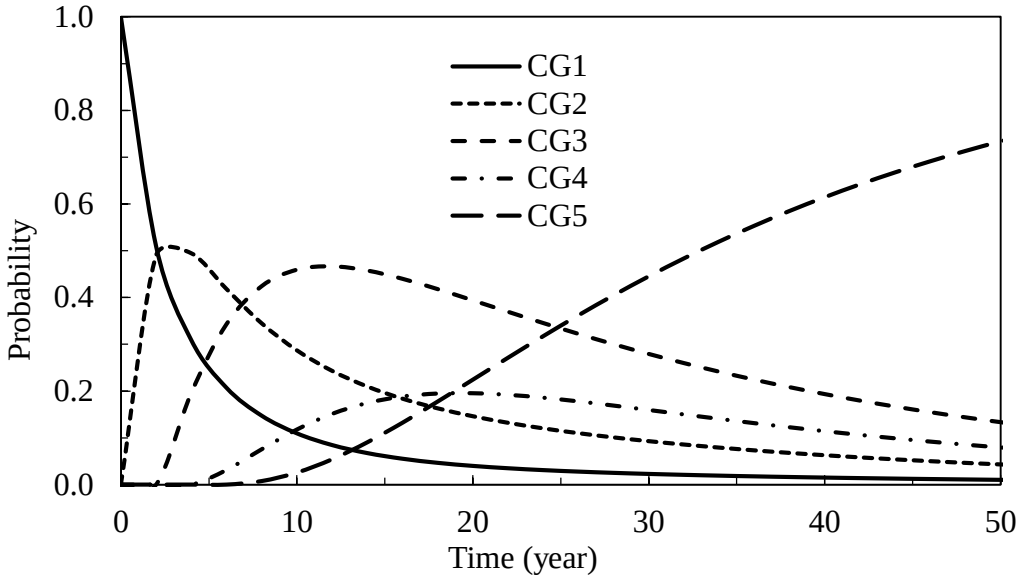

Figure 4.10 Effect of maintenance on time-dependent condition grade probabilities from the Markov model for the earth sea dyke subject to fast deterioration rate.

4.6. Case study at Thames estuary

A case study for a simplified sea dyke as shown in Figure 4.11 along Thames estuary flood defence system, described by Gouldby et al. (2007), is employed to demonstrate the applicability of the proposed non-homogeneous Markov model. The structure has a crest height of 6.40 mAOD, the seaside slope of $Cot(\alpha_1) = 4.20$, the landside slope of $Cot(\alpha_2) = 3.20$, and foreshore slope of 1:30. The seaside slope protected by berm and coarse gravels to reduce the destructive effects of the sea waves. It is assumed that the sea dyke is in a very good initial condition (Condition grade 1).

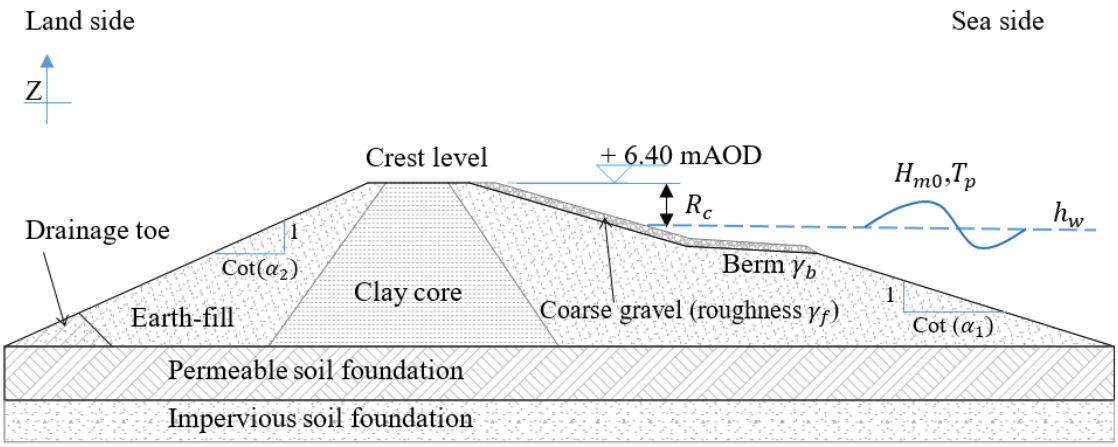

Figure 4.11 Sketch of the earth sea dyke section along Thames estuary.

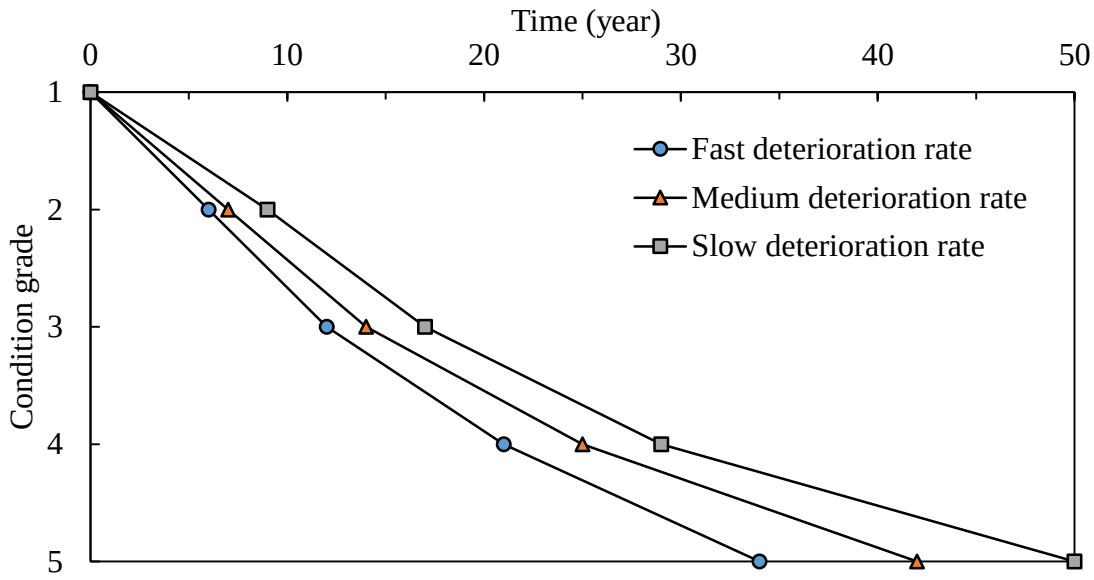

Figure 4.12 Deterioration times to specified condition grades from new with various deterioration rates (Halcrow group 2013).

4.6.1. Survival probabilities estimated from two-state approach

The deterministic deterioration curves for the asset is provided in the case study by Gouldby et al. (2007) concerning different deterioration rates on a scale of 1 to 5 (1 for very good condition and 5 for very poor condition), as presented in Figure 4.12. The deterioration curves are utilised in the numerical example to evaluate the lifecycle of the condition grades for the sea dyke. The parameters of the Weibull function are estimated using Equations (4.28- (4.30). Trust-Region algorithm is utilised to solve the minimisation function to estimate the parameters for different condition grades are presented in Table 4.3.The estimated parameters in the tables are applied to Monte Carlo simulations to generate the cumulative survival distributions of the transition process, and their changes over time under the mentioned scenarios are shown in Figure 4.13 to Figure 4.15.

Table 4.3 Parameter estimation for three different scenarios using two-state approach.

CG	Fast rate			Medium rate			Slow rate		
	τ (Year)	κ_i	θ_i	τ (Year)	κ_i	θ_i	τ (Year)	κ_i	θ_i
1(→ 2)	6	3.325	0.111	7	5.362	0.097	9	5.362	0.079
2(→ 3)	6	4.251	0.122	6	4.333	0.087	8	7.746	0.079
3(→ 4)	9	4.732	0.067	12	5.745	0.061	12	7.562	0.054
4(→ 5)	13	3.634	0.100	17	3.915	0.081	21	6.632	0.064

For example, for the sea dyke subject to fast deterioration rate, the probability of being in condition grade CG2 and CG3 after 15 years from the present day is about 22% and 57%, respectively, as shown in Figure 4.13. While, for the same year and but subject to medium deterioration rate, the probability of being in CG2 and CG3 is about 31% and 54%, respectively, as shown in Figure 4.14. Two examples of the estimated transition probabilities subject to slow deterioration rate at years 4 and 7 are presented here as

$$P^{4,5} = \begin{bmatrix} 0.852 & 0.148 & 0 & 0 & 0 \\ 0 & 0.742 & 0.258 & 0 & 0 \\ 0 & 0 & 0.653 & 0.347 & 0 \\ 0 & 0 & 0 & 0.648 & 0.352 \\ 0 & 0 & 0 & 0 & 1 \end{bmatrix} \quad (4.36)$$

$$P^{7,8} = \begin{bmatrix} 0.583 & 0.417 & 0 & 0 & 0 \\ 0 & 0.642 & 0.358 & 0 & 0 \\ 0 & 0 & 0.613 & 0.387 & 0 \\ 0 & 0 & 0 & 0.558 & 0.442 \\ 0 & 0 & 0 & 0 & 1 \end{bmatrix} \quad (4.37)$$

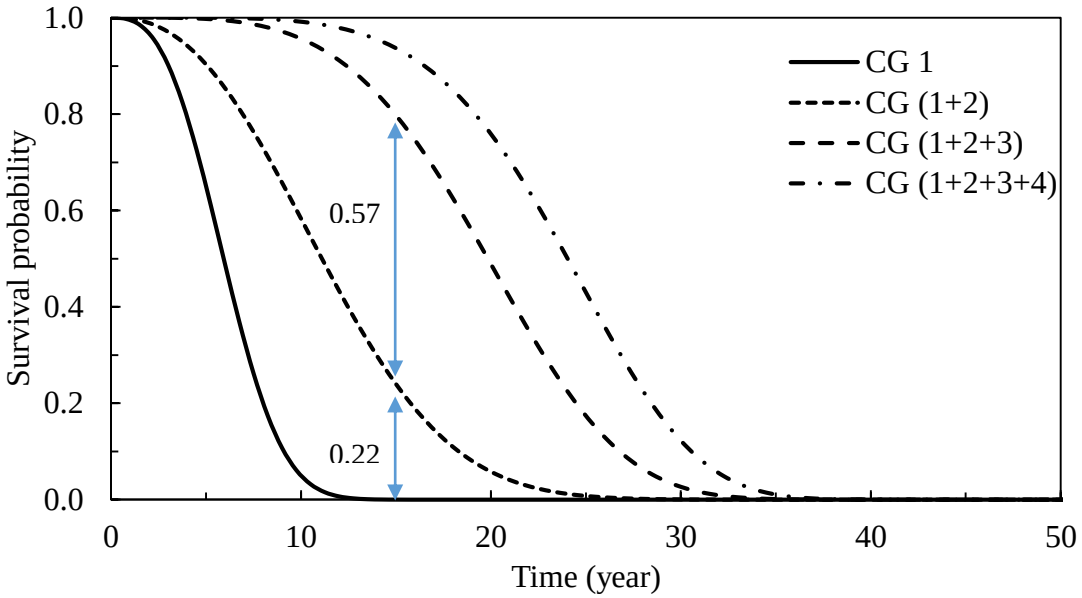

Figure 4.13 Survival functions of cumulative waiting times in different condition grades (CG) subject to fast deterioration rate.

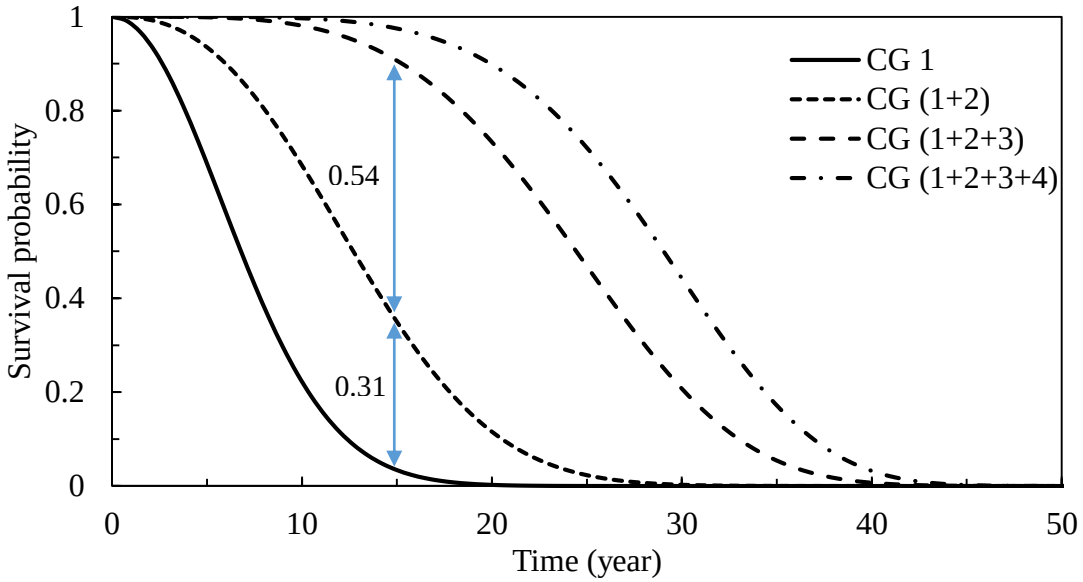

Figure 4.14 Survival functions of cumulative waiting times in different condition grades (CG) subject to medium deterioration rate.

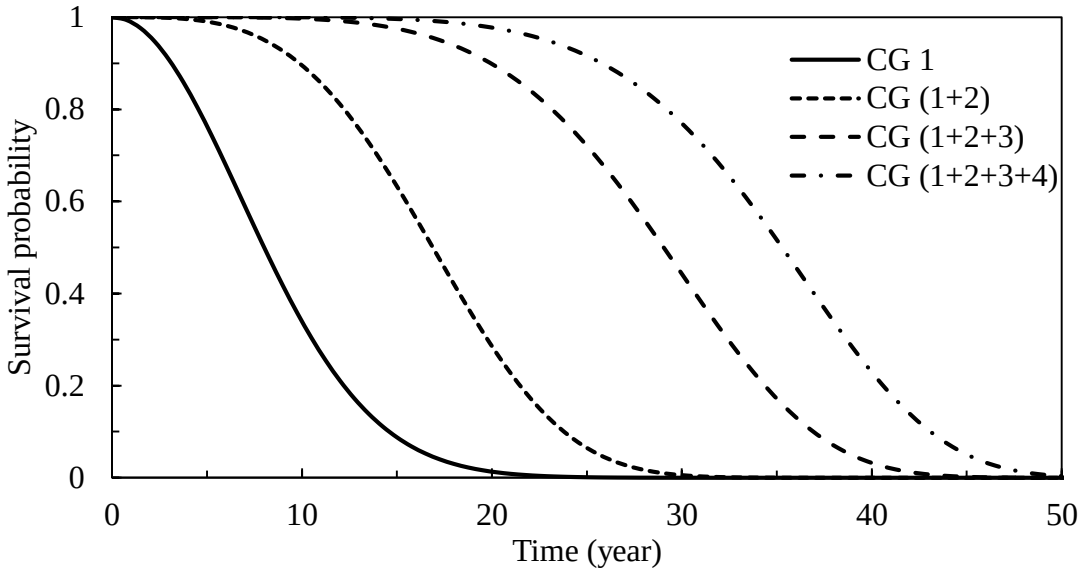

Figure 4.15 Survival functions of cumulative waiting times in different condition grades (CG) subject to slow deterioration rate.

4.6.2. Survival probabilities estimated from transition approach

The parameters of the Weibull function are estimated using Equations (4.32- (4.33). Trust-Region algorithm is utilised to solve the minimisation function to estimate the parameters for different condition grades, and results are presented in Table 4.4. The estimated parameters in the tables are applied to Monte Carlo simulations to generate the cumulative survival distributions of the transition process and their changes over time are shown in Figure 4.16.

For the same year and but subject to medium deterioration rate, the probability of being in CG2 and CG3 is about 37% and 52%, respectively, as shown in Figure 4.17. For the sea dyke subject to the slow deterioration rate, the probability of being in fair conditions CG2 and CG3 at the same year, i.e. 15 years after the initial day, is about 50% and 31%, respectively, as shown in Figure 4.18. On the other hand, the probability of being in very good conditions (CG1) is negligible for a 10-year old sea dyke subject to fast and medium deterioration rates, while it is about 12% for slow deterioration rate.

Table 4.4 Parameter estimation for three different scenarios using transition approach.

CG	Fast rate				Medium rate				Slow rate			
	τ_{50} (Year)	τ_0	κ_i	θ_i	τ_{50} (Year)	τ_0	κ_i	θ_i	τ_{50} (Year)	τ_0	κ_i	θ_i
1(→ 2)	6	11	3.212	0.111	6	14	2.851	0.097	8	16	2.815	0.079
2(→ 3)	5	9	2.410	0.122	8	13	2.831	0.087	8	12	2.776	0.079
3(→ 4)	9	14	2.855	0.067	10	15	2.523	0.061	12	21	2.525	0.054
4(→ 5)	7	14	3.663	0.100	9	17	3.441	0.081	10	16	3.655	0.064

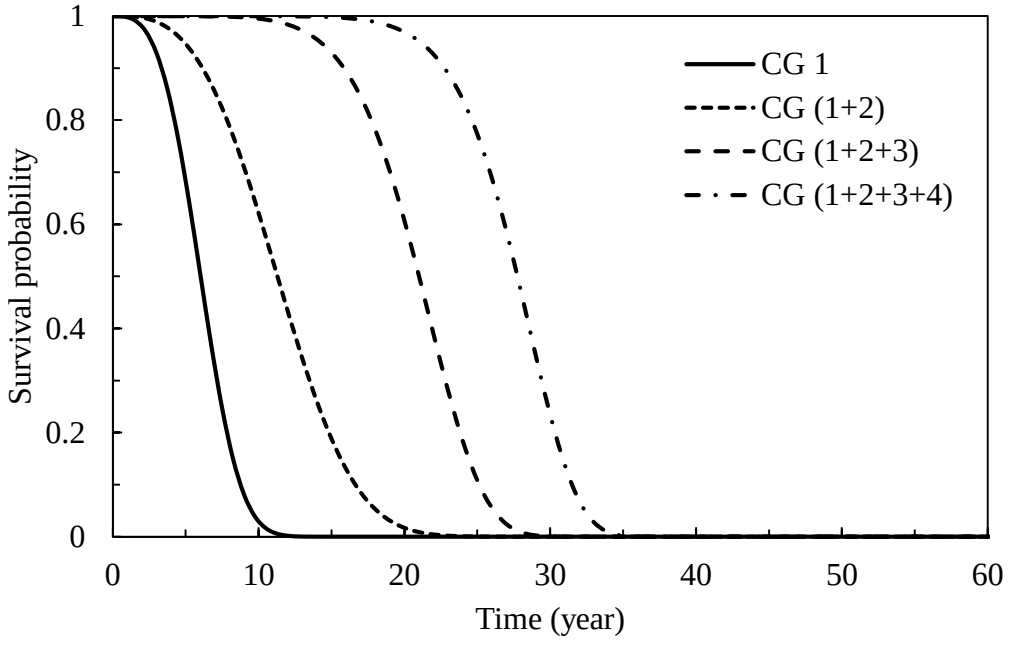

Figure 4.16 Survival functions of cumulative waiting times in different condition grades (CG) subject to fast deterioration rate.

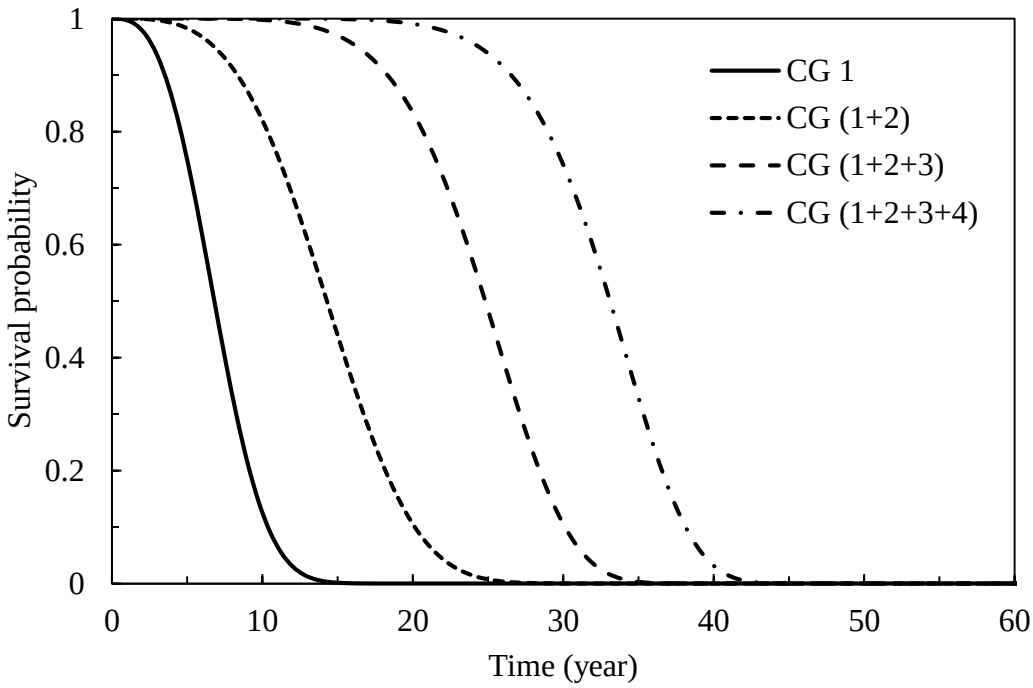

Figure 4.17 Survival functions of cumulative waiting times in different condition grades (CG) subject to medium deterioration rate.

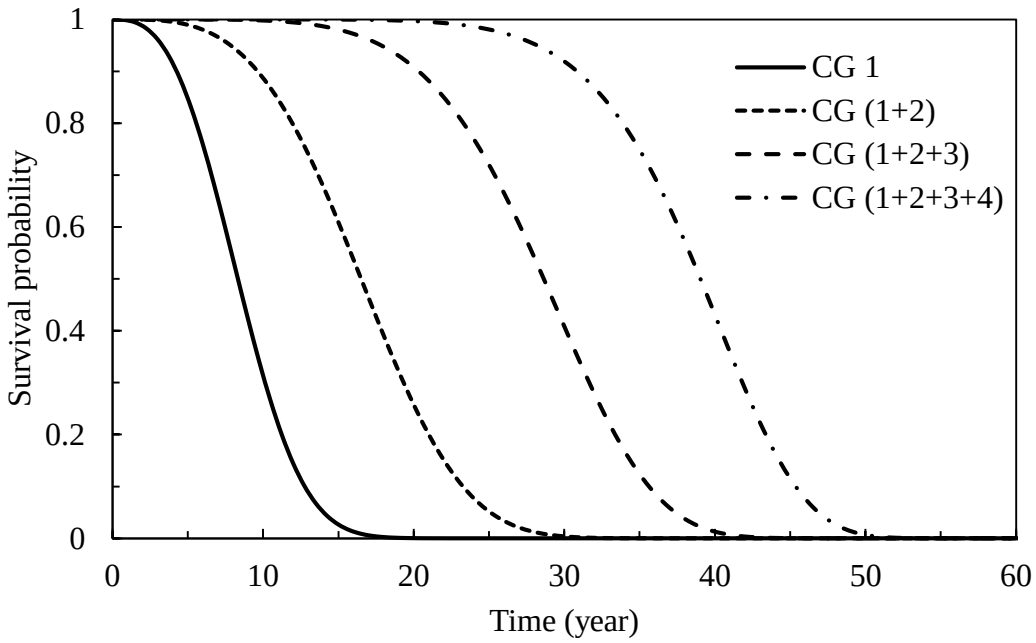

Figure 4.18 Survival functions of cumulative waiting times in different condition grades (CG) subject to slow deterioration.

4.6.3. Comparison of results from two approaches

The evolution of the condition grades over time is estimated using the non-homogeneous Markov model by assuming that the waiting times follow a Weibull distribution. The parameters of the Weibull distribution are evaluated via two-state and transition approaches. In the two-state approach, it is assumed that the asset deteriorates according to a two-state homogeneous Markov model. While in the transition approach, the asset deteriorates gradually by assuming the survival probability at the deterministic transition year is 50%.

A quick comparison between the estimated results shows that the two-state approach estimates a more conservative estimates, suggesting the asset reaches to the higher condition grades faster. The probability of the good condition grades 1 and 2 are closer to the reality if the transition approach utilised, suggesting higher probabilities at the early ages. The comparison between the estimated results and the available inspection data from the case studies shows that the transition approach provides a closer estimation to the observed condition grades.

4.7. Summary and conclusions

In this chapter, a gamma process model is investigated to simulate the deterioration process in flood defences. Additionally, two stochastic and state-based models are proposed to evaluate the future deterioration of flood defence structures by utilising Markov model with consideration of the structure's current condition. The gamma process model was already developed in other studies, e.g. Chen and Alani (2012), and in this chapter only the simulation process is developed in order to compare and study of the deterioration process with other models. The state-based deterioration models (Markov models) are developed to characterise the deterioration process with a condition grading system, which is useful for risk management and maintenance optimisation.

In order to characterise the deterioration models and to adopt them into the condition grading system (state-based), the geometrical damage tables, e.g. crest level loss in different condition grades, are utilised. The parameters for both homogeneous and inhomogeneous Markov models are estimated based on inspection results and available data, e.g. the data published by Environment Agency (2006). A Weibull function is

utilised to define the length the waiting time between the different condition grades with consideration of different deterioration rates. Two different approaches are suggested to evaluate the Weibull parameters, two-state and transition approaches, namely. Finally, case studies are provided for the developed models in order to show the applicability of the models and to illustrate the future deterioration process in coastal defence structures.

From the results obtained by the proposed models, following conclusions are drawn: a) the stationary Markov process is used to model deterioration process that will be useful in the fragility curve estimations. Although the model is practical, it is not recommanded for simulation of the deterioration process of far future, e.g more than 40 year, because the possible change in the deterioration rate in the future is not considered in this model ; b) the semi Markov model is capable of simulating time-dependent deterioration process, and it will be useful for time-dependent reliability analysis. However, the simulation and calulation process is complex, and many parametres need to be considered carefully; c) the probability distributions of condition grades of the structures provide information regarding the performance deterioration over time with uncertainties; d) the transition probability matrix is critical for the Markov chain deterioration models and can be determined by using robust non-linear optimisation techniques on the basis of estimated performance deterioration rates; e) and the estimation of the transition probaility matrices mainly depends on the available data, e.g. the detrioration curves published by Environment Agency, which is a limitation for the proposed model.

5. Reliability-based performance assessment for coastal defences

5.1. Introduction

The challenge of an accurate failure probability and reliability evaluation for coastal flood defence structures has been addressed in many studies. Changes in the resistance of coastal defence structures and hydraulic loading conditions over time are two significant challenges for risk assessment. Risk assessment methodologies for the coastal defence structures still need to be developed due to the impact of climate change or other changing environments. As discussed in literature reviews, wave overtopping and piping are two primary failure mechanisms in coastal defences, and this thesis focuses on them. The main contributions of this chapter are as follows:

- Fragility curves are developed by utilising the proposed stationary deterioration model to analyse the reliability of the coastal defences.
- Fragility surface is proposed for a time-dependent reliability analysis associated with a particular load.
- Time-dependent reliability model is developed by utilising the proposed non-stationary deterioration model for coastal defences.

5.2. Failure risk assessment

Sea defences provide essential protection for coastal lowlands against flooding. The risk of land flooding can increase in the future due to the rise of sea level and change of wave conditions caused by climate change. The sea level rise also affects the future hydraulic loading on sea defence structures, leading to further deterioration of structural resistance. In order to effectively manage these risks, reliability analysis is often employed to provide a useful tool for quantitatively evaluating the risks of sea defence structures under future conditions in order to predict the probability of failure for the structures over time. The probability of failure of coastal flood defences is relevant to the type of the structure and its conditions. A proper reliability analysis needs three main steps (Buijs, 2005; Steenbergen and Lassing 2004):

1. Defining the flood defence system and its structure types, its boundary conditions and the floodplain protected by the flood defence.

2. Identifying failure mechanisms and their mutual relationships, developing fault tree, and formulating limit state functions.
3. Discretion the flood defence system into flood defence sections, using the information from the flood defence system as a basis for probabilistic calculations.

Failure probability of coastal defence structures is often calculated regarding annual and extreme hydraulic conditions. The annual probability of failure is used to determine the state of the asset, and the event probability of failure is used for risk analysis models (Buijs et al. 2009). In the reliability-based analysis, the first step is to define the desired/required performance level of the structure. The asset is prioritised to the required service life and the most extreme event in the fault tree that identifies the end of service life. Performance of the structure is the combination of the short-term and long-term fulfilment of the functional requirements, which includes safety, serviceability and functionality of the structure during the lifespan that may be expressed by limit state equations. As mentioned in literature reviews, the failure is defined when limit state equation is equal or less than zero, as shown in Figure 5.1.

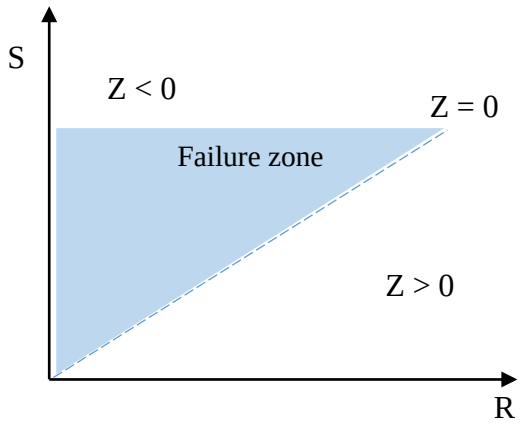

Figure 5.1 Schematic of a reliability function.

Acceptable target limits or desired performance levels have to be set for the reliability assessment of the structures. In reliability analysis, the threshold for damage and deterioration is defined as a serviceability limit state, and the threshold between damage and break is defined as an ultimate limit state (Birolini 2007):

- Serviceability limit state (SLS), defined as the limit between two states: 1) the state that the performance of the structure is acceptable, and 2) the state where

the structure is no longer serviceable. Excessive wave overtopping is most crucial failure mechanism in coastal flood defences in the category of serviceability failure modes.

- Ultimate limit state (ULS), defined as the limit between two states: 1) the state that the structure is no longer serviceable, and 2) the state that the structure has collapsed. Piping and uplifting are two critical failure modes in this category.

In the limit state equation, both strength and load may interpret in time-dependent stochastic random variables. The time-dependent failure probability is expressed as

$$P_f(t) = Pr(Z(t) \leq 0) = Pr(S(t) \geq R(t)) \tag{5.1}$$

The reliability is the counterpart of the probability of failure:

$$Pr(Z(t) > 0) = 1 - P_f(t) \tag{5.2}$$

Hence, if the distribution and the density of the strength and load variables are known, it is possible to estimate the probability of failure. In the reliability function, the strength and load variables are assumed to be stochastic variables. It means the variables are defined by statistical distributions and probability density functions. The load variables are discussed in Chapter 3, and the variables of strength deteriorating over time are discussed in Chapter 4. The deterioration level is estimated by utilising stochastic processes, which are discussed in detail in the previous chapter. The failure probability for different time can be determined if the loads and deterioration level at the desired time is known. The failure probability over time can be described in a small time-step to estimate the rate of failure probability with respect to lifetime L (Buijs et al. 2009).

$$\eta(t)dt = \Pr[failure\ for\ (t, t+dt) | (no\ failure\ for\ (0,t)] = \frac{f_L(t)dt}{1 - F_L(t)} \tag{5.3}$$

with the definition of hazard rate and lifetime distribution the following equation is derived

$$\eta(t) = \frac{f_L(t)}{1 - F_L(t)} \tag{5.4}$$

Now by considering the time-dependent limit state equation $Z(t)$, time-dependent reliability analysis is calculated by means of at least one statistical distribution function for load or strength or both at time t, which provides the failure probability as well. The

statistical distribution functions can be extreme water levels, significant wave heights, etc. Consequently, time-dependent reliability analysis describes a stochastic process and calculates the failure probability per unit of time as

$$P_f(t) = \int_{Z \leq 0} f_{RS}(s(t), r(t)) dr ds \tag{5.5}$$

where f_{RS} is the joint probability density function of load S with value of s at time t, and strength R with value of r at time t. The integral implies that the time-dependent reliability problem is joint probability density function of loading and strength parameters, and continuously changes with time. Let $F_R(x)$ be the cumulative density function that returns the failure probability given the value x of a certain load variable, e.g. sea water level. With the definition of limit state function, the annual failure probability of variable x is given here as (Van der Meer et al. 2009)

$$P_f = \int_{-\infty}^{\infty} f_S(x) F_R(x) dx \tag{5.6}$$

where the strength and the load are independent. The above function is the basis for estimating annual failure probability in this study. It was discussed in the previous chapters that the strength and load in coastal flood defence structures are always a function of multiple variables such as water level h_w and significant wave height H_{m0}.

Simulation process

Monte Carlo simulations are adopted to evaluate the time-dependent failure probability due to its flexibility. In the Monte Carlo simulations, a large number of samples ($> 10e6$) are generated corresponding to the variable parameters, and the probability of failures are estimated as follows

$$P_f \approx \frac{1}{N} \sum_{1}^{N} I\{Z(R(t), S(t)) \leq 0\} \tag{5.7}$$

where N is the total number of simulations; and $I[.]$ is an indicator function which takes values when $Z(t) \leq 0$. During the Monte Carlo simulations, the desired period of the analysis is divided into uniform time intervals, and then the stochastic processes are sampled. Therefore, for example for time $t = 1$, sampling is undertaken for all random variables $X_1, .., X_n$. X_n(t), which is a time-dependent function $X_n(t) = f(v_1, \dots v_n)$

where v is the effective variable in a time-dependant process. The required number of sample for an acceptable level of accuracy is given in Melchers (1999) as

$$N > \frac{-ln(1-L_c)}{P_f} \tag{5.8}$$

where L_c is the confidence level. Based on the sample of the random variables the limit state equations corresponding to the different failure mechanisms are computed and evaluated whether $Z(t) \leq 0$. Then, the failure probability is

$$P_f(t) = \frac{N_f}{N} \tag{5.9}$$

where N_f is the numbers of simulations that the limit state function is equal or less than zero.

5.3. Fragility curves and fragility surfaces

A fragility curve provides information on the structure's reliability associated with the loads as well as its uncertainty. The shape of the curve approaches to a form of step function when the uncertainty becomes lower, while high uncertainty makes it an *S* shape curve. The step function shows a critical load that causes the system to fail, and it is appropriate for a well-understood system (Schultz et al. 2010) and also for a deterministic analysis as discussed in chapter 2. On the other hand, for a complex and changeable system with high level of uncertainty, the S-shaped function is more appropriate in order to illustrate the performance level of the system for a specific range of load/demand (Hall et al. 2009), as shown in Figure 5.2.

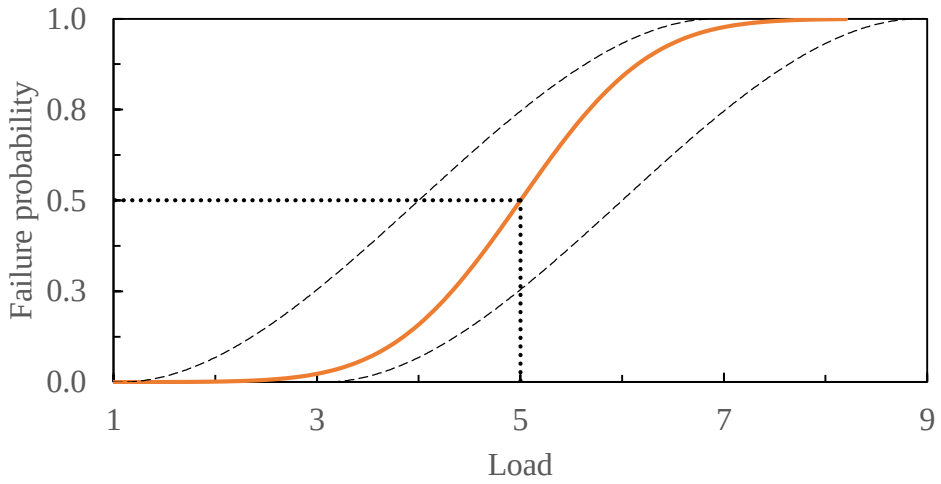

Figure 5.2 Typical S-shape fragility curves (solid line) and the uncertainty area (dashed line).

Let the load variable to be considered in the fragility curve be water level. The failure probability P_f corresponding to water level h_w is rewritten as

$$P_f = \Pr(S \geq R|h_w) = \int_{-\infty}^{\infty} f_{h_w}(h_w) \cdot F_{\mathrm{R}}(h_w) \cdot dh_w \tag{5.10}$$

where $f_{h_w}(h_w)$is the probability distribution function of the water level; and $F_{\mathrm{R}}(h_w)$ is the cumulative distribution of the available strength for the water level load parameter which is called fragility curve. The above function can be expressed for any other load parameters similarly. The cumulative distribution function of the strength of the structure, e.g. sea dyke, gives the relationships between the load and the failure probability for the desired load, as shown in Figure 5.2. Therefore, by considering the relationship between the water level h_w at time t, the failure probability can be expressed as

$$P_f = P(S \geq R|h_w, t) = \int_{h_w \geq R} f_{h_w}(h_w(t)) F_R(h_w(t)) dh_w(t) \tag{5.11}$$

where $f_s(h_w(t))$ is joint probability density for water level h_w at time t; and $F_R(h_w(t))$ is cumulative density function which represents the failure probability given the water level h_w at time t with consideration of the residual strength, and the fragility surface is shown in Figure 5.3.

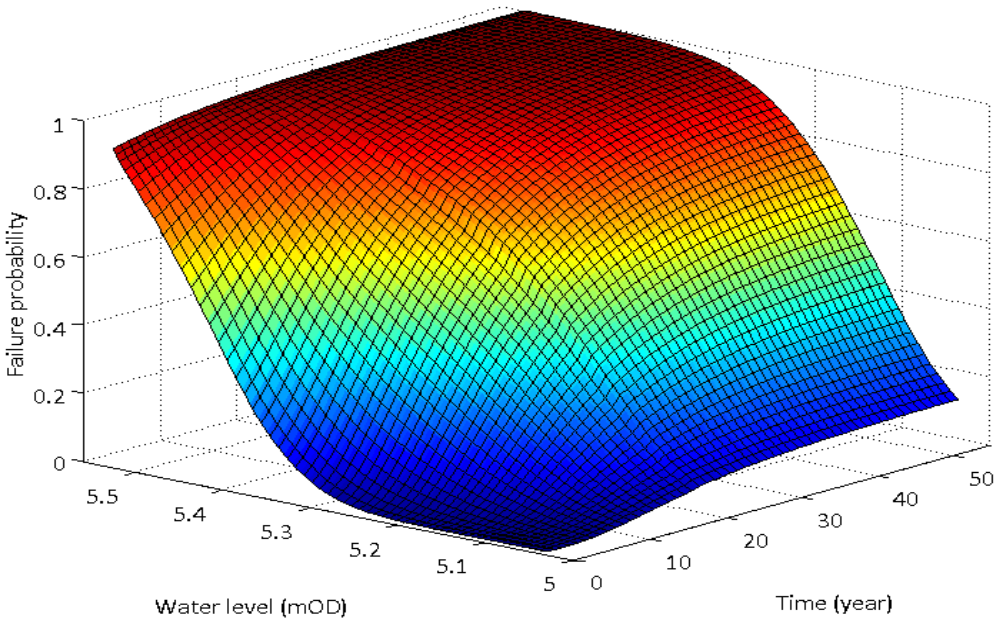

Figure 5.3 Fragility surf as a failure mechanism as a function of water level and time after initial date.

5.4. Excessive wave overtopping failure

In a reliability analysis of a sea dyke, a critical failure mode such as the excessive wave overtopping might be dominant. The demand defined is based on allowable overtopping discharge over the dyke. The overtopping discharge related to the structure's freeboard which is between the still water level and the crest level. The crest height will degrade over time as it ages and wears, and will cause decrease in capacity of freeboard. The probability of failure is the probability that the overtopping discharge exceeds allowable limit. When the overall failure probability exceeds a certain level, the maintenance should be applied on the dyke's crest level.

Wave overtopping discharge is one of the critical parameters in the failure mode. Depending on the structure's type and importance, some rates of overtopping discharge are allowed (Van der Meer et al. 2016). However, excessive overtopping discharge may result in erosion and damage to the dyke. The influence of deterioration processes during structure's lifespan such as settlement may reduce the resistance of the sea dyke, and ongoing excessive overtopping may cause the serviceability failure. Overtopping discharge rate is calculated based on an exponential function, with consideration of boundary conditions and structure strength, e.g. wave height, inner slope, wave angle and berm width, and given as (Pullen et al. 2007; Van der Meer et al. 2016)

$$q = A\ exp(BR_c) \tag{5.12}$$

where coefficients A and B in the function are related to the method concerned; and R_c is the freeboard defined by the height of the crest above still water level.

Hydraulic conditions and structural resistance especially crest level control the failure probability of coastal defences due to excessive wave overtopping. Hydraulic loads vary due to changing environments significantly and often become more severe due to sea level rise. In the meantime, the structural resistance of coastal defences such as the crest level of earth sea dykes may decrease due to degradation, e.g. due to traffic and soil consolidation. Excessive wave overtopping may lead to the landslide slope and slope failure by eroding the dyke crest. Figure 5.4 illustrates schematic of excessive failure

mechanism for a sea dyke regarding changes in hydraulic conditions and deteriorations on the crest level over time.

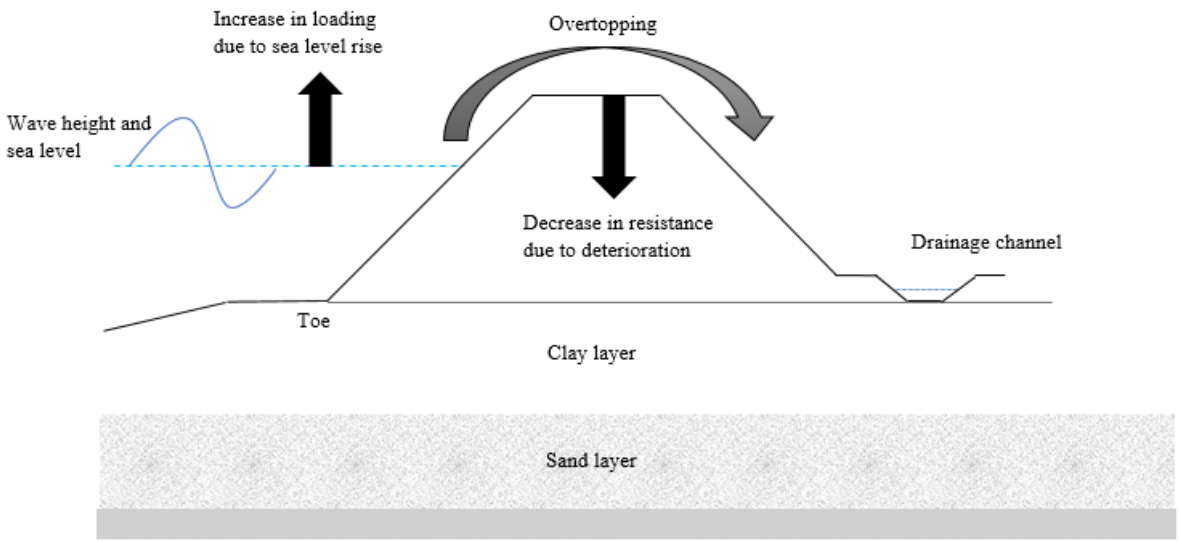

Figure 5.4 Schematic diagram of wave overtopping discharge over a sea dyke.

Basic approaches for overtopping discharge calculations are divided into three groups, depending on the structure type:

- Smooth slopes.
- Rough slopes.
- Special conditions.

For smooth slopes and rough slopes the approaches for estimating overtopping by Owen (1980) and TAW (2002) are suggested in the most literature (e.g. Chini and Stansby 2012; Sierra et al. 2016)). For special conditions such as oblique waves, and rough slopes with crest walls, approaches by TAW (2002) and Hawkes et al. (2000) are suggested. This study only focuses on TAW (2002) model as this method is the most comprehensive method and suggested by EurOtop manual II (Van der Meer et al. 2016).

In order to protect seaside slope of earth sea dykes and embankments from wave overtopping, different kinds of revetment such as grass, asphalt, concrete and natural blocks are used. For consideration of the influence of surface roughness γ_f , berm γ_b and oblique waves γ_β , the values of reduction factors are available in CIRIA and EurOtop

manual. For example, concrete and grass revetments have roughness factor of 1.00, and ribs have roughness factor of 0.75. The limit state equation for overtopping failure mechanism Z_q is modified here as

$$Z_q(t) = q_{cr} - \chi_q q(t) \tag{5.13}$$

where q_{cr} is the critical or predefined overtopping rate; χ_q is model uncertainty coefficient associated with overtopping; and $q(t)$ is average overtopping discharge over time, expressed here as (Van der Meer et al. 2016)

$$\frac{q(t)}{\sqrt{g{H_{m0}}^3(t)}} = \frac{0.023}{\sqrt{\tan\alpha_1}}\gamma_b\xi_{m-1,0}(t)\exp\left[-\left(2.7\frac{R_{c,i}(t)}{\xi_{m-1,0}\,\gamma_b\gamma_f\gamma_\beta H_{m0}(t)}\right)^{1.3}\right] \tag{5.14}$$

with a maximum of:

$$\frac{q(t)}{\sqrt{g{H_{m0}}^3(t)}} = 0.09\exp\left[-\left(1.5\frac{R_{c,i}(t)}{\gamma_f\gamma_\beta H_{m0}(t)}\right)^{1.3}\right] \tag{5.15}$$

where γ_b, γ_f and γ_β are correction factors for berm, roughness and oblique wave attack, respectively; $H_{m0}(t)$ is depth-limited significant wave height at the toe of structure at time t; $R_c(t)$ is crest freeboard of the structure at time; and $\xi_{m-1,0}(\mathrm{t})$ is local breaker parameter over time which is related to the slope steepness $\tan\alpha_1$.The breaker parameter or Iribarren number $\xi_{m-1,0}$ (also known as the surf similarity parameter) is a dimensionless parameter to model several effects of (breaking) surface gravity waves on sea bed and coastal structures, and describes as follow

$$\xi_{m-1,0}(t) = \frac{tan\,\alpha_1}{\sqrt{\frac{H_{m0}(t)}{L_{op}}}} \tag{5.16}$$

where α_1 is the slope of the horizontal and the overall structure slope; and L_{op} is deep water wavelength expresses as

$$L_{op} = \frac{g\cdot {T_{m-1,0}}^2}{2\pi} \tag{5.17}$$

where g is the gravitational acceleration; and $T_{m-1,0}$ is spectral wave period.

Freeboard deterioration modelling using gamma process

For the existing coastal defence structures subjected to sea level rise, by considering crest level settlement over time, the future freeboard $R(t)$ at time t can be determined by

$$R_c(t) = R_c(0) - \Delta h_w(t) - \sum \Delta H_d(t) \tag{5.18}$$

where $R_c(0)$ is initial freeboard at present day; $\Delta h_w(t)$ is the sea level rise at time t; and $\Delta H_d(t)$ is the time-dependent deterioration of dyke crest height due to settlement. The settlement of dyke crest level is often estimated with uncertainties, requiring a stochastic modelling for the deterioration process. The gamma process is a stochastic process with independent non-negative increments having a gamma distribution with a given average of deterioration, therefore it is an appropriate model for the resistance degradation process such as crest level settlement over time. From the definition of the gamma process described in Chapter 4, the probability density function of the deterioration of dyke crest height due to settlement ΔH_d occurring at time t ($t \geq 0$) can be described as

$$f_{\Delta H_d(\mathrm{t})}(\Delta H_d) =$$

$$Ga(\Delta H_d|\kappa_d(t), \theta_d) = \begin{cases} \dfrac{{\theta_d}^{\kappa_d(t)}}{\Gamma[\kappa_d(t)]} {\Delta H_d}^{\kappa_d(t)-1} e^{-\theta_d \Delta H_d}, & for\ \Delta H_d \geq 0 \\ 0\ , & \text{elsewhere} \end{cases} \tag{5.19}$$

where $\Gamma[\eta_d(t)] = \int_0^\infty V^{\kappa_d(t)-1}\, e^{-\nu} d\nu$ for $\kappa_d(t) > 0$ is the gamma function. The scale parameter θ_d with $\theta_d > 0$ and the shape function $\kappa_d(t)$ could be estimated from maximum likelihood method by using in-situ measurements about the dyke crest settlement, expressed here as

$$\theta_d = \frac{\mu_d}{{\sigma_d}^2}$$
$$\kappa_d(t) = \frac{{\mu_d}^2 t}{{\sigma_d}^2} \tag{5.20}$$

where μ_d and σ_d are the mean value and standard deviation for the average decrease in the crest level, respectively.

Freeboard deterioration modelling using Markov process

The crest freeboard of the structure at time t, $R_c(t)$, can be denoted as $R_{c,i}$, given condition grade $i \in \{1,2,3,4,5\}$. The future freeboard $R_{c,i}(t)$ at time t is described here as

$$R_{c,i}(t) = R_{c,i}(0) - \Delta h_w(t) - \Delta L_{Z,i}(t) \tag{5.21}$$

where $R_{c,i}(0)$ is initial freeboard at initial time; $\Delta h_w(t)$ is the sea level rise at time t; and $\Delta L_{Z,i}(t)$ is the deterioration of crest level in vertical direction, associated with certain condition grade at time t. In order to characterise the deterioration level $\Delta L_{Z,i}$ regarding the initial freeboard, Table 5.1 is suggested. The values in the below table are general and derived from the Environment Agency publications, and might be slightly different for each case study.

Table 5.1 Suggested vertical crest level loss (Long et al. 2013) for a sea dyke related to condition grade system.

Grade	Crest level loss, $\Delta L_{Z,i}$ (m)	Distribution of deterioration intensity
1	$0.00 \leq \Delta L_{Z,1} < 0.05$	Lognormal
2	$0.05 \leq \Delta L_{Z,2} < 0.10$	Normal
3	$0.10 \leq \Delta L_{Z,3} < 0.20$	Normal
4	$0.20 \leq \Delta L_{Z,4} < 0.40$	Normal
5	$0.40 \leq \Delta L_{Z,5}$	Lognormal

Risk of failure due to wave overtopping

The effects of dyke failure due to wave overtopping depend on the importance of the structure and the protected lands. Although the implications of failure in reality are random variables, this thesis is focused on the expected values of loss regarding likely damage and replacements. The annual risk $R_f(t)$ in monetary term is expressed (Allsop et al. 2008; Barone and Frangpol 2014) as

$$R_f(t) = E(C_R) = P_f(t) \cdot \sum C_{tot}(t) \tag{5.22}$$

where $E(C_R)$ is the expected value of loss due to wave overtopping; and $C_{tot}(t)$ is total cost of loss at time t. The total cost of loss C_{tot} at time t is estimated as the sum of three different losses due to the dyke failure (Allsop et al. 2008), given here as

$$C_{tot}(t) = \frac{C_{hazard} + C_{direct} + C_{erosion}}{(1+r)^t} \tag{5.23}$$

where C_{hazard} is the direct hazard of injury or death to people immediately behind the defence including direct and indirect costs expressed in monetary term; C_{direct} is the damage to property and infrastructure in the area defended, including the defence structure; $C_{erosion}$ is the damage to the environment and erosion of the coastline; and r is the annual discount rate.

5.5. Piping failure

Underground water seepage in the water-conductive layer carries soil particles from the permeable layer due to water head difference. If this process continues long enough, pipes generate in the water-conductive soils underneath the earth dyke, eventually leading to collapse of the structure. As shown in Figure 5.5, the structure fails as a consequence of piping if the water pressure head across the structure exceeds the time-dependent critical head difference $h_{crp}(t)$. The limit state equation for this failure mechanism is given by Allsop et al. (2007) and modified here as

$$Z_p(t) = h_{crp}(t) - \Delta h(t) \tag{5.24 }$$

where $\Delta h(t)$ is the difference between seaside water level at time t, and landside water level h_b, defined as

$$\Delta h(t) = h_w(t) - h_b \tag{5.25}$$

The earliest model to estimate the critical head difference was suggested by Bligh (1912). Lane (1935) developed Bligh's formula to take into account the vertical component of the seepage length. Selmeijer (1989) further developed these models to consider more sophisticated soil properties, as well as seepage flow in different directions. Later, the model developed based on experiments in Weijer and Selmeijers (1993) with consideration of the sand layer thickness, given here as

$$h_{crp} = C\beta \cdot (\frac{\gamma_s}{\gamma_w} - 1) \cdot \tan\theta_s \cdot (0.68 - 0.1\, ln\, C) L_P(t) \tag{5.26}$$

where γ_s is weight per unit volume of sand particles; γ_w is weight per unit volume of water; θ_s is soil friction angle; L_P is seepage length; β reflects the effect of a finite thickness and coefficient C describe the characteristic of soils during erosion, defined as

$$C = (\frac{D_s}{L_P})^{\frac{0.28}{(\frac{D_s}{L_P})^{2.8} - 1}} \tag{5.27}$$

$$\beta = \omega d_{70} \left(\frac{1}{\varepsilon L_P}\right)^{\frac{1}{3}} \tag{5.28}$$

where ω is drag force factor; d_{70} the sand particle diameter of 70% weight grain size distribution; ε is intrinsic permeability; D_s sand layer thickness. According to Vorogushyn et al. (2009), the Weijer and Selmeijers (1993) model has good results for fine sandy coastlines, but the poor prediction for coarse sands due to laminar flow through the sands.

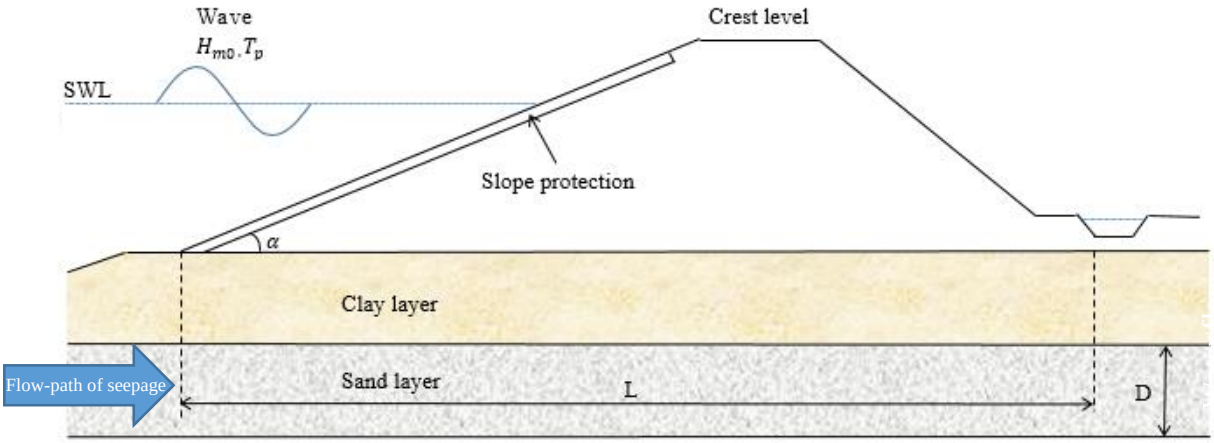

Figure 5.5 Schematic diagram of piping under a typical sea dyke over time.

Seepage length deterioration modelling using gamma process

The time-dependent critical head difference $h_{crp}(t)$ represents the resistance of seepage in soils over time. The resistance of seepage in the water-conductive layer deteriorates due to internal erosion in soils, which can be indicated by the reduction of seepage length over time (Buijs et al. 2009). The reduction of seepage length ΔL_P, occurring at time t as

a result of the deteriorating filter materials, and is described here as a stochastic gamma process. The probability density function of the increment of seepage length is modelled as

$$f_{\Delta L_p(\Delta t)}(\Delta L_p) = Ga(\Delta L_p|\kappa_p(t), \theta_p) \tag{5.29}$$

where the scale parameter θ_p with $\theta_p > 0$ and the shape function $\kappa_p(t)$ could be estimated from maximum likelihood method. The seepage length $L_P(t)$ at time t is then calculated from

$$L_P(t) = L_P(0) - \sum \Delta L_p(t) \tag{5.30}$$

where $L_P(0)$ is initial seepage length.

Seepage length deterioration modelling using Markov process

Seepage length of the structure at time t, $L_P(t)$, can be denoted it as $L_{P,i}$ given condition grade $i \in \{1,2,3,4,5\}$. The future seepage length $L_{P,i}(t)$ at time t is expressed here as

$$L_{P,i}(t) = L_P(0) - \Delta L_{X,i}(t) \tag{5.31}$$

where $L_P(0)$ is the initial seepage length at initial time; and $\Delta L_{X,i}(t)$ is the deterioration of dyke in water flow direction associated with certain condition grade at time t. In order to characterise the deterioration level $\Delta L_{X,i}$ regarding the initial seepage length, Table 5.2 is suggested. The values in the below table are general and derived from the Environment Agency publications, and might be slightly different for each case study.

Table 5.2 Suggested seepage length loss (Long et al. 2013) in water flow direction for a sea dyke related with condition grade system.

Grade	Seepage length loss, $\Delta L_{X,i}$, (m)	Distribution of deterioration intensity
1	$0.00 \leq \Delta L_{Z,1} < 0.05$	Lognormal
2	$0.05 \leq \Delta L_{Z,2} < 0.15$	Normal
3	$0.15 \leq \Delta L_{Z,3} < 0.30$	Normal
4	$0.30 \leq \Delta L_{Z,4} < 0.60$	Normal
5	$0.60 \leq \Delta L_{Z,5}$	Lognormal

5.6. Case Study at Sheerness

The same case study for an earth sea dyke that discussed in the previous chapter for the homogeneous Markov model is used here to demonstrate the reliability analysis. The deterioration process for different rates was provided, and the results from the previous chapter will be used in the current fragility curve evaluation. In this example, the parameters relevant to deterioration of crest level are considered. It is assumed that the structure is in very good conditions with the initial condition vector of (1 0 0 0 0). The transition probabilities between the condition grades were estimated using the proposed homogenous Markov deterioration model in Chapter 4. The extreme water levels and significant wave heights for a 1000-year return period are evaluated as 3.30 mOD and 2.25 m, respectively.

The projected sea level rises due to low, medium and high emission scenarios are adopted from UKCP09 (Jenkins et al. 2011) to analyse the future hydraulic conditions. According to UKCP09 low emission scenario, the projected sea level rise including vertical land movements over a period of 1990-2095 is between 18-42 cm, or 3.3 mm/year in average (Jenkins et al. 2011). According to UKCP09 medium emission scenario, the projected sea level rise including vertical land movements over a period of 1990-2095 is between 24-62 cm, or 4.5 mm/year in average (Dahl et al. 2017). The estimated sea level rise for high emission scenario including vertical land movements over the same period is between 32-86 cm, or 5.9 mm/year (Dahl et al. 2017).

5.6.1. Evaluation of the fragility curves

A reliability analysis is carried out for the excessive wave overtopping through the dyke crest. The deterioration of crest level was considered for estimation of the overtopping failure probability. Figure 5.6 shows wave overtopping fragility curves for the sea dyke in different condition grades at 1 and 2 l/s/m wave overtopping limit, where the deterioration rate is medium. The failure fragility curves shift to the right when the critical values for overtopping increases. For example, the failure probability when the dyke is at condition grade 1 and water level 2.4 mOD is about 36% for 1 l/s/m wave overtopping, while the failure probability for the same situation for 2 l/s/m is about 11%.

The results show the failure probability was not critical for the structure when it is in condition grades 1 and 2 at the water level of less than 2.2 mOD. However, the sea dyke needs immediate maintenance to raise the dyke crest level when it is in condition grade 3 for the same water level to improve the performance. The failure probability for condition grades 4 and 5 is high for the water levels more than 1.80 mOD, and the structure was not reliable due to the significant deterioration.

The overall probability of failure over time subject to medium deterioration rate is also analysed regarding various values of water levels and 1 and 2 l/s/m wave overtopping discharge limits as shown in Figure 5.7. The results emphasise that for the water levels less than 1.8 m the structure is reliable after 50 years from the present day. The changes of structure response over time are also represented in Figure 5.8 for certain various times, e.g. 0, 10, 20, 30, and 40 years after the initial day for two allowable overtopping rates. The results show that the reliability of the sea dyke decreases significantly due to the crest level settlement and sea level rise. All figures have similar trends between 1 and 2 l/s/m wave overtopping discharge limits, as expected.

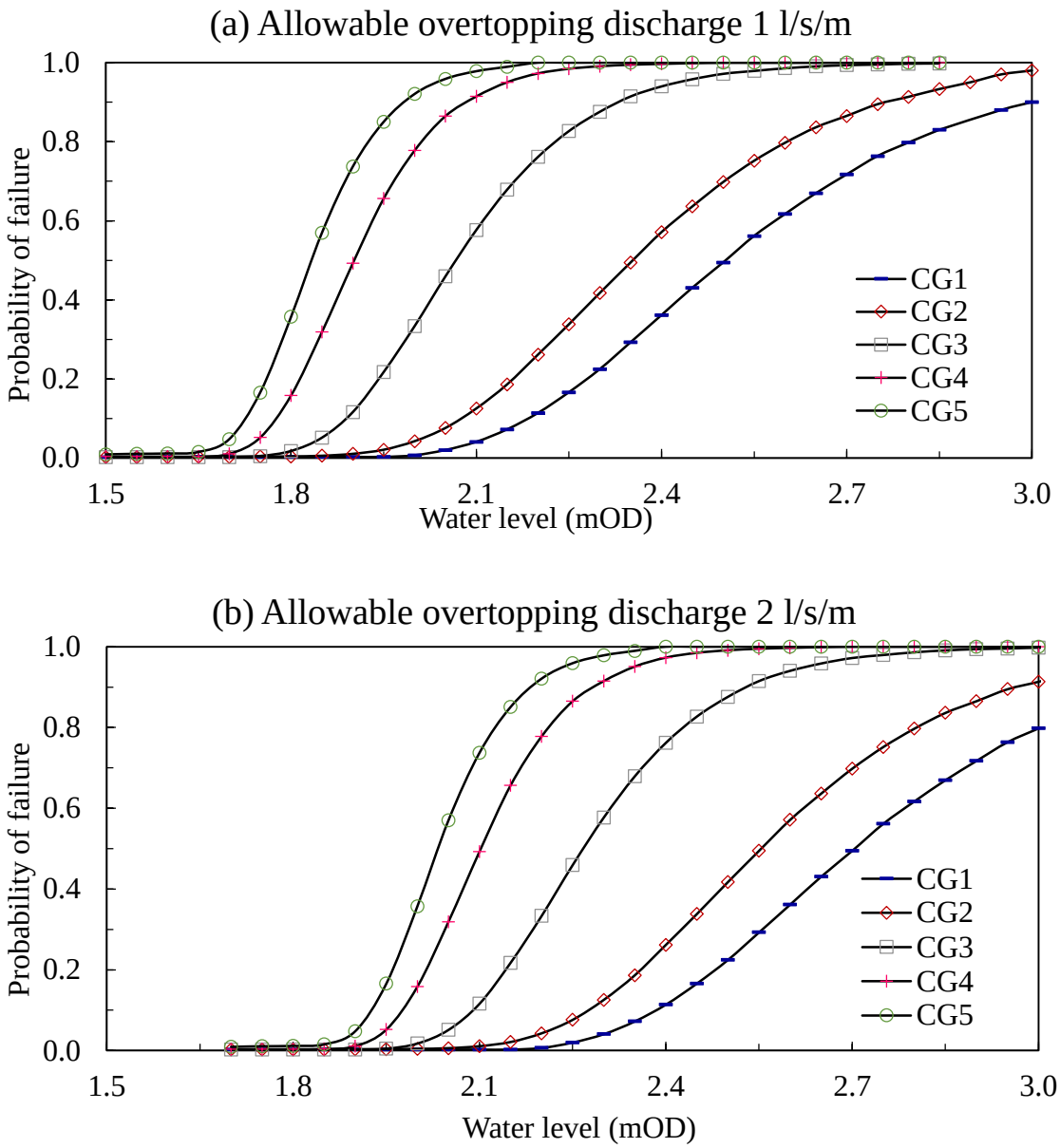

Figure 5.6 Fragility curves for diffrent wave overtopping discharge limits in specific condition grades and medium deterioration rate.

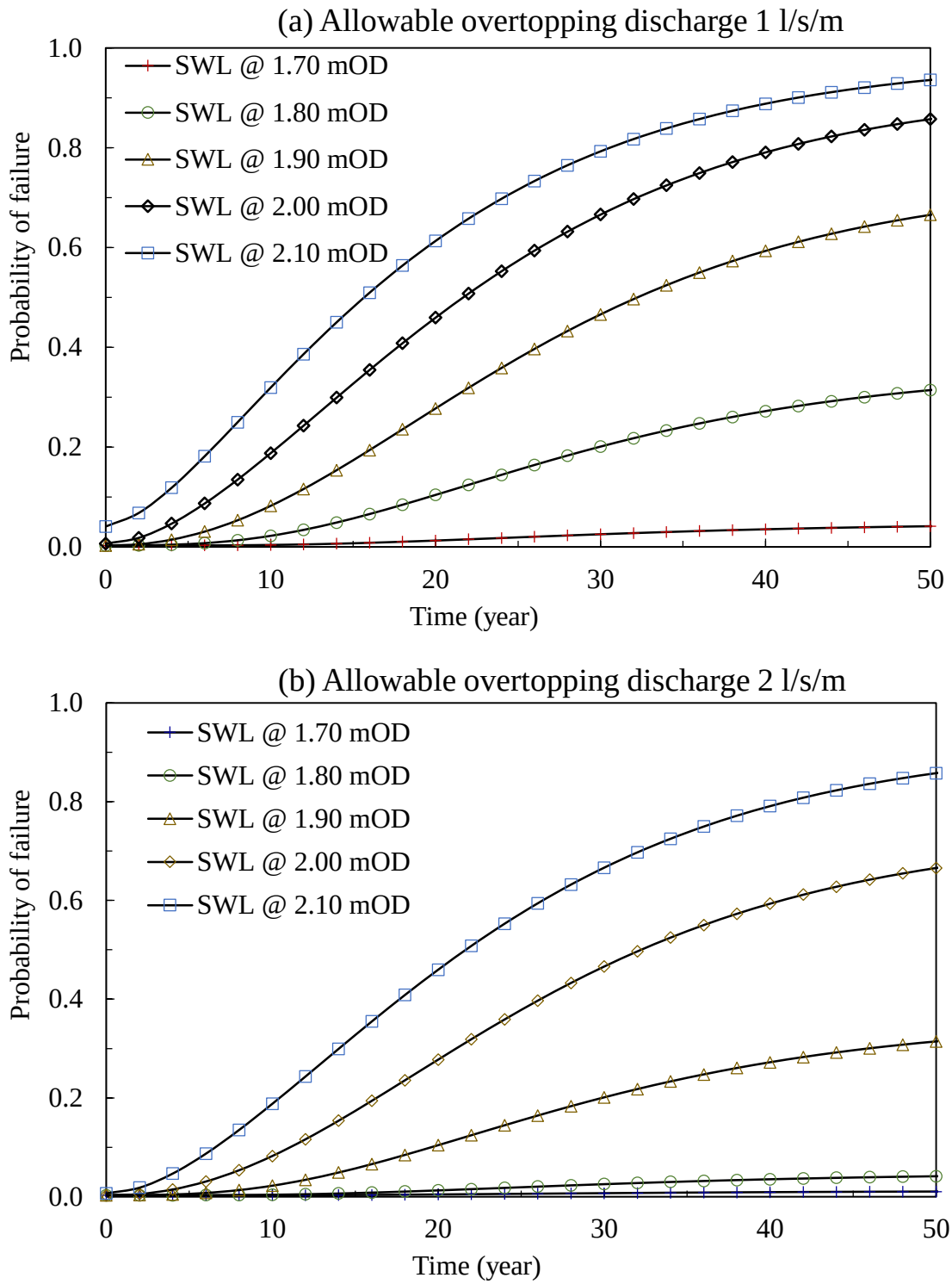

Figure 5.7 Failure probability over time at certain sea water levels for various wave overtopping discharge imits.

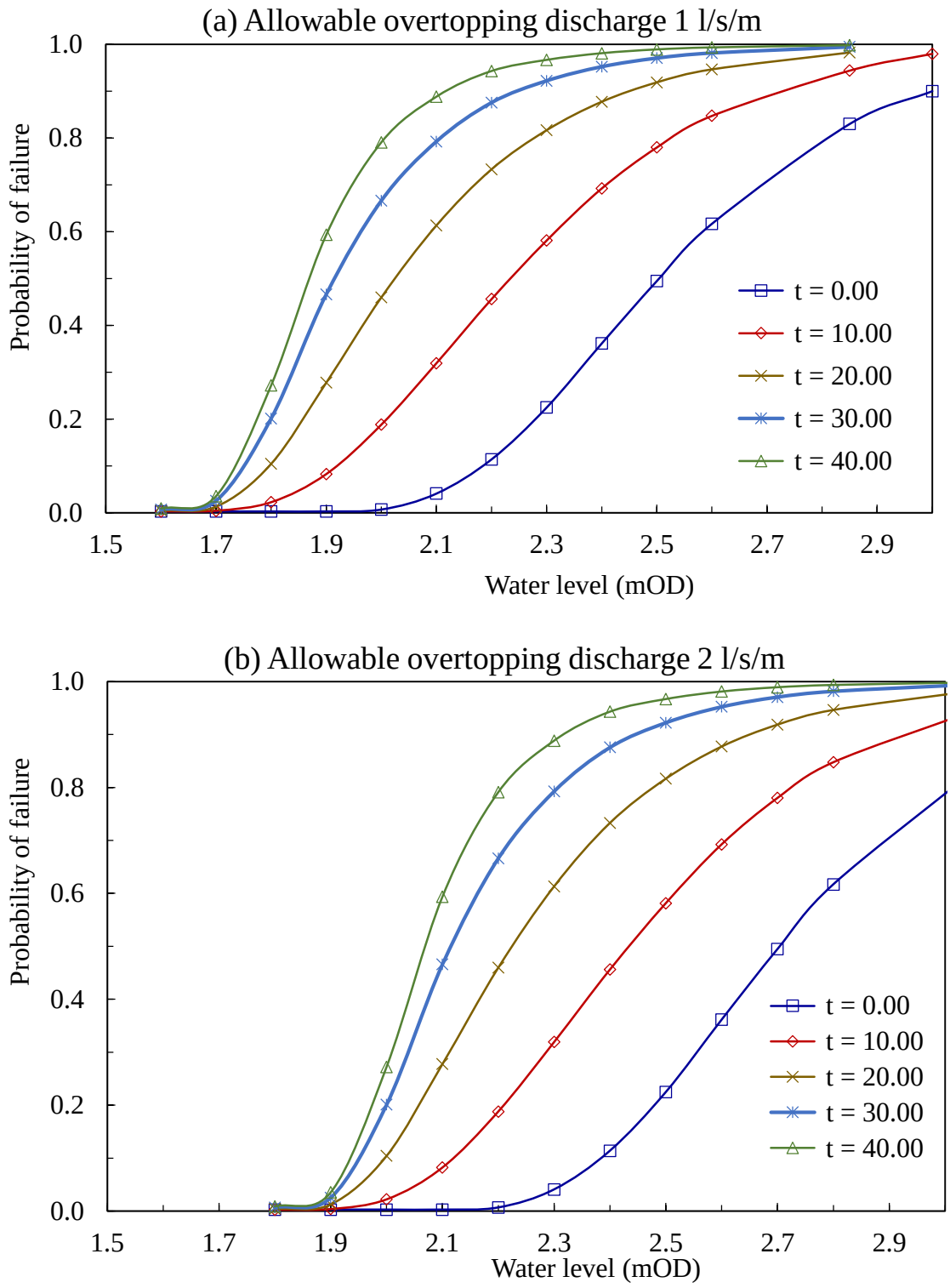

Figure 5.8 Fragility curves for various wave overtopping discharge limits with sea level rise after present day.

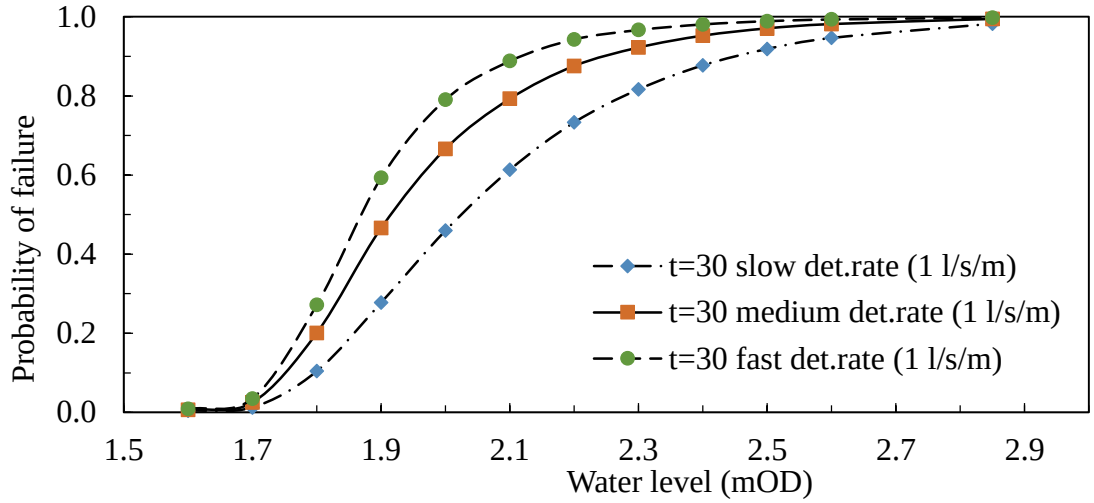

Figure 5.9 Fragility curves for 1 l/s/m wave overtopping as a function of water level at 30 years after present condition subject to different deterioration rates.

5.6.2. Effects of deterioration rates on the fragility curves

The effects of different deterioration rates for 1 and 2 l/s/m overtopping rate limits are provided in Figure 5.9 and Figure 5.10, respectively. The deterioration rates are fast, medium and slow, and the transition probabilities were estimated in the previous chapter, as shown in Figure 4.7. The failure probability steadily increases with the increase of the water level, but with the different pace regarding the rate of the deterioration as shown in the figures. The increase in the rate of deterioration from slow to medium and fast (at year 30, water level 2.1 and overtopping rate 1 l/s/m) leads to the increase in the failure probability about 18% and 30%, respectively. The increase in failure probability from slow rate to medium and fast rates for the same water level and time, but 2 l/s/m discharge, is about 20% and 34%, respectively, as shown in Figure 5.10.

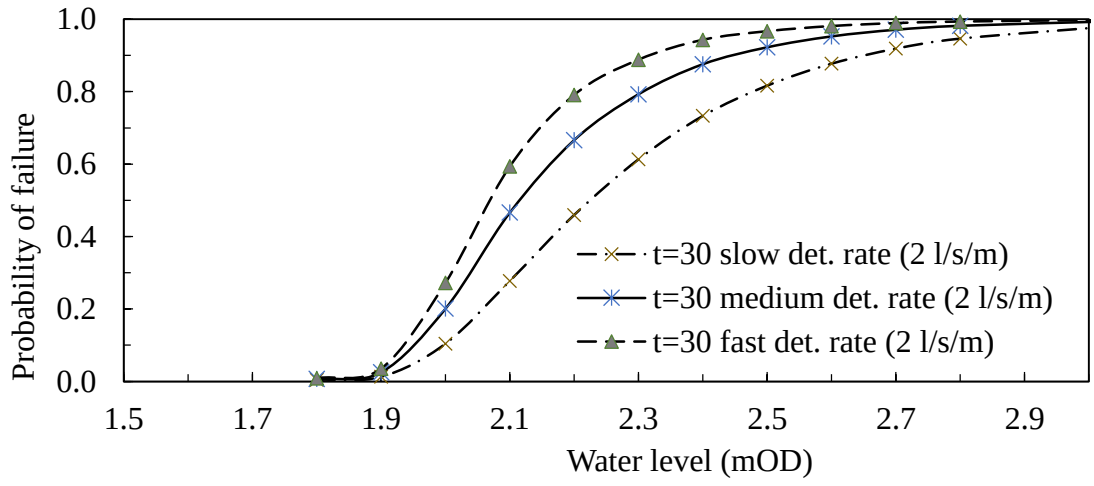

Figure 5.10 Fragility curves for 2 l/s/m wave overtopping as a function of water level at 30 years after present condition subject to different deterioration rates.

5.6.3. Effects of repair maintenance on fragility curves

In the maintenance plan, it is assumed that the dyke is refurbished to a better condition grade due to the maintenance implemented every 4 years. The effects of maintenance over different deterioration rates were estimated in the previous chapter, and the essential transition probabilities were calculated. Figure 5.13-5.16 demonstrate the effect of maintenance plan on three deterioration rates, by assuming the structure is at age 30 for a 1 l/s/m wave overtopping discharge limits. The deterioration rates are assumed to be fast, medium and slow.

The maintenance decreases the probability of the failure due to the wave overtopping in all scenarios as expected, but with different effectiveness. The improvement in the reliability of the sea dyke due to the maintenance is higher when the deterioration rate is slower. For example, the decreases in the probability of failure when the structure is at age 30 and water level is at 2.2 mOD, are about 25%, 18% and 10% for deterioration rates of slow, medium and fast, respectively. This is because in a slow deterioration rate the lifecycle of the asset is longer. Hence it is possible to apply more maintenance intervals especially when the condition are better. It is also noticed that beside the decrease in the rate of deterioration due to the maintenance, the fragility curves are also shifted to the right.

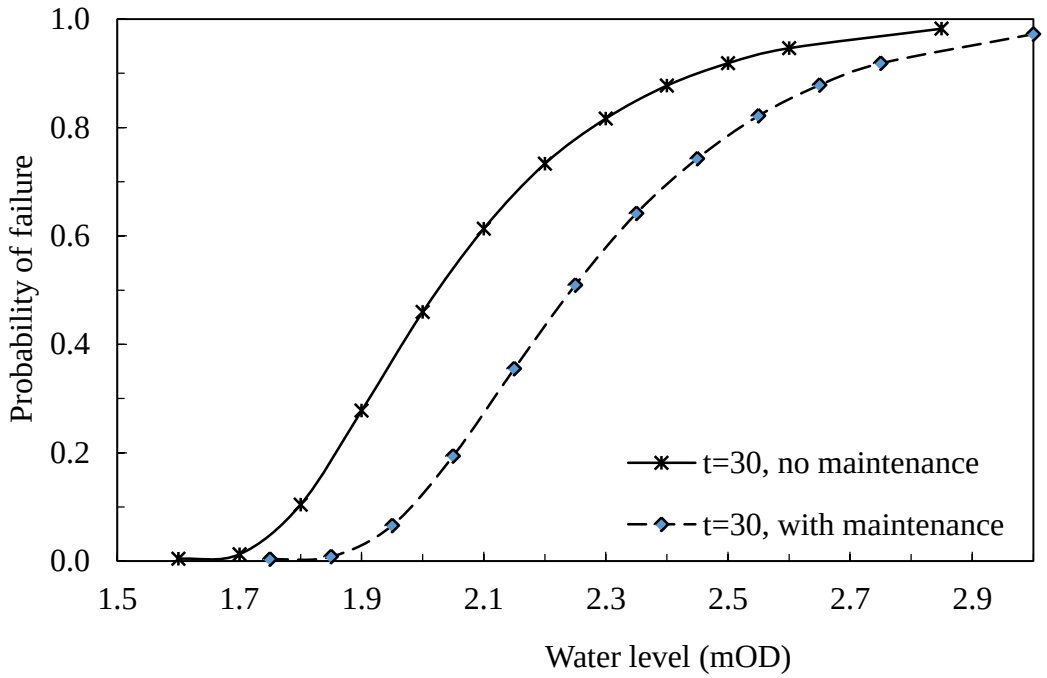

Figure 5.11 Fragility curves for 1 l/s/m wave overtopping as a function of water level at 30 years subject to slow deterioration rate and two maintenance plans.

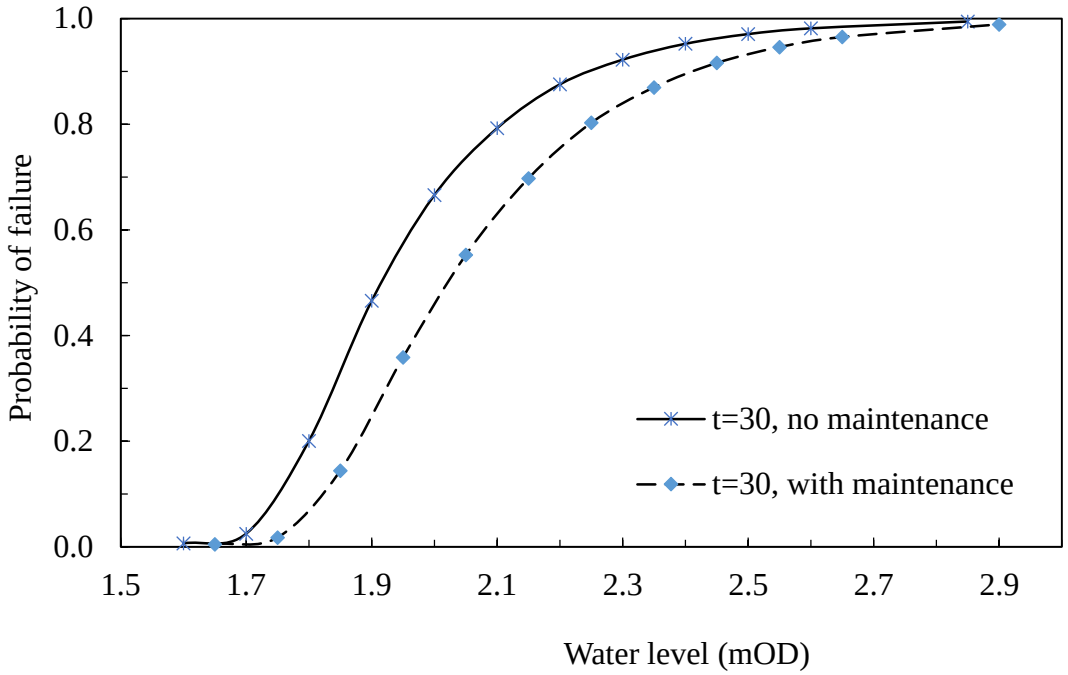

Figure 5.12 Fragility curves for 1 l/s/m wave overtopping as a function of water level at 30 years subject to medium rate and two maintenance plans.

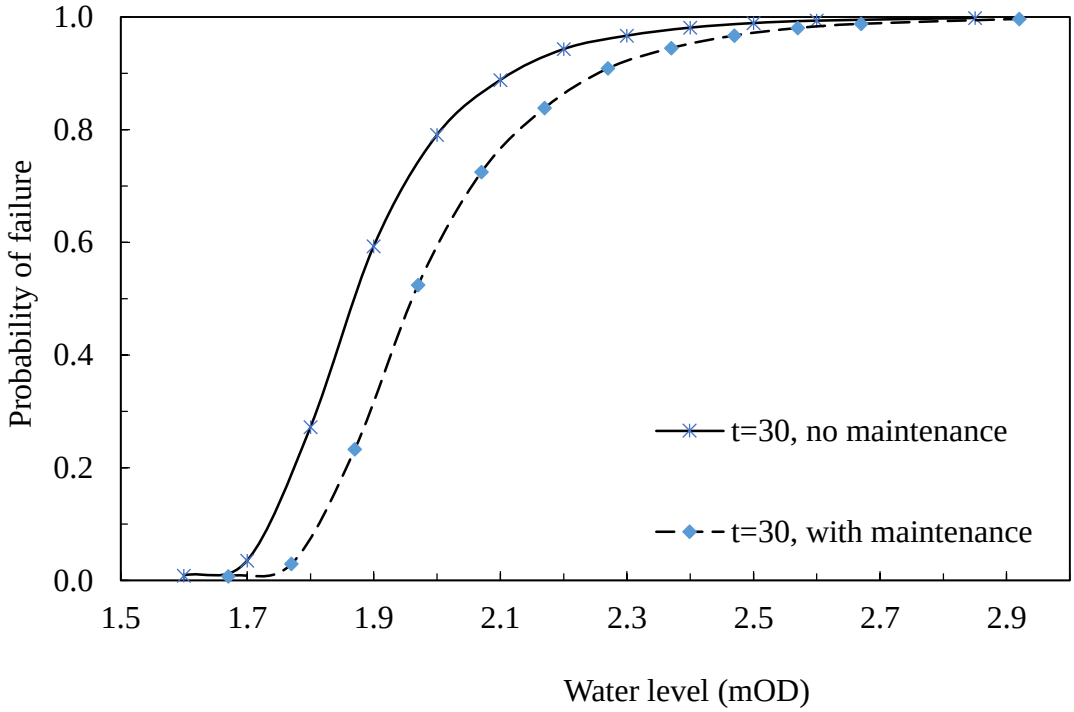

Figure 5.13 Fragility curves for 1 l/s/m wave overtopping as a function of water level at 30 years subject to fast deterioration rate and two maintenance plans.

5.7. Case study at Thames estuary

The Thames estuary case study described in the previous chapter is utilised to show the applicability of the proposed model for overtopping and piping failure mechanisms for the sea dyke. It is assumed that the structure is subjected to three different deterioration rates: slow, medium and fast. The extreme values for water level and significant wave height at 1000-year retrun period are 4.56 mOD and 1.20 m, respectively. It is expected to have sea level rises at 3.5 mm/year, 4.6 mm/year and 5.8 mm/year for low, medium and high emission scenarios, respectively, according to UKCP09. The data from the selected deterioration curves are utilised to estimate the deterioration of the structure, and given in the previous chapter.

The survival functions of the transition processes and their changes over time are generated by Monte Carlo simulations using the estimated parameters. Then, the time-dependent transition probabilities are generated using the proposed method in Chapter 4. A reliability analysis is carried out for each of the potential failure modes of the earth dyke section, such as wave overtopping through the dyke crest and piping in the sand layer underneath the sea dyke section, by assuming 2 l/s/m overtopping discharge as critical rate for overtopping failure.

Since these two failure modes occur at different locations of the sea defence system, it is assumed that the failure modes are independent. A total number of 10e6 samples are utilised in the Monte Carlo simulations to estimate the failure probability for each failure mode. Reduction factors for berm γ_b and slope roughness γ_f are considered 0.85 and 0.90, respectively. Figure 5.14 shows the expected deterioration in crest level and seepage length for different condition grades, as discussed in previous sections.

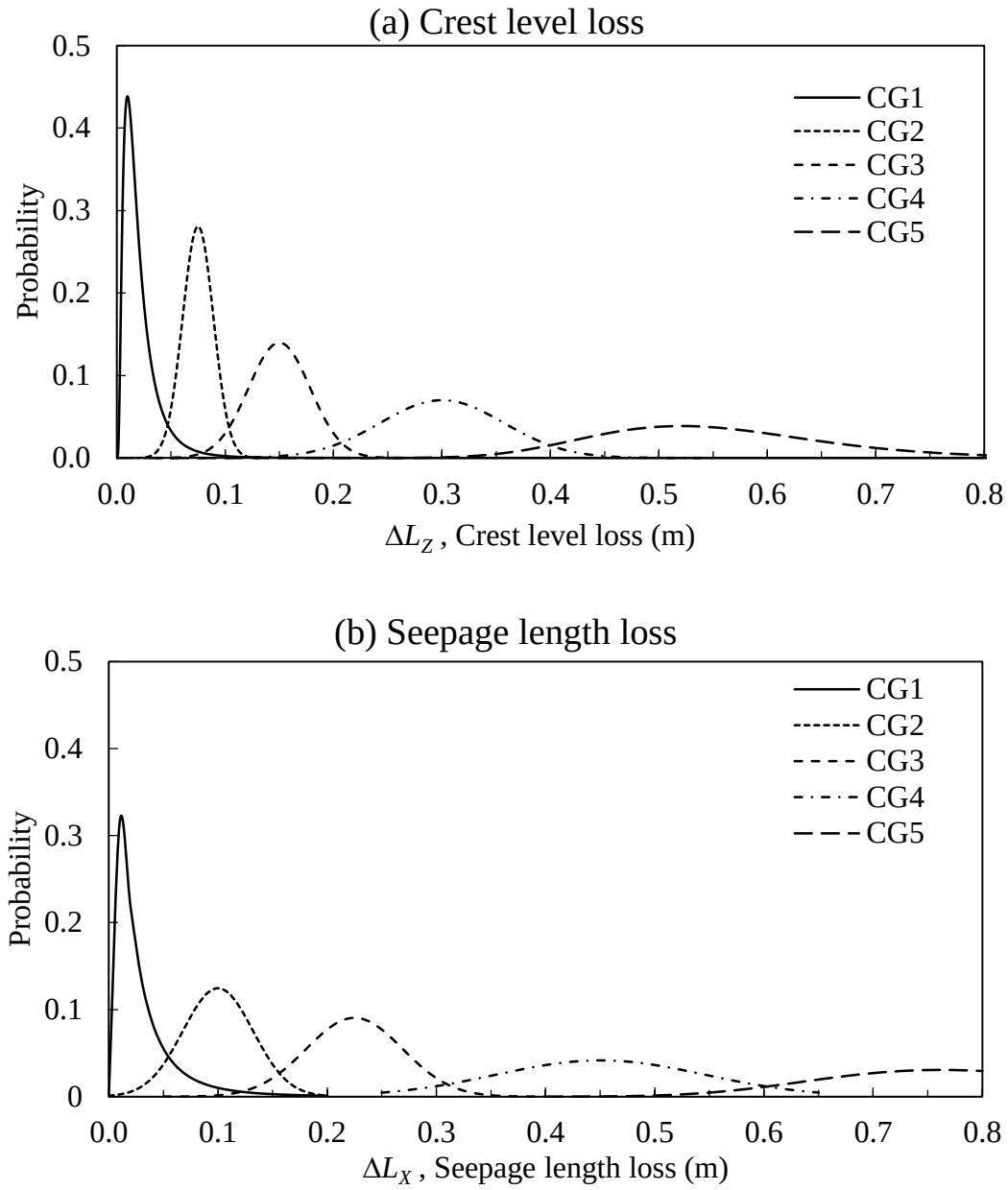

Figure 5.14 Probability density distribution of the sea dyke crest level and seepage length loss associated with condition grade (CG).

5.7.1. Effects of sea level rise on overtopping

Figure 5.15 shows the effect of the decrease in the crest level on the overtopping discharge rate after 50 years from the present day for 1000-year return period event. The increase in the overtopping discharge is significant especially for medium and fast deterioration rates, and it is expected the dyke is no longer capable for servicing against the overtopping failure.

The relative increases in the overtopping discharge rate for various return period events are also provided for better understanding of the future conditions as shown in Figure 5.16. For the events higher than 50-year return period, the dyke needs a comprehensive maintenance repairs to improve the overtopping reliability performance.

Figure 5.17 shows the average mean overtopping discharge for the 1000-year return period event associated with the sea level rise over 50 years from the initial date. The uncertainty in the discharge prediction is significant for sea level rise more than 30 cm due to the uncertainty in the projection of the sea level rise for higher values. It is expected to experience overtopping discharges of more than 10 l/s/m for about 25 cm increase in the sea level rise.

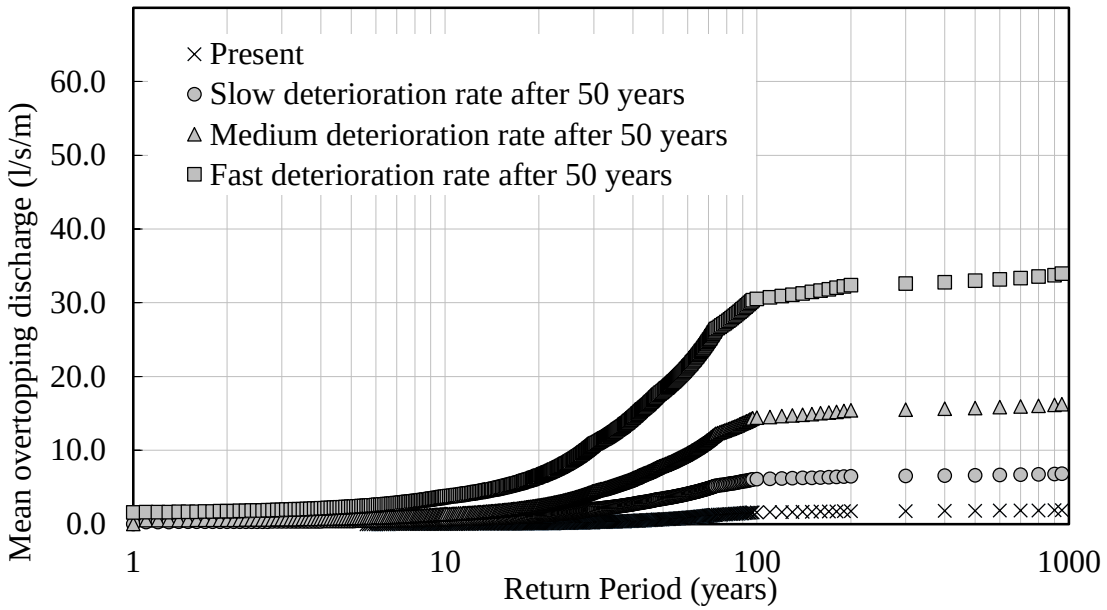

Figure 5.15 Different rates of crest level deterioration to give the same overtopping rate at 1000-year return period after 50 years from the initial date.

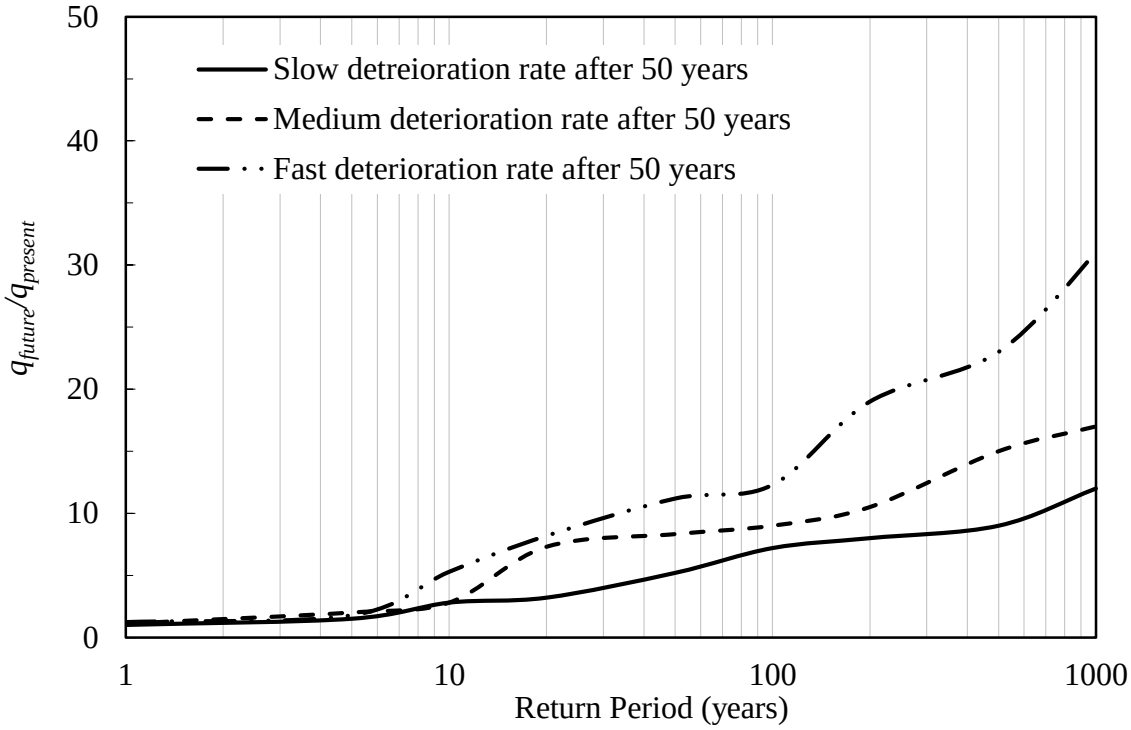

Figure 5.16 The relative changes of overtopping discharge in the future subject to different deterioration rates.

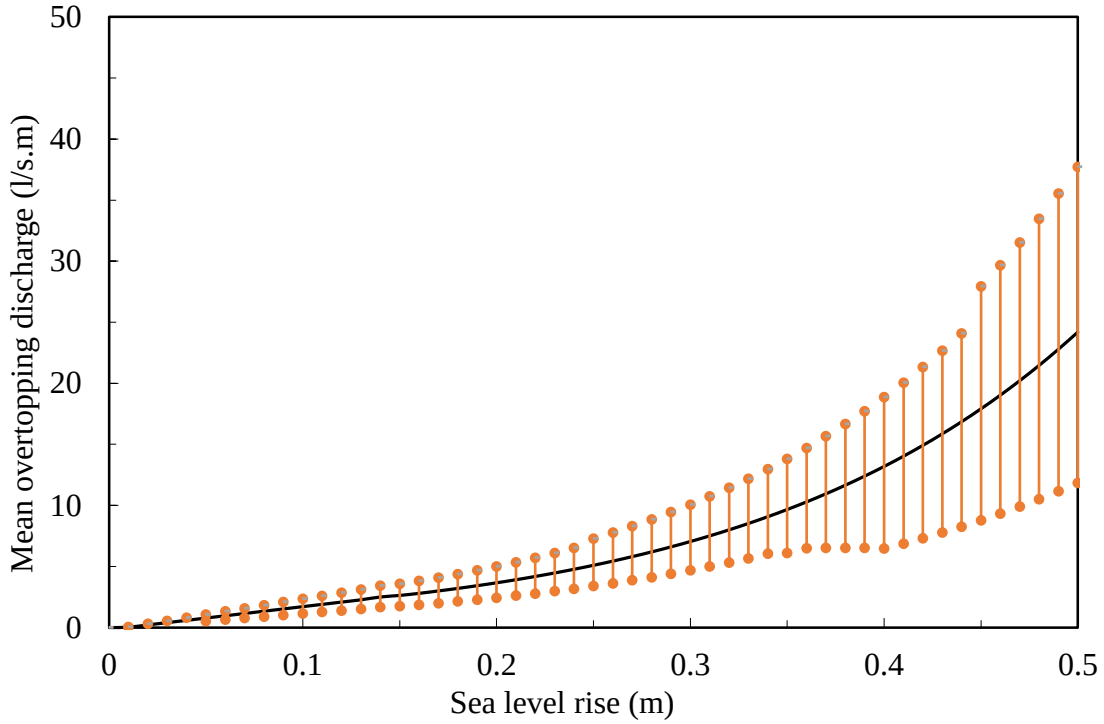

Figure 5.17 Average mean overtopping discharge for the 1000-year return period event associated with the sea level rise after 50 years from the initial day with 95% percentiles shown by bars.

5.7.2. Evaluation of time-dependent failure probability

Figure 5.18 shows the failure probability caused by wave overtopping and piping over 50 years after the initial construction date subject to three deterioration rates. It is demonstrated that the probability of failure increases over time due to deterioration processes and sea level rise. The failure risk of overtopping and piping varies with the type of deterioration rate, as expected. For example, the risk of failure due to wave overtopping at age 20 years is about 67% for the sea dyke under fast deterioration rate, while it is about 18% and about 28% lower for the sea dyke under medium and fast deterioration rates, respectively.

Piping failure mechanisms are associated with the deterioration of seepage resistance and the increase in water pressure head between the water levels at the seaside and land side. The water level on the seaside is increasing due to the rising sea level, and the water level on the land side is assumed at ground level. The permeable sand layer has soil parameters of saturated density $\gamma_s = 17$ kN/m3, soil friction angle of $35°$, intrinsic permeability $\kappa = 1.28 \times 10^{-10}$, drag force factor $\eta = 0.25$, and large grain fraction $d_{70} = 0.3$ mm. The results show that the probability of failure caused by piping in the sand layer increases rapidly after approximately 20 year, reaching a failure probability close to 1.00 in approximately 80 years. The failure probability due to piping shows less risk in comparison with overtopping failure mode. However, the risk of failure due to piping is still significant.

Figure 5.19 and Figure 5.20 show the overall overtopping and piping fragility surfaces of the sea dyke associated with time and water level subject to various deterioration rates. The overall failure probability of the structure can be assessed by integration of failure probability for a specific water level and all possible condition grades with consideration of their probability distributions over time. The results show that the probability of failure due to wave overtopping for 4.50 mOD water level reached over $90\%, 80\%$ and 50% about 25 years after the initial date, subject to fast, medium and slow deterioration rates, respectively.

It implies that the overtopping failure probabilities increase significantly due to the settlement of crest level over time. A quick comparison between the results provided in

Figure 5.18, Figure 5.19 and Figure 5.20 shows that the critical probability of failure occur when load variable (the water level) is lower than extreme values. Piping fragility surface shows that the probability of failure is critical when the water level is higher than 4.5 mOD, even in the early stages of the asset lifecycle.

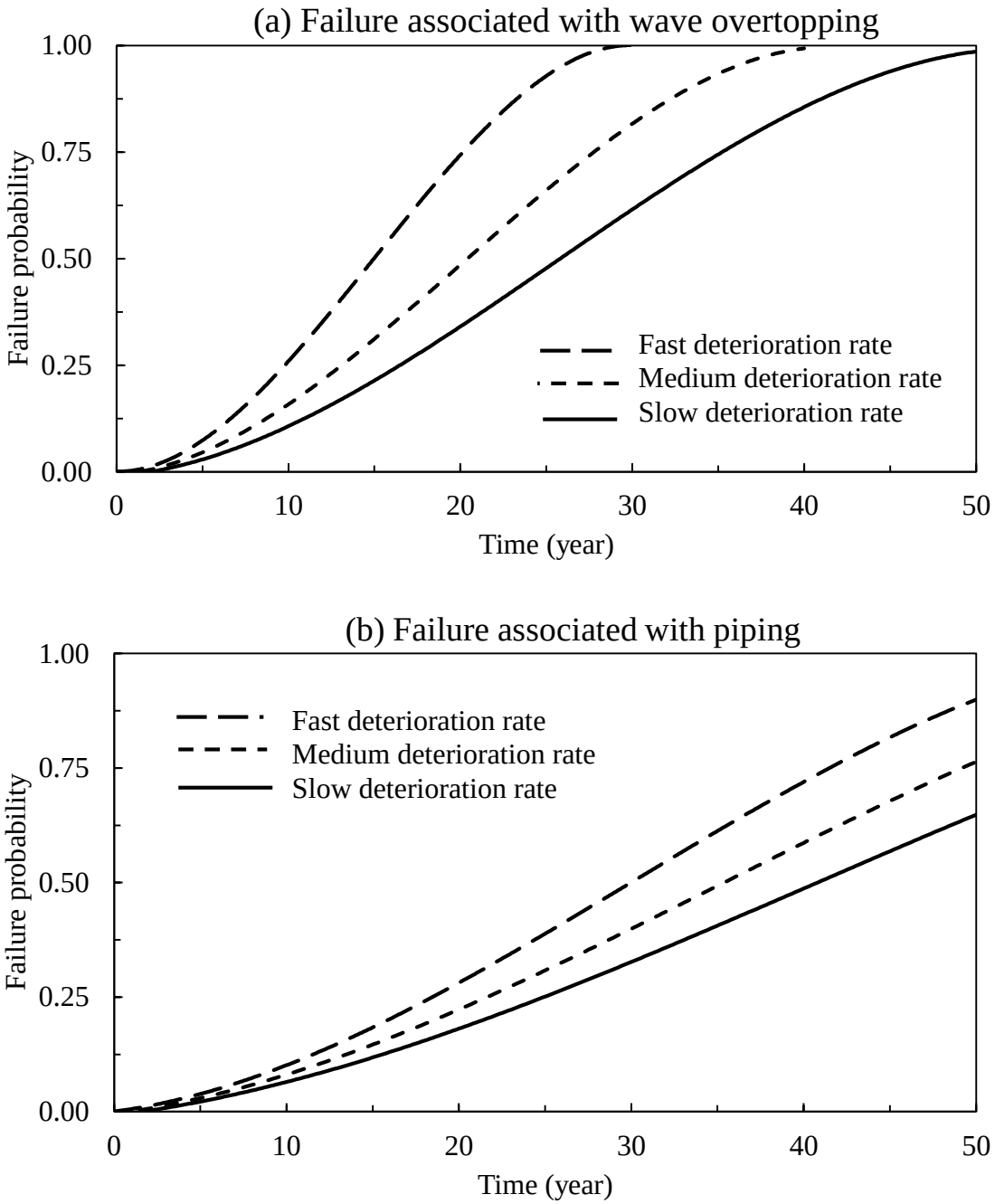

Figure 5.18 Failure probability of the sea dyke due to wave overtopping and piping subject to different deterioration rate.

(c) Slow deterioration rate

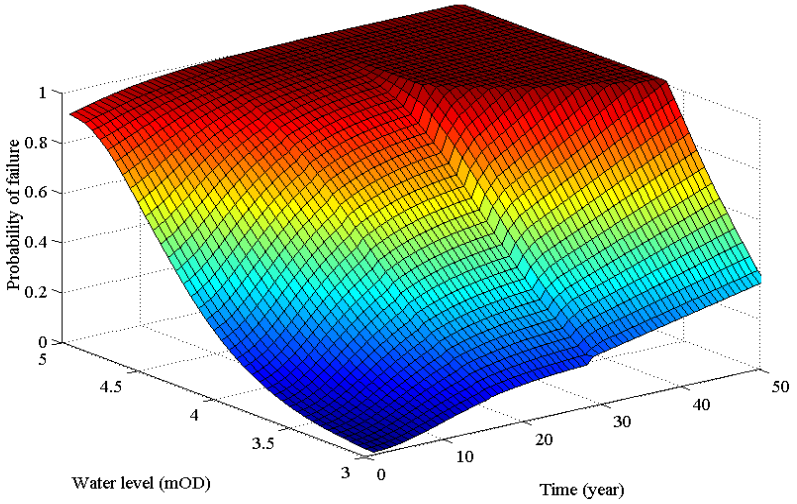

(b) Medium deterioration rate

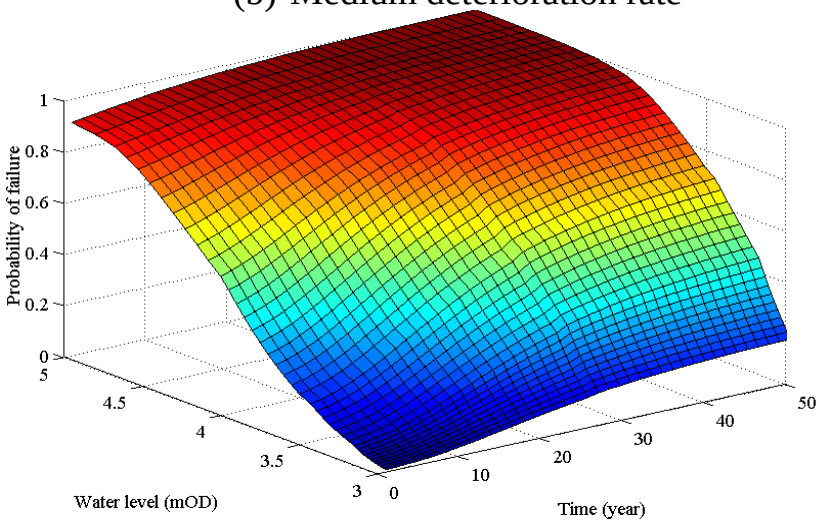

(a) Fast deterioration rate

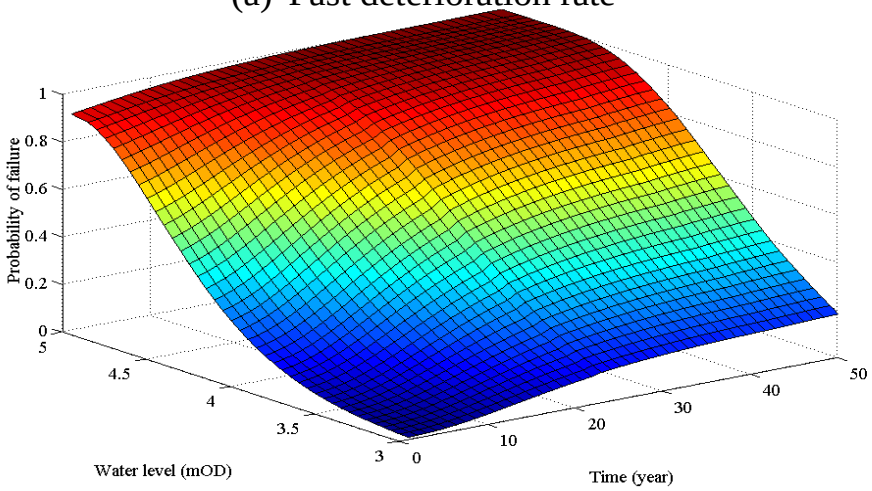

Figure 5.19 Fragility surface for overtopping failure mechanism subject to various deterioration rates.

(a) Slow deterioration rate

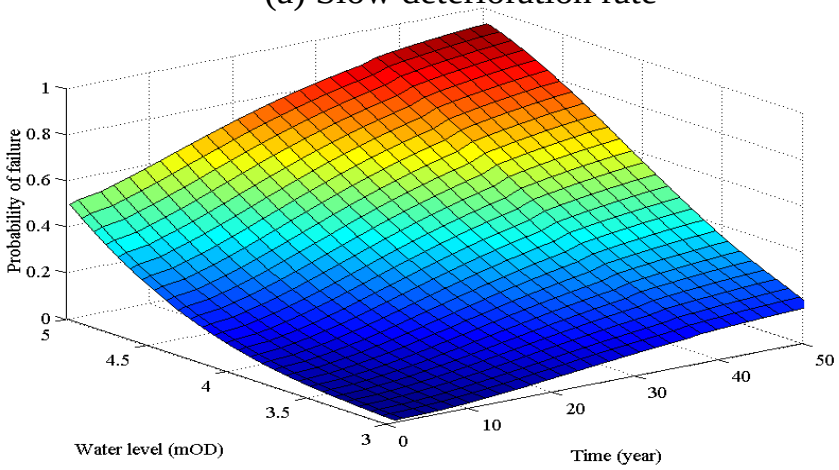

(b) Medium deterioration rate

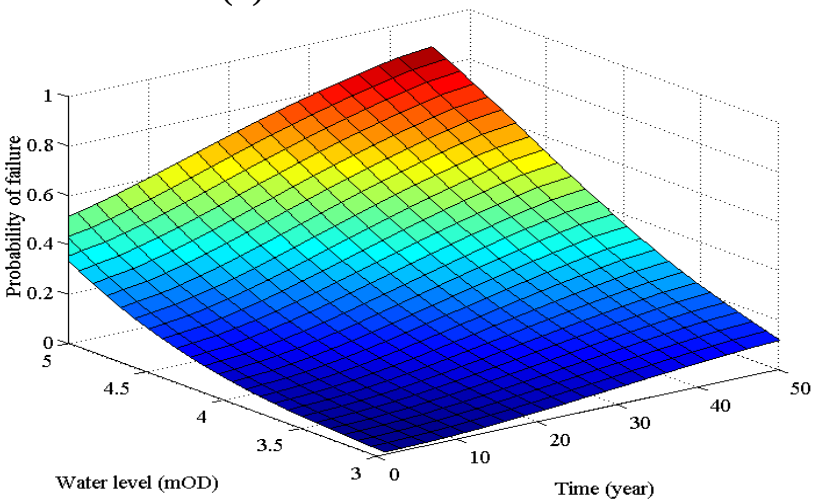

(c) Fast deterioration rate

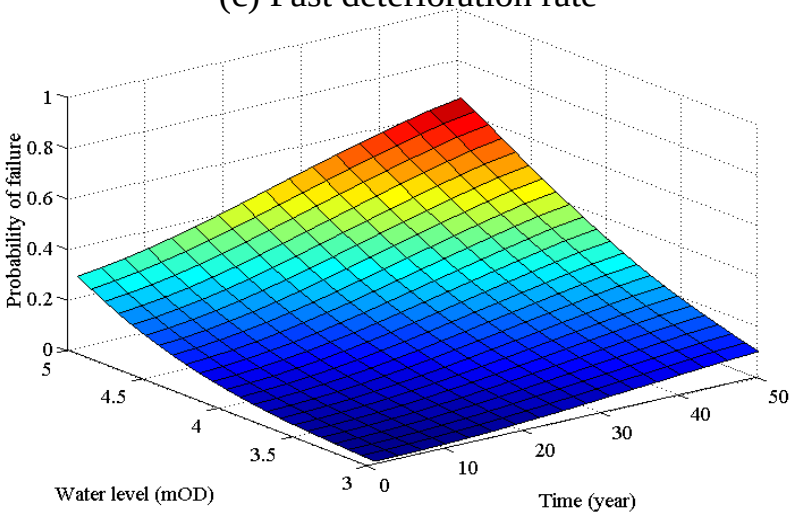

Figure 5.20 Fragility surface for piping failure mechanism subject to various deterioration rates.

5.8. Summary and conclusions

In this chapter, time-dependent reliability analyses of flood defences with consideration of changing environment and deterioration process is undertaken. The effects of climate change in the future such as sea level rise are adopted in the limit state equations for different failure modes. The decrease in the strength of the coastal defences over time due to deterioration process is also considered in the reliability analyses by utilising the proposed model in Chapter 4, and adopted into the limit state equations. Fragility curves and fragility surfs are provided to demonstrate the performance deterioration associated with various parameters such as deterioration rate.

The stationary and non-stationary effects of the deterioration process over the reliability of the assets in the future are studied. Wave overtopping and piping failure mechanisms are investigated specifically in this chapter as two major failure mechanism in sea defences. The effects of different parameters on wave overtopping discharge are investigated, such as the crest level settlement, wave parameters and sea level rise. The effects of seepage length loss is also investigated for piping failure mechanism with consideration of the sea level rise. The sea level rise is mainly responsible for the failure of overtopping discharge due to its double effect of the rise of design water level at the toe and the increase in local depth-limited significant wave height. Piping in the underlain water-conductive sand also make the earth dyke vulnerable due to sea level rise and internal erosion of the soils underneath the dyke in the future.

From the results obtained by the proposed models, following conclusions are drawn: a) the proposed grade-based and non-stationary deterioration model in Chapter 4 can be utilised to evaluate the time-dependent reliability performance of the coastal defence structures; b) the reliability of the coastal defence structures is decreased significantly due to the deterioration processes such as crest level settlement and seepage length loss; c) the obtained fragility surface is capable of providing time-dependent behavior of the coastal defences associated with specific water level; and d) the failure probabilities estimated in reliability analysis that uses non-stationary deterioration process are higher than the failure probabilities associated with stationary deterioration processes. This is due to the consideration of faster deterioration rate when the structure is in higher condition grades.

6. Optimal maintenance strategy for coastal defences

6.1. Introduction

Effective maintenance planning is necessary to keep the deteriorating sea defence structure safe and reliable. If no repair is undertaken, the resistance of the structure will deteriorate further until reaching the ultimate limit or collapse. Therefore, structural repairs should be organised to improve the resistance of the deteriorating structure against increasing hydraulic loads before collapse during its service life. The repair strategy for the deteriorating earth sea dyke could be determined by the statistical estimations of failure probability and the costs for the repairs. The main contribution of this chapter includes:

- The cost of errors in inspection results on the maintenance optimisation process is considered. In order to optimise the maintenance strategy, Partially Observable Markov Decision Process (POMDP) model is utilised for determining optimal maintenance strategy for coastal defence structures.
- A renewal maintenance model is also studied to evaluate the optimal repair and inspection intervals.

6.2. Single-objective vs multi-objective decision process

In coastal flood defence structures, the typical objectives are: to minimise the risk consequences, to minimise the failure probability of failure mechanisms, to minimise maintenance costs, and to keep the structure above a specific condition grade. The decision maker may choose one (single-objective) or many (multiple-objective) goals to be achieved in an optimal maintenance policy regarding the importance of the assets or budgetary matters. A single-objective optimisation is a process to find the best policy or solution to minimise or maximise the value of a single objective function, e.g. to minimise the costs of maintenance. In this process, the other objectives are not considered, and the method cannot provide alternative solutions that might improve or worsen other aspects of a maintenance strategy (Alex et al. 2009; Madanat and Ben-Akiva 1994). While in a multi-objective optimisation a set of solutions are computed with consideration of the interaction between different objectives, e.g. minimising the costs and maximising the asset reliability at the same time.

The optimisation process for a single-objective problem is much easier and more straightforward than a multi-objective problem. However, it does not mean that for solving a multi-objective problem is required to have a particular multi-objective mathematical model. In a multi objective optimisation problem, the dominated solutions are required. The definition of domination is a key concept in a multi-objective optimisation problems. In a minimisation problem, the mathematical expression of a dominant solution is given as (Soh and Demiris 2011)

$$\hat{x_i}\ dominates\ \hat{x_j}\ if;\ \forall k\ \in\ \mathbb{N},\ Obj_k(\hat{x_i}) \leq Obj_k(\hat{x_j}) \tag{6.1}$$

where Obj_k is objective function of objective k. This is illustrated in a two-objective optimisation example in Figure 6.1. In the figure, objective function f_1 and f_2 need to be maximised and minimised, respectively. Each dot demonstrates a possible solution for the problem. Solution C dominates solution B as it is better in both objectives, while it does not dominate objective E in any functions. However, solution C dominates solution A in maximisation objective function, while they have the same value for minimisation objective function.

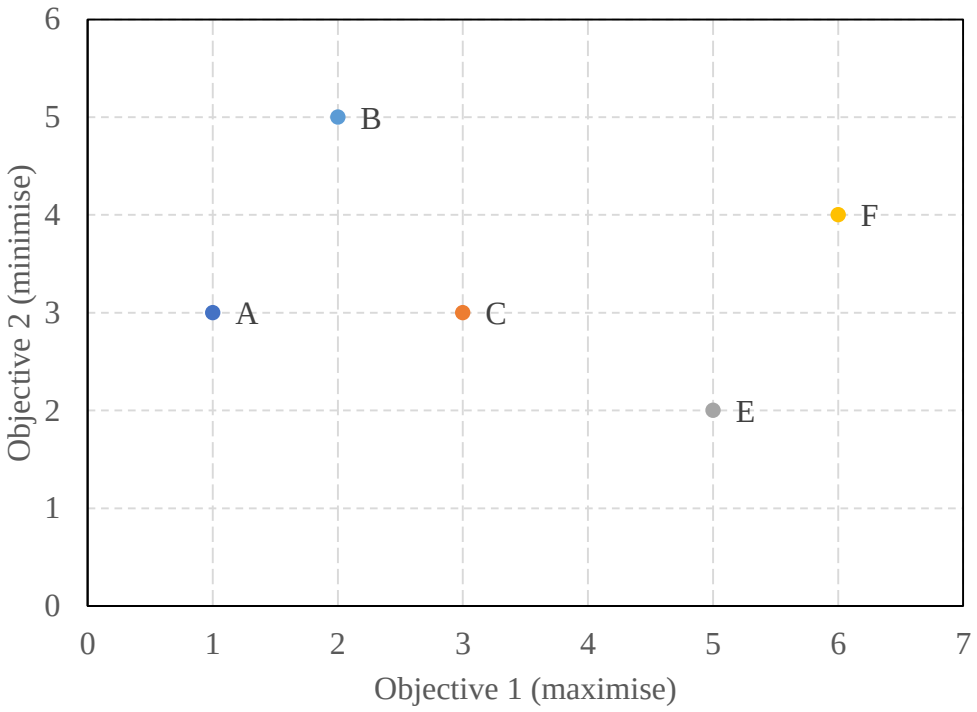

Figure 6.1 Example of the dominance and Pareto optimally.

6.3. Evaluating effectiveness matrices for repair actions

In a Markov process, the effect of maintenance action is defined in a probability form that improves the condition of the sea defence from grade i (before maintenance action a) to grade j (after maintenance action a) at time step t. Let $\mathbf{P}_a$ be the effectiveness matrix of the action a. The transition probability due to action a is expressed as

$$p_{ij,a}^{t} = \Pr(s_t = j | s_{t-1} = i, a) \tag{6.2}$$

where $p_{ij,a}^{t}$ is the probability of improving from condition grade i to condition grade j at time t if action a is implemented on the structure.

A common approach to estimate the effectiveness transition matrices for repair actions is expert judgments. A considerable number of existing studies used expert judgment to estimate the transition action matrices (e.g. Corotis et al. 2005; Grall et al. 2002). Another way to estimate repair effectiveness matrix is to calculate the increase in average structure performance due to repair actions, by computing the change in the new performance index relative to the old performance index before the repair (Lavrenz et al. 2014). As mentioned in Chapter 3, deterioration curves for structures subjected to different maintenance regimes are available and provided by Environment Agency, and it is used here as a basis for the estimations.

In order to estimate the effectiveness of a maintenance action, non-linear equations of deterioration curves before $f_{ini}(t)$, and after maintenance action $f_a(t)$ are derived. Then, the difference between the two areas under the deterioration curves are calculated as (Lavrenz et al. 2014)

$$\Delta Area_{j \to i} = \int_{t_i}^{t_j} f_{a,i \to j}(t)\, dt - \int_{t_i}^{t_j} f_{ini,i \to j}(t)\, dt \qquad i < j;\ i,j \in \{1,2,3,4,5\} \tag{6.3}$$

where f_{ini} is the equation of asset deterioration curve before maintenance; f_a is the equation of deterioration curve after maintenance a; t_i and t_j are times (year) that the asset is in condition grade i and j, respectively. The above equation estimates the cumulative difference between two diagrams shown in Figure 6.2. The figure shows deterioration curves for a sea dyke subject to do-nothing and major maintenance plan.

The area between two lines is considered as the improvement due to the maintenance action.

For evaluating more than one condition grade improvement, Equation (6.3) is repeated for all condition grades. For example, to estimate the repair influence at condition grade 4, $\Delta Area_{4\to3}$, $\Delta Area_{4\to2}$, and $\Delta Area_{4\to1}$ are calculated, which provide cumulative differences in the areas from condition grade 1 to condition grade 4. Hence, the probability of improvement from condition grade j to i due to action a can be estimated as

$$p_{a_{j\to i}} = \frac{\Delta Area_{j\to i`} - \Delta Area_{i`\to i}}{\Delta Area_{j\to i}} \qquad i < i` < j \tag{6.4}$$

where $a_{j\to i}$ is the improvement effectiveness from condition grade j to condition grade i after performing action a.

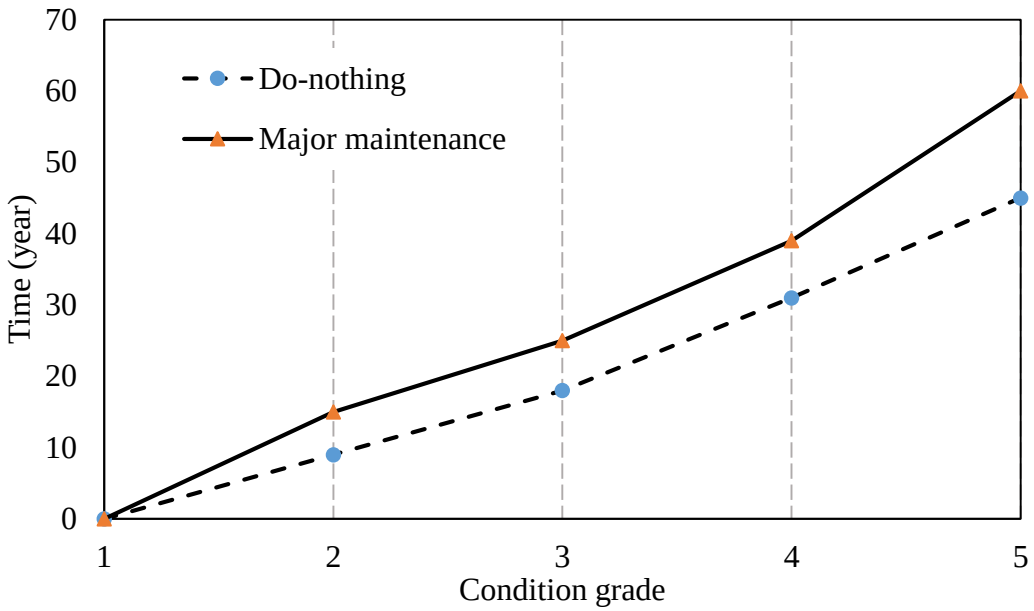

Figure 6.2 The deterioration curve for a class-44 sea dyke subject to do-nothing and major maintenance action.

6.4. Cost of inspection error in decision making process

As discussed in Chapter 2, Markov Decision Process (MDP) is a useful model to evaluate optimal policy in civil infrastructures. In a Markov process, the effect of maintenance action is defined in a probability form, which improves the condition of the sea defence from grade i (before maintenance action a) to grade j (after maintenance action a) at time step n. In the MDP approach, it is assumed that inspection outcome is certain and

confirms the actual condition state of the asset, thus the maintenance action can be performed directly after each time step. For some civil infrastructures such as steel bridges, the condition state of the asset may be identified with high level of certainty by condition assessment techniques (Golroo and Tighe 2009) with reasonable costs compared to coastal defence structures.

However, in coastal flood defence structures, the information about the current state of the asset is not complete due to many factors such as errors in inspection outcomes. Coastal defence assets deteriorate in an environment that is difficult or expensive to be observed or inspected with a high level of certainty. For example, visual indicators contributing to piping failure mode, such as porous in the soil, are changing over time and cannot be inspected easily. Additionally, as discussed in Chapter 3, the inspection strategies in flood defence structures have different level of accuracy with the correct results about 80% to 96% regarding the inspection method. Consequently, the deterioration rate can be accelerated by unnoticed factors.

In order to model inspection error and the inability of capturing the condition grade of the flood defence to have results with 100% accuracy, Partially Observable MDP (POMDP) introduce the inspection (observation) matrix ($\mathbf{O_I}$). The inspection matrix represents the reliability of the inspection strategy as it gives the probability of inspecting the asset in a certain condition grade with consideration of the actually being in that condition grade, which provides the possible error in that inspection results. For example, for Tier 1 inspection strategy (e.g. visual inspection), if a sea dyke is in condition grade 1 then there is 80% probability of observing the asset in condition grade 1. Accordingly, O_{ij} is the probability of observing an asset in state i when the actual condition is j, hence it represents the error in the condition assessment technique.

Hence, the decision maker needs to choose the policies based on incomplete or uncertain information. The process starts by multiplying the inspection matrix by the transition matrix producing what is called belief state b. This will update expected deterioration by updating the transition matrix with the reliability of the condition assessment method.
As the difference between the belief state and the actual condition grade decreases, the reliability of information increases. A belief state b is a probability distribution to show

the available information over all state spaces, and the sum of beliefs over the states equal to 1.0 (Kaelbling et al. 1998). The process of a single objective POMDP is illustrated in Figure 6.3.

Figure 6.3 shows the sequences of a POMDP process in each time step. For example, at time step t, the structure is in state s_t, while s_t is the outcome of the latest implemented action a_{t-1} on state s_{t-1}. However, the decision maker can update the information via inspection outcome o_{t-1} that is the outcome of the inspection strategy in the last time step. The available information about the current condition of the structure is summarised into the current belief state b_t. Consequently, the next decision or action a_t will be implemented based on the current information or belief state b_t, and an immediate reward R^t will be assigned.

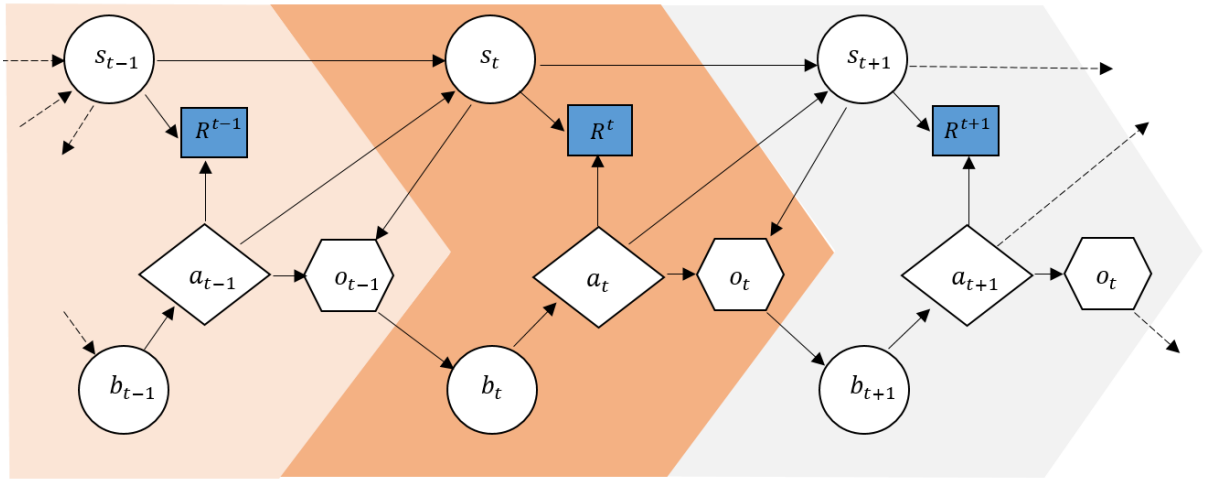

Figure 6.3 Sequential decision process with partial information. s_k: states, a_k: actions, o_k: observations, b_k: belief states, R^k: reward value.

The error for different inspection strategies in coastal defences, e.g. Tier1, 2 and 3, are estimated and discussed in Chapter 3. The value of information is described as the cost of the imperfect information plus the cost of the implementing the inspection strategy, and it is discussed in many literatures, e.g. by Keisler et al. (2013) and Osman et al. (2012). In order to quantify the errors, the cost of failure is described as cost matrix **C**. Then the cost matrix is multiplied by the inspection matrix to describe the errors in monetary values. Hence, the value of information V_I^t after t time steps can be estimated by adding the cost of inspection strategy C_I to the cost of imperfect information (Osman et al. 2011), given here as

$$V_I^t = C_I + \mathbf{CI_I^t} = \mathbf{C} \cdot \mathbf{P^t}(\mathbf{O}_I - \mathbf{I}) \tag{6.5}$$

where $\mathbf{CI_I^t}$ is the costs of imperfect information at time t using inspection strategy I; $\mathbf{P^t}$ is the transition probability matrix**;** $\mathbf{O_I}$ is the inspection matrix for inspection strategy I; and **I** is the identity matrix.

6.5. Bi-objective optimised inspection strategy regarding risk consequences

During the life cycle of coastal defences affected by deterioration process, a series of inspection and maintenance actions may be needed, which requires the planned inspection and maintenance strategy to be scheduled and optimised. As discussed earlier, different inspection strategies may require different amount of resources, and they improve the condition of the asset to different levels. The primary objective of optimisation is to allocate minimum costs based on criticality to reduce the probability of unexpected failures. As such, each coastal defence asset will have two main objective functions: 1) minimum cost of condition assessment strategy to be applied with optimised interval; and 2) minimum consequences of risks due to a failure mode e.g. wave overtopping.

Changing the time between inspection intervals can decrease or increase failure costs. The maintenance cost objective function aims to reduce the cost incurred by imperfect inspection, as discussed in previous section. Additionally, the risk consequence objective function aims to keep the asset above a certain performance level with respect to the monetary consequence of a concerned failure mode. In this chapter, the risk consequence due to wave overtopping is considered by utilising Equation (5.22), and the evaluation process is discussed in Section 5.4. Hence, the objective function is expressed here as

$$\begin{aligned} &\textit{To minimise}: \begin{cases} V_I^t \\ R_f(t) \end{cases} \\ &\textit{Subject to:} \begin{cases} t_{insp} > 0 \\ t_{min} \le t_{insp} \le t_{max} \\ \sum C_I \le B \end{cases} \end{aligned} \tag{6.6}$$

where $R_f(t)$ is the consequence of failure in a monetary value; t_{insp} is the optimal inspection time that need to be estimated from the objective function; t_{min} and t_{max} are the minimum and maximum allowable time between condition assessments, respectively; B is the available budget for conducting the maintenance, which only applies to single objective problems. Genetic Algorithms are considered suitable to solve

this optimisation problem because of the evolutionary process, and the ability to solve the large number of spaces. GA toolbox is available through MATLAB software.

6.6. Optimal maintenance and replacement policy

Renewal maintenance model are another common model to optimise maintenance strategies for infrastructures. In order to find out the optimum inspection/repair interval, the balance between the risk of failure and the total cost of repair and inspection should be considered at the same time. Hence, the maintenance models can be defined according to the risk models as condition-based models and reliability-based models. Both models can find the optimal solution of the maintenance strategy problems with minimum cost and predefined risk level (Noortwijk and Frangopol 2004). The reliability-based model treats the multi-component, and multi-failure modes, while condition-based model treats only one component and one failure mode.

Kim et al. (2016) compared two distinct maintenance policies: reliability-based maintenance and condition-based maintenance under different cost environments for stochastically deteriorating infrastructures. The study showed that reliability-based maintenance causes some unexpected deterioration that leads to high cost, while condition-based maintenance maintains a certain level of condition steadily under consistent inspection, which enables steady spending at the management level. Also, life cycle cost under condition-based maintenance is relatively symmetric and has a more concentrated distribution than condition-based maintenance.

The maintenance actions may bring back a flood defence into its original condition or as-good-as-new condition where the quantification of the maintenance costs can be obtained by modelling the maintenance of deteriorated flood defence structures as a discrete-time renewal process (Noortwijk, 2009). Therefore, the costs of actions that are performed to restore an asset or structure to the initial condition are considered as the cost of maintenance and can be defined as the cost parameter. Let a discrete renewal process be $X_n, n = \{1,2, \dots\}$, which is a stochastic process with specific time intervals $T_k, k = \{1,2, \dots\}$. The interval times are expressed here as (Van Noortwijk and Frangopol, 2004)

$$\Pr(T_k = i) = q_i \tag{6.7}$$

where time intervals are identically distributed with random variables; and q_i represents the probability of a renewal in unit time i. Assuming c_i as the renewal cost in this unit time i, the expected average costs over the horizon $(0, n]$ can be obtained by averaging sum of the cost associated with the renewal and the additional expected cost during the interval $(i, n]$, given by

$$C(n) = \sum_{1}^{n} q_i[c_i + C(n-1)] \tag{6.8}$$

According to the renew reward theory and age replacement policy, the expected costs of maintenance over a finite horizon per unit time depend on the preventive maintenance cost C_p, and the corrective maintenance cost C_F. The preventive and corrective maintenances are defined with respect to the failure probability, and the expected renew cycle length, expressed as the ratio of the expected cycle cost and expected cycle length, given here as (Van Noortwijk, 2003; Chen and Alani 2012)

$$C(k) = \lim_{n\to\infty} \frac{C(n)}{n} = \frac{\left(\sum_1^k p_i\right)C_F + \left(1 - \sum_1^k p_i\right)C_P}{\left(\sum_1^k ip_i\right) + k\left(1 - \sum_1^k p_i\right)} \tag{6.9}$$

where p_i is the failure probability per unit time at ith time interval. Once the failure probability p_f at time t is estimated, the probability of failure per unit time at the time interval p_i can be computed from

$$p_i = p_f(t_i) - p_f(t_{i-1}), \quad for\ i = 1,2,3, \ldots \tag{6.10}$$

in which the time interval could be taken as one year for the convenience in calculations. In order to compare the maintenance costs at present day and in the future, the future cost needs to be discounted to its present value by a discount factor. The expected discounted costs over time intervals $(0, k)$ are then given by (Chen and Alani 2012)

$$C_d(k) = \frac{\left(\sum_1^k d^i p_i\right)C_F + d^k\left(1 - \sum_1^k p_i\right)C_P}{1 - \left[\left(\sum_1^k d^i p_i\right) + d^k\left(1 - \sum_1^k p_i\right)\right]} \tag{6.11}$$

where coefficient $d = (1 + r)^{-1}$ represents discount factor per unit time and r is discount rate per unit time. The optimal maintenance time interval k^* without and with discounting are evaluated by minimising the expected average costs per unit time given in Equations (6.9) and (6.11).

6.7. Case study at Thames estuary: POMDP optimisation

6.7.1. Single objective optimisation

A single objective POMDP optimisation is carried out for the Thames estuary case study in Chapter 5 to find the optimal maintenance strategy with respect to budgetary constraints. The performance of the sea dyke for different condition grades was discussed and transition matrix was estimated with respect to the initial condition state. The failure probability of the sea dyke due to excessive wave overtopping will be considered in this optimisation model. A yearly time interval for possible inspection is assumed, and the available inspection strategies are: (1) no inspection with inspection cost=0 unit; (2) Tier 1 inspection such as visual inspection with inspection cost=30 units; and (3) Tier 3 such as detailed survey with inspection cost=120 units. Unit in this example means an arbitrary currency value, and it should be noted that the monetary values in this example are hypothesis. The outcome (observations) of the inspection strategies are five possible condition grades (CG1-CG5). The costs of inspection strategies are independent of the sea dyke condition grades. The inspection matrices regarding the accuracy of the inspection strategies are given here as

$$\mathbf{I_1} = \begin{bmatrix} 1.00 & 0.00 & 0.00 & 0.00 & 0.00 \\ 1.00 & 0.00 & 0.00 & 0.00 & 0.00 \\ 1.00 & 0.00 & 0.00 & 0.00 & 0.00 \\ 1.00 & 0.00 & 0.00 & 0.00 & 0.00 \\ 1.00 & 0.00 & 0.00 & 0.00 & 0.00 \end{bmatrix}$$

$$\mathbf{I_2} = \begin{bmatrix} 0.80 & 0.20 & 0.00 & 0.00 & 0.00 \\ 0.10 & 0.80 & 0.10 & 0.00 & 0.00 \\ 0.00 & 0.10 & 0.80 & 0.10 & 0.00 \\ 0.00 & 0.00 & 0.10 & 0.80 & 0.10 \\ 0.00 & 0.00 & 0.00 & 0.20 & 0.80 \end{bmatrix} \quad (6.12)$$

$$\mathbf{I_3} = \begin{bmatrix} 0.92 & 0.08 & 0.00 & 0.00 & 0.00 \\ 0.04 & 0.92 & 0.04 & 0.00 & 0.00 \\ 0.00 & 0.04 & 0.92 & 0.04 & 0.00 \\ 0.00 & 0.00 & 0.04 & 0.92 & 0.04 \\ 0.00 & 0.00 & 0.00 & 0.08 & 0.92 \end{bmatrix}$$

Penalty costs are associated with CG4 (poor) and CG5 (failure) states and reflect the actual cost of overtopping failure. The failure costs are taken as 0, 0, 200, 500, and 1000 units for CG1 to CG5, respectively. The transition matrix represents the expected deterioration process of the sea dyke in the future. As the partial reliability of the inspection techniques affects the accuracy of determining the current condition of the sea dyke, belief state is utilised to evaluate the current condition state as discussed previously. The condition that is evaluated via inspection matrix with respect to the transition matrix is called belief state, which shows the difference between the transition matrix and the belief state with respect to the expected error.

The single objective optimisation model only minimised Equation (6.5) to utilises the value of information model V_I to select the appropriate condition assessment and use the Genetic Algorithm to alter the time between inspection intervals. This is mainly constrained with budgetary limitations and in finding the optimal solution with respect to the risk exposure for the sea dyke. In this example the budgetary limitations are given in Table 6.1 with the following GA parameters: probability of mutation (0.1), probability of crossover (0.4), population size (600), and the upper and lower bounds for time between inspections (t_{min} = 3, t_{max} = 12). The obtained optimal results are presented in Tables 6.1. For example, for the dyke subject to fast deterioration rate the total cost for inspection is 9,453 units with Tier 1 and Tier 3 inspection time intervals for every 3 and 8 years, respectively.

Table 6.1 Pareto optimum samples for single-objective optimisation.

Deterioration rate	Budget limit (unit)	Total cost of inspection (unit)	Tier 1 time interval	Tier 3 time interval
Fast	10000	9453	3	8
Medium	14000	13823	4	10
Slow	18000	16785	6	12

6.7.2. Multi-objective POMDP optimisation

In the multi-objective model, it is aimed to balance between decreasing inspection costs while the minimum consequence of failure in sea dyke due to wave overtopping is obtained by minimising Equation (6.6). The model uses the same GA parameters with the upper and lower bounds for time between inspections as (t_{min} = 3, t_{max} = 12). The parameters for the second objective or the annual failure risk are assumed as follow: C_{hazard}=7,000 units, C_{direct} =4,500 units, and C_{erosion} =600 units. The results are shown in Fig 6.4. Table 6.2 provides a sample of the pareto optimal solutions over the solution space. In each solution, the appropriate condition assessment technique, time interval, costs, and risk consequence are shown for the sea dyke. Each solution dominates the optimal space in one objective e.g. maintenance cost or risk consequence.

For example, solution A1 in Table 6.2 has an expected risk consequence of 2361 units, which is lower than solution A2 (3880 units). However, solution A2 is cheaper than solution A1 in terms of overall inspection cost, which is 9860 units for the sea dyke subject to fast deterioration rate. Solution B2 can be preferred when the decision maker has budgetary limitation, hence the decision will cost less inspection cost (13369 units) with reasonable inspection intervals for the sea dyke subject to medium deterioration rate. There are more dominated and non-dominated solutions for different deterioration rates with balance between the risk consequence and total inspection cost as shown in Fig. 6.4. The pareto space allows a decision maker to choose the best solution based on available resources and the importance of the asset.

Table 6.2 Pareto optimum samples for multi-objective optimisation.

Pareto solution	Deterioration rate	Expected risk consequence (unit)	Total cost of inspection (unit)	Tier 1 time interval	Tier 3 time interval
A1	Fast	2361	23370	2	6
A2	Fast	3880	9860	4	10
B1	Medium	1858	28083	2	5
B2	Medium	3138	13369	4	8
C1	Slow	2227	25707	2	5
C2	Slow	4736	9329	5	9

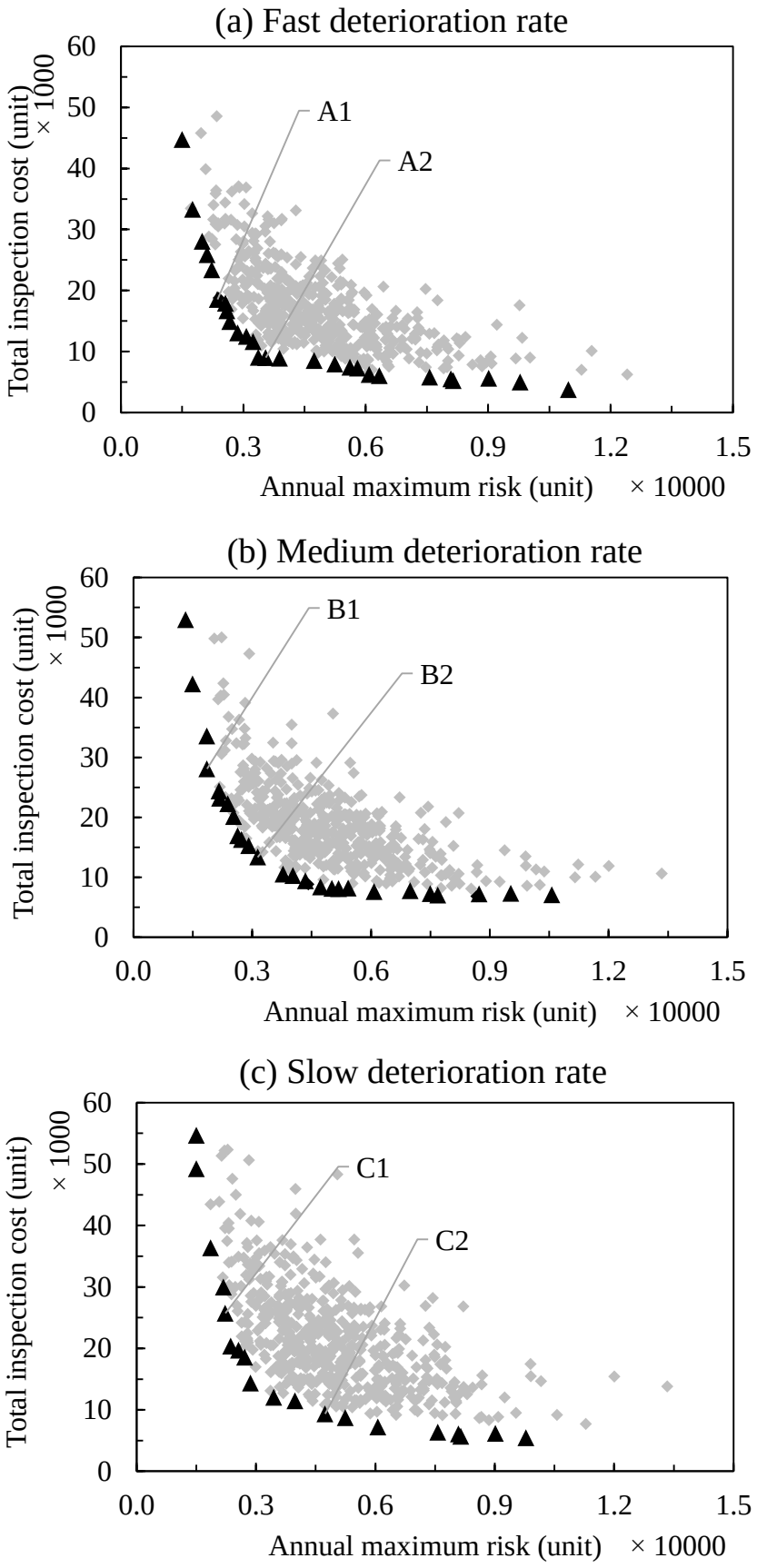

Figure 6.4 Pareto sets of solutions for the sea dyke subject to different deterioration rates.

6.8. Case study at Thames estuary: Renewal maintenance optimisation

The risk caused by the failures due to sea level rise and structural performance deterioration needs to be properly managed, while the costs for the maintenance of the deteriorating sea defence should be minimised. Here, the cost rates defined in Equation (6.9) or (6.11) are minimised with respect to the number of time interval k to find an optimal value of the repair time. Only relative costs are needed to be considered in calculations, assuming here the corrective maintenance cost C_F =1.00 and the preventive maintenance cost $C_P = 0.05C_F$ for the failure due to excessive wave overtopping. It is more convenient to calculate relative costs at time intervals within a time period and then to find the optimum repair time corresponding to the minimum relative cost.

Figure 6.5 and Figure 6.6 show the results for the expected relative costs without and with discounting as a function of the repair time for different average annual crest level deterioration rates. The results without discounting in Figure 6.5 give optimal repair time at 20 years for the fast deterioration rate, at 29 years for the medium deterioration rate and at 32 years for the slow deterioration rate, respectively. Results in Figure 6.6 suggest the optimal repair time obtained with annual discounting rate of 5% is close to, but 2 to 4 years longer than, that from without discounting for each case of settlement rates considered.

Figure 6.7 shows the influence of the preventive maintenance cost C_P on the optimal repair time where the preventive maintenance cost with different ratios to the corrective maintenance is assumed. The medium crest level deterioration rate is adopted in calculations and the annual discount rate is again assumed to be 5%. As expected, the value of the optimal repair time increases when the preventive maintenance cost goes up, increasing from 17 years when $C_P = 0.01C_F$ to 37 years when $C_P = 0.10C_F$. Therefore, an earlier repair is necessary to reduce the risk of failure if the preventive maintenance cost is relatively low. When the preventive maintenance cost is higher the optimal repair time interval could be longer. The repair however should be undertaken well before the expected time to failure caused by excessive wave overtopping.

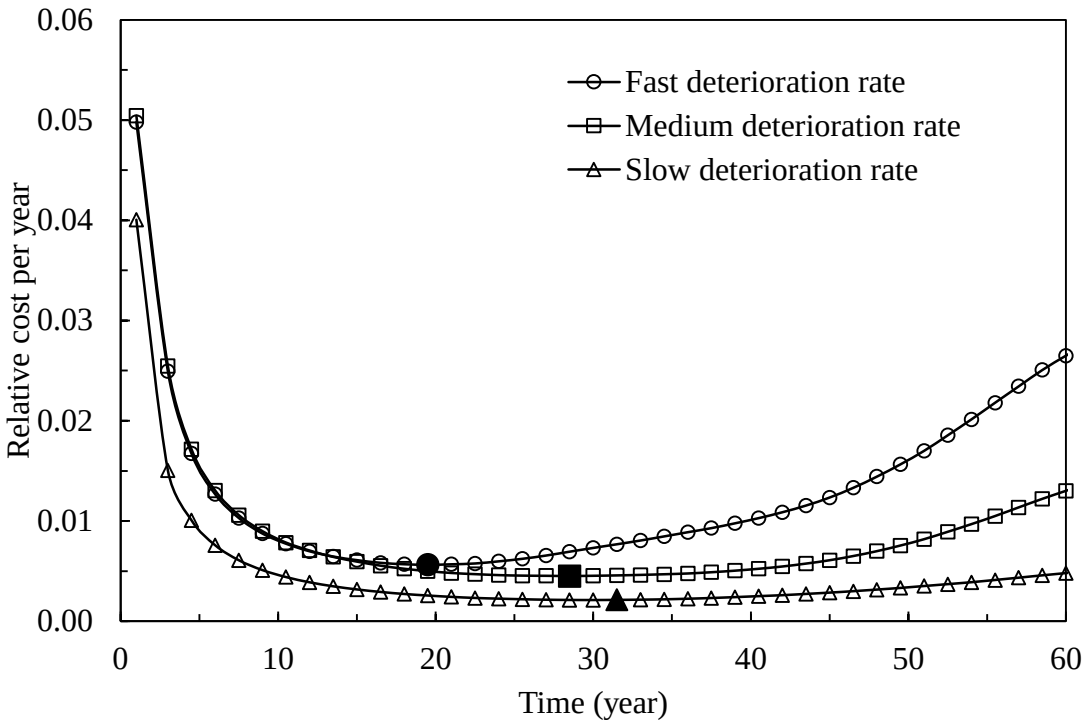

Figure 6.5 Expected annual relative costs without discounting as a function of time for different deterioration rates of the crest level.

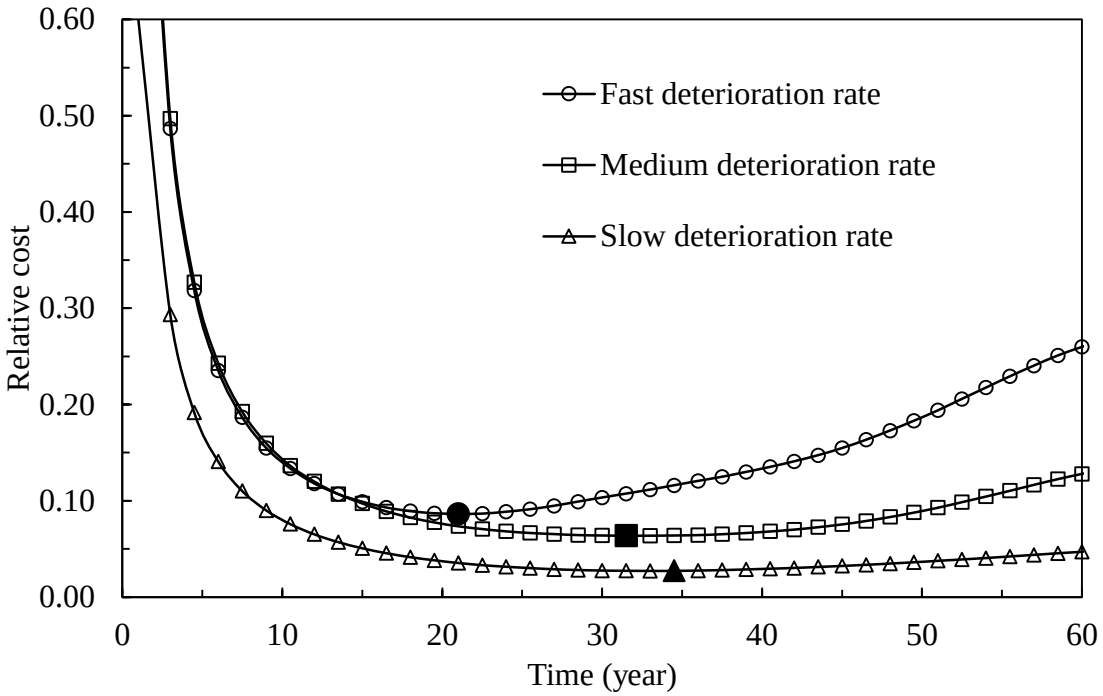

Figure 6.6 Expected relative costs with discounting at an annual rate of 5% as a function of time for various deterioration rates of crest level.

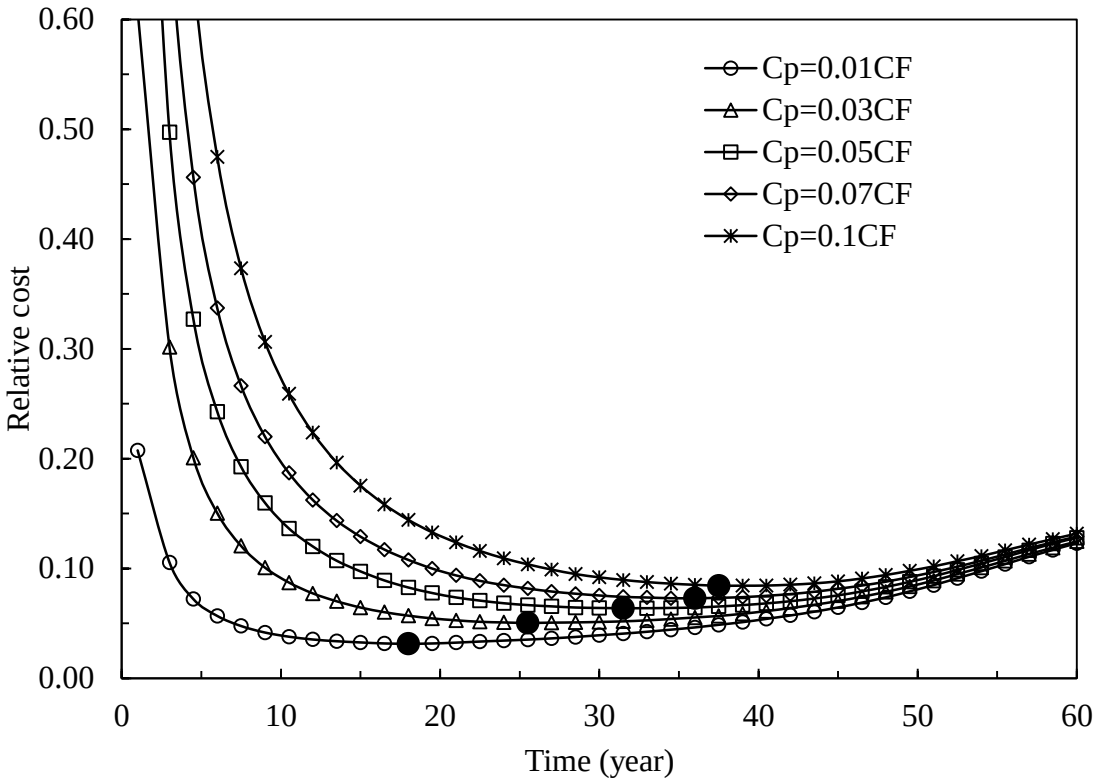

Figure 6.7 Expected relative costs with discounting and the medium deterioration rate of crest level as a function of time for various preventive maintenance costs Cp.

6.9. Summary and conclusions

In this chapter maintenance optimisation models for coastal defences are proposed with consideration of the deterioration process and possible inspection errors in this field. Two maintenance models are investigated: partially observable Markov decision process (POMDP), and renewal maintenance model, namely. The POMDP model provides a grade-based optimal maintenance solution and this model is able to consider the costs of imperfect information with respect to the available inspection strategies. As discussed in precious chapters, it is difficult to have accurate inspection results in coastal defences due to the nature of the structures, hence, consideration of the imperfect information in the maintenance optimisation process is essential.

Single-objective and multi-objective models are adopted evolutionary Genetic Algorithm is utilised to solve optimisation functions that provides optimal policies for with respect to the defined constraints. Additionally, optimal repair planning during the service life is determined by optimising the balance between the risk of failure and the costs for maintenance by utilising renewal maintenance model. Numerical examples are

given to illustrate the applicability of both the renewal and POMDP models for coastal defences. The optimal maintenance strategy during the service life of the sea defences affected by sea level rise and structural resistance deterioration can be determined with consideration of single or multiple objectives and available conventional repair and inspection strategies.

From the results obtained by the proposed models, following conclusions are drawn: a) the POMDP model is capable of considering the inspection error and cost of imperfect information in the process of decision making and leads to decrease in the total expected maintenance cost significantly; b) the POMDP model is also capable of optimising the maintenance strategies for multiple objectives with consideration of necessary constraints by utilising evolutionary algorithms; c) both POMDP and renewal models are flexible to be applied to different reliability models and different failure modes in coastal defences with respect to changing environment and different deterioration rates; and d) the renewal model is capable of estimating optimal inspection and repair time intervals with and without consideration of the discount factor. The optimal repair time largely depends on the deterioration rate, available actions, quality of the inspection strategies, number of the objectives, and little influence from discounting in the maintenance costs.

7. Conclusions and suggestions for future research

7.1. Summary and conclusions

The main aim of this research is to improve the understanding and performance prediction of the structural behaviour of coastal defences with special attention to two major causes: 1) deterioration processes in the coastal defences, and 2) changes in the hydraulic parameters in the future due to sea level rise. The research also aims to investigate the lifecycle management of coastal defence structures based on point-based Markov Decision Process (MDP) by considering realistic effects of partial information with inspection errors.

First, probabilistic models developed to translate the current condition grade system and quantitative damage measurements to a probabilistic form. Then, the translated models are utilised in stochastic and grade-based Markov models to simulate deterioration processes in the future such as crest level and seepage length. The results obtained from the developed models validated with the field and experimental data available. Furthermore, performance deterioration also investigated by considering stationary and non-stationary parameters in the Markovian models. The time-dependent reliability analysis and fragility curves are also provided to analyse the behaviour and reliability of the structures in the future with consideration of the sea level rise impacts. Finally, the optimal repair planning and maintenance strategies during the lifetime are determined by balancing the maintenance cost and failure consequences using multi-objective POMDP maintenance model. A full set of conclusions are included at the end of each chapter. The most significant conclusions are now summarised in this chapter.

Effects of sea level rise on hydraulic variables

A practical approach is proposed to consider the effects of sea level on the extreme values of hydraulic variables such as sea level, wave heights and wave periods. A new approach to estimate the dependence value between the joint extreme variables is proposed based on a Copula function. The joint extreme value model is described and the common models for the coastal defences to evaluate extreme values are investigated and compared. It is found that the GEV model estimates higher extreme values than the GPD model. It is suggested that the GPD model is more realistic and cost-efficient. The

simulations for the future events show that the new dependence model is capable of generating the data in a flexible and efficient process, which improves the quality of the simulated data in comparison with the original data.

Probabilistic condition grading system

A probabilistic condition grading framework is developed to translate the deterministic deterioration curves to a probabilistic form with respect to the quality/error of inspection strategies. The visual indicators in the structures, which are defined by Environment Agency to rank the asset, are linked to relevant failure mechanisms based on quantitative values to be applied in the deterioration models. The quality of the available inspection strategies for flood defences is translated into a probabilistic framework and validated with the published data from various case studies.

Stochastic grade-based deterioration models

Two stochastic deterioration models are adopted to predict the deterioration of the coastal defence resistances by utilising state-based Markov models, i.e. homogeneous Markov model for stationary deterioration process, and inhomogeneous Markov model for non-stationary deterioration process. A Gamma deterioration model is also utilised to simulate the process of the deterioration in coastal defences regardless of the condition grade system. The parameters of the stochastic state-based deterioration models are estimated using the available inspection data and deterministic deterioration curves. The proposed models are capable of providing reliable results when compared with available data. The essential parameters for the models are estimated using the available data from Environment Agency.

It is suggested that the stationary Markov process is more appropriate for short-time reliability analyses and for the fragility curve evaluations. The non-stationary Markov and Gamma models are capable of simulating time-dependent deterioration rates, and they are useful for time-dependent reliability analysis. It is noted that the transition probability matrices are critical for the Markov chain models and can be determined by using robust non-linear optimisation techniques on the basis of estimated performance deterioration rates. The deterioration processes have significant impact on the performance of the coastal defences in the future.

Reliability assessment models

A practical approach has been proposed to investigate the reliability of the coastal defences for overtopping and piping failure modes through fragility curves and time-dependent reliability evaluation. In lifecycle performance assessment, Markov process was adopted for stochastic deterioration modelling to take uncertainties into account. The time-dependent reliability analysis is then employed to evaluate the probability of failure of the coastal defences with consideration of the sea level rise. The results from the analysis showed that the proposed stochastic deterioration model based on the Markov process can be applied to assess the lifecycle performance with uncertainties, such as deterioration of crest level and seepage length. The proposed fragility surfaces are capable of providing time-dependent behaviour of the coastal defences associated with specific load variable. During the analysis it has also been found that the structural reliability depends not only on deterioration rates but also on the sea level rise. The reliability of the coastal defence structures is decreased significantly due to the deterioration processes such as crest level settlement and seepage length loss.

Optimal maintenance strategies

A point-based optimisation model is adopted to find optimal maintenance strategies in coastal defence structures with respect to the imperfect information and inspection errors using POMDP model. A renewal maintenance model is also investigated using a corrective-predictive maintenance framework. The POMDP model is used to provide a state-based optimal solution with consideration of the errors in the available inspection strategies for single or multiple-objective problems. The POMDP model is capable of optimising the maintenance strategies for multiple objectives without considering complex constraints, and it is compatible with the different reliability models provided in this thesis. The optimal repair time largely depends on the deterioration rate, available actions, quality of the inspection strategies, number of the objectives, and little influence from discounting in the maintenance costs.

7.2. Recommendations for future study

Following recommendations are suggested for future study:

- The proposed model in Chapter 3 to translate the current deterministic data to a probabilistic form has a limitation that is dependent on the quality of the available data especially available quantitative data. Although the available quantitative data are sufficient to develop the model, more studies and investigations are needed to enrich the accuracy of the quantitative values that describe the intensity of the damage in an asset. Moreover, more studies are required to define a more comprehensive link between the structural damage in different part of a structure and the failure mechanisms, especially laboratory and field studies.
- Further investigations are needed for the effects of sea level rise on the future hydraulic conditions acting on existing coastal defences and the response of the structures regarding various failure mechanisms such as piping and uplifting. It is assumed that the increase in water level usually leads to decrease in the reliability of the coastal defences against different failure modes. However, more investigations are needed concerning piping and uplifting failures modes, in order to investigate the influence of the change in hydraulic loading over the structure's resistance.
- Further studies are required to investigate the dependence between the different failure mechanisms. It is often assumed that the failure mechanisms that occur in different parts of a structure are independent, such as overtopping and piping failure mechanisms. However, from studies, there are some dependency, either positive or negative, between the so-called parallel failure mechanisms. The hypothesis of independency between the parallel failure mechanisms needs to be investigated.
- The effect of imperfect information in a maintenance repair model needs to be studied. The effects of imperfect information on decision making are studied in this study e.g. considering the errors to update the information and inspection strategy. However, the cost of identifying an incorrect state that lead to implementing inappropriate repair actions is still not clear. This parameter may increase the importance of the inspection strategies with higher accuracy, although they are more expensive, in order to improve the quality of optimal repair and inspection solutions.

Reference

Abdel-Hameed, M., 1975. A Gamma Wear Process. IEEE Transactions on Reliability, 24(2), pp.152-153.

Agrawala, S., Bosello, F., Carraro, C., De Cian, E. And Lanzi, E., 2011. Adapting To Climate Change: Costs, Benefits, and Modelling Approaches. International Review of Environmental and Resource Economics, 5(3), pp.245-284.

Alex, D.P., Al Hussein, M., Bouferguene, A. And Fernando, S., 2009. Artificial Neural Network Model For Cost Estimation: City Of Edmonton's Water and Sewer Installation Services. Journal of Construction Engineering and Management, 136(7), pp.745-756.

Allsop, W., Bruce, T., Pullen, T.A. And Van Der Meer, J.E.N.T.S.J.E., 2008. Direct Hazards from Wave Overtopping-The Forgotten Aspect of Coastal Flood Risk Assessment.

Allsop, W., Kortenhaus, A., Morris, M., Buijs, F., Hassan, R., Young, M., Doorn, N., Van Der Meer, J., Van Gelder, P.H.A.J.M., Dyer, M. And Redaelli, M., 2007. Failure Mechanisms for Flood Defence Structures. Floodsite Report. T04_06_01.

Ang, A., And Tang, W., Probability Concepts in Engineering: Emphasis on Applications to Civil and Environmental Engineering, 2nd Edition. John Wiley and Sons, 2007. ISBN-13: 978-0471720645.

Antonioli, F., Anzidei, M., Amorosi, A., Presti, V.L., Mastronuzzi, G., Deiana, G., De Falco, G., Fontana, A., Fontolan, G., Lisco, S. And Marsico, A., 2017. Sea-Level Rise and Potential Drowning Of the Italian Coastal Plains: Flooding Risk Scenarios for 2100. Quaternary Science Reviews, 158, pp.29-43.

Armagan, A., Dunson, D.B. And Lee, J., 2013. Generalized Double Pareto Shrinkage. Statistica Sinica, 23(1), pp.119-127.

Arns, A., Dangendorf, S., Jensen, J., Talke, S., Bender, J. And Pattiaratchi, C., 2017. Sea-Level Rise Induced Amplification of Coastal Protection Design Heights. Scientific Reports, 7, Report No. 40171.

Osman, H., Atef, A. And Moselhi, O., 2011. Optimizing Inspection Policies for Buried Municipal Pipe Infrastructure. Journal of Performance of Constructed Facilities, 26(3), Pp.345-352.

Atwater, B.F., Musumi-Rokkaku, S., Satake, K., Tsuji, Y., Ueda, K. And Yamaguchi, D.K., 2016. The Orphan Tsunami of 1700: Japanese Clues to a Parent Earthquake in North America. University of Washington Press.

Baars, S. Van and Kempen, I.M. Van, 2009. The Causes and Mechanisms of Historical Dike Failures in the Netherlands. E-Water, 2009(06), Pp.1–14. Available at: Http://Www.Ewa-Online.Eu/E-Water-Documents.Html.

Baik, H.S., Jeong, H.S. And Abraham, D.M., 2006. Estimating Transition Probabilities In Markov Chain-Based Deterioration Models For Management of Wastewater Systems. Journal of Water Resources Planning and Management, 132(1), pp.15-24.

Bali, T.G., 2003. The Generalized Extreme Value Distribution. Economics Letters, 79(3), pp.423-427.

Barone, G. And Frangopol, D.M., 2014. Life-Cycle Maintenance of Deteriorating Structures By Multi-Objective Optimization Involving Reliability, Risk, Availability, Hazard And Cost. Structural Safety, 48, pp.40-50.

Batstone, C., Lawless, M., Tawn, J., Horsburgh, K., Blackman, D., Mcmillan, A., Worth, D., Laeger, S. And Hunt, T., 2013. A UK Best-Practice Approach for Extreme Sea-Level Analysis along Complex Topographic Coastlines. Ocean Engineering, 71, pp.28-39.

Battjes, J.A. And Groenendijk, H.W., 2000. Wave Height Distributions on Shallow Foreshores. Coastal Engineering, 40(3), pp.161-182.

Bennett, C.C. And Hauser, K., 2013. Artificial Intelligence Framework for Simulating Clinical Decision-Making: A Markov Decision Process Approach. Artificial Intelligence in Medicine, 57(1), pp.9-19.

Binder, K., Heermann, D., Roelofs, L., Mallinckrodt, A.J. And Mckay, S., 1993. Monte Carlo Simulation in Statistical Physics. Computers in Physics, 7(2), pp.156-157.

Birolini, Reliability Engineering: Theory and Practice. 7th Edition. Heidelberg: Springer, 2007. DOI: 10.1007/978-3-642-39535-2.

Blong, R., 2003. A Review of Damage Intensity Scales. Natural Hazards, 29(1), pp.57-76.

Bocchini, P., Saydam, D. And Frangopol, D. M., 2012. Efficient, Accurate, and Simple Markov Chain Model for the Life-Cycle Analysis of Bridge Groups. Structural Safety, Volume 40, pp. 51-64.

Bonelli, S., 2013. Erosion In Geomechanics Applied To Dams And Levees. John Wiley and Sons.

Bosello, F. And Cian, E. D., 2013. Climate Change, Sea Level Rise, and Coastal Disasters. A Review of Modelling Practices. Energy Economics, Volume Article In Press, pp. 1-13.

Bown, J. Chatterton, and Purcell A., Asset Performance Tools – Asset Inspection Guidance, Bristol: Environment Agency, 2014.

British Geological Survey 1998 - 2017 NERC, 2017. Meteotsunami, South West England, British Geological Survey (BGS). Available at: Http://Www.Bgs.Ac.Uk/Research/Highlights/2011/Tsunamiswengland2011.Html. [Accessed 16 June 2017].

Bu, G., Lee, J., Guan, H., Blumenstein, M. And Loo, Y.C., 2012. Development of an Integrated Method for Probabilistic Bridge-Deterioration Modelling. Journal of Performance of Constructed Facilities, 28(2), pp.330-340.

Buijs, F.A., Hall, J.W., Sayers, P.B. And Van Gelder, P.H.A.J.M., 2009. Time-Dependent Reliability Analysis of Flood Defences. Reliability Engineering and System Safety, 94(12), pp.1942-1953.

Buijs, F.A., Hall, J.W., Van Noortwijk, J.M. And Sayers, P.B., 2005. Time-Dependent Reliability Analysis of Flood Defences Using Gamma Processes. Safety and Reliability of Engineering Systems and Structures, pp.2209-2216.

Burcharth, H.F., Andersen, T.L. And Lara, J.L., 2014. Upgrade of Coastal Defence Structures against Increased Loadings Caused By Climate Change: A First Methodological Approach. Coastal Engineering, 87, pp.112-121.

Cai, Y. And Reeve, D.E., 2013. Extreme Value Prediction via a Quantile Function Model. Coastal Engineering, 77, pp.91-98. Available At: Http://Dx.Doi.Org/10.1016/J.Coastaleng.2013.02.003.

Cai, Y., Gouldby, B., Dunning, P. And Hawkes, P., 2007. A Simulation Method for Flood Risk Variables, In Flood Risk Assessment. Plymouth, U.K., September 4th–5th, 2007, IMA, Univ. Of Minn., Minneapolis, ISBN: 978-0-905091-20-4., Proceedings of a Conference Held By the Institute of Mathematics and Its Applications.

Carter, A., Magar, V., Simm, J., Gouldby, B. And Wallis, M., 2013, October. Accounting For Multivariate Probabilities of Failure in Vertical Seawall Reliability Assessments. In ICE Conference on Coasts, Marine Structures and Breakwaters.

Castillo, J. And Daoudi, J., 2009. Estimation of the Generalized Pareto Distribution. Statistics & Probability Letters, 79(5), pp.684-688.

Castillo, E. And Hadi, A.S., 1997. Fitting the Generalized Pareto Distribution to Data. Journal of The American Statistical Association, 92(440), pp.1609-1620.

Chen, H.P. And Alani, A.M., 2012. Reliability and Optimised Maintenance for Sea Defences. In Proceedings of the Institution of Civil Engineers-Maritime Engineering (Vol. 165, No. 2, pp. 51-64). Thomas Telford Ltd.

Chen, H.P. And Alani, A.M., 2013. Optimized Maintenance Strategy For Concrete Structures Affected By Cracking Due To Reinforcement Corrosion. ACI Structural Journal, 110(2), pp.229-237.

Chen, H.P., 2006. Efficient Methods for Determining Modal Parameters of Dynamic Structures with Large Modifications. Journal of Sound and Vibration, 298(1), pp.462-470.

Chen, H.P., 2015. Time-Dependent Reliability Analysis Of Coastal Defences Subjected To Changing Environments. Structural Monitoring and Maintenance, 2(1), pp.49-64.

Cheng, Z., Qiao, Y. And Guo, B., 2015, June. Imperfect Maintenance Model of Pavement Based On Markov Decision Process. In The Ninth International Conference on Mathematical Methods in Reliability the Ninth International Conference on Mathematical Methods in Reliability (pp. 1-4).

Chini, N. And Stansby, P., 2012. Extreme Values of Coastal Wave Overtopping Accounting for Climate Change and Sea Level Rise. Coastal Engineering, Volume 65, pp. 27-37.

CIRIA, Construction Industry Research, Information Association, 2007. The Rock Manual: The Use of Rock in Hydraulic Engineering. CIRIA, London, UK, Report C683.

Coles, S., Bawa, J., Trenner, L. And Dorazio, P., 2001. An Introduction to Statistical Modelling of Extreme Values, 3rd Edition. London: Springer.

Dahl, K.A., Fitzpatrick, M.F. And Spanger-Siegfried, E., 2017. Sea Level Rise Drives Increased Tidal Flooding Frequency at Tide Gauges Along The US East And Gulf Coasts: Projections for 2030 and 2045. Plos One, 12(2), Report.E0170949.

Damnjanovic, I. And Zhang, Z., 2008. Risk-Based Model for Valuation of Performance-Specified Pavement Maintenance Contracts. Journal of Construction Engineering and Management, 134(7), pp.492-500.

Davison, A.C. And Smith, R.L., 1990. Models for Exceedances over High Thresholds. Journal of the Royal Statistical Society. Series B (Methodological), pp.393-442.

Diakakis, M., Deligiannakis, G., Katsetsiadou, K. And Lekkas, E., 2015. Hurricane Sandy Mortality in the Caribbean and Continental North America. Disaster Prevention and Management, 24(1), pp.132-148.

Donovan, B., Horsburgh, K., Ball, T. And Westbrook, G., 2013. Impacts of Climate Change on Coastal Flooding. MCCIP Science Review, 2013, pp.211-218.

Duchesne, S., Beard sell, G., Villeneuve, J., And Bouchard, K., 2013. A Survival Analysis Model For Sewer Pipe Structural Deterioration. Computer-Aided Civil and Infrastructure Engineering, 28(2), pp.146-160.

Edirisinghe, R., Setunge, S. And Zhang, G., 2013. Application of Gamma Process for Building Deterioration Prediction. Journal of Performance of Constructed Facilities, 27(6), pp.763-773.

Environment Agency, Condition Assessment Manual; Managing Flood Risk, Document Reference 116-03-SD01. Environment Agency, Bristol, 2006. Pdf Download Available From: Http://Publications.Environmentagency.Gov.Uk.

Environment Agency, Asset performance tools – asset inspection guidance, Document Reference SC110008/R2. Environment Agency, Bristol, 2014.

Environment Agency, 2017, Flood Map for Planning, [Online] https://flood-map-for-planning.service.gov.uk/, Accessed: September 2017.

Esteban, M., Takagi, H. And Shibayama, T., 2014. Adoptation to an Increase in Typhoon Intensity and Sea Level Rise by Japanese Ports. Climate Change and Adaptation Planning For Ports, pp. 117-132.

Ewans, K. And Jonathan, P., 2014. Evaluating Environmental Joint Extremes for the Offshore Industry Using the Conditional Extremes Model. Journal of Marine Systems, 130, pp.124-130.

Firth, L.B., Mieszkowska, N., Thompson, R.C. And Hawkins, S.J., 2013. Climate Change and Adaptational Impacts in Coastal Systems: The Case of Sea Defences. Environmental Science: Processes and Impacts, 15(9), pp.1665-1670.

Flikweert J., Lawton P., Collel MR., And Simm J., Guidance on Determining Asset Deterioration and The Use of Condition Grade Deterioration Curves. Bristol: Environment Agency, 2009. Pdf Download Available From: Http://Publications.Environmentagency.Gov.Uk.

Flikweert, J. And Simm, J., 2008. Improving Performance Targets for Flood Defence Assets. Journal of Flood Risk Management, 1(4), pp.201-212.

Frangopol, D.M. And Liu, M., 2007. Maintenance And Management of Civil Infrastructure Based On Condition, Safety, Optimization, and Life-Cycle Cost. Structure and Infrastructure Engineering, 3(1), pp.29-41.

Frangopool, D.M., Kallen, M.J. And Van Noortwijk, J.M., 2004. Probabilistic Models for Life-Cycle Performance of Deteriorating Structures: Review and Future Directions. Progress in Structural Engineering and Materials, 6(4), pp.197-212.

Garrity, N.J., Battalio, R., Hawkes, P.J. and Roupe, D., 2007. Evaluation of Event and Response Approaches to Estimate the 100-Year Coastal Flood for Pacific Coast Sheltered Waters. In 30th International Conference On Coastal Engineering, ICCE 2006, 3 September 2006 Through 8 September 2006, San Diego, CA, United States (pp. 1651-1663).

Garthwaite, P.H., Kadane, J.B. and O'Hagan, A., 2005. Statistical Methods for Eliciting Probability Distributions. Journal of The American Statistical Association, 100(470), pp.680-701.

Gelder, P., Buijs, F., Horst, W., Kanning, W., Van, C.M., Rajabalinejad, M., Boer, E., Gupta, S., Shams, R., Erp, N. and Gouldby, B., 2008. Reliability Analysis of Flood Defence Structures and Systems in Europe.

Gelder, P.H.A.J., 2013. Flood Risk Management, Quantitative Methods. Wiley Statsref: Statistics Reference Online.Gelder 201

Genest, C., Favre, A.C., Béliveau, J. and Jacques, C., 2007. Metaelliptical Copulas and Their Use in Frequency Analysis of Multivariate Hydrological Data. Water Resources Research, 43(9) pp.237-245.

Goda, Y., 2010. Random Seas and Design of Maritime Structures. Advanced Series On Ocean Engineering. Third Ed. Japan: World Scientific Press.

Gouldby, B., Méndez, F.J., Guanche, Y., Rueda, A. and Mínguez, R., 2014. A Methodology for Deriving Extreme Nearshore Sea Conditions for Structural Design and Flood Risk Analysis. Coastal Engineering, 88, pp.15-26.

Gouldby, B., Sayers, P., Mulet-Marti, J., Hassan, M.A.A.M. and Benwell, D., 2008, June. A Methodology for Regional-Scale Flood Risk Assessment. In Proceedings of the Institution of Civil Engineers-Water Management (Vol. 161, No. 3, pp. 169-182). Thomas Telford Ltd.

Gouldby, B., Sayers, P., Tarrant, O. and Kavanagh, D., 2007. Thames Estuary 2100: Performance Based Asset Management. Technical Report IA8/10, Hrwallingford.

Grall, A., Bérenguer, C. and Dieulle, L., 2002. A Condition-Based Maintenance Policy for Stochastically Deteriorating Systems. Reliability Engineering and System Safety, 76(2), pp.167-180.

Grimaldi, S. and Serinaldi, F., 2006. Asymmetric Copula in Multivariate Flood Frequency Analysis. Advances in Water Resources, 29(8), pp.1155-1167.

Halcrow Group, 2013. Practical Guidance On Determining Asset Deterioration and The Use Of Condition Grade Deterioration Curves: Revision 1, Bristol: Environment Agency.

Hall, J.W., Dawson, R.J., Sayers, P.B., Rosu, C., Chatterton, J.B. and Deakin, R., 2003, September. A Methodology for National-Scale Flood Risk Assessment. In Proceedings of the Institution of Civil Engineers-Water Maritime and Engineering, Vol. 156, No. 3, pp. 235-248.

Hallegatte, S., Green, C., Nicholls, R.J. and Corfee-Morlot, J., 2013. Future Flood Losses in Major Coastal Cities. Nature Climate Change, 3(9), pp.802-806.

Hallegatte, S., Ranger, N., Mestre, O., Dumas, P., Corfee-Morlot, J., Herweijer, C. and Wood, R.M., 2011. Assessing Climate Change Impacts, Sea Level Rise and Storm Surge Risk In Port Cities: A Case Study On Copenhagen. Climatic Change, 104(1), pp.113-137.

Hames, D. and Reeve, D., 2007. The Joint Probability of Waves and High Sea Levels in Coastal Defence. Cradiff, Institute Of Mathematics and Its Applications (IMA).

Hansen, H.S., 2010. Modelling The Future Coastal Zone Urban Development As Implied By The IPCC SRES and Assessing The Impact From Sea Level Rise. Landscape and Urban Planning, 98(3-4), pp.141–149.

Hawkes P., 2008, Joint Probability Analysis for Estimation of Extremes. Journal of Hydraulic Research 46(2), pp. 246–256.

Hawkes, P.J. and Svensson, C., 2006. Joint Probability: Dependence Mapping and Best Practice. T02-06-16.

Hawkes, P.J., Gonzalez-Marco, D., Sánchez-Arcilla, A. and Prinos, P., 2008. Best Practice for the Estimation of Extremes: A Review. Journal of Hydraulic Research, 46(S2), p.324-332.

Hawkes, P.J., Gouldby, B.P., Tawn, J.A. and Owen, M.W., 2002. The Joint Probability of Waves and Water Levels in Coastal Engineering Design. Journal of Hydraulic Research, 40(3), pp.241-251.

Hawkes, P.J., Svensson, C. and Surendran, S., 2005. The Joint Probability of Pairs of Variables Relevant To Flood Risk: Dependence Mapping and Best Practice.

Hinkel, J., Lincke, D., Vafeidis, A.T., Perrette, M., Nicholls, R.J., Tol, R.S., Marzeion, B., Fettweis, X., Ionescu, C. and Levermann, A., 2014. Coastal Flood Damage and Adaptation Costs under 21st Century Sea-Level Rise. Proceedings of the National Academy of Sciences, 111(9), pp.3292-3297.

Hong, H.P., Zhou, W., Zhang, S. and Ye, W., 2014. Optimal Condition-Based Maintenance Decisions for Systems with Dependent Stochastic Degradation of Components. Reliability Engineering and System Safety, 121, pp.276-288.

HR Wallingford, 2000. The Joint Probability of Waves and Water Levels: JOIN-SEA-A Rigorous but Practical New Approach. HR Wallingford Report SR, 537.

HR Wallingford, 2006. Tidal/Fluvial Interaction on Tributaries of the Tidal Thames, HR Wallingford Technical Report EP4, January. Pdf Available At: Www.HR-Wallingford.Com

Jenkins G, Murphy J, Sexton D and Lowe J, 2011. UK Climate Projections: Briefing Report. Version 2, Met Office Hadley Centre, Newcastle, UK.

Jiang, Y., and Sinha, K.C., 1989. Bridge Service Life Prediction Model Using the Markov Chain. Transportation Research Record 1223, Transportation Research Board. Washington, DC. pp. 24-30.

Jonathan, P., Ewans, K. and Randell, D., 2013. Joint Modelling Of Extreme Ocean Environments Incorporating Covariate Effects. Coastal Engineering, Volume 79, pp. 22-31.

Kaelbling, L.P., Littman, M.L. and Cassandra, A.R., 1998. Planning and Acting In Partially Observable Stochastic Domains. Artificial Intelligence, 101(1), pp.99-134.

Karamouz, M., Razmi, A., Nazif, S. and Zahmatkesh, Z., 2017. Integration of Inland and Coastal Storms for Flood Hazard Assessment Using a Distributed Hydrologic Model. Environmental Earth Sciences, 76(11), pp.395-403.

Karim, M.F. and Mimura, N., 2008. Impacts of Climate Change and Sea-Level Rise on Cyclonic Storm Surge Floods in Bangladesh. Global Environmental Change, 18(3), pp.490-500.

Khon, V.C., Mokhov, I.I., Pogarskiy, F.A., Babanin, A., Dethloff, K., Rinke, A. and Matthes, H., 2014. Wave Heights In The 21st Century Arctic Ocean Simulated With A Regional Climate Model. Geophysical Research Letters, 41(8), pp.2956-2961.

Kim, J., Ahn, Y. and Yeo, H., 2016. A Comparative Study of Time-Based Maintenance and Condition-Based Maintenance for Optimal Choice of Maintenance Policy. Structure and Infrastructure Engineering, 12(12), pp.1525-1536.

Kleiner, Y., 2001. Scheduling Inspection and Renewal of Large Infrastructure Assets. Journal of Infrastructure Systems, 7(4), pp.136-143.

Komen, G.J., Cavaleri, L. and Donelan, M., 1996. Dynamics and Modelling Of Ocean Waves. Cambridge University Press.

Konency, F. and Nachtnebel, H. P., 1985. Extreme Value Processes and the Evaluation of Risk in Flood Analysis. Application of Mathematics Modell, Volume 19, pp. 11-15.

Kortenhaus, A., Oumeraci, H., Weissman, R. and Richwien, W., 2002. Failure Mode and Fault Tree Analysis for Sea and Estuary Dikes. In Coastal Engineering Conference (Vol. 2, pp. 2386-2398). ASCE American Society of Civil Engineers.

Kuczera, G., Lambert, M., Heneker, T., Jennings, S., Frost, A. and Coombes, P., 2006. Joint Probability and Design Storms at the Crossroads. Australian Journal of Water Resources, 10(1), pp.63-79.

Lane, A., 2004. Bathymetric Evolution of the Mersey Estuary, UK, 1906–1997: Causes and Effects. Estuarine, Coastal and Shelf Science, 59(2), pp.249-263

Lavrenz, S., Hoyos, J.M. and Labi, S., 2014. Constructs For Quantifying The Long-Term Effectiveness Of Civil Infrastructure Interventions. Maintenance and Safety of Aging Infrastructure: Structures and Infrastructures Book Series, 10, pp.379-386.

Le Son, K., Fouladirad, M., Barros, A., Levrat, E. and Iung, B., 2013. Remaining Useful Life Estimation Based On Stochastic Deterioration Models: A Comparative Study. Reliability Engineering and System Safety, 112, pp.165-175.

Lee, C.-E., Kim, S.-W., Park, D.-H. and Suh, K.-D., 2013. Risk Assessment of Wave Run-Up Height and Armor Stability of Inclined Coastal Structures Subject To Long Term Sea Level Rise. Ocean Engineering, Volume 71, pp. 130-136.

Lehner, B., Döll, P., Alcamo, J., Henrichs, T. and Kaspar, F., 2006. Estimating the Impact of Global Change on Flood and Drought Risks in Europe: A Continental, Integrated Analysis. Climatic Change, 75(3), pp.273-299.

Li, Q., Wang, C. and Ellingwood, B.R., 2015. Time-Dependent Reliability of Aging Structures In The Presence Of Non-Stationary Loads and Degradation. Structural Safety, 52, pp.132-141.

Lin, X. and Breslow, N.E., 1996. Bias Correction in Generalized Linear Mixed Models with Multiple Components of Dispersion. Journal of The American Statistical Association, 91(435), pp.1007-1016.

Liu, D., Pang, L., Fu, G., Shi, H. and Fan, W., 2006, January. Joint Probability Analysis of Hurricane Katrina 2005. In The Sixteenth International Offshore and Polar Engineering Conference. International Society of Offshore and Polar Engineers.

Long, G., Smith, M., Mawdesley, M. and Taha, A., 2013. A Methods for the Monitoring and Inspection of Flood Defences: New Techniques Flood Defences: New Techniques. CIRIA, London: Classic House.

Lorenzoni, I., Benson, D. and Cook, H., 2016. Regional Rescaling In Adaptation Governance: From Agency To Collaborative Control In Flood Management In England. Climate Adaptation Governance in Cities and Regions: Theoretical Fundamentals and Practical Evidence. Wiley.

Madanat, S. and Ben-Akiva, M., 1994. Optimal Inspection and Repair Policies for Infrastructure Facilities. Transportation Science, 28(1), pp.55-62.

Mai, C.V., Van Gelder, P.H.A.J.M., Vrijling, J.K. and Mai, T.C., 2008. Risk Analysis of Coastal Flood Defences: A Vietnam Case. In 4th International Symposium on Flood Defence" Managing Flood Risk, Reliability and Vulnerability", Toronto, Canada, 6-8 May 2008. Institute for Catastrophic Loss Reduction.

Martins, E.S. and Stedinger, J.R., 2000. Generalized Maximum-Likelihood Generalized Extreme-Value Quantile Estimators for Hydrologic Data. Water Resources Research, 36(3), pp.737-744.

Masselink, G. and Russell, P., 2013. Impacts of Climate Change on Coastal Erosion. MCCIP Science Review, 2013, pp.71-86.

Mazas, F., Kergadallan, X., Garat, P. and Hamm, L., 2014. Applying POT Methods to the Revised Joint Probability Method for Determining Extreme Sea Levels. Coastal Engineering, 91, pp.140-150.

Mcmillan, A., Batstone, C., Worth, D., Tawn, J., Horsburgh, K. and Lawless, M., 2011. Coastal Flood Boundary Conditions for UK Mainland and Islands. Project SC060064/TR2: Design Sea Levels.

Mehrabani, M.B. and Chen, H.P., 2015. Risk Assessment of Wave Overtopping of Sea Dykes Due to Changing Environments. In The 3rd International Conference on Flood Risk Assessment (IMA3), Swansea, UK.

Mehrabani, M.B. and Chen, H.P., 2016. Grading-Based Deterioration Models for Future Performance Predictions of Coastal Flood Defences. In International Conference on Smart Infrastructure and Construction (ICSIC). Cambridge, UK.

Mehrabani, M.B., Chen, H.P. and Stevenson, M.W., 2015. Overtopping Failure Analysis Of Coastal Flood Defences Affected By Climate Change. In Journal Of Physics: Conference Series (Vol. 628, No. 1, pp. 152-163). IOP Publishing.

Mishalani, R.G. and Madanat, S.M., 2002. Computation of Infrastructure Transition Probabilities Using Stochastic Duration Models. Journal of Infrastructure Systems, 8(4), pp.139-148.

Muller, G., Allsop, W., Bruce, T., Kortenhaus, A., Pearce, A. and Sutherland, J., 2007, December. The Occurrence and Effects of Wave Impacts. In Proceedings-Institution Of Civil Engineers Maritime Engineering (Vol. 160, No. 4, pp. 167-172).

Nagy, L., and Toth, S., 2005. Detailed Technical Report On The Collation and Analysis Of Dike Breach Data With Regards To Formation Process and Location Factors. Technical Report, H-Euraqua Ltd. Hungary.

Naulina, M., Kortenhaus, A. and Oumeraci, H., 2011. Failure Probability of Flood Defence Structures/Systems in Risk Analysis for Extreme Storm Surges. Coastal Engineering Proceedings, 1(32), pp.13-23.

Naulinb, M., Kortenhaus, A. and Oumeraci, H., 2011. Reliability Analysis and Breach Modelling Of Coastal and Estuarine Flood Defences. In Proceedings 3rd International Symposium on Geotechnical Safety and Risk (ISGSR 2011), Munich, Germany (pp. 577-586).

Nicholls, R.J. and Cazenave, A., 2010. Sea-Level Rise and Its Impact on Coastal Zones. Science, 328(5985), pp.1517-1520.

Norris, J.R., 1997. Markov Chains, Cambridge Series in Statistical and Probabilistic Mathematics, Cambridge U.

Oh, S.H., Suh, K.D., Son, S.Y. and Lee, D.Y., 2009. Performance Comparison Of Spectral Wave Models Based On Different Governing Equations Including Wave Breaking. KSCE Journal of Civil Engineering, 13(2), pp.75-84.

Olbert, A.I., Comer, J., Nash, S. and Hartnett, M., 2017. High-Resolution Multi-Scale Modelling Of Coastal Flooding Due To Tides, Storm Surges and Rivers Inflows. A Cork City Example. Coastal Engineering, 121, pp.278-296.

Ortiz-García, J. Costello, S. and Snaith, M. 2006. Derivation of Transition Probability Matrices for Pavement Deterioration Modelling, Journal of Transportation Engineering, 132, pp.141–161.

Osman, Y., Fealy, R. and Sweeney, J., 2013. Downscaling Extreme Precipitation In Ireland Using Combined Peak-Over-Threshold Generalised Pareto Distribution Model Of Varying Parameters. Journal of Water and Climate Change, pp. 1-16.

Ossai, C.I., Boswell, B. and Davies, I.J., 2016. Stochastic Modelling of Perfect Inspection and Repair Actions for Leak–Failure Prone Internal Corroded Pipelines. Engineering Failure Analysis, 60, pp.40-56.

Oumeraci, H., 2005. Integrated Risk-Based Design and Management of Coastal Flood Defences. Die Küste, 70, pp.151-172.

Owen, M.W., 1980. Design of Seawalls Allowing For Wave Overtopping. Report Ex, 924, pp.39-51.

Papakonstantinou, K.G. and Shinozuka, M., 2014. Optimum Inspection and Maintenance Policies for Corroded Structures Using Partially Observable Markov Decision Processes and Stochastic, Physically Based Models. Probabilistic Engineering Mechanics, 37, pp.93-108.

Phillips, T., Hall, J.H., Dawson, R.J., Barr, S., Ford, A., Batty, M., Dagoumas, A. and Sayers, P.B., 2008. Strategic Appraisal of Flood Risk Management Options over Extended Timescales: Combining Scenario Analysis with Optimization.

Pinsky M., and Karlin S., an Introduction to Stochastic Modelling, 4th Edition. Burlington, USA: Academic Press, 2011, ISBN-13: 978-0123814166.

Pirazzoli, P. A. and Tomasin, A., 2002. Recent Evolution of Surge-Related Events in the Northern Adriatic Area. Journal of Coastal Research, 18(3), pp. 537-554.

Pugh, D.T. and Vassie, J.M., 1980. Applications of the Joint Probability Method for Extreme Sea Level Computations. Proceedings of The Institution of Civil Engineers, 69(4), pp.959-975.

Pullen, T., Allsop, N.W.H., Bruce, T., Kortenhaus, A., Schuttrumpf, H. and Van Der Meer, J.W., 2007. Eurotop—Wave Overtopping Of Sea Defences and Related Structures. Assessment Manual, August. ISBN, Pp.978-3.

Purvis, M.J., Bates, P.D. and Hayes, C.M., 2008. A Probabilistic Methodology to Estimate Future Coastal Flood Risk Due To Sea Level Rise. Coastal Engineering, 55(12), pp.1062-1073.

Rakonczai, P. and Zempléni, A., 2012. Bivariate Generalized Pareto Distribution in Practice: Models and Estimation. Environmetrics, 23(3), pp.219-227.

Rangel-Buitragoa, N. G., Anfusob, G. and Williams, A. T., 2015. Coastal Erosion along the Caribbean Coast of Colombia: Magnitudes, Causes and Management. Ocean and Coastal Management, Volume 114, pp. 129-144.

Reeve, D., 2009. Risk and Reliability: Coastal and Hydraulic Engineering. CRC Press.

Reeve, D., Rozynskib, G. and Li, Y., 2008. Extreme Water Levels of the Vistula River and Gdansk Harbour. Journal of Hydraulic Research, Volume 46, pp. 235-245.

Rinker, J., 2013. Peak-Over-Threshold Method for Extreme Values, North Carolina: Duke University.

Roijers, D.M., Vamplew, P., Whiteson, S. and Dazeley, R., 2013. A Survey of Multi-Objective Sequential Decision-Making. Journal of Artificial Intelligence Research, 48, pp.67-113.

Rosenzweig, C., Solecki, W.D., Blake, R., Bowman, M., Faris, C., Gornitz, V., Horton, R., Jacob, K., Leblanc, A., Leichenko, R. and Linkin, M., 2011. Developing Coastal Adaptation to Climate Change in the New York City Infrastructure-Shed: Process, Approach, Tools, and Strategies. Climatic Change, 106(1), pp.93-127.

Saydam, D. and Frangopol, D.M., 2014. Risk-Based Maintenance Optimization of Deteriorating Bridges. Journal of Structural Engineering, 141(4), pp.141-152.

Saydam, D., Frangopol, D. and Dong, Y., 2013. Assessment of Risk Using Bridge Element Condition Ratings. Journal of Infrastructure Systems, 19, pp.252-265.

Sayers, P., Walsh, C. and Dawson, R., 2015. Climate Impacts on Flood and Coastal Erosion Infrastructure. Infrastructure Asset Management, 2(2), pp. 69-83.

Schaller, N., Kay, A.L., Lamb, R., Massey, N.R., Van Oldenborgh, G.J., Otto, F.E., Sparrow, S.N., Vautard, R., Yiou, P., Ashpole, I. and Bowery, A., 2016. Human Influence on Climate in the 2014 Southern England Winter Floods and Their Impacts. Nature Climate Change, 6(6), pp.627-634.

Schultz, M.T., Gouldby, B.P., Simm, J.D. and Wibowo, J.L., 2010. Beyond The Factor Of Safety: Developing Fragility Curves To Characterize System Reliability (No. ERDC-SR-10-1). Engineer Research and Development Center Vicksburg Ms Geotechnical and Structures Lab.

Sekimoto, T., Isobe, M., Anno, K. and Nakajima, S., 2013. A New Criterion and Probabilistic Approach to the Performance Assessment of Coastal Facilities In Relation To Their Adaptation to Global Climate Change. Ocean Engineering, 71, pp.113-121.

Sierra, J.P., Casanovas, I., Mösso, C., Mestres, M. and Sánchez-Arcilla, A., 2016. Vulnerability Of Catalan (NW Mediterranean) Ports To Wave Overtopping Due To Different Scenarios Of Sea Level Rise. Regional Environmental Change, 16(5), pp.1457-1468.

Simm, J.D., Gouldby, B.P., Sayers, P.B., Flikweert, J., Wersching, S. and Bramley, M.E., 2008. Representing Fragility of Flood and Coastal Defences: Getting Into the Detail.

Soh, H. and Demiris, Y., 2011, July. Evolving Policies for Multi-Reward Partially Observable Markov Decision Processes (MR-Pomdps). In Proceedings of the 13th Annual Conference on Genetic and Evolutionary Computation (pp. 713-720). ACM.

Steenbergen, H. and Lassing, B., 2004. Reliability Analysis of Flood Defence Systems. Heron, 49(1), pp.51–73.

Sterr, H., 2007. Assessment of Vulnerability and Adaptation to Sea-Level Rise for the Coastal Zone Of Germany. Journal of Coastal Research, 24(2), pp. 380-393.

Strauss, A., Wendner, R., Vidovic, A., Zambon, I. and Frangopol, D.M., 2015. Prediction of Creep and Shrinkage Based On Gamma Process Models.

Strauss, B., Tebaldi, C. and Ziemlinski, R., 2012. Sea Level Rise, Storms and Global Warming's Threat to the US Coast. Climate Central.

Suppasri, A., Mas, E., Koshimura, S., Imai, K., Harada, K. and Imamura, F., 2012. Developing Tsunami Fragility Curves from the Surveyed Data of the 2011 Great East Japan Tsunami in Sendai and Ishinomaki Plains. Coastal Engineering Journal, 54(01), pp.125-136.

Tajvidi, N., 1996. Multivariate Generalised Pareto Distributions, University In Gothenburg, Sweden: Chalmers.

TAW, 2002. Technical Report – Wave Run-Up and Wave Overtopping At Dikes. Technical Advisory Committee for Flood Defence in the Netherlands (TAW), Delft.

Tawn, J. A., 1992. Estimating Probabilities of Extreme Sea-Levels. Journal of the Royal Statistical Society, 41(Series C), pp. 77-93.

Taylor, J. Short, D. Dales, River Hamble to Portchester Coastal Flood and Erosion Risk Management Strategy, Ref: 47067754/JPWOR_4. URS, Basingstoke, 2014.

Thorne, C., 2014. Geographies of UK Flooding In 2013/4. The Geographical Journal, 180(4), pp.297-309.

Townend, I. and Burgess, K.E.V.I.N., 2004. Methodology for Assessing the Impact of Climate Change upon Coastal Defence Structures. In Coastal Engineering Conference (Vol. 29, No. 4, pp. 39-53). ASCE American Society of Civil Engineers.

Udale-Clarke, H., 2009. Floodsite Fact Sheets, Summary of Key Project Outputs. T32-09-02.

Van Der Meer, J.W., Pullen T., Allsop, N.W.H., Bruce, T., Kortenhaus, A., Sch, H., and Eurotop II: Wave Overtopping Of Sea Defences and Related Structures: Assessment Manual. Environment Agency, London, 2016. Pdf Download Available From: Www.Overtopping-Manual.Com.

Van Der Meer, J.W., 1998. Wave Run-Up and Overtopping. Dikes and Revetments: Design, Maintenance and Safety Assessment, Ed. KW Pilarczyk (AA Balkema, Rotterdam, The Netherlands), pp.145-159.

Van Der Meer, J.W., Horst, W.L.A. and Velzen E.H., 2009. Cal-Culation Of Fragility Curves For Flood Defence Assets, Flood. Risk Management: Research and Practice, pp.567-573.

Van Der Meij, R., Van Den Ham, G.A., Morris, M., Lhomme, J., Tourment, R. and Maurel, P., 2012, November. Combining Different Data Sources for Assessment of Urban Flood Defences. In 2nd European Conference on Floodrisk Management. London: Taylor and Francis Group.

Van Gelder, P.H.A.J.M., Vrijling, J.K. and Van Haaren, D.H., 2004. Joint Probability Distributions for Wave Height, Wind Setup and Wind Speed. In Coastal Engineering Conference (Vol. 29, No. 1, pp. 19-32). ASCE American Society of Civil Engineers.

Van Noortwijk, J.M. and Frangopol, D.M., 2004. Two Probabilistic Life-Cycle Maintenance Models for Deteriorating Civil Infrastructures. Probabilistic Engineering Mechanics, 19(4), pp.345-359.

Van Noortwijk, J.M., 2009. A Survey of the Application of Gamma Processes in Maintenance. Reliability Engineering and System Safety, 94(1), pp.2-21.

Van, C.M., Van Gelder, P.H.A.J.M. and Vrijling, J.K., 2007, July. Failure Mechanisms of Sea Dikes-Inventory and Sensitivity Analysis. In COPRI-ASCE-Coastal Structures 2007 International Conference.

Vincest, L., 1982. Technical Report No.82-3, Depth-Lomited Significant Wave Height: A Spectral Approach, Coastal Engineering Research Center.

Voortman, H.G. and Vrijling, J.K., 2001. A Risk-Based Optimisation Strategy for Large-Scale Flood Defence Systems. In Proceedings IABSE Conference Safety Risk and Reliability, Trends in Engineering.

Vorogushyn, S., Merz, B. and Apel, H., 2009. Development of Dike Fragility Curves for Piping and Micro-Instability Breach Mechanisms. Natural Hazards and Earth System Sciences, 9(4), pp.1383-1401.

Wadey, M.P., Haigh, I.D. and Brown, J.M., 2014. A Century of Sea Level Data and the UK's 2013/14 Storm Surges: An Assessment of Extremes and Clustering Using the Newlyn Tide Gauge Record. Ocean Science, 10(6), pp.10-31.

Weggel, J.R., 1973. Maximum Breaker Height for Design. In Coastal Engineering 1972 (pp. 419-432).

Weijers, J.B.A. and Sellmeijer, J.B., 1993. A New Model to Deal with the Piping Mechanism. Filters in Geotechnical and Hydraulic Engineering, pp.349-355.

Weisse, R., Bellafiore, D., Menéndez, M., Méndez, F., Nicholls, R.J., Umgiesser, G. and Willems, P., 2014. Changing Extreme Sea Levels along European Coasts. Coastal Engineering, 87, pp.4-14.

Wellalage, N. K. W., Zhang, T. and Dwight, R., 2015. Calibrating Markov Chain–Based Deterioration Models For Predicting Future Conditions Of Railway Bridge Elements. Journal of Bridge Engineering, 20(2).

White, C.C. and Kim, K.W., 1980. Solution Procedures for Vector Criterion Markov Decision Processes. Large Scale Systems, 1(4), Pp.129-140.

Wilby, R. and Keenan, R., 2012. Adapting To Flood Risk under Climate Change. Progress in Physical Geography, Volume 36, pp. 348-378.

Wilks, D. S., 2011. Statistical Methods in the Atmospheric Sciences. Third Ed. Academic Press: International Geophysics Series.

Wray, K.H. and Zilberstein, S., 2015, July. Multi-Objective Pomdps with Lexicographic Reward Preferences. In IJCAI (pp. 1719-1725).

Zhang, L. and Singh, P., 2006. Bivariate Flood Frequency Analysis Using the Copula Method. Hydrologic Engineering, pp. 150–164.

Zhang, L. and Singh, V. P., 2007. Trivariate Flood Frequency Analysis Using the Gumbel–Hougaard Copula. Journal of Hydrologic Engineering, 12 (Special Issue: Copulas in Hydrology), pp. 431–439.

Appendices

Appendix 1: List of publications

1. Mehrabani, M.B. and Chen, H.P., 2015. Risk Assessment of Wave Overtopping of Sea Dykes Due To Changing Environments. In The 3rd International Conference on Flood Risk Assessment (IMA3), Swansea, UK.

2. Mehrabani, M.B., Chen, H.P. and Stevenson, M.W., 2015. Overtopping Failure Analysis of Coastal Flood Defences Affected By Climate Change. In Journal of Physics: Conference Series (Vol. 628, No. 1, pp. 120-132). IOP Publishing.

3. Mehrabani, M.B. and Chen, H.P., 2016. Grading-Based Deterioration Models for Future Performance Predictions of Coastal Flood Defences. In International Conference on Smart Infrastructure and Construction (ICSIC). Cambridge, UK.

4. Mehrabani, M.B. and Chen, H.P., 2016. Markov Chain Modelling For Life-Cycle Performance Assessment of Coastal Flood Defences. Life-Cycle of Engineering Systems: Emphasis on Sustainable Civil Infrastructure: Proceedings of the Fifth International Symposium on Life-Cycle Civil Engineering, pp.184-192, Delft, The Netherlands.

5. Chen, H.P., Nepal, J., and Mehrabani M.B., 2016. Lifetime Performance Assessment of Flood Defence Structures Utilising Condition Grading Data, Journal of flood and coast.

6. Mehrabani, M.B. and Chen, H.P., 2017. Performance Predictions of Coastal Defences Using Stochastic Deterioration Modelling. In International Conference on Uncertainty Quantification in Computational Sciences and Engineering, pp.131-142, UNCECOMP, Greece.

7. Overtopping failure probability of coastal defences under changing environments, submitted to Journal of Lifecycle Performance Engineering in January 2018. Under review.

8. Performance Prediction and Overtopping Risk Assessment of Coastal Defences Using Stochastic Deterioration Modelling, submitted to Journal of Engineering Failure Analysis in February 2018. Under review.

Appendix 2: Summary of condition grade assessment in UK adopted from Environment Agency 2014.

A2.1 Assessing condition

Condition Assessment Manual (CAM) is a condition grade assessment criterion in the context of grade-based asset management (Environment Agency 2006). Condition grades are defined to offer a standardised approach to assess the deterioration of flood defence structures and to assist decision makers to manage the maintenance strategies. In an inspection process based on CAM, each component is visually inspected by a trained inspector, and it is ranked into one of five condition grades from 1 to 5 (1 for very good and 5 for very poor).

Table A.2.1 Definitions of condition grades in Condition Assessment Manual.

Grade	Rating	Description
1	Very Good	Cosmetic defects that will have no effect on performance.
2	Good	Minor defects that will not reduce the overall performance of the asset.
3	Fair	Defects that could reduce the performance of the asset.
4	Poor	Defects that would significantly reduce the performance of the asset.
5	Very poor	Severe defects are resulting in complete performance failure.

A2.2 Weighting of elements

Weightings in the Environment Agency approach can be used to indicate the importance of each element to the overall condition grade of the asset. The weightings used in this model range from 1 (elements that do not have a function) to 9 (critical elements function). The Environment Agency method is described as:

- The overall grade of the asset is the sum of (weightings × condition grades) divided by the sum of the weightings.
- If any individual element with a weighting of 9 (a critical element) falls below the target condition and the above calculation shows the asset is numerically

meeting its target condition, this should be overridden to give an overall condition grade below the target.

A2.3 Assessment of data quality

General descriptions of data quality regardless of the inspection method are provided in Table A2.3.1. The quality of data are categorised into 5 condition grades from good (condition grade 1) to missing (condition grade 5). Data quality is dominant to data management, however, should be proportional to the needs of users (level of decision), availability of data, the benefits, the costs and the risks associated with collecting, improving or not collecting of data. The quality of data (or dataset) is inherent in its associated attributes such as accuracy, age (how old the data is), and competence (dependent on the skill and experience of the data originator).

Table A.2.1 Data quality indicators and their definitions.

Grade	Rating	Description
1	Good	All elements visually assessed.
2	Adequate	One or more elements were not inspected but a detailed engineering survey has been undertaken.
3	Suspect	A single element that was inspected on the last inspection is not visible at the current inspection.
4	Poor	Two or more single elements that were inspected on the last inspection is not visible at the current inspection.
5	Missing	One or more single elements are not visible for two or more consecutive inspections.

In case of missing elements (Grades 3 to 5 data quality) Flowchart A2.1 should be considered for next actions. The flowchart explains the necessary actions for the described situations and provides the relevant performance assessment activities for the suggested inspection activities.

Flowchart A2.1 Missing element data instruction.

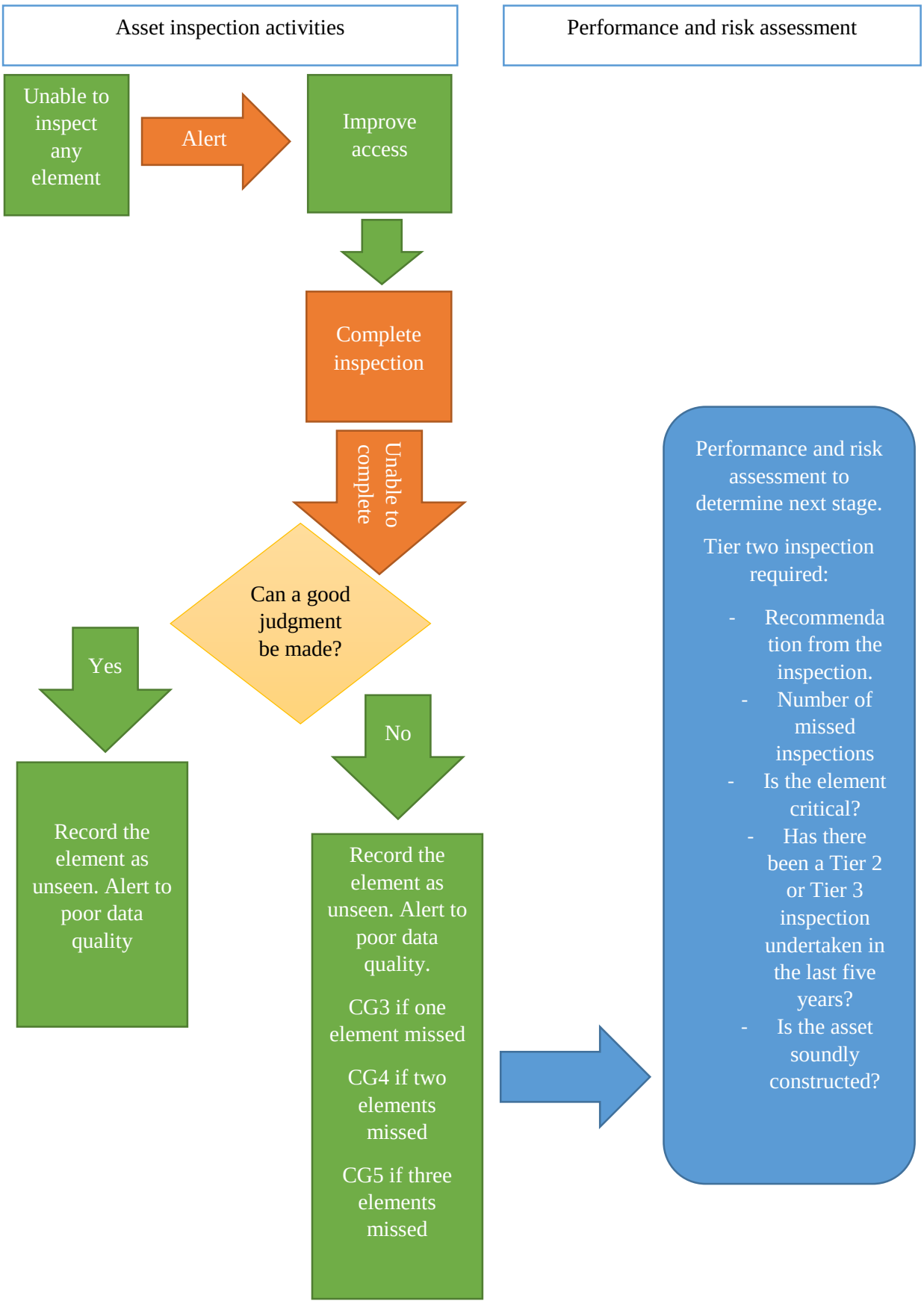

Reference

Environment Agency, Asset performance tools – asset inspection guidance, Document Reference SC110008/R2. Environment Agency, Bristol, 2014.